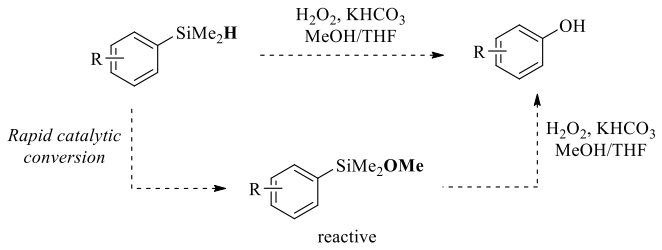
Synthetic and Mechanistic Studies of Arylsilane Oxidation

Doctor of Philosophy **Elizabeth Rayment**

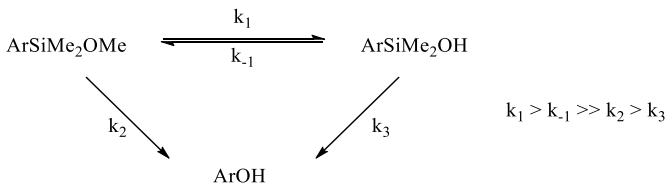
Trinity Term, 2013 **Balliol College**

Abstract: In this thesis, we study arylsilane oxidation from both a synthetic and a mechanistic perspective. Building upon previous work within our group, we demonstrate in an early chapter that aryl*hydro*silanes are surprisingly reactive to oxidation (Scheme 1). This disproves the previous assumptions of the Tamao oxidation and provides new insights into the mechanism of the reaction. Furthermore, we find that the best substrates for oxidation are aryl*methoxy*silanes, and we describe rapid and efficient syntheses for these compounds. A further chapter addresses applications of arylsilane oxidation to natural product synthesis, protecting group chemistry and cycloadditions.



Scheme 1: Arylsilane oxidation methodology

By collecting concentration profiles of the oxidation of various arylsilanes, we reveal a rapid equilibration between arylmethoxysilanes and arylsilanols. By comparison, phenol formation (especially from silanol) is often slow (Scheme 2). The rate of oxidation turns out to be highly sensitive to both the concentration of the oxidising agent and the substituents of the aromatic ring. In the final chapter we discuss in detail the consequences of these observations for the mechanism of arylsilane oxidation.



Scheme 2: Arylsilane oxidation mechanism

Acknowledgements

I would like to extend my thanks to a number of people who have played an important role during my preparation of this thesis:

To Ed, for his enthusiastic supervision and encouragement. I am grateful (now!) for being pushed to unfamiliar fringes of organic chemistry. Although the challenge was daunting a lot of the time, I feel that I learnt a lot!

To Will Unsworth, who helped me begin to understand and enjoy Organic Chemistry. I would also like to acknowledge Jeremy Robertson and his group for such an enjoyable Part II year which convinced me I'd like to study for a DPhil.

To the former members of the EAA group: MC, Dave, Sonia, Jem and Birgit. Your help and advice was always very much appreciated and I missed you all when you left.

My thanks go to Diane for our extremely useful silicon chats, and for her uplifting, thoughtful and funny responses to the daily grind!

To Craig, for his thorough proof reading of this thesis, and for helping me to answer the nitty gritty questions I'd been worrying about.

To the current EAA group, especially Becky, Bobby, Bryony, Ross and Shermin, for always making me feel welcome whenever I came back to lab during my write up.

To the NMR staff of the CRL, for training me, answering my many questions and allowing me so much use of the department's machines. Also to John Brown, for his time listening to our progress and his advice for moving the project forward.

To my housemates from Cripley Road, Kingston Road, and the residents of Inverness Terrace. Thank you so much for your excellent company and for drinking gin and tonic with me whenever necessary.

To David and my family, for their constant support and encouragement.

Abbreviations

Ac	Acetyl
app	apparent
aq.	aqueous
Ar	Aryl
Bu	Butyl
^{13}C	carbon 13
cat.	catalytic
DA	Diels Alder
DCM	dichloromethane
DMAP	4-dimethylaminopyridine
DMEDA	*N*,*N'*-dimethylethylenediamine
DMF	*N*,*N'*-dimethylformamide
DMSO	dimethylsulfoxide
equiv	equivalents
Et	Ethyl
ESI	electrospray ionisation
FI	field ionisation
FT-IR	Fourier transform infra red spectroscopy
^{1}H	proton
h	hour(s)
HMPA	hexamethylphosphoramide
H_2O_2	hydrogen peroxide
HRMS	high resolution mass spectrometry
Hz	Hertz
i-	iso
imid,	imidazole
IPA	*iso*-propanol
IR	infra red
J	coupling constant
KCN	potassium cyanide
L_n	unspecified number of ligands
m-	meta
M	molar , mol dm^{-3}
Me	methyl
mg	milligram
MHz	megahertz

min	minute(s)
mL	millilitre
mm Hg	millimetre of mercury
mmol	millimole
m-CPBA	*meta*-chloroperbenzoic acid
NMR	Nuclear Magnetic Resonance
n.r.	no reaction
o-	ortho
p-	para
P.E.	petroleum ether
PG	protecting group
Ph	phenyl
Pr	propyl
*p*TSA	*para*-toluenesulfonic acid
ppm	parts per million
PPTS	pyridinium *para* toluenesulfonate
quant.	quantitative
R	unspecified subsituent
RDS	rate determining step
R_f	thin layer chromatography retention factor
RSD	relative standard deviation
RT	room temperature
s-	sec
sat.	saturated
t-	tertiary
TBAF	tetrabutylammonium fluoride
TBDPS	*tert*-butyldiphenylsilyl
TBS	*tert*-butyldimethylsilyl
THF	tetrahydrofuran
TLC	thin layer chromatography
TMEDA	*N,N,N',N'*-tetramethylethylenediamine
TMS	trimethylsilyl
TS	transition state
w/w	weight/weight

Contents

1. Introduction 1

1.1. The prevalence of phenols 1

1.2. The synthesis of phenols 3

1.3. Latent phenols 10

1.4. The Kumada-Tamao oxidation 12

1.5. Thesis summary 19

2. Methodology Development 20

2.1. Introduction 20

2.2. Synthesis of arylsilanes 23

2.3. Synthesis of arylsilanols and arylalkoxysilanes 27

2.4. Oxidation of arylsilanes; preliminary results 30

2.5. Preliminary mechanism studies 32

2.6. Optimised oxidation of arylsilanes and arylmethoxysilanes 38

2.7. Heterogeneous catalysis 41

2.8. Conclusion 46

3. Applications of the arylsilane oxidation 48

3.1. The natural polyphenol khellinone 48

3.2. Cycloaddition routes to phenols 64

3.3. Controlled cleavage of Si–O bonds 68

3.4. Development of a flow reactor 72

3.5. Conclusion and future work 80

4. A mechanistic study of arylsilane oxidation 81

4.1. Introduction 81

4.2. Summary of previous observations 94

4.3. Preliminary investigation 95

4.4. Observing the oxidation by ^{19}F NMR spectroscopy 99

4.5. Equilibrium experiments 107

4.6. The addition of TBAF 109

4.7. Initial rate experiments 116

4.8. Initial rate experiment results 122

4.9. Further equilibrium experiments 127

4.10. Modelling the oxidation 128

4.11. Conclusion and future work 133

5. Experimental 136

5.1. General Experimental 136

5.2. Methodology development 138

5.3. Applications of the arylsilane oxidation 171

5.4. Mechanism 208

6. References 229

1. Introduction

For almost 50 years, the organosilane oxidation reaction has been widely used as an efficient method to prepare aliphatic alcohols in a highly stereospecific manner.[1] Despite the reactivity of arylsilanes towards oxidation, and the prevalence of phenols in many areas of chemical industry and research, this process has not been fully exploited for the synthesis of phenols. It has therefore been a recent focus of research in our group to use and develop arylsilane oxidation towards phenol synthesis.

1.1. The prevalence of phenols

Phenols are widespread throughout the natural world with plant polyphenols often described as the most common secondary metabolite in plants.[2] These natural phenols exhibit great structural diversity, from the cresols to the tannins (see *p*-cresol **1** and castalagin **2**, Figure 1.1).[3-4] The chemical properties of the phenol motif can be used to explain many complex natural phenomena including natural pigments and flavours.[5-7] For example, the phenol-stabilised system of double bonds in cyanidin **3** (Figure 1.1) is responsible for the colour observed from this pigment and contributes to the deep red bloom of roses. Meanwhile the gingerols **4** are responsible for the spicy flavour of ginger.[7]

Many naturally occurring phenols are bioactive and have been used for centuries as medicines. (–)-Epigallocatechin **5** is responsible for the medicinal properties of green tea and is now

understood to promote human health through its antioxidant properties. Phenolic antioxidants are able to quench reactive peroxyl radical species (ROO•, Figure 1.1) by hydrogen atom transfer. The radical is thereby 'trapped' within the phenolic compound and the following rapid peroxyl and aryloxyl radical recombination removes the damaging species which can otherwise cause harm to biological systems. Uninhibited peroxyl radical is reported to be implicated in a variety of degenerative diseases such as cancer and heart disease.[8] Thus, many naturally occurring phenols are currently being tested for their potential anti-cancer properties, such as resveratrol **6**.

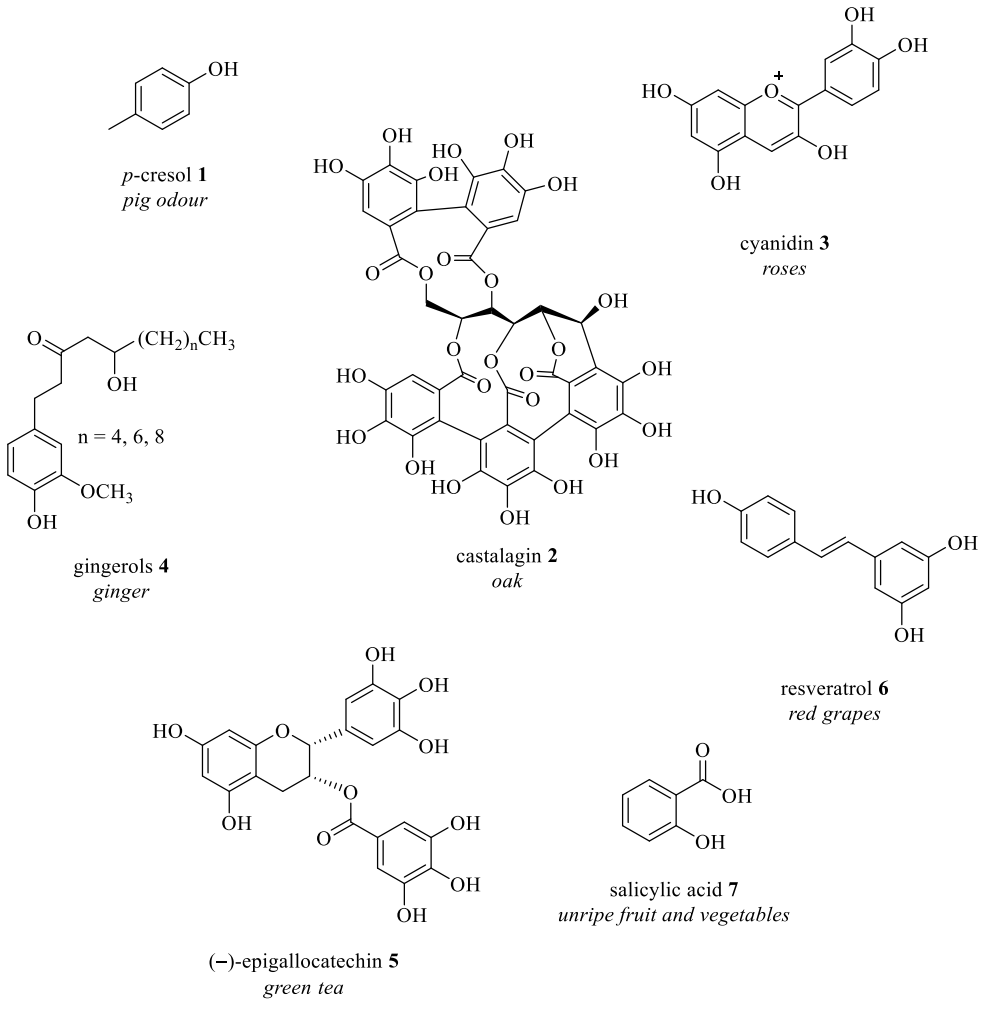


Figure 1.1: Naturally occurring phenols

Salicylic acid **7** has been used for thousands of years to treat fevers and pain, despite the gastrointestinal irritation which can occur after long-term use of the compound. In 1895, Felix Hoffmann discovered that the acetylated derivative of salicylic acid, aspirin, could be ingested by the human body without irritation.[9] The strength of the medicine was not affected, and aspirin is now believed to be the most widely used pharmaceutical drug in the world. It was later discovered that, as a result of decomposition of the molecule to salicylic acid in the stomach, liver and blood after ingestion, the drug remained effective yet innocuous.

The most common industrial use of phenols is in the preparation of polymers for plastics.[10] One of the first synthetic polymers was prepared through the reaction of phenol with formaldehyde. The resulting phenolic resin was commercialised by Leo H. Bakeland in 1907, under the trade name 'Bakelite', as a heat-resistant plastic.[8, 11] A vast array of phenol polymerisation has since been developed and applied to the preparation of adhesives, thermal insulation and electronics.[8]

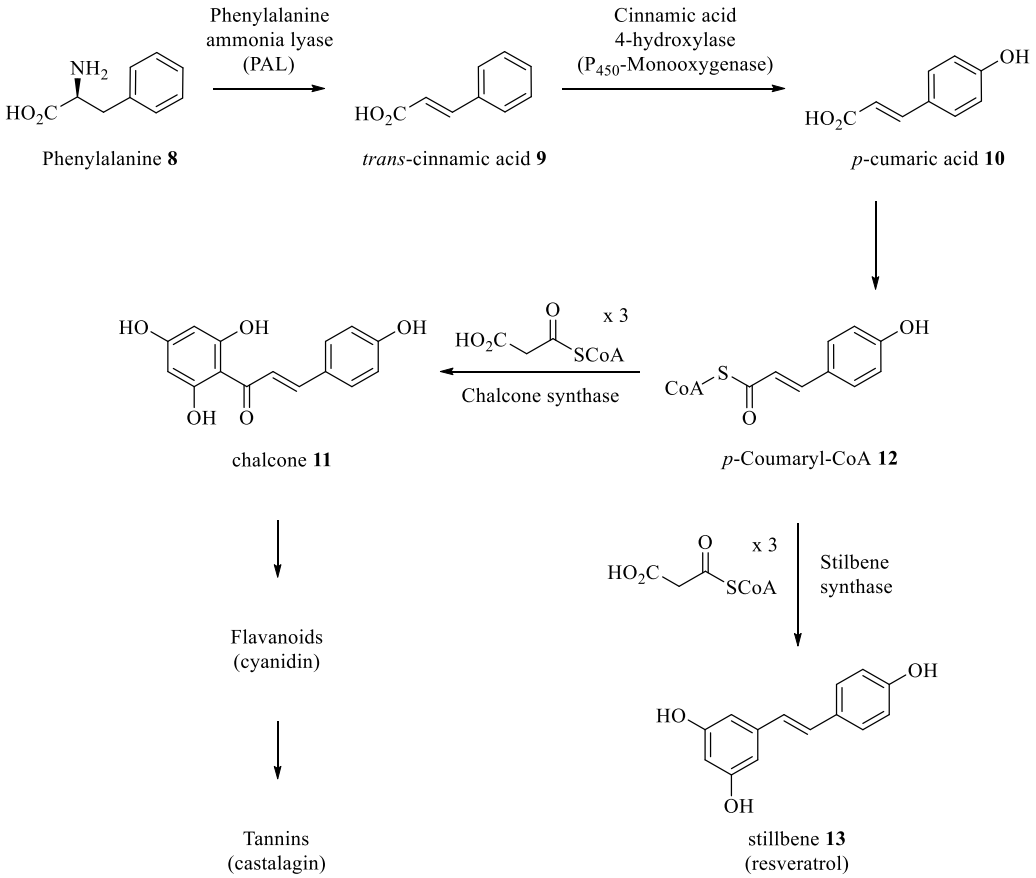
Naturally occurring phenols have been utilised in other industries, for example the complex tannin castalagin **2** is added to whisky *via* the oak barrels used to flavour the liquor. Although this tannin has not been isolated from the complex mixture of polyphenols present in final whisky products, its hydrolyzed derivatives have been identified and are believed to contribute to both the flavour and colour of whisky.[12]

1.2. The synthesis of phenols

1.2.1. Biosynthesis

As a motif so widespread in the natural world, it is not surprising that there are a number of metabolic pathways to the biosynthesis of phenols. Most plant phenolic compounds are derived from phenylpropanoids, which are in turn usually derived from the aromatic amino acid phenylalanine **8** (see *trans*-cinammic acid **9** and *p*-cumaric acid **10**, Scheme 1.1).

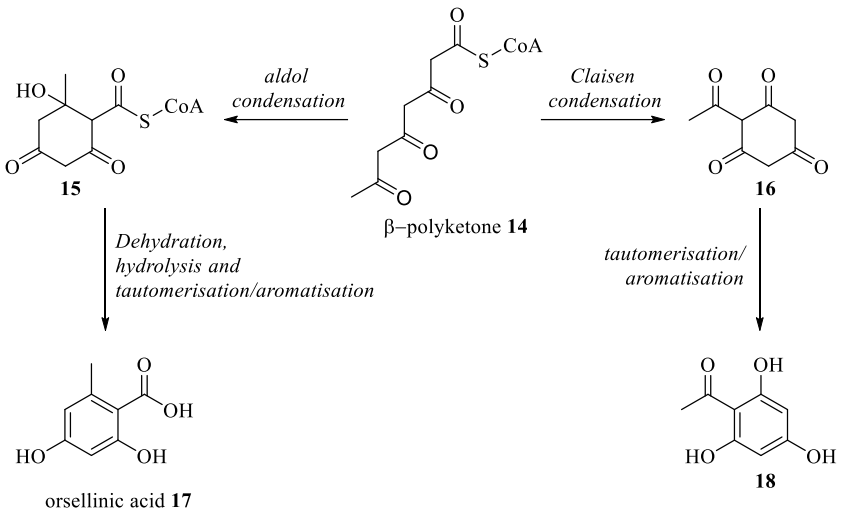
Phenylalanine **8** is synthesised in plants through the shikimate pathway.[13] Following deamination of phenylalanine, *trans*-cinammic acid **9** can be hydroxylated *via* a monooxygenase-catalysed reaction. Direct hydroxylation of aromatic compounds is observed in animals also, but the biosynthesis of aromatic amino acids is very limited, making the inclusion of plants in the diets of animals essential.[14-15] An additional aromatic ring is linked to the system, *via* malonic acid pathways, to produce chalcones (**11**), stilbenes (**13**), flavanoids and tannins as shown.



Scheme 1.1: Common phenolic biosynthetic pathways in plants

The malonic acid transformations are familiar to the organic chemist as classic carbonyl condensation reactions, and are utilised in bacteria and fungi for the synthesis of simple phenols (Scheme 1.2).[16] β-Polyketones such as **14** (which are products of condensation reactions of several molecules of acetyl-CoA) are common precursors to a large group of natural polyketides. During the biosynthesis of phenols, intramolecular aldol or Claisen condensations form highly oxygenated

6-membered rings **15** or **16** respectively. These intermediates are primed for aromatisation, through thermodynamically favourable tautomerization, to form phenols **17** and **18**.[16]



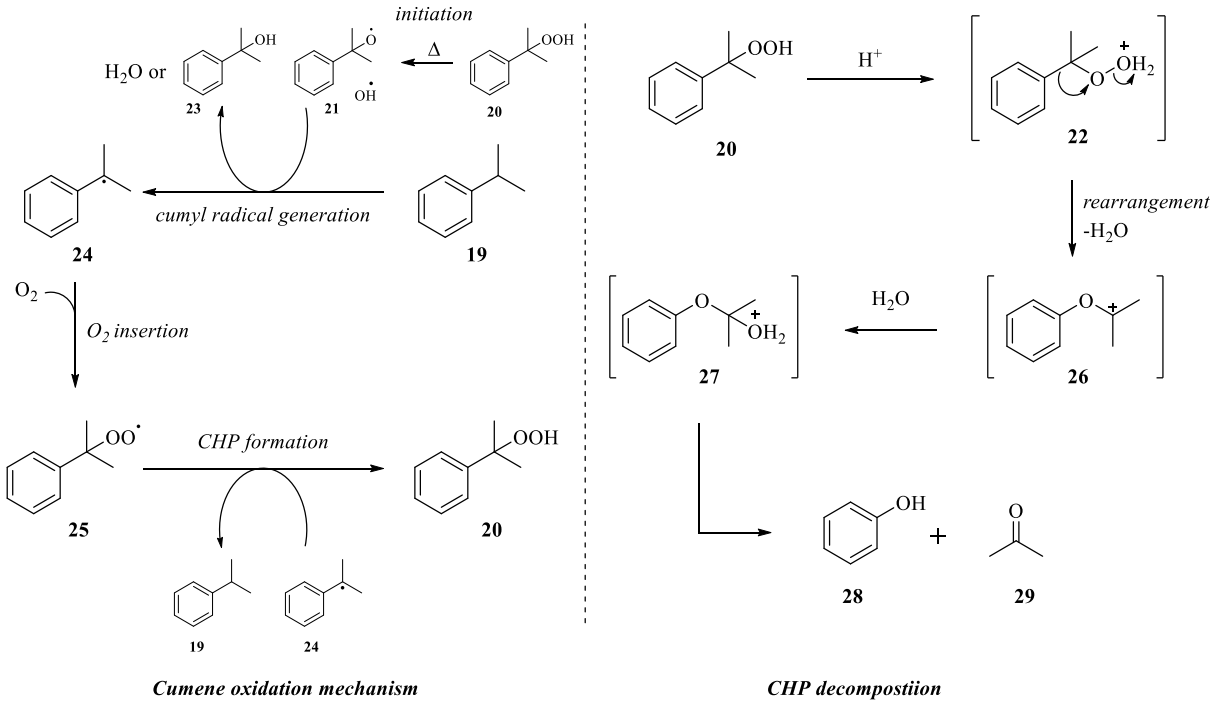
Scheme 1.2: Biosynthesis of phenols *via* polyketide condensation reactions

1.2.2. Chemical Synthesis

In 2008, the world-wide demand for phenol itself amounted to approximately 8.7 million tons. Of the world-wide production capacity at that time, 98.5% was based on the Hock process (Scheme 1.3). This process is based on the oxidation of cumene **19** to phenol **28** and was first discovered by Hock and co-workers in 1944.[17]

The Hock process begins with oxidation of cumene **19** to cumene hydroperoxide (CHP, **20**) which proceeds *via* a radical mechanism. Cumene itself has, most recently, been commercially produced from benzene and propylene using zeolite based catalyst systems.[18] Typically, a solution of CHP (**20**) and cumene (**19**), containing pH moderator sodium carbonate, is submitted to either transition metal catalysis or pressurized conditions. CHP is included in the initial mixture because it acts as an initiator in the radical mechanism (Scheme 1.3).[19] The radical products of cumene thermal decomposition (**21** and **HO**$^{\bullet}$) are able to abstract a hydrogen from cumene **19** to begin the oxidation to CHP. The product CHP (**20**) is explosive and cannot be concentrated. Instead, the

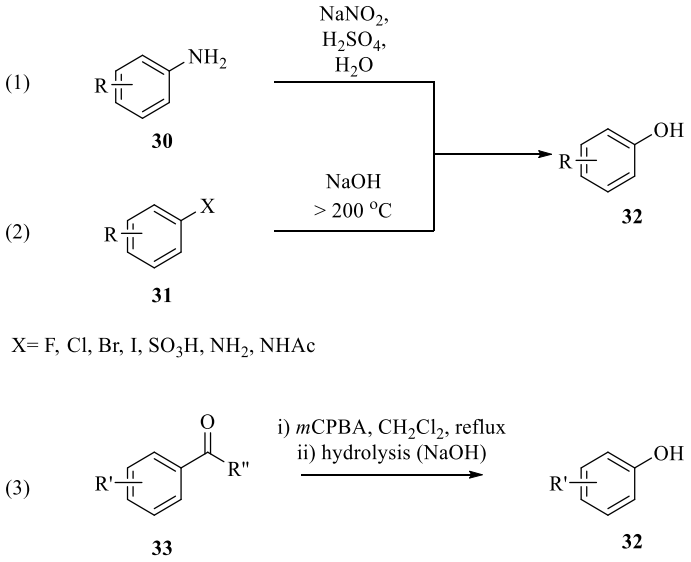
hydroperoxide is immediately exposed to an acid catalyst, in the presence of which rearrangement (intermediate **22**) and subsequent decomposition occurs.[8, 20]



Scheme 1.3: Cumene oxidation mechanism

The laboratory synthesis of phenols is of fundamental importance to the development of a number of areas of chemical research. Many pharmaceutical initiatives are centred on phenolic organic compounds and methods to prepare and test libraries of similar hydroxylated aromatic compounds are essential for progress in this area of research. The development of phenolic resins also requires efficient preparation of phenolic monomers.

Unfortunately, traditional methods of aromatic hydroxylation involve harsh reaction conditions towards which many functional groups are intolerant.[21] Scheme 1.4 highlights some typical methods of laboratory scale phenol synthesis. The difficulty of hydroxylating aromatic rings can be understood by the propensity of both hydroxyl groups and aromatic rings to behave as nucleophiles. Additionally, the stability of aromatic rings often renders the reactions thermodynamically unfavourable. Process (1), otherwise known as the Sandmeyer reaction, proceeds *via* a diazonium ion and aryl cation, to which water may attack.



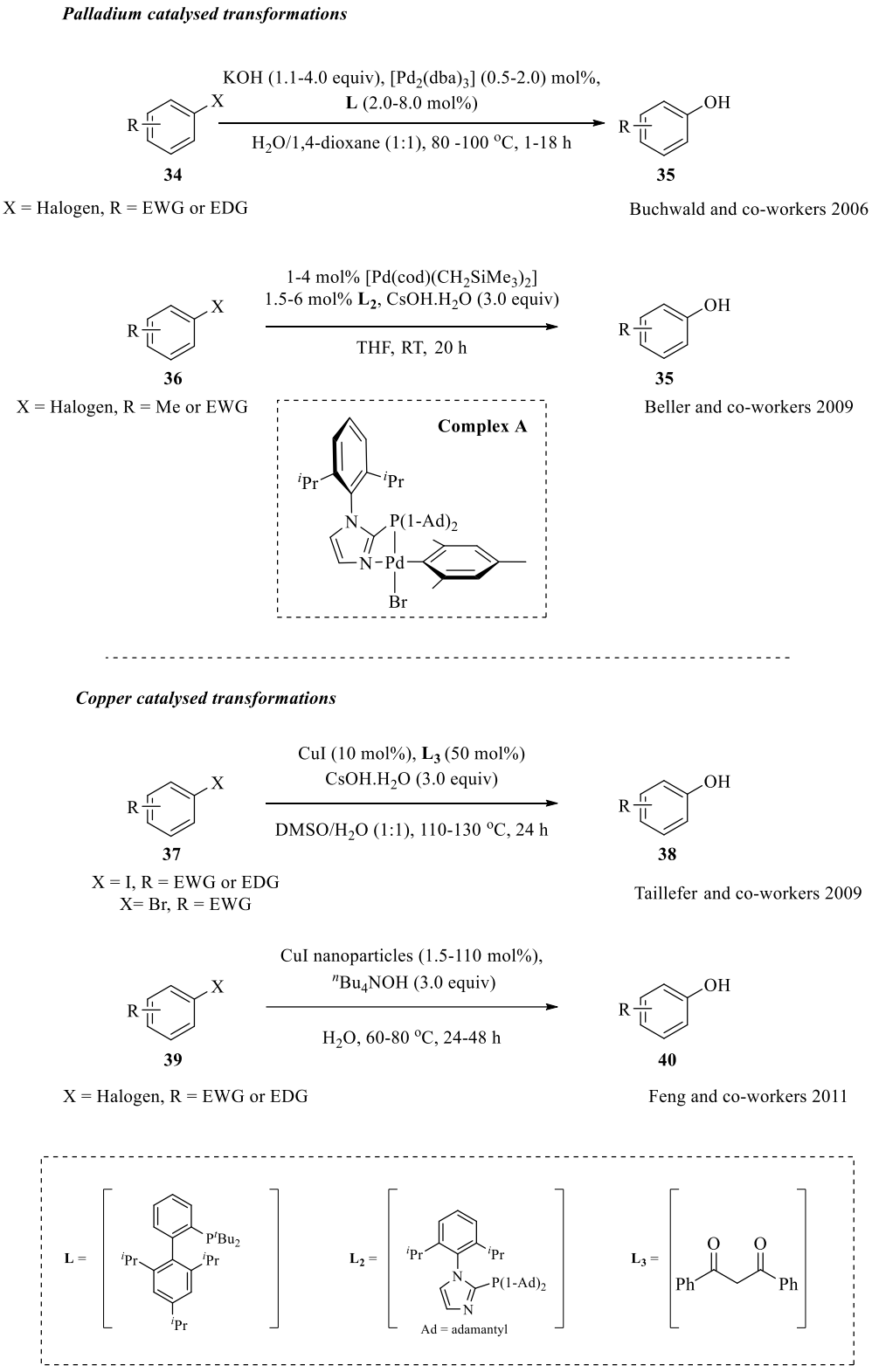
Scheme 1.4: Traditional methods of phenol preparation

The Baeyer-Villiger oxidation (also known as the Dakin oxidation for the synthesis of phenols) described in process (3) utilises the migrating group ability of aromatic rings. In the presence of a peroxyacid, aryl ketone **33** will undergo a 1,2 aryl shift to an O-acylphenol, which can undergo hydrolysis to phenol under standard conditions.[22-23]

Despite the forcing conditions described above, it was not until relatively recently that considerable improvements were made on these traditional methods. Through the development of enzymatic hydroxylation of aromatic compounds, impressive methods of selective hydroxylation have been demonstrated in recent work.[24] Alternatively, from the development of transition metal-catalysed oxidations of aryl halides, a great number of reports have appeared in the recent literature and have subsequently been reviewed.[25-27] Recent selected examples are shown in Scheme 1.5.[28-31]

A relatively early example of palladium catalysed oxidation was achieved by Buchwald and co-workers.[29] This system however, required high reaction temperatures and long reactions times. Although the hydroxylation of aryl bromides could be carried out at 80 °C, an increase in temperature to 100 °C was necessary to fully convert aryl chlorides to phenols. A subsequent system developed by Beller and co-workers could instead be carried out at room temperature and represents one of the mildest systems in the literature, although it is limited by an exotic catalyst

and ligand combination.[28] Within this work, the oxidative addition **complex A** was successfully isolated and characterised.

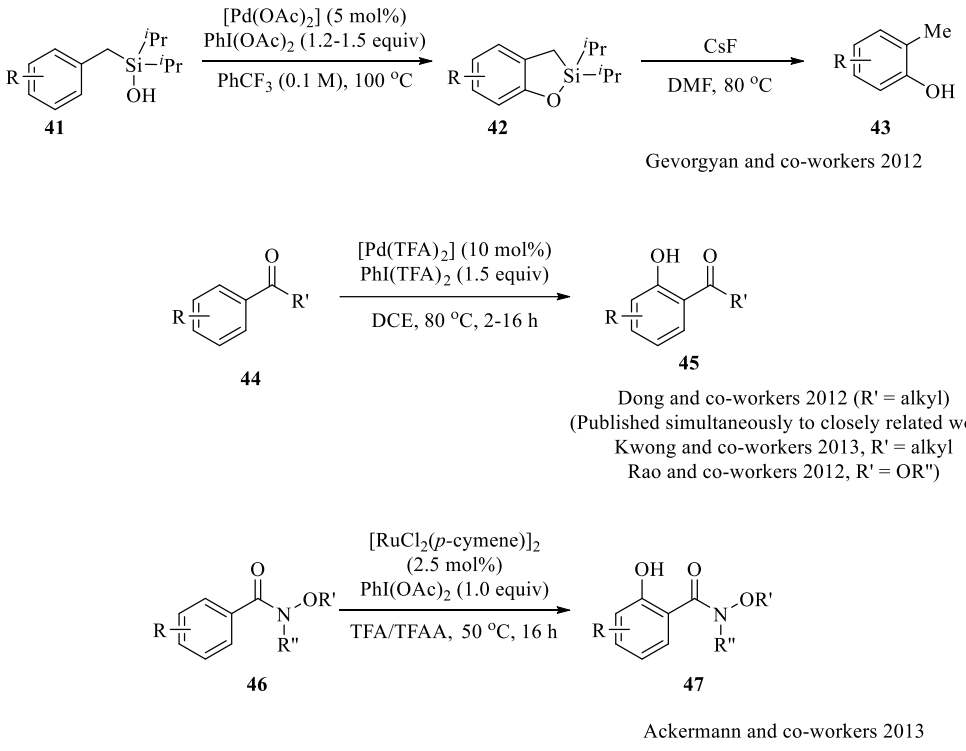


Scheme 1.5: Metal-catalysed synthesis of phenols from aryl halides

When an attempt to isolate the following hydroxo complex was made, within 20 minutes full conversion to phenol at room temperature was observed, demonstrating extremely rapid C–O bond formation (*via* reductive elimination) and explaining the reactivity of this catalyst system.

Of the copper catalysed systems also developed, nanoparticles have been employed (see Scheme 1.5), in addition to many further examples which include microwave chemistry and aqueous media.[32-36] There have also been attempts to develop iron-catalysed hydroxylation of aryl halides, however these methods may in reality be mediated by copper impurities in the system.[27, 37]

Following the success of aryl halide hydroxylation reactions, direct arene C-H oxyfunctionalisation has also been developed. The most successful reports have relied on a directing group substituted *ortho* to the activation site, or, as in the work of Gevorgyan and co-workers, the oxygenating agent has been substituted at a pendant position (substrate **41**, Scheme 1.6).[38-41]



Scheme 1.6: C-H activation and phenolation

Very recent work utilised carbonyl functional groups (useful synthetic handles) to direct palladium or ruthenium catalysed hydroxylations.[42-46] The work of Ackermann and co-workers included

mechanistic studies which suggested that C–H activation was irreversible and kinetically relevant. Additionally, through $LiAlH_4$ reduction of the hydroxylated products, *ortho*-hydroxylated benzaldehydes were easily accessed, which improved the synthetic utility of the methodology further.

Efforts have been made with palladium, copper and iron catalysts to hydroxylate aromatics in the absence of a directing group, however, these reactions currently still exhibit low selectivity.[27, 47]

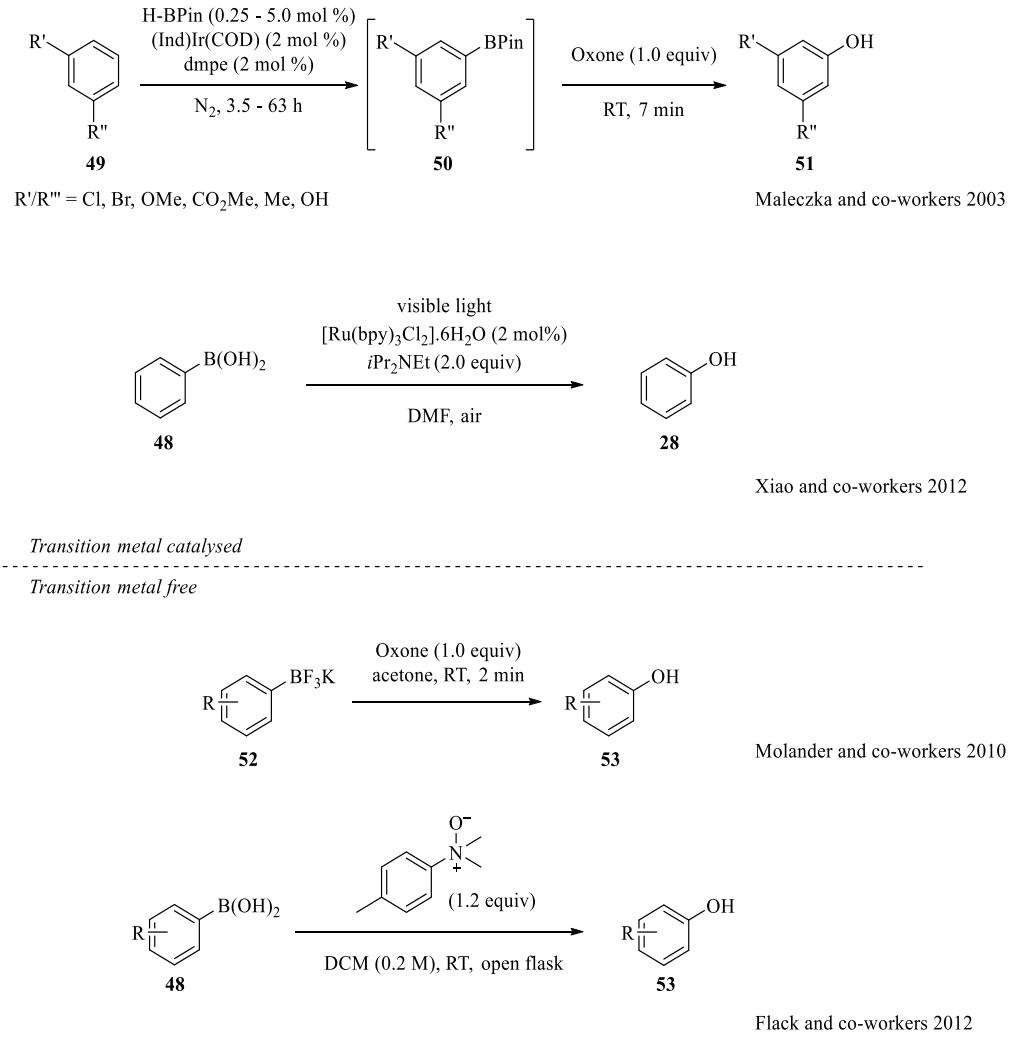
1.3. Latent phenols

Despite the impressive development of transition metal catalysed methods for the synthesis of phenols, nearly all systems so far discussed are limited by harsh reactions conditions and a lack of functional group tolerance. If used during multi-step syntheses of complex phenolic compounds, these hydroxylation reactions would have to take place at an early stage to avoid cleavage of any labile moieties within the compound, greatly inhibiting synthetic flexibility. In the synthesis of polyphenols, it would be preferable for hydroxyl groups to be introduced sequentially in a synthesis, so that each phenol may be differentiated where necessary. Additionally, the mesomerically electron donating nature of oxygen, when substituted to an aromatic ring, increases the reactivity (and therefore, instability) of the arene and ideally would be introduced at a late stage in a complex synthesis. A synthetic strategy that addresses these wishes may be found in the form of a phenol surrogate. Ideally, this would be a species which can be easily introduced, is inert to many chemical reagents and could thus be carried through a synthetic sequence before late stage oxidation under mild conditions.

Arylboron and arylsilane derivatives offer a potential realisation of this vision. The former is well established in the literature and examples of transition metal catalysed processes are shown in Scheme 1.7.[48] The ground-breaking C-H activation/borylation sequence from aryl halides (Scheme 1.7), developed by Maleczka and co-workers, allowed exclusively *meta*- substituted phenols to be

prepared.[49] More recently, an arylboronic acid oxidation was developed with the use of visible light, and this process was also later adapted under electrolytic conditions (Xiao and co-workers).[50-51]

The transition metal free oxidation of arylboronic acids has also been successful (Scheme 1.7). After the use of Oxone® as a rapid and efficient oxidant was reported by Levy and co-workers, a powerful latent phenol system was developed by Molander and co-workers.[52-53] Aryltrifluoroborate salts were found to convert to phenols in high yields and an impressive range of substrates were successfully oxidised within this work, including electron-rich and electron-deficient arenes, heteroaromatics, vinyl and alkyl substrates.



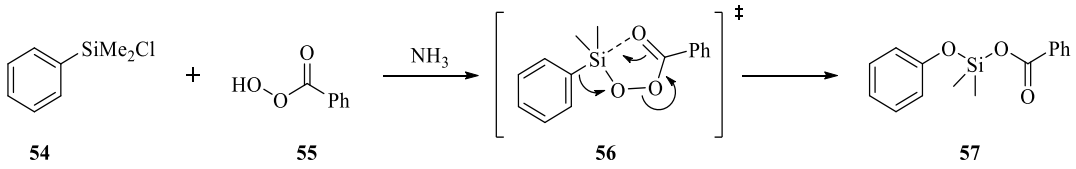
Scheme 1.7: Oxidation of arylboranes

The need for corrosive reagent KHF_2, for the preparation of trifluoroborate salts, was a drawback to this process until recently when an improved procedure using KF and tartaric acid was reported.[54] Most recently, *N*-oxides have also been utilised for the fast oxidation of boronic acids.[55]

The oxidation of arylborane derivatives has been established as an efficient route to phenols. The polar intermediates however, limit their use as latent phenols. Arylsilane compounds potentially present a complementary alternative. Silyl groups can easily be introduced to aromatic rings and display very low toxicity. Additionally, arylsilanes have been found to be stable to a variety of chemical conditions, especially through their use as protecting groups.

1.4. The Kumada-Tamao oxidation

An early report in 1958 of a 1,2-aryl shift of silicon to oxygen by Davies and co-workers can be considered as the first report of an arylsilane oxidation (Scheme 1.8).[56]



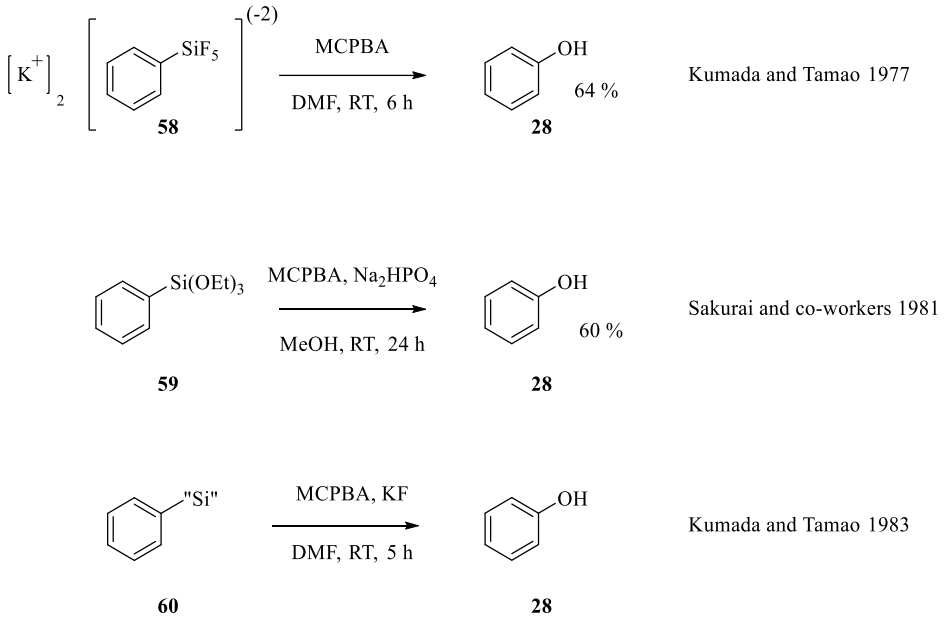
54 **55** **56** **57**

Scheme 1.8: 1,2 silicon to oxygen aryl shift reported by Davies and co-workers

During an attempt to prepare peroxysilanes, alkylsilylperbenzoates (**56**) in particular were found to decompose to the corresponding alkoxysilyl benzoates (**57**). Notably, the phenyl group migrated in preference to the methyl group.

Some twenty years later, Kumada and Tamao reported an *m*CPBA oxidation of pentafluorosilanes **58**, which included an example of phenol formation (Scheme 1.9).[57] The reaction performed best in DMF, and reasonably good yields were obtained over a range of organosilanes.[57] The reaction was also studied by Sakurai and co-workers, who found that triethoxysilanes **59** would oxidise in methanol with *m*CPBA and sodium hydrogen phosphate.[58] Interestingly, the NMR chemical shifts

of the silicon centres (**59**) indicated a similarly low charge density to the organopentafluorides (**58**) that had previously been reported. This suggested to the authors that an electron deficient silicon was responsible for the success of the oxidation. During the following years, the oxidation was developed by Kumada and Tamao and a variety of silicon derivatives were found to be suitable for oxidation.[59-60] During this time, the rate increasing effects of KF were discovered, in addition to the stereospecific nature of the oxidation.



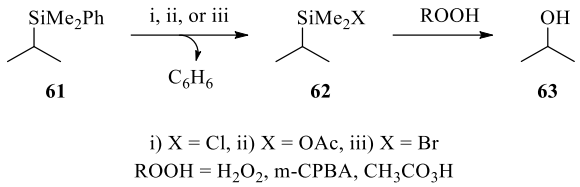
58 **28** **59** **28** **60** **28**

"Si" = SiF_3 (no KF added), $SiMe_2F$, $Si(C_8H_{17})_2Cl$, $Si(C_8H_{17})_2F$, $Si(C_8H_{17})_2OEt$

Scheme 1.9: Kumada oxidation of pentafluorosilicates

The use of *hydrogen peroxide* as an oxidising agent was subsequently optimised by Tamao and co-workers until the classic conditions, recognised today as Tamao oxidation conditions, were settled upon. Initially, this work was limited to alkylsilane substrates.[61-65]

The prolific work of Fleming and co-workers took place concurrently with these investigations. The main aim of this research was to prepare chiral alcohols from enantiopure alkylsilanes; this work therefore was never intended for the preparation of phenols. Phenyldimethylsilane was presented as a masked hydroxyl group, but the phenyl group would be removed *via* an *ipso*-substitution reaction before formal oxidation was carried out (Scheme 1.10).[66-67]



Scheme 1.10: The Fleming Oxidation. Reagents Conditions: (i) HCl (gas), $CHCl_3$, RT, 22.5 h; (ii) $Hg(OAc)_2$, (1.0 equiv), CH_3CO_3H, RT, 4 h; (iii) Br_2 (1 M in acetic acid, 0.5 equiv), CH_3CO_3H, 0 °C, 5 h.

The synthesis of phenols from arylsilanes was published some years later by Tamao and co-workers, alongside a mechanistic investigation into the reaction. The conditions which had previously been optimised by the authors were successfully applied to a range of arylfluorosilane substrates (Scheme 1.11).[68] Oxidation of all substrates was observed under these conditions. $PhSiMeF_3^-$ was even found to oxidise in the absence of a fluoride source, however $PhSiMeF_2$ would not oxidise without fluoride activation. Substrates were also tested with varying substitution to the aromatic ring and a rate dependence on electron density of the arene was observed.

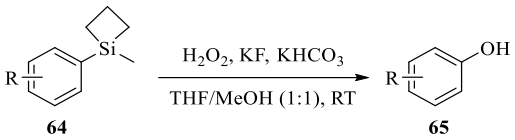


Scheme 1.11: Tamao arylsilane oxidation

Within this publication, Tamao highlighted the need for at least one heteroatom to be substituted on silicon for oxidation to occur. This condition, and the need of a fluoride source for most silicon substrates, was repeatedly corroborated by subsequent reports and developments of the Tamao and Fleming oxidations.[69]

Further examples of arylsilane oxidations have been sporadic. Some cases have exploited the reactivity of arylsilanes to prepare aliphatic alcohols, including work produced by Molander and co-workers.[70] Through a hydrosilylation/oxidation sequence, alkenes were converted to their homologated alcohols. Phenols, however, were not isolated from these reactions. Similarly, Simitrovich and co-workers developed a base catalysed oxidation of alkylsilanes with phenyl substituted silicon centres.[71]

During studies on the oxidation of siletanes by Dudley and co-workers (**64**, Scheme 1.12), a number of phenols were prepared.[72] As an alternative to electronegative heteroatom substitution to silicon, this methodology exploited the reactivity of siletanes.



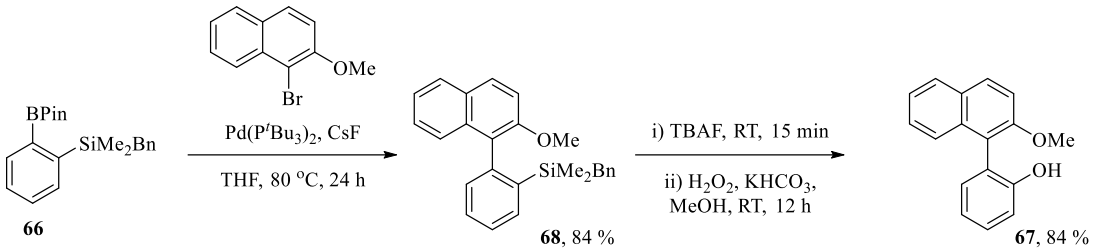
64 **65**

R = Me, OMe, Ph, CF_3 Dudley and co-workers, 2003

Scheme 1.12: Oxidation of strained siletanes

Siletanes possess 'strain release' Lewis acidic properties, which allows them to react under the Tamao oxidation conditions normally reserved for fluorosilanes. Although successful, a limited number of phenols were prepared. The chemistry has since been used in the context of novel protecting groups which can be removed under Tamao oxidation conditions.[73-74]

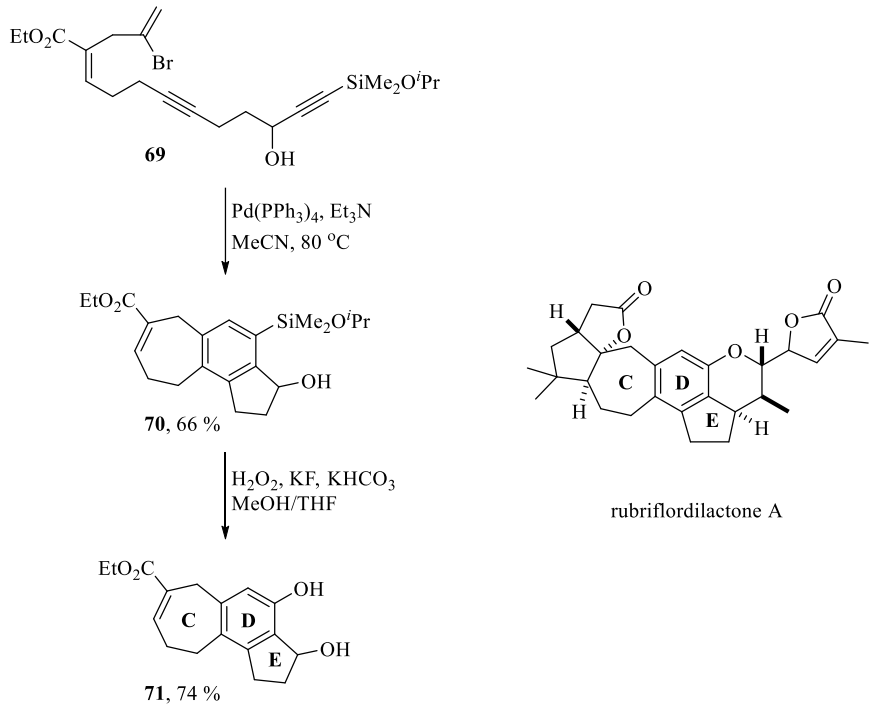
Further isolated examples of phenol synthesis through arylsilane oxidation exist but are limited to studies which are focused on the synthesis of arylsilanes. In these cases, an oxidation is only carried out as proof of the synthetic utility of arylsilanes and throughout nearly all these systems, a heteroatom was substituted to the silicon centre and a fluoride source was used to promote the reaction.[75-77] For example, a recent study into the orthogonal reactivity of arylboranes and arylsilanes included a final Tamao oxidation to prepare polyaromatic **67** (Scheme 1.13).[78] After a Suzuki-Miyaura coupling, arylsilane **68** was activated *via* hydrolysis of the 'safety catch' benzylsilane group. In the presence of TBAF, benzylsilanes have been found to reveal the more reactive silanols, through which oxidation may occur.[79] Additional isolated examples of oxidation in the absence of a fluoride source can be found but in each case the silicon centre is substituted with fluorine.[80-81]



Ihara and co-workers, 2009

Scheme 1.13: Orthogonal arylboranes and arylsilanes

Recent studies by Cordonnier within our group represented the first use of arylsilanes as latent phenols in multi-step synthesis (Scheme 1.14). During studies towards the total synthesis of rubriflordilactone A, an *iso*-propoxysilyl acetylene was installed on alicyclic substrate **69**, which produced arylsilane **70** through a palladium-catalysed cascade transformation. The subsequent oxidation installed a hydroxyl group, mirroring the natural product's CDE ring system.[82]

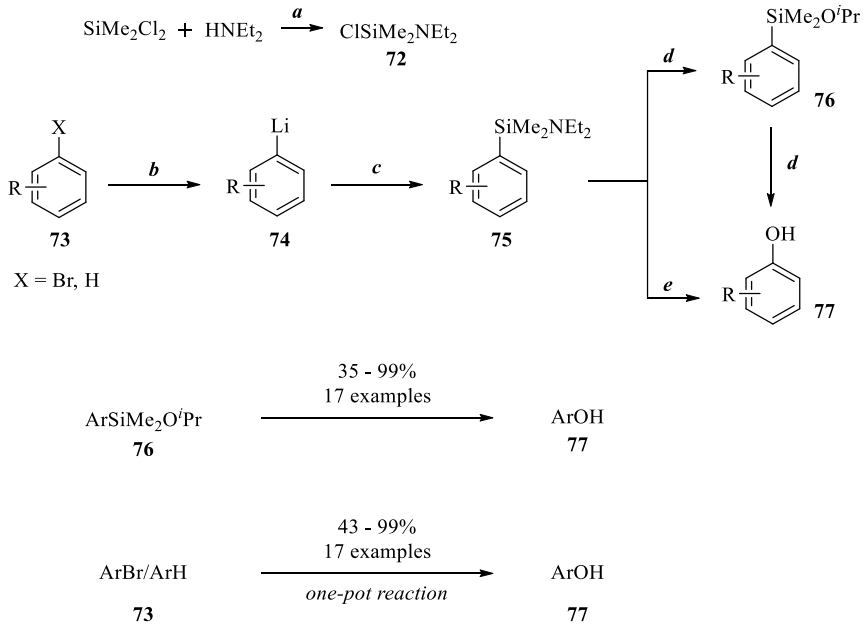


Scheme 1.14: Latent phenol synthesis

1.4.1. "New routes to hydroxylated aromatics"

Following the success of this approach, a detailed study of the oxidation of *iso*-propoxysilanes was carried out by Bracegirdle within our group.[83] This work represented the first general synthesis of phenols from arylsilanes and included the development of efficient methods to prepare arylsilanes.

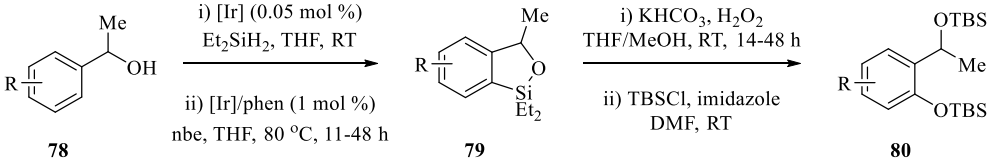
Chloroaminosilane **72** was used to introduce silicon to aromatic substrates, and was easily prepared on a multigram scale from dichlorodimethylsilane and diethylamine. After either bromine-lithium exchange or directed *ortho*-metallation (D*o*M) of an aromatic substrate, chloroaminosilane **72** underwent only a single addition of aryllithium species **74** at low temperature to form aryl amino silane **75**. This species was then primed for either isolation as the isopropoxyaryl silane **76**, or direct oxidation to phenol **77** in a one pot procedure. Isopropoxysilane (**76**) was chosen as the most suitable "latent phenol" group under the belief that it would remain untouched under most chemical conditions, that it would be stable to column chromatography but also would display sufficient reactivity towards oxidation.



Scheme 1.15: Directed phenolation methodology. Reagents and conditions: (a) NEt_3 (1.1 eq), THF, 0 °C, $HNEt_3$ (1.0 eq) added over 2 h then stirred for 16 h (b) *n*- or *t*-BuLi (1.2–2.0 eq), THF, -78 °C, 2 h; (c) **72** (1.4 eq) (d) *i*-PrOH (excess), DMAP (cat), rt, 16 h; (e) $KHCO_3$ (2.0 eq), TBAF (0.1–2.0 eq), H_2O_2 (6.0 eq), MeOH/THF (1:1), rt, 16 h.

The synthesis of arylsilanes was successful over a range of substrates, including electron rich and electron deficient arenes and a heteroaromatic substrate. The subsequent oxidation was also carried out in excellent yield for most substrates, both through the one-pot reaction (**73** -**77**) and the oxidation of arylisopropoxysilanes **76**. Notably, the optimised conditions required only a sub-stoichiometric amount of the fluoride source, TBAF (0.1 equiv), which improved the efficiency and functional group tolerance of the transformation. It was observed within this work that the oxidation could proceed in the absence of *any* fluoride source. However, the reaction rate was greatly reduced under these conditions, and the addition of 0.1 equivalents of TBAF was considered a reasonable price to pay for significantly improved reactivity. Overall, this methodology provided a previously unattainable degree of synthetic flexibility. Hydroxyl groups could now be introduced to an aromatic compound in a relatively mild and regiocontrolled manner and potentially carried through many synthetic steps as latent phenols.

Following this work, a C-H activation/silylation/oxidation sequence was reported by Hartwig and co-workers (Scheme 1.16). After iridium catalysed C-H activation *via* a pendant hydroxyl group, the product cyclic alkoxysilane could be oxidised in the absence of any fluoride source.[84]



78 **79** **80**

Scheme 1.16: Sequenced silylation/oxidation procedure

This work corroborated the results within our group that a fluoride source was not essential to the oxidation. The length of time needed for full conversion of each substrate was not reported, instead a range of 14-18 h was given.

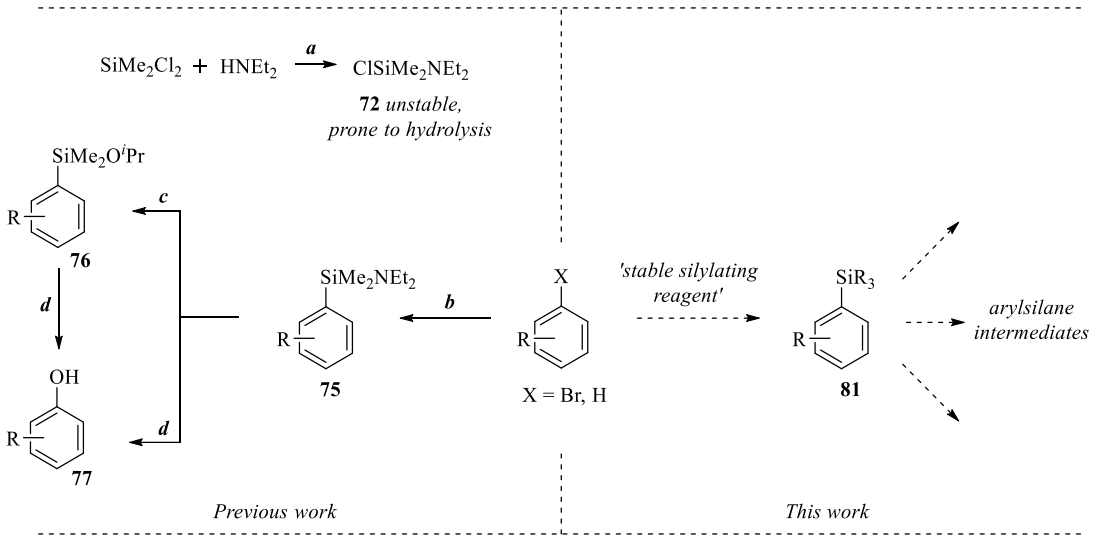
1.5. Thesis summary

Following the establishment of a general method for the synthesis of phenols from arylsilanes, the methodology was further developed in terms of generality and practicality and has since been published (Chapter 2).[85] It was our hope that this methodology could be applied to the synthesis of pharmacologically important natural phenol compounds. The success of this endeavour is described in Chapter 3, alongside efforts to adapt the methodology to protecting groups, cycloadditions and flow chemistry. Finally, some detail of the mechanism of the arylsilane oxidation, which had intrigued our group for some time, was revealed through a series of studies using NMR spectroscopic techniques and is described in Chapter 4.

2. Methodology Development

2.1. Introduction

Despite the success of the methodology developed by Bracegirdle, it was felt that the procedures were limited by the use of silylating reagent chloroaminosilane **72**. Although the reagent was ideally suited to the one-pot silylation/hydroxylation of aromatics, it was difficult to prepare arylsilane derivatives beyond isopropoxysilane **76** through arylaminosilane **75**.

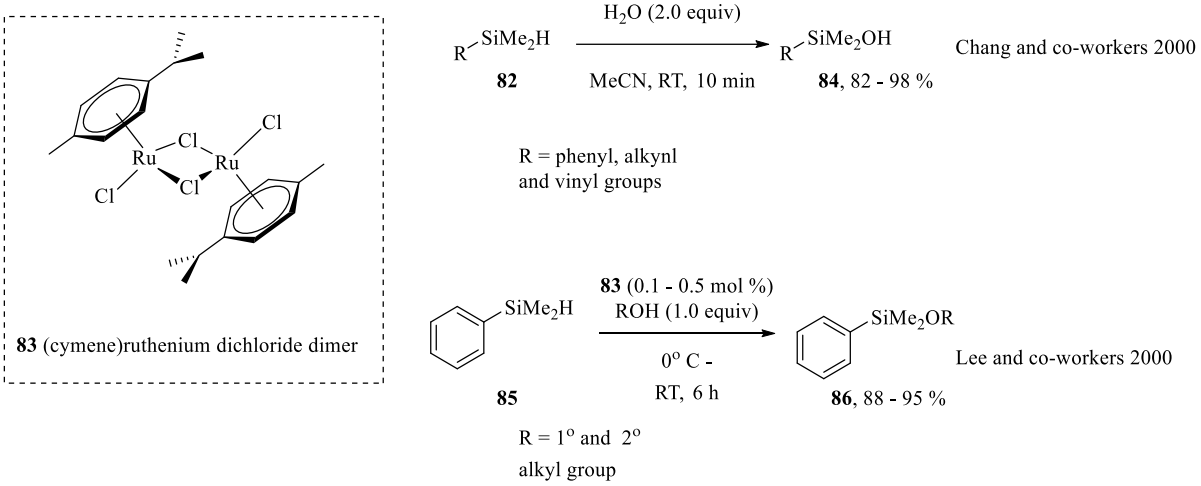


Scheme 2.1: Directed phenolation methodology. Reagents and conditions: (a) NEt_3 (1.1 eq), THF, 0 °C, $HNEt_3$ (1.0 eq) added over 2 h then stirred for 16 h; (b) *n*- or *t*-BuLi (1.2–2.0 eq), **72** (1.4 eq), THF, –78 °C, 2 h; (c) *i*-PrOH (excess), DMAP (cat), RT, 16 h; (d) $KHCO_3$ (2.0 eq), TBAF (0.1–2.0 eq), H_2O_2 (6.0 eq), 1:1 MeOH/THF, rt, 16 h.

Additionally, although reagent **72** could be prepared in house in multi-gram quantities, it would begin to hydrolyse within days despite storage under argon at a reduced temperature. Thus a less

sensitive silylating reagent was sought which could also begin an efficient route to a more diverse range of arylsilanes.

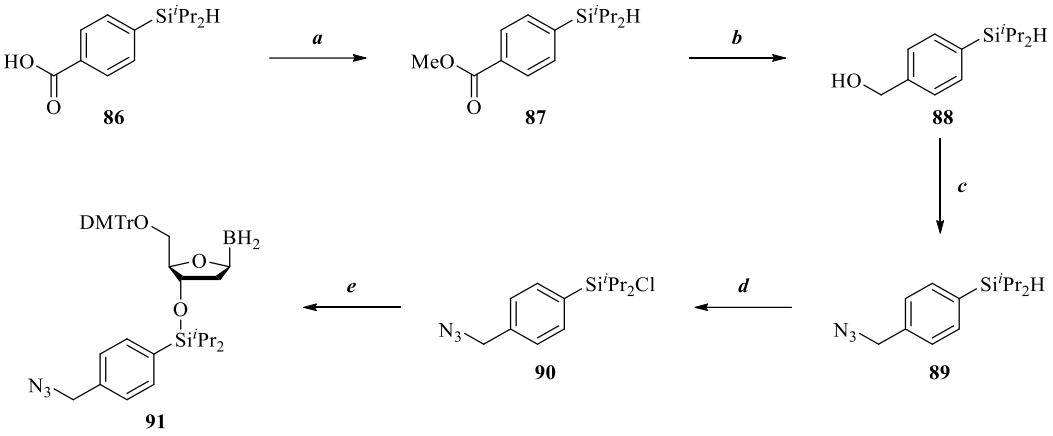
The work of Chang and co-workers and the subsequent studies by Lee and co-workers prompted us to consider preparing aryl*hydro*silanes (**82**) as intermediates (Scheme 2.2).[86-88]



Scheme 2.2 Ruthenium catalysed silanol synthesis

Ruthenium catalyst **83** was found to display impressive efficiency in activating Si–H bonds. During the synthesis of silanols **84**, complete conversion was observed in 10 minutes for a variety of substrates. Lee and co-workers were able to conduct the dehydrogenation reactions at a low loading of 0.1 mol%, though this may well have lowered the rate of reaction.

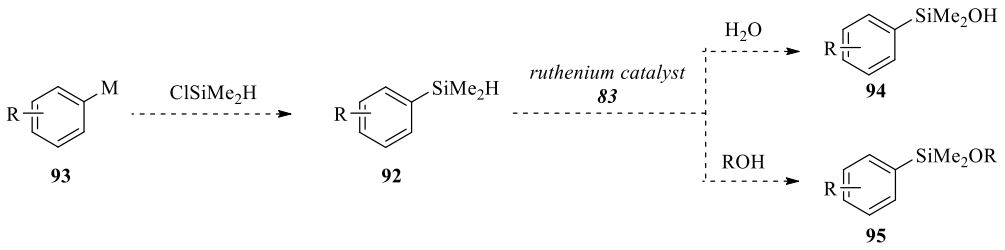
When considering arylhydrosilanes as intermediates in the synthesis of oxidation substrates, we were pleased to discover evidence in the literature of their stability to many chemical conditions. Examples of organometallic reactions and redox processes in the presence of arylhydrosilanes were found during which the Si–H bond remain untouched.[89-93] We were particularly pleased to find an example of an arylhydrosilane carried through a multi-step synthesis (Scheme 2.3). Sekine and co-workers prepared 3'-terminal deoxyribonucleoside-loading reagents which contained silyl-type linkers for introduction onto a polymer support, using relatively inert arylhydrosilanes for much of the synthesis.[89]



Scheme 2.3: An arylhydrosilane carried through multi-step synthesis. Reagents and conditions: a) 5% H_2SO_4, MeOH, reflux, 1 h, 76%; b) $LiAlH_4$, THF, RT, 15 min, 85%; c) CBr_4, Ph_3P, NaN_3, DMF, RT, 12 h, 78%; d) 1,3 dichloro-5,5-dimethylhydantoin, CH_2Cl_2, RT, 2 h; e) 5'-*O*-DMTr-Th, CH_2Cl_2, RT, 2h, 93%.

Within this synthesis, hydrosilane **89** was successfully converted to chlorosilane **90** to facilitate silylether formation, only after the necessary functional group transformations elsewhere in the molecule had taken place.

It was hoped that after preparing arylhydrosilanes (**92**, Scheme 2.4), many arylsilane derivatives would be available to us through the ruthenium catalysed systems described above. We were hopeful that this hydrosilane would be much easier to handle than the previously described arylaminosilanes **75** (Scheme 2.1). The commercial availability, low cost and stability of silylating reagent $ClSiMe_2H$ were also appealing; it was thought that this would significantly increase the attractiveness of the methodology to the synthetic community.



Scheme 2.4: Summary of intended arysilane synthesis

As discussed in Chapter 1.4, an electronegative substituent on silicon was believed to be essential to a Tamao-Kumada oxidation. Commonly, a fluoride source was also thought necessary to

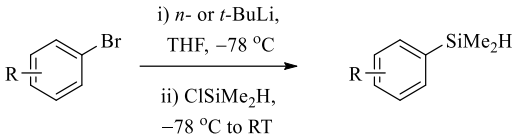
activate the silicon towards oxidation. We hoped that with the range of arylsilanes available to us through the reactions described above, we would be able to test these assumptions through attempted oxidations of all arylsilanes prepared. We were particularly interested in the possible oxidation of arylhydrosilanes **92**. Although trisubstituted hydrosilanes lack an electronegative substituent to promote nucleophilic attack at silicon, an isolated example of alkylhydrosilane oxidation did exist (reported by Tamao and co-workers).[61] This suggested that oxidation of arylhydrosilanes **92** might be successful and that the full potential of the Tamao-Kumada oxidation was still to be unlocked.

2.2. Synthesis of arylsilanes

Our study began with the synthesis of arylhydrosilanes. We hoped to synthesise a range of arylsilanes which would allow us to test the oxidation reaction both in terms of electronic and steric effects.

2.2.1. Butyllithium chemistry

The majority of our arylhydrosilanes substrates were prepared *via* lithium/halogen exchange of aryl bromides.[94] Although butyllithium reagents are limited by their need for stoichiometric loading and cryogenic moisture free conditions, they have been used to great effect in previous work within the group and throughout organic chemistry.[83] Full conversion of all aryl halides listed in Table 2.1 was observed following a brief optimisation of lithiation time. Notably, only when bromine/lithium exchange was left for two or more hours were many substrates fully converted. Additionally, substrates with electron-rich aromatic rings generally required the stronger reagent, *t*-BuLi (see Table 2.1).



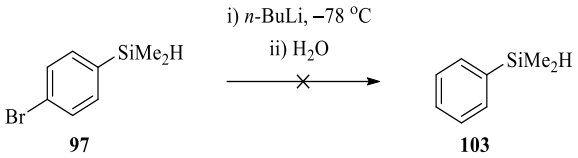
Entry	R (σ value)	*n*- or *t*-BuLi	Time given for lithiation	Product	Yield of hydrosilane (%)
1	4-CF_3 (0.43)	*n*-BuLi	2 h	**96**	52
2	4-Br (0.23)	*n*-BuLi	3 h	**97**	89
3	3-OMe (0.12)	*t*-BuLi	30 min	**98**	81
4	4-F (0.06)	*n*-BuLi	3 h	**99**	67
5	4-Me (-0.17)	*n*-BuLi	2 h	**100**	80
6	4-OMe (-0.27)	*t*-BuLi	40 min	**101**	85
7	4-NMe_2 (–0.83)	*t*-BuLi	2 h	**102**	84

Table 2.1 Synthesis of arylhydrosilanes *via* bromine/lithium exchange.

We were pleased to prepare successfully substrates that varied greatly in electron density, as described by the Hammett sigma constant shown in Table 2.1. Most substrates could be isolated in good yield from these reactions, with the exception of fluorinated substrates **96** and **99**. These products had relatively low boiling points and, although care was taken, it is possible that some product was lost during concentration *in vacuo* before vacuum distillation was carried out.

We had hoped that after bromine-lithium exchange of arylhydrosilane **97**, we would be able to quench the lithiated product with DMF and that an aldehyde could be afforded. This reaction was not successful, and subsequent studies on the reaction informed us that bromine-lithium exchange of compound **97** must be complicated by the Si–H bond, despite literature precedent to the contrary.[93] Even after a simple aqueous work up following bromine-lithium exchange, no evidence

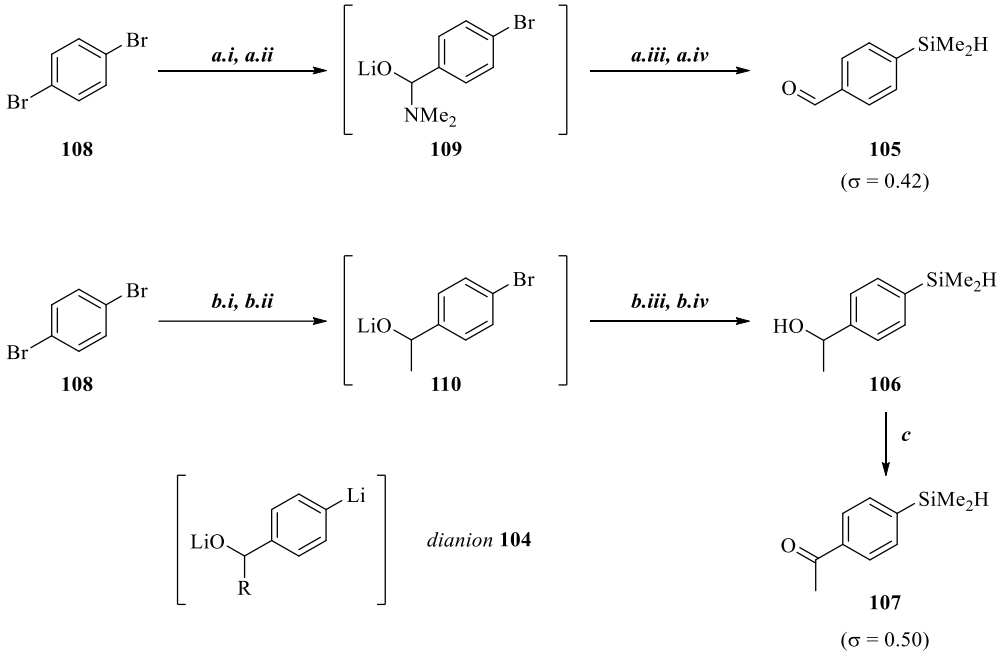
of arylhydrosilane **103** formation was found. One product that was observed from this reaction was seen to possess a symmetrical structure around the aromatic ring, which suggested that aryllithium addition to the hydrosilane may be occurring to produce a 1,4-disilyl product.



97 **103**

Scheme 2.5: Attempted bromine/lithium exchange of arylhydrosilanes X

Following the procedures of Kim and co-workers, the synthesis of electron deficient arylhydrosilanes was instead achieved *via* sequential one-pot bromine/lithium exchange of 1,4-dibromobenzene **108** (Scheme 2.6).[95]



108 **109** **105** (σ = 0.42)

108 **110** **106**

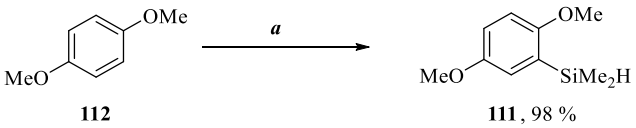
107 (σ = 0.50)

Scheme 2.6: Synthesis of electron deficient arylhydrosilanes. (a.i) *t*-BuLi (2.0 equiv) 1 h, THF –78 °C;(a.ii) DMF (1.1 equiv) 15 min; (a.iii) *t*-BuLi (2.0 equiv); (a.iv) $ClSiMe_2H$ (1.0 equiv), 59%; (b.i) *t*-BuLi (2.0 equiv), 1 h, THF –78 °C; (b.ii) Acetaldehyde (1.1 equiv), 30 min; (b.iii) *t*-BuLi (2.2 equiv) (b.iv) $ClSiMe_2H$ (1.3 equiv), 78%; c) SO_3.pyridine (3.0 equiv), DMSO (10.0 equiv), DIPEA (5.0 equiv), CH_2Cl_2, 1 h, RT, 97%.

Through the sequential lithiation described in Scheme 2.6, the otherwise reactive aldehyde and ketone products remained inert in their lithiated state, allowing dianion **104** to form. Subsequent

silylation proceeded selectively with the least stable organolithium bond and following work up, products **105** and **106** were isolated in reasonable yields of 54% and 78% respectively. A Parikh-Doering oxidation of benzylic alcohol **106** efficiently afforded ketone **107** in 97% yield. This provided a pleasing example of the stability of the arylhydrosilane group.

Directed *ortho* metalation (D*o*M) was employed to prepare slightly more complex hydrosilane **111**. Lithiation and subsequent silylation of 1,4-dimethoxybenzene **112** (Scheme 2.7) was repeatedly high yielding, and the 98% yield reported was carried out on a 60 mmol scale.[96-97]

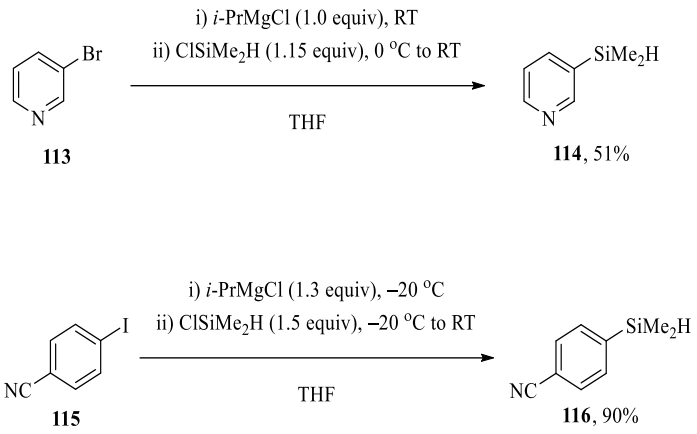


112 **111**, 98 %

Scheme 2.7: Synthesis of arylhydrosilanes *via* D*o*M. (a.i) *s*-BuLi (1.2 equiv), TMEDA (1.2 equiv), 2 h, –78 °C; (a.ii) $ClSiMe_2H$ (1.3 equiv), THF, –78 °C to RT, 98%

2.2.2. Grignard Reagents

It was hoped that the substrate scope could be expanded further with the use of Grignard reagents, specifically to access heteroaromatic and aromatic hydrosilanes of greater sigma (Hammett) values than those previously prepared. After comparison of literature conditions and a brief optimisation, 2-pyridyl silane **114** and arylnitrile silane **116** were prepared through their Grignard derivatives (Scheme 2.8).[98-100] The Grignard intermediate to nitrile substrate **116** was found to only be stable below –10 °C; above this temperature a drastic lowering of the final isolated yield was observed. In contrast, formation of the Grignard precurser to pyridyl silane **114** required temperatures above 0 °C; below this temperature Grignard formation was very slow and an insoluble solid formed. However, once conversion to the organometallic had occurred the chlorosilane quench was performed at 0 °C.



113 **114**, 51%

115 **116**, 90%

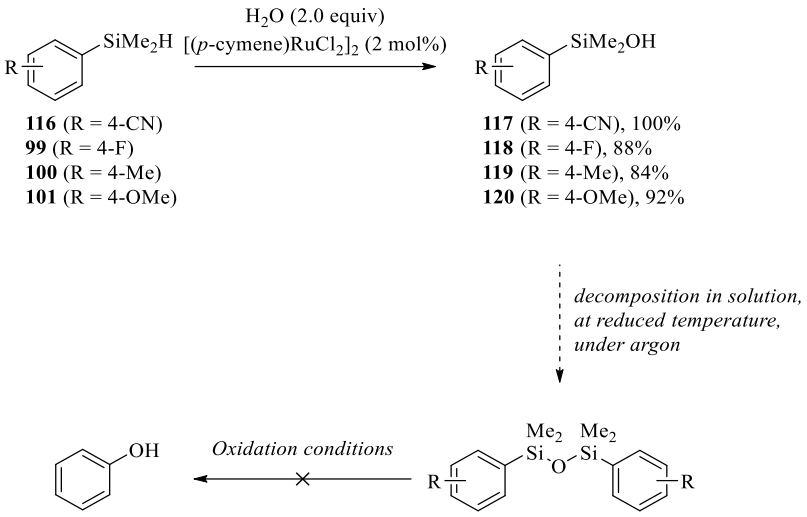
Scheme 2.8 Synthesis of arylhydrosilanes *via* Grignard reagents

Throughout the synthesis of these arylhydrosilanes we were very pleased to observe that all hydrosilane products prepared were air and moisture stable. The compounds were easily purified by either vacuum distillation or flash column chromatography, and retained analytical purity when stored under air for several months at room temperature.

2.3. Synthesis of arylsilanols and arylalkoxysilanes

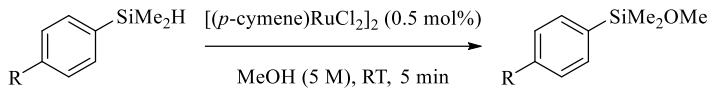
We were pleased to find that the synthesis of silanols from the corresponding hydrosilanes, using the ruthenium catalysed system developed by Chang and co-workers, was a very reliable method (Scheme 2.9).[86] Silanols **117** to **120** were isolated in excellent yields.

These silanols, however, were found to be extremely susceptible to disiloxane formation. Even when stored in solution, under argon and in the freezer, the transformation would occur. The oxidative potential of arylsilane substrates was tested simultaneously with their synthesis and through these studies we learnt that disiloxanes are inert to Tamao-Kumada oxidation conditions.



Scheme 2.9 Synthesis of arylsilanols

Once this unreactivity was realised, it appeared that silanols might not be suitable substrates for the development of the methodology as any formation of disiloxane in the silanol substrates prepared would result in a lower final yield of phenol. Instead, it was considered whether alkoxy-silanes might be better substrates for arylsilane oxidation. Under the intention that an aryl*hydro*silane would be carried through any multistep synthesis as a latent phenol, as long as the alkoxysilane was not susceptible to disiloxane formation, the intrinsic stability of the alkoxysilane was not a concern and instead the most important factor was reactivity. With this in mind, the synthesis of methoxysilanes was attempted. We were subsequently very pleased to find the dehydrogenative silyl ether formation under ruthenium catalysis was an extremely reliable reaction for the synthesis of methoxysilanes **121**-**132** (Table 2.2). Unlike the conditions for silyl ether formation reported by Lee and co-workers (with 1.0 equivalents of alcohol added to the reaction), methanol was added in a large excess as the reaction solvent. The reaction was found to be so rapid that some dilution of the reaction mixture was necessary to prevent a large exotherm and to dampen the vigorous nature of hydrogen effervescence. Thus, the transformation was often complete within seconds but after TLC analysis to confirm full conversion the reaction would be worked-up after 5 minutes. To isolate arylmethoxysilanes **121**-**132**, only a small silica plug was necessary, to remove the ruthenium catalyst. Pleasingly, these species were far more stable than the silanols previously prepared and could retain analytical purity at room temperature for months.



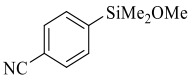
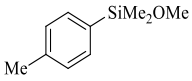
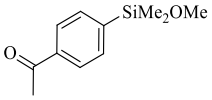
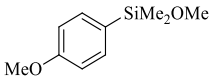
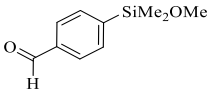
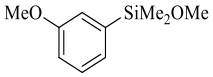
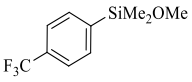
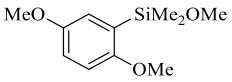
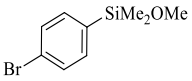
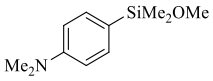
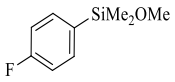
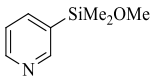
Entry	Methoxysilane		Yield	Entry	Methoxysilane		Yield
1		**121**	95	7		**127**	89
2		**122**	96	8		**128**	99
3		**123**	98	9		**129**	100
4		**124**	89	10		**130**	89
5		**125**	85	11		**131**	75
6		**126**	86	12		**132**	n.r.

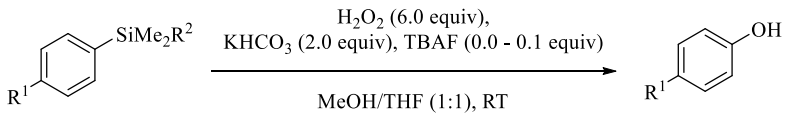
Table 2.2 Synthesis of methoxysilanes

The reaction was successful for nearly all arylsilane substrates to hand, and exhibited pleasing functional group tolerance to carbonyl groups, amines and aryl halides, although aldehyde **123** was found to decompose rapidly after its preparation. The late stage activation of a hydrosilane to methoxysilane, in a multi-step synthesis, should therefore be successful for highly functionalised intermediates. The catalyst was not active, however, in the presence of pyridyl substrate **114**; suggesting that coordination of the pyridine nitrogen may be inhibiting.

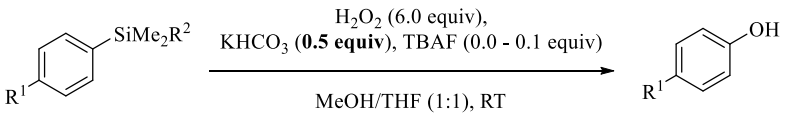
2.4. Oxidation of arylsilanes; preliminary results

Following the optimisation of the arylsilane oxidation previously carried out in the group, we were pleased to find that the conditions previously identified could be applied to the successful oxidation of arylmethoxysilanes and arylsilanols (Scheme 2.10). In addition, we found that the amount of base needed in the reaction was much lower than two equivalents; 2.0 equivalents of base would not, in fact, completely dissolve in the reaction mixture. Instead, the reaction proceeded to completion with just 0.5 equivalents of $KHCO_3$. When the solvent system was scrutinised we found that the MeOH/THF mixture was indeed necessary, mainly to allow full miscibility of the aqueous hydrogen peroxide polar solution, the base and the fairly non-polar arylsilane substrates.

Previously optimised procedure



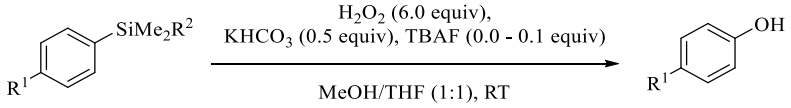
Updated procedure



Scheme 2.10: Arylsilane oxidation procedures

Some preliminary results of the oxidation of arylmethoxysilanes and arylsilanols are shown in Table 3.3. The use of silanols as oxidation substrates became even more unappealing as it appeared in these initial studies that methoxysilanes were better substrates for oxidation (Entries 1 and 3).

The results, however, were blighted by incomplete phenol formation. Although all of these reactions had been quenched after full starting material consumption according to TLC analysis, unknown arylsilane derivatives were observed in the crude product, through NMR analysis. Thus, the final yields of phenol obtained were much lower than expected.

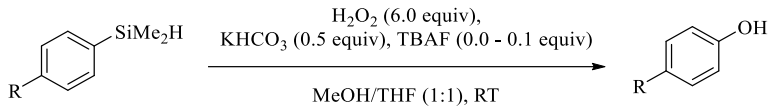


Entry	Substrate	TBAF equivalents	Reaction length	Phenol/ Yield (Conversion (%)[a])
1	R^1 = Me, R^2 = OMe, **127**	0.0	2 h	**133** / n.d. (80)
2	R^1 = Me, R^2 = OMe, **127**	0.1	1 h	**133** / n.d. (62)
3	R^1 = F, R^2 = OH, **88**	0.0	6 h	**134** / 61 (100)
4	R^1 = F, R^2 = OH, **88**	0.1	90 min	**134** / n.d. (41)

Table 2.3 Preliminary results of arylsilane oxidation; [a]conversion was calculated from crude NMR spectroscopic data

Towards the end of these oxidations, only one 'spot' was observed by TLC analysis, but it quickly became clear that the mechanism of phenol formation involved a multi-step pathway and that complete phenol formation was not equivalent to full consumption of starting material. Instead, phenol formation was only complete after the unknown arylsilane intermediates were also consumed. Unfortunately however, these species were indistinguishable from the product by TLC analysis.

In this preliminary work, we were delighted to observe that hydrosilanes were also susceptible to arylsilane oxidation (Table 2.4). This result contradicted the general consensus of previous publications which repeatedly claimed that an electronegative heteroatom substitution was essential to the Tamao-Kumada oxidation. Additionally, most substrates could be converted to phenol in the absence of a fluoride promoter. The reactivity of this substrate could not be immediately explained however. It was not obvious how the silicon centre could be sufficiently electrophilic enough to facilitate hydrogen peroxide addition. Additionally, nucleophilic substitution, of a hydride or methyl anion, at the silicon centre was thought impossible.



Entry	Substrate	TBAF equivalents	Reaction length	Phenol / Yield /% (Conversion/%)
1	R^1 = F, **99**	0.0	7 h	**134** / 69 (85)
2	R^1 = F, **99**	0.1	5 h	**134** / 45 (96)
3	R = Me, **100**	0.0	7.5 h	**133** / 56 (75)
4	R = Me, **100**	0.1	4 h 20 min	**133** / 75 (90)
5	R = OMe, **101**	0.0	24 h	**135** / n.d. (33)
6	R = OMe, **101**	0.1	24 h	**135** / 65 (80)

Table 2.4 Preliminary results of arylhydrosilane oxidation

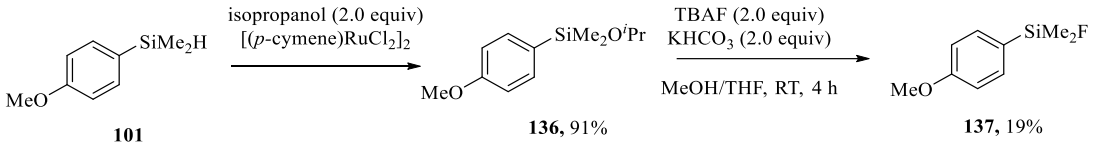
In agreement with the linear free energy relationship of alkyl trifluorosilanes observed by Tamao and co-workers, a striking effect of substrate aromatic electron density was observed on the rate of reaction.[68] Hydrosilanes with electron withdrawing groups substituted on the aromatic ring displayed much faster rates of oxidation than electron rich substrates (Entry 1 and 2), which were very slow to react (Entry 6 and 7).

Unfortunately, these reactions were also quenched before complete conversion because of the inaccuracy of TLC analysis in observing the reaction. Most previous examples of the Tamao oxidation had reaction times of 16 h or more, thus problems of incomplete oxidation were rarely an issue. However, to highlight the speed of the oxidation it was necessary for us to confirm and quantify the varying rates of arylsilane oxidation. Therefore, before further substrates were tested, efforts were directed towards a greater understanding of the mechanism of the reactions.

2.5. Preliminary mechanism studies

To gain a better understanding of the reaction mechanism, we aimed to identify the components of the reaction as it progressed. With routes to silanols, methoxysilanes and disiloxane already in hand, we also attempted to synthesise fluorosilanes to allow identification of the compounds if

evidence of their existence arose. From our substrate library we chose to prepare derivatives of *para*-methoxyarylsilane **101**, due to its slow reactivity and distinct ^{1}H NMR chemical shifts (well separated arylsilane aromatic resonances and a single, well separated phenol, aromatic resonance). The slow reactivity would allow us to observe the reaction at a convenient rate, while the spectroscopic resonances allowed us make more accurate observations from the ^{1}H NMR spectra obtained.



Scheme 2.11: Preparation of further reaction possible reaction intermediates

Following a procedure which had previously been successful within the group, we were able to prepare fluorosilane **137**.[83] Unfortunately, this product partially decomposed during column chromatography to a mixture of fluorosilane and disiloxane. Nevertheless, with this mixture we were able to assign the ^{1}H NMR resonances of the fluorosilane.

The reaction was followed *via* aliquot sampling of an oxidation in progress. The upfield region (highlighted in Figure 2.1) of the aliquot's ^{1}H NMR spectra, relating to the methyl silicon substituents, was most informative. To avoid decomposition of reaction intermediates, the aliquots were quenched with sodium thiosulphate instead of the acidic wash used in our general procedure.

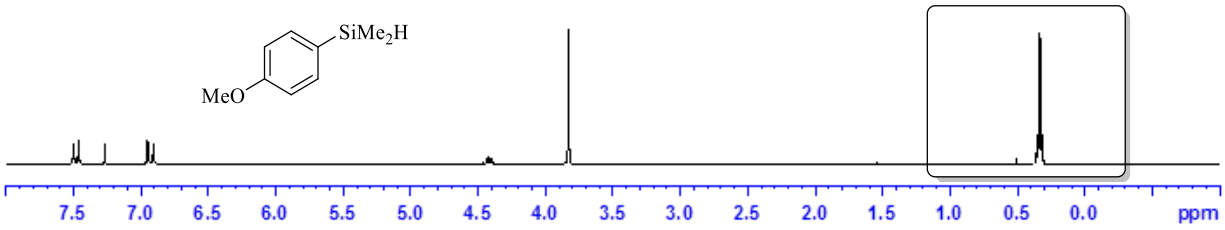


Figure 2.1: 1H NMR spectra of (4-methoxyphenyl)dimethylsilane

Aliquots from an arylhydrosilane oxidation are shown in Figure 2.2. From these spectra, we were able to observe the formation of silanol during the oxidation of hydrosilanes. It was thought that an

explanation for the reactivity of arylhydrosilanes may therefore lie in their ability to form silanols, which would then be prone to further oxidation.

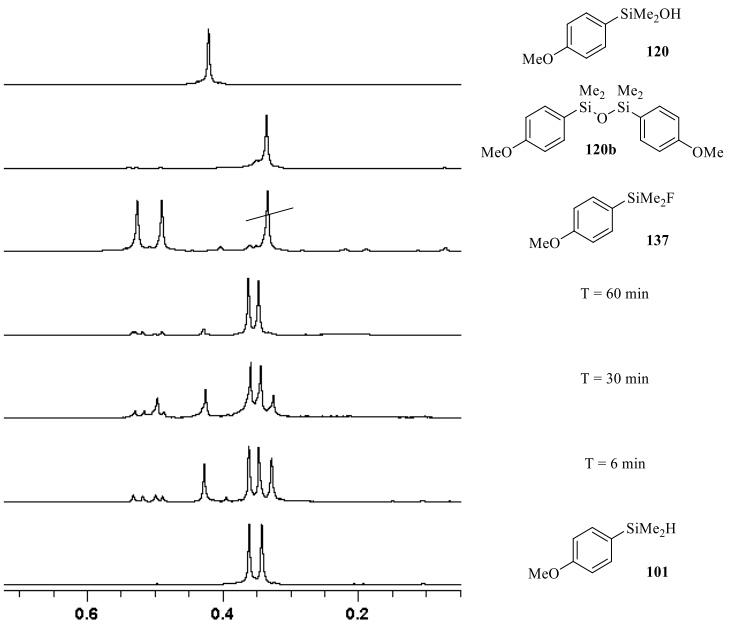


Figure 2.2: Progression of TBAF catalysed oxidation

Fluorosilane **137** and disiloxane **120b** can also be identified in the ^{1}H NMR spectra obtained. However, their concentrations appear to be inconsistent. Despite our efforts to quench the reaction in as mild a manner as possible it appeared likely that this procedure was distorting the data collected, and that accurate observations would have to be made *in situ*. This was later found to be possible through ^{19}F NMR spectroscopy, and will be discussed in full in Chapter 4.

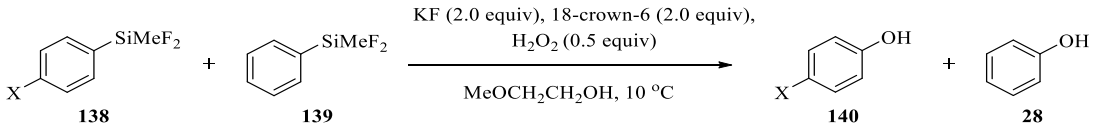
The formation of silanol in the reaction provided an explanation for the unpredictable nature of the reaction by TLC. On further investigation we discovered that for many of our substrates, silanol and phenol would co-elute, thereby explaining how an incomplete oxidation could be represented by a single spot in TLC analysis of reaction mixtures.

2.5.1. Hammett study

In the belief that silanols were common intermediates to the oxidations of all our substrates, we chose to begin a Hammett study of the oxidation of silanols. We envisaged that confirmation of a

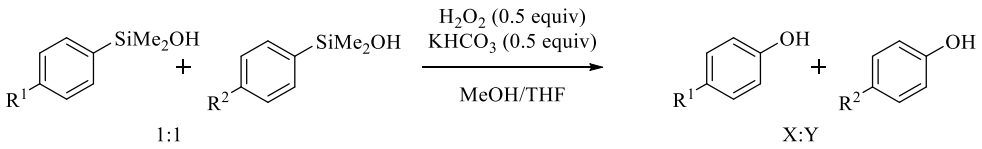
linear free energy relationship would contribute to our mechanistic understanding of the oxidation, as well as provide guidance to appropriate reaction lengths.

Within the mechanistic work of Tamao and co-workers, the effect of aromatic electron density on oxidation rates of fluorosilanes was observed by comparing the crude NMR spectra of incomplete oxidations. Equimolar mixtures of substituted arylsilanes and phenyl arylsilane were prepared and submitted to oxidation conditions with a limited amount of hydrogen peroxide.[68] This system appealed to us as the relative rates of the two substrates could easily be found without the need to find absolute rate constants.



Scheme 2.12 Tamao procedure for relative rate determination

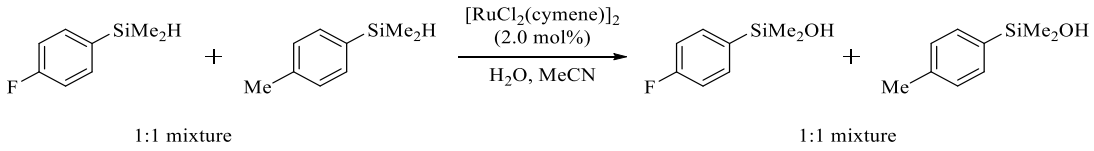
We hoped to replicate this procedure with our own system to gain information on the relative rates of oxidation of our substrates. Our attempt to follow a similar procedure is shown in Table 3.2. Although we were able to identify the fastest and slowest substrate through this method (nitrile and methoxy respectively) the accuracy of our data was disappointing (see disparity between entry 1 and 2, Table 2.5). We also found that substrate pairs that differed greatly in reactivity were unsuitable for this experiment (Entry 3, Table 2.5) as the reactive substrate appeared infinitely faster, which we knew was not the case.



Entry	R_1/R_2	R_1 conversion:R_2 conversion (X:Y)
1	Me/OMe	15:14
2	Me/OMe (repeat)	15:22
3	CN/Me	63:0
4	F/Me	6.3:5
5	CN/Me	38:2

Table 2.5 Study of relative rates of oxidation of arylsilanols I

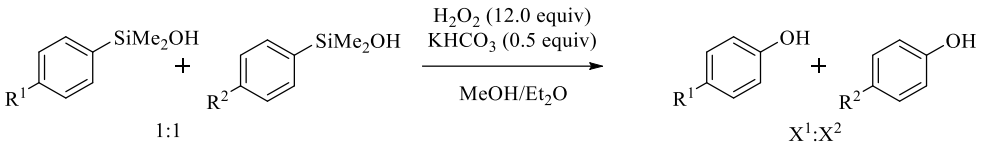
We believed the formation of a 1:1 mixture of silanols may have been the most challenging part to the procedure, as these intermediates were difficult to prepare without disiloxane formation, and much more difficult to purify than their hydrosilane equivalents. Thus, we tested whether a 1:1 mixture of silanols could be prepared more easily from a 1:1 mixture of hydrosilanes. We were pleased to find that this was indeed the case. However, despite this improved method of sample preparation the competition results were still not reproducible.



Scheme 2.13: Synthesis of equimolar silanol mixtures

Extremely low levels of conversion were observed with this limited loading of hydrogen peroxide, and the subsequent NMR spectra obtained were difficult to analyse due to a high noise to signal ratio. We chose instead to repeat the procedure with a large excess of oxidising agent, and took aliquots from the reaction at close intervals at the beginning of the oxidation reaction when the concentration of all substrates and reagents was considered constant (Table 2.6). We were pleased to find that the relative conversions observed at the very beginning of these arylsilanol oxidations

were consistent, and the values reported in Table 2.6 are average values of the data obtained across 3 aliquots (from a single reaction).



Entry	R^1/R^2	Relative R_1 conversion: Relative R_2 conversion
1	Me/OMe	1.05:1.0
2	F/Me	1.33:1.0
3	Br/F	2.12:1.0
4	Ac/Br	1.52:1.0
5	CN/Ac	2.36:1.0

Table 2.6 Study of relative rates of oxidation of arylsilanols II

This result was of great interest to us mechanistically, and the data obtained could be plotted against the Hammett values for these substrates, to afford a graph of linear dependence (Figure 2.3).

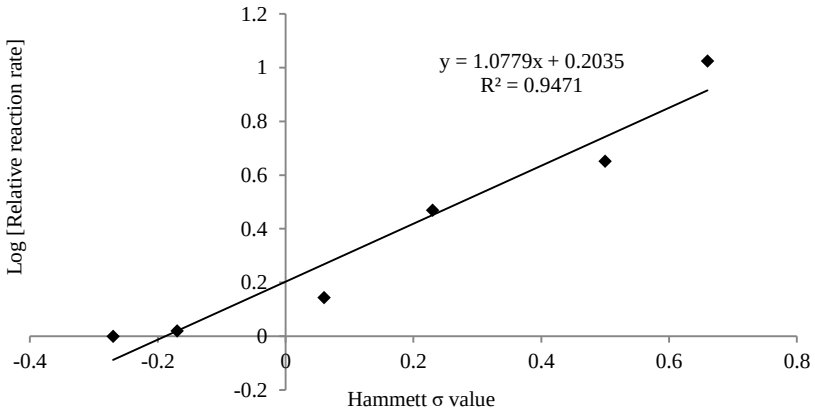


Figure 2.3: Hammett relationship observed

The ρ value obtained for this Hammett relationship was relatively low, and it was felt necessary to test that this value (1.08) was not an indication that the reaction's isoequilibrium temperature was close to room temperature. This could simply be done by repeating an example at 0 °C. The

relative rates were found to be the same at this temperature, which confirmed that the ρ value obtained was not distorted by isoequilbrium effects.[101]

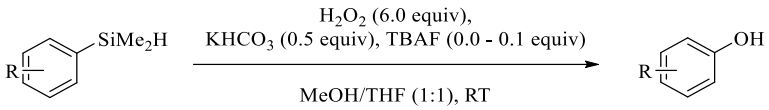
This result added to our interest in the mechanism of the arylsilane oxidation. A positive gradient from this Hammett graph is usually attributed to a build up in negative charge in the transition state of the rate determining step of a reaction. This can be understood most simply to correlate with the coordination of hydroperoxide anion to silicon in the rate determining step of the oxidation, which is also the explanation presented by Tamao.[68] This will be discussed again in greater detail in Chapter 4.

2.6. Optimised oxidation of arylsilanes and arylmethoxysilanes

By combining the results of our Hammett study with further trial oxidations, we were able to divide our substrates into groups of similar oxidative reactivity, and settle upon reliable reaction times which would bring about full conversion to phenols (with the exception of particularly electron rich substrates which did not fully convert within 24 h under fluoride free conditions). We were pleased to obtain good yields for many substrates, particularly electron deficient nitrile-silane **116**. Oxidation of pyridyl silane **114** was rapid, presumably due to the electronegative nitrogen in the aromatic ring. Throughout these oxidations, it was found that full conversion could be achieved in a reduced time when 0.1 equivalents of TBAF was added. Explanations for this apparent catalytic activity will be discussed in Chapter 4.

Two substrates were found to be unsuitable for the oxidation. Aldehyde **105** (Entry 3) appeared to decompose in the presence of hydrogen peroxide, which could be explained by competitive Dakin type processes. Following the attempted oxidation of amino substrate **102** (Entry 11), an insoluble black solid formed. It was thought that oxidation of the amine to an *N*-oxide may have occurred which subsequently decomposed upon work-up. In all successful oxidations it was observed that after two or three hours of oxidation, a colourless white insoluble solid would form in the reaction

flask. This had also been observed by Tamao and co-workers.[61] The yields of these reactions generally decrease as the time required for full oxidation increases and it was therefore envisaged that this solid may have include some trapped phenolic product and was responsible for the drop in yield.



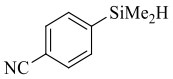
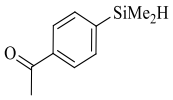
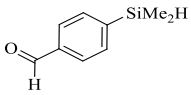
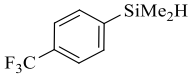
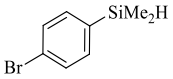
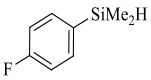
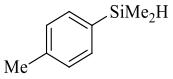
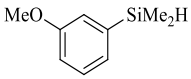
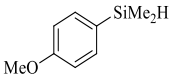
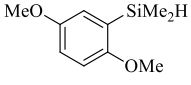
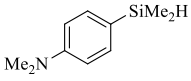
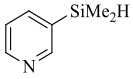
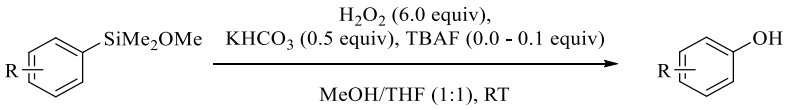
Entry	Hydrosilane		Phenol	Equivalents of TBAF	Time (h)	Yield (%)
1		**116**	**141**	none 0.1	5 3	99 93
2		**107**	**142**	none 0.1	7 3	73 66
3		**105**	**143**	none 0.1	7 5	*only decomposition of starting material observed*
4		**96**	**144**	none 0.1	7 5	91 73
5		**97**	**145**	none 0.1	7 5	57 75
6		**99**	**134**	none 0.1	12 7	71 64
7		**100**	**133**	none 0.1	12 7	67 85
8		**98**	**146**	none 0.1	24 16	40 32
9		**101**	**135**	none 0.1	24 24	33[a] 65 (80)[a]
10		**111**	**147**	0.1	24	< 5[a]
11		**102**	**148**	none 0.1	24 24	*only decomposition of starting material observed*
12		**114**	**149**	none 0.1	2 1	78 71

Table 2.7 Oxidation of Arylhydrosilanes. [a]determined by analysis of crude ^{1}H NMR spectra

The oxidation of arylmethoxysilanes was also optimised and the results are shown in Table 2.8. We were delighted to find that many substrates could reach full conversion within 1 hour while good to excellent yields were obtained for nearly all substrates.



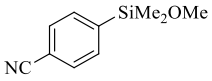
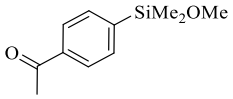
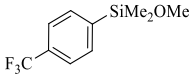
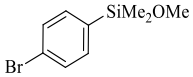
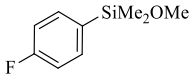
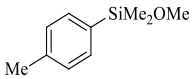
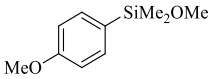
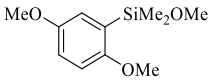
Entry	Methoxysilane		Phenol	Equivalents of TBAF	Time /Yield (%)
1		**121**	**141**	none 0.1	45 min / 89 30 min / 93
2		**122**	**142**	none 0.1	45 min / 81 30 min / 87
3		**124**	**144**	none 0.1	60 min / 73 30 min / 76
4		**125**	**145**	none 0.1	90 min / 86 60 min / 86
5		**126**	**134**	none 0.1	90 min / 91 60 min / 87
6		**127**	**133**	none 0.1	2.5 h / 79 90 min / 80
7		**128**	**135**	none 0.1	3 h / 88 2 h / 93
8		**130**	**147**	none 0.1	4.5 h / 78 3 h / 91

Table 2.8 Oxidation of arylmethoxysilanes

As discussed in the synthesis of arylhydrosilanes, fluorine-substituted aromatics were particularly volatile and although care was taken, the low yields observed may be due to a loss of mass when concentrating the isolated product *in vacuo*.

The oxidation of arylhydrosilanes had provided an interesting contradiction to the assumed limitations of the Tamao-Kumada oxidation in the literature. However, the speed and high yielding nature of the methoxysilane oxidation provided a more appealing synthetic tool. It was envisaged that in most circumstances, silyl ether formation and subsequent oxidation could be applied, but for particularly delicate substrates, which may not be stable to the ruthenium catalysed reaction, the arylhydrosilane could be oxidised directly.

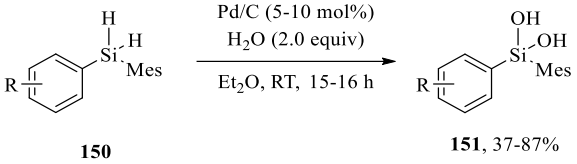
2.7. Heterogeneous catalysis

Despite our progress with arylhydrosilane oxidations, it was felt that the homogenous nature of the catalyst had begun to limit the overall methodology. The ruthenium catalyst, like most transition metal complexes, catalysed the decomposition of hydrogen peroxide, and it was therefore essential that the methoxysilane was submitted to the oxidation completely catalyst free. Although only a silica plug was needed to bring this about, we felt that the sequence would be significantly improved if less handling of the methoxysilane intermediate were necessary. Although methoxysilane was generally stable on silica, we feared hydrolysis to disiloxane could become a problem on greater reaction scales. Ideally, a telescoped procedure could be developed where the methoxysilane formation and subsequent oxidation could be carried out without any change in solvent.

Efforts have been made to prepare solid supported homogenous catalysts to allow for easy catalyst removal and recycling, however these systems remain expensive and impractical at present.[102-103] A heterogeneous catalyst, with similar reactivity to [*p*-cymene)$RuCl_2]_2$ was sought instead. We were delighted to find that Pd/C and Raney Nickel had been proven, some time ago, to be suitable catalysts for this transformation.[104] Surprisingly, despite the inexpensive nature of Pd/C in particular, there are few examples of its use in the synthesis of silyl ethers.[105-107]

2.7.1. Pd/C catalysed arylmethoxysilane synthesis

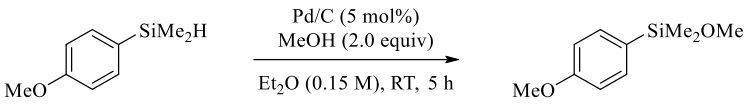
The synthesis of arylsilanols through Pd/C catalysed dehydrogenation held slightly wider precedent than the synthesis of arylmethoxysilanes.[108-109] Thus, we began our study of the synthesis of methoxysilanes using procedures adapted from these examples. During studies on hydrogen bonding interactions of silanediols and carbonyl compounds, Franz and co-workers prepared silanediols **151** with Pd/C as described in Scheme 2.14.



150 **151**, 37-87%

Scheme 2.14: Literature example of Pd/C catalysed synthesis of silanols

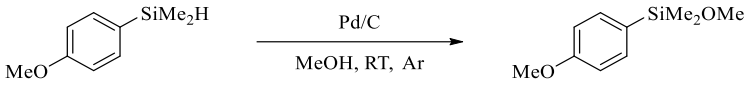
We tested the synthesis of arylmethoxysilanes using a similar procedure and were pleased to observe full conversion of hydrosilane **101** to methoxysilane **128** (Scheme 2.15). The increased reaction rate of our system can be explained by the far less sterically hindered nature of the silicon centre in hydrosilane **101**.



101 **128**, 94 %

Scheme 2.15: Synthesis of arylmethoxysilanes *via* Pd/C catalysis

We hoped that by replacing the solvent diethyl ether with methanol and increasing the concentration, we would be able lower the amount of catalyst added to the system. This was indeed the case and a short optimisation of the reaction is described in Table 2.9.



101 **128**

Entry	Pd/C loading (mol%)	Si–H Concentration (M in MeOH)	Time	Yield (%)
1	5	0.4	30 min	93
2	0.5	5.0	5 min	93
3	0.2	5.0	> 30 min	n/d

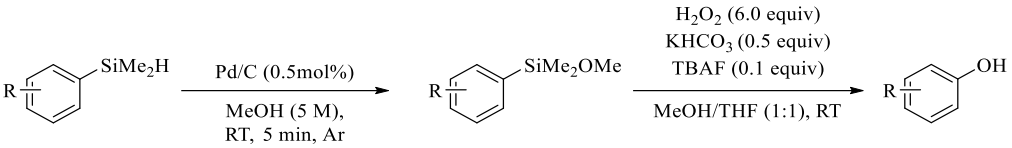
Table 2.9 Pd/C alcoholysis optimisation

The optimum catalyst loading was thought to be 0.5 mol%. At some point below this amount of catalyst, the reaction rate began to drop. We settled at this loading, it was considered very reasonable when the cost of the catalyst was considered. As a safety precaution, these reactions were carried out under an atmosphere of argon. Although the catalyst is of course stable in air, the potential hazards of generating hydrogen gas under aerobic conditions with flammable methanol were to be avoided.

This improved procedure for methoxysilane formation was substituted into our hydrosilane activation/oxidation procedure. For large scale reactions, it was possible to filter the crude Pd/C mixture through Celite® without adding any extra solvent. The Pd/C free solution could then be taken directly onto oxidation. Our substrate screen, however, was conducted on a 0.5 mmol scale which necessitated the addition of extra methanol to rinse the Celite® after filtration. Partial concentration *in vacuo* of the resulting methoxysilane solution followed by addition of tetrahydrofuran provided the solution ready for oxidation.

Nearly all substrates were successfully oxidised through the Pd/C activation/oxidation sequence and excellent yields were obtained for the overall conversions of hydrosilane to phenol (Table 2.10). Although arylbromide hydrosilane **97** required a diluted procedure to avoid partial decomposition: Pd catalysed Br–C cleavage and subsequent substrate decomposition appeared to occur in concentrated methanol solution. Unfortunately, both nitrile substrate **116** and pyridyl

substrate **114** were found to be unsuited to the Pd/C catalysed reaction. It was thought that the nitrile group may be reduced in the presence of Pd/C and the hydrogen produced from silyl ether formation. Again, the pyridyl substrate appeared to deactivate the catalyst.



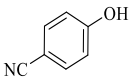
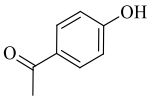
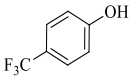
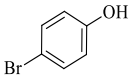
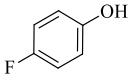
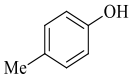
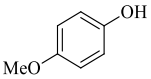
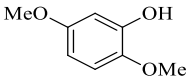
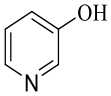
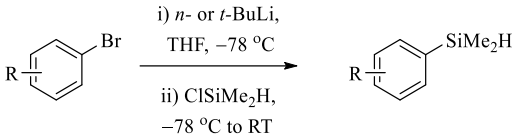
Entry	Hydrosilane	Phenol		Oxidation time	Yield over 2 steps (%)
1	**116**		**141**	-	hydrosilane **190** decomposed in the presence of Pd/C
2	**107**		**142**	30 min	72
3	**96**		**144**	30 min	89
4	**97**		**145**	30 min	85[a]
5	**99**		**134**	1 h	88
6	**100**		**133**	1.5 h	92
7	**101**		**135**	3 h	80
8	**111**		**147**	3 h	79
9	**114**		**149**	-	n.r:.:hydrosilane **192** unreactive to Pd/C

Table 2.10: Pd/C activation/oxidation sequence: [a]Pd/C catalysed reaction diluted with ether to prevent side product formation.

With this optimised methodology in hand, it was hoped that further substrates could be prepared to test the reaction both in terms of steric hindrance and functional group tolerance.

2.7.2. Additional substrates

Once again, butyllithium reagents were utilised to prepare reliably arylhydrosilane substrates (Table 2.11). The precursors to hydrosilanes **153** and **154** were derived from the corresponding carbonyl compounds *via* sodium borohydride reduction and silyl group protection under standard conditions.

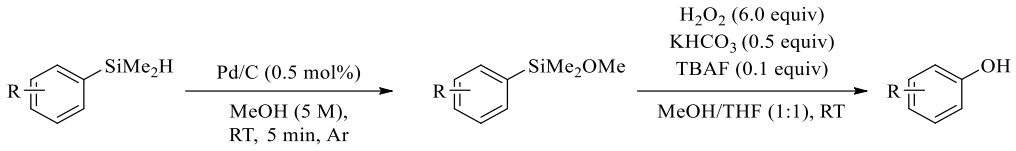


Entry	R	*n*- or *t*-BuLi	Time given for lithiation	Product	Yield of hydrosilane (%)
1	3-CF_3	*n*-BuLi	3 h	**152**	72
2	4-CH_2OTBS	*n*-BuLi	2 h	**153**	68
3	4-CH(CH_3)OTMS	*t*-BuLi	2 h	**154**	42
4	2,5-Me	*t*-BuLi	1 h	**155**	59

Table 2.11: Synthesis of additional arylhydrosilanes *via* bromine/lithium exchange

By preparing substrates **153** and **154** we hoped to test the functional group tolerance of the reaction. Although arylhydrosilane **154** could be isolated *via* vacuum distillation, it was unstable to column chromatography. Therefore it was thought that this substrate was unlikely to be suitable for our methodology, as the phenolic product could not likely be isolated through our standard procedures. Substrate **155** was prepared with the intention of testing the degree of steric hindrance the arylsilane oxidation was able to tolerate. These arylhydrosilanes were submitted to our

sequenced Pd/C/oxidation procedure with pleasing results; all substrates could be converted to phenols in reasonable to excellent yield.



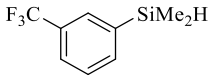
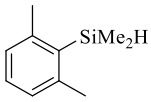
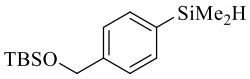
Entry	Hydrosilane		Phenol	Oxidation time	Yield over 2 steps (%)	$ArMe_2OMe$	Yield (*via* 'Ru',%)
1		**152**	**156**	30 min	68	**157**	83
2		**155**	**158**	3 h /	88	**159**	84
3		**153**	**160**	3 h	74[a]	**161**	96

Table 2.12: Pd/C activation / oxidation of additional substrates; [a] Oxidation performed in the absence of TBAF and quenched with aq. $Na_2S_2O_3$

These substrates were also successfully converted to methoxysilanes under ruthenium-catalysed conditions. Should the homogeneous catalyst system be preferred it was reassuring to see the functional group tolerance of this reaction.

2.8. Conclusion

Our methods to prepare and oxidise arylsilanes have been significantly improved through the studies described in this chapter. In contradiction to most previous Tamao oxidation studies, all but the most electron rich aryl*hydro*silanes we had prepared would oxidise to phenols in the absence of TBAF. Through dehydrogenative silyl ether forming reactions under ruthenium or Pd/C catalysis we were able to prepare arylmethoxysilanes reliably, using practical procedures. These

intermediates were found to be excellent oxidation substrates, and would all rapidly convert to phenols. The relationship between reaction rate and substrate electron density, which had previously been observed, was confirmed and a new understanding of the reaction was gained through the identification of silanol as a major component in the mechanisms of both arylhydrosilane and arylmethoxysilane oxidations. The role of this species, and the mechanism in general, remained of great interest to us and will be the focus of Chapter 4 of this thesis.

3. Applications of the arylsilane oxidation

While developing the arylsilane oxidation, we hoped to apply the methodology to significant challenges in organic chemistry. This work began with studies towards the synthesis of biologically relevant natural phenols. Additionally, we attempted to prepare hydroxylated aromatics *in situ* from silylated acyclic starting materials. Following the conclusion of our methodology development (described in Chapter 2), and inspired by current efforts to improve the environmental impact of chemical synthesis, we also attempted to adapt our optimised conditions to flow chemistry procedures.

3.1. The natural polyphenol khellinone

Khellinone (**162**, Figure 3.1**)** was initially chosen as an ideal synthetic target with which to demonstrate the power of the arylsilane oxidation. Khellinone **162** and its tricyclic derivative khellin **163** were first structurally determined by Späth and Gruber in 1938.[110] For thousands of years, khellin **163** has been taken as a medicine by Egyptians as a natural diuretic and antispasmodic by ingestion of the fruits and seeds of *Amni visnaga*, a plant that grows wild in many Eastern Mediterranean countries.[111-112] Since this time, the compound has been noted for its smooth muscle relaxation and vasodilator activity. A more recent line of pharmaceutical research was prompted by the observation that khellinone is capable of inhibiting voltage-gated potassium channels, albeit weakly. Facile derivatization of the compound *via* the free phenol and/or acetyl group has allowed medicinal chemists to optimise this bioactivity (Figure 3.1). Khellinone

derivatives **164** and **165** were found to show particular potency and thus to be promising lead compounds for small molecule immunosuppresants.[113-114]

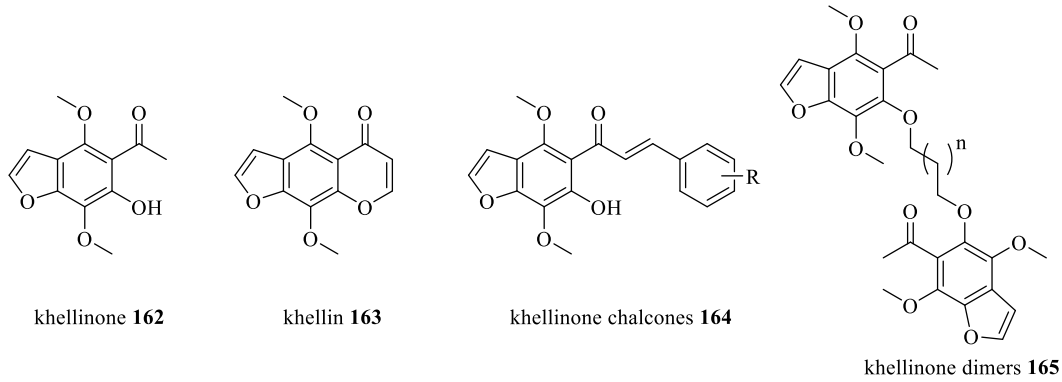
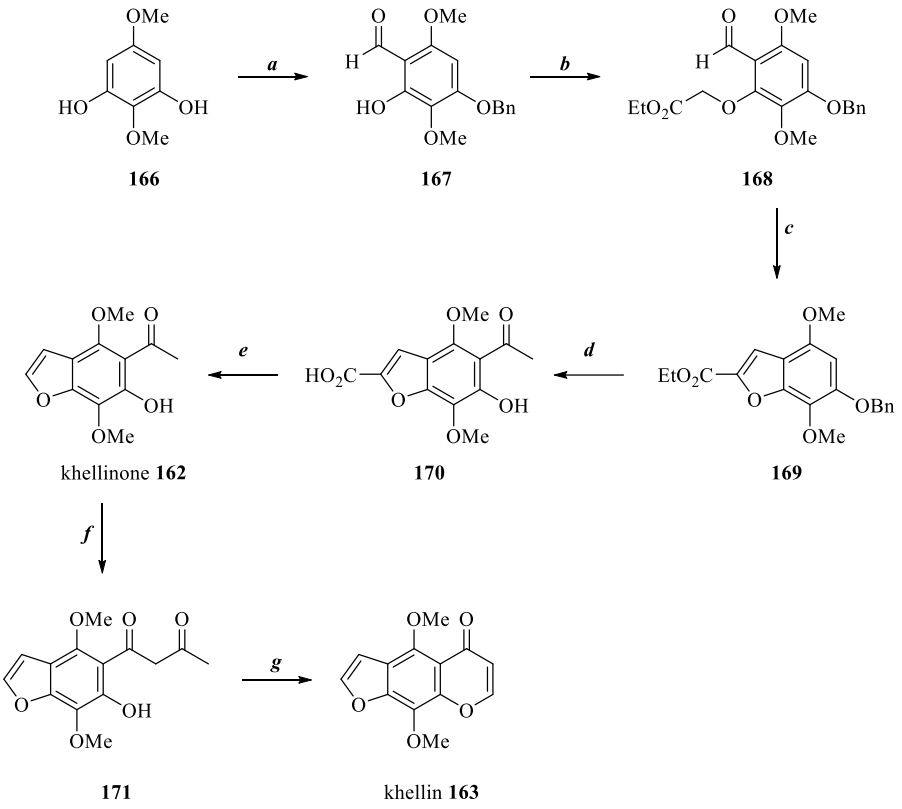


Figure 3.1: Khellinone and its bioactive derivatives

A convenient synthetic route to both khellinone and khellin would be of great interest to medicinal chemists currently studying derivatives of the natural polyphenols. Unfortunately, previous syntheses of the natural product have been limited by inefficient sequences to differentiate the four aromatic oxygen substituents in the compound. Protecting groups were often called upon, and the length of functional group manipulations even extended to dearomatisation in one case.[111, 115-125]

Approximately a decade after the structure of khellin was determined, a total synthesis was reported by Clarke and Robertson (Scheme 3.1).[118] This synthesis began with the highly oxygenated starting material 2,5-dimethoxyresorcinol **166** which, after acetylation, could undergo selective benzylation. This phenol differentiation can be explained through the hydrogen bond that is likely to have formed between the acetyl and phenol group, which deactivates this particular phenol towards electrophilic attack. Following an aldol-type cyclisation and dehydration, benzofuran **169** was prepared. The benzyl ether could be cleaved through Pd/C-catalysed hydrogenation, and the ethyl ester hydrolysed with acid, before a Friedel-Crafts acetylation afforded intermediate **170**. Copper catalysed decarboxylation of this species produced the natural product khellinone. The subsequent conversion to khellin was achieved in two steps through a Claisen condensation and cyclisation. The ease of transformation between khellin and khellinone

has since allowed the total synthesis of khellinone to be considered also as a formal synthesis of khellin.



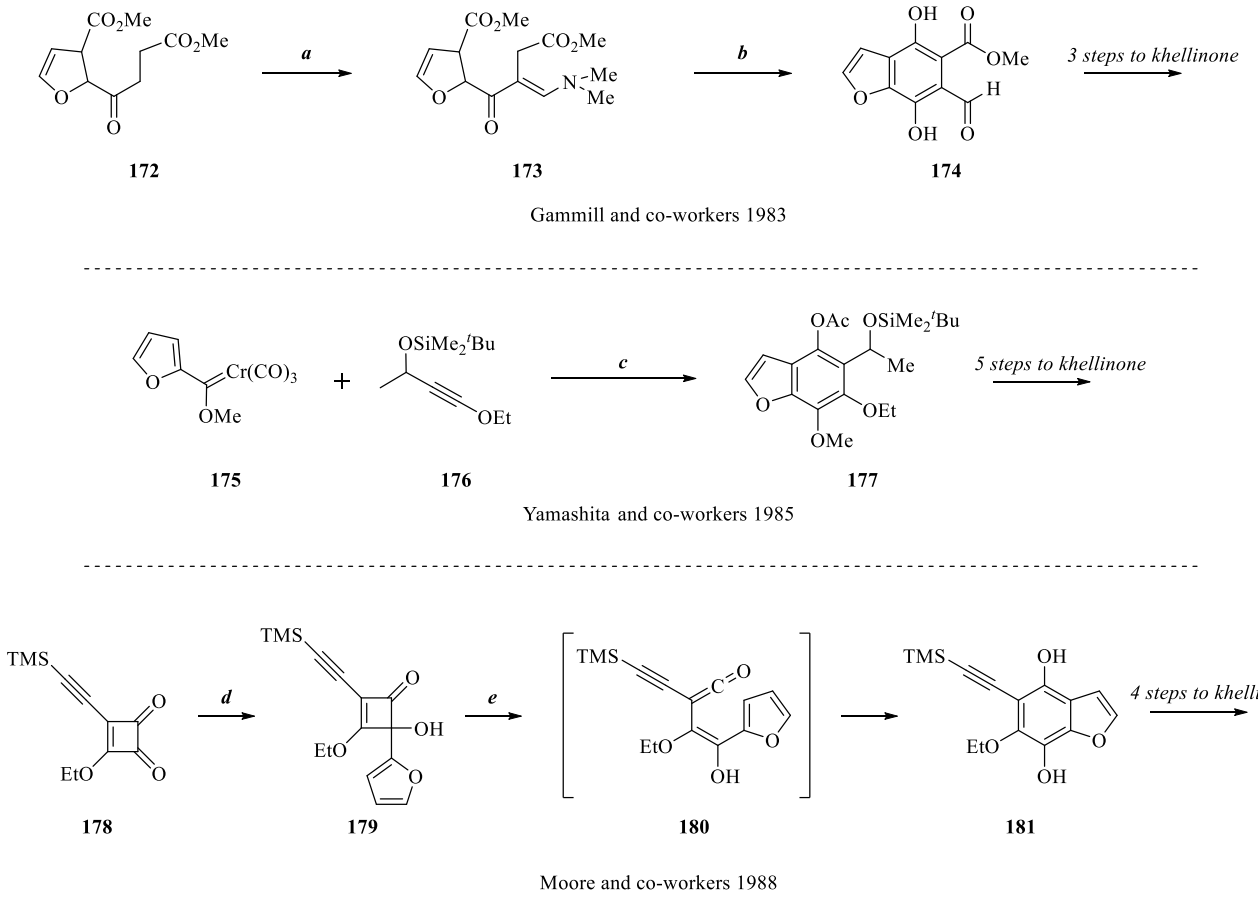
Scheme 3.1: Synthesis of khellin and khellinone as reported by Clarke and Robertson. Reagents and conditions: (a.i) HCN, HCl, Et_2O, 16 h, 0 °C - RT; (a.ii) BnBr, K_2CO_3, acetone, 2 h, reflux; (b) $BrCH_2CO_2Et$, K_2CO_3, acetone, 5 h, reflux; (c) NaOEt, EtOH, 1 h, RT; (d.i) HCl, H_2O; (d.ii) Pd/C (cat.), H_2, acetic acid, 15 min, RT; (d.iii) $AlCl_3$, AcCl, $PhNO_2$, 50 h, 4 °C - RT (e) quinoline, bronze, 25 min, reflux; (f) EtOAc, Na, 5 h, 100 °C; (g) HCl, EtOH, 1 min, reflux.

The structural assignment made by Späth and Gruber was confirmed through this work, and further derivatives of the natural compounds were made. Shortly afterwards, a number syntheses of khellin, khellinone and their derivatives were reported.[121-122, 124-125] A similar approach to the synthesis of polyphenols was carried out throughout: aromatic hydroxyl substitution was not often attempted and highly oxygenated starting materials were used instead. The conditions needed for functional group transformations were often harsh and included high temperatures and strong acids.

Subsequent attempts to prepare the natural compound aimed to construct highly functionalised aromatic intermediates from starting materials which could be derivatised more easily than benzene

(Scheme 3.2). Although highly substituted aromatic rings could successfully be prepared, further steps were always needed to prepare the natural product khellinone **162**.

During the synthesis reported by Gammill and co-workers, a Dieckmann cyclisation of acyclic precursor **173** afforded diphenol **174** before a global methylation, Baeyer-Villiger oxidation and final methyl Grignard addition produced the natural product. After developing a cycloaddition reaction of furan chromium carbene complexes, Yamashita and co-workers were able to prepare the highly advanced intermediate **177** from relatively simple starting materials. Following acetate removal and methylation, khellinone could be accessed *via* silyl group deprotection, benzyl alcohol oxidation and ethyl ether cleavage.



Scheme 3.2: *In situ* synthesis of khellinone; Reagents and Conditions: (a) *N*,*N*-dimethylformamide dimethyl acetyl (1.1 equiv), TsOH, 6 days, RT, 80%; (b.i) KO^{t}Bu (2.0 equiv), THF, −78 °C; (b.ii) 2N HCl, THF, 4 h, 75%; (c) Ac_2O, NEt_3, THF, 10 h, 66 °C, 43%; (d) 2-lithiofuran, THF/ether, 25 min, −100 to −78 °C; (e) Toluene, 1 h, reflux.

During the studies of Reed and co-workers, thermal rearrangement of hydroxycyclobutenone **179** afforded conjugated ketene intermediate **180** which can form diphenol **181** after an electrocyclic ring closure. Methylation, hydrolysis of the alkyne and ethyl ether cleavage then also afforded khellinone. Despite some impressive efficiency of synthesis, all of the routes to khellinone shown above required protecting groups to carry reactive species through the cyclisation step. Extra final steps were also required to bring about simple functional group transformations which inhibited the effectiveness of these synthetic routes.

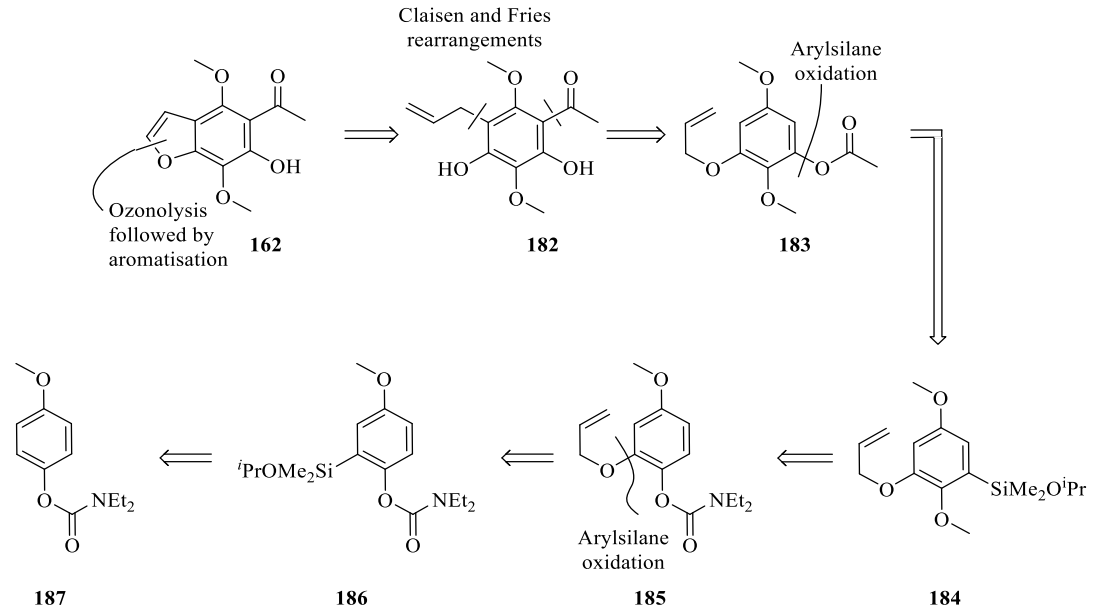
We hoped that it would be possible to develop a synthesis that could introduce hydroxyl groups to the aromatic in a stepwise fashion, thereby limiting the need for protecting groups and phenol differentiation. Additionally, we hoped to demonstrate the use of arylsilanes as latent phenols and believed that this approach could significantly simplify the synthesis of khellin and khellinone.

3.1.1. Retrosynthesis

Our first synthetic attempts were carried out before the utility of aryl*hydro*silanes had been discovered. Thus, the procedures developed by Bracegirdle were used initially.

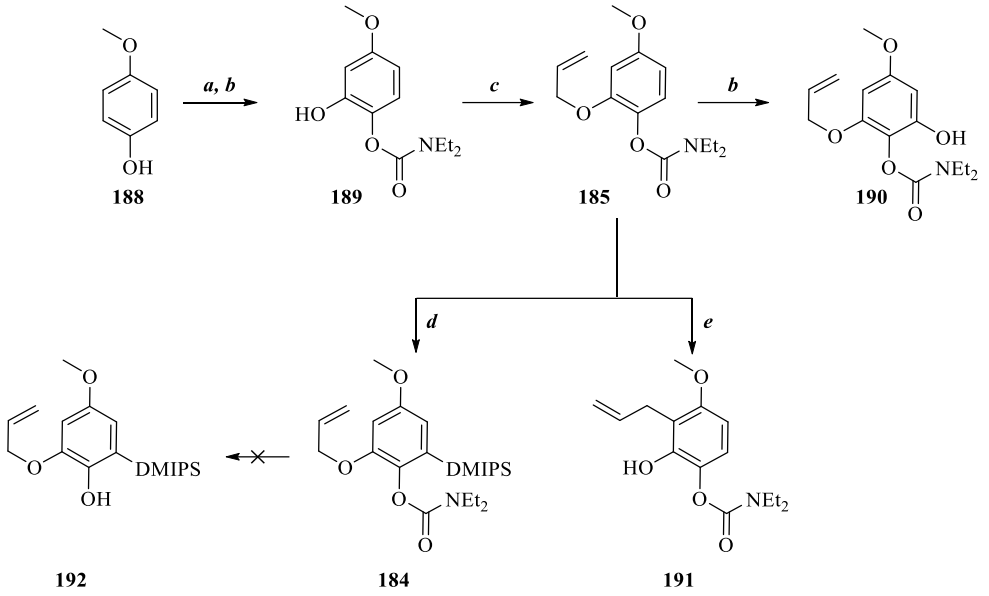
Our inital retrosynthetic approach to khellinone **162** relied on the construction of a benzofuran unit from diphenol **182**; ozonolysis of the allyl double bond would form an aldehyde which we hoped would be capable of condensing with the nearby phenol to give benzofuran product **162** (Scheme 3.3). We then envisaged that diphenol **182** could be prepared through two consecutive phenol-based rearrangements (the Fries, and the aromatic Claisen) of poly-phenolic intermediate **183**. We considered **183** a key intermediate, and one which could be readily prepared in a stepwise and regiocontrolled manner using our directed phenolation procedure. Acetate **183** would be derived from aryl silane **184**, through oxidation and subsequent acetylation. We hoped to install the neighbouring methoxy group from an *N,N*-diethylamine carbamate (**185)** in the presence of the latent phenol, and expected that the dimethylisopropoxy silane (DMIPS) would be stable to hydrolysis and methylation of the carbamate. Finally, we envisaged the allyl ether in **185** could

also be readily prepared *via* our directed phenolation strategy from carbamate protected *para*-methoxy phenol **187**.



Scheme 3.3: Retrosynthetic analysis

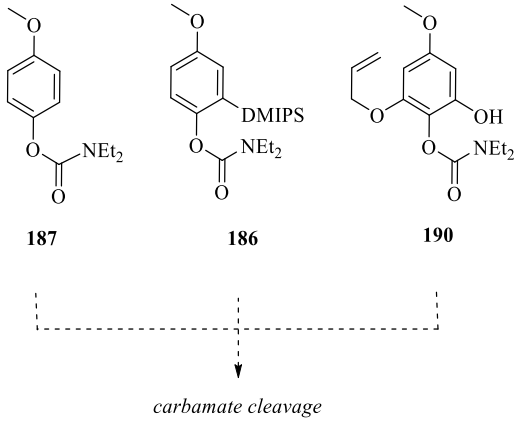
Previous work within the group had found *N*,*N*-dimethyl carbamates to be reliable directing groups, and we were confident from literature precedent that it would compete successfully with the *para* methoxy group in directing metallation of substrate **187**.[97] Hence the *para*-methoxy carbamate was prepared from phenol **188** (Scheme 3.4). Pleasingly, the D*o*M was selective and phenol **189** was isolated in 77% yield through our one pot procedure. After allylation of the phenol under standard conditions we successfully tested both the aromatic Claisen rearrangement and an *ortho*-phenolation, on allyl ether **185**, to provide further confidence in our route.[126] However, the D*o*M and subsequent isopropoxysilylation of **185** did not proceed as easily as hoped. Although full conversion was observed by TLC, and the crude ^{1}H NMR spectrum was promising, aryl silane **184** could only be isolated in 14% yield. Furthermore, initial attempts to cleave carbamate **184** with $LiAlH_4$ resulted in a complex mixture of products.



Scheme 3.4: Synthetic progress. Reagents and conditions: (a) NaH (3.0 eq), THF, rt, 2 h then $ClCONEt_2$, 16 h, 94%; (b) *s*-BuLi (1.3 eq), TMEDA (1.3 eq), THF, –78 °C, 1.5 h then **72** (1.4 eq), –78 °C, 2 h and finally $KHCO_3$ (2.0 eq), TBAF (0.1 eq), H_2O_2 (6.0 eq), 1:1 MeOH/THF, rt, 16 h, 77%; (c) K_2CO_3 (3.0 eq), allyl bromide (1.1 eq), acetone , reflux 16 h, 54%; (d) *s*-BuLi (1.3 eq), TMEDA (1.3 eq), THF, –78 °C, 1.5 h then **72** (1.4 eq), –78 °C, 2 h and finally *i*-PrOH (excess), DMAP (cat.), rt, 16 h, 14%; (e) DMA, 170 °C, 2 h, 30%; (f)

As a result of this problem, efforts were directed towards carbamate cleavage across three substrates **187**, **186** and **190** (Table 3.1). Although carbamate **187** was easily cleaved by $LiAlH_4$ (Entry 1), this method was not successful with the more hindered substrates. Isopropoxysilane **186** only delivered SM and some decomposition.

Scouring of the literature did not present many alternative methods to force carbamate cleavage; various conditions, from hydrated hydrazine and MeLi, to KOH in refluxing ethanol were attempted but carbamate cleavage remained elusive.[127-128] Substrate **190** could be treated with less sensitivity due the absence of an isopropoxysilyl group but after submitting the phenol to increasingly forcing conditions, still the carbamate group could not be removed (Entries 7-11). As an alternative, rearrangement of the carbamate group onto the free phenol of substrate **190** (in analogy to the anionic Fries rearrangement[129]) was also attempted with NaH, although this approach was ultimately also unsuccessful.



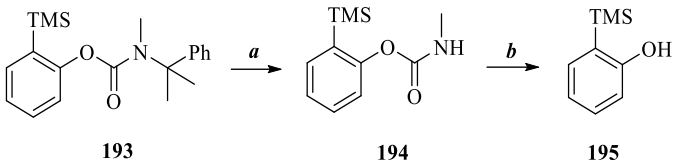
Entry	Substrate	Conditions	Result
1	**187**	$LiAlH_4$, THF, RT, 16 hr	94% conversion[a]
2	**186**	$LiAlH_4$, THF, RT, 16 hr	SM and some decomposition
3	**186**	2N NaOH, DMA, dioxane, RT, 2 hr	Silanol formation (61% recovered)
4	**186**	Hydrazine hydrate, DMA, RT, 3 hr	Only SM recovered
5	**186**	$KOH_{(s,\ 1.2\ eq)}$, IPA, reflux, 2.5 hr	89% aryl silane cleavage[a]
6	**186**	MeLi, THF, -65 °C, 15 min	SM and some decomposition
7	**190**	KOH/EtOH, reflux, 16 hr	Only SM recovered
8	**190**	KOH/IPA, reflux, 16 hr	Only SM recovered
9	**190**	1.3 – 5eq $LiAlH_4$ THF, RT- reflux	Only SM recovered
10	**190**	5 eq TBAF, THF, reflux 16 hr	Only SM recovered
11	**190**	MeLi, THF, -65 °C – RT, 30 min	Only SM recovered

Table 3.1: Attempted carbamate group removal. [a]determined by crude ^{1}H NMR spectra

This issue presented a major drawback in the synthesis and highlighted a flaw in using an *N,N*-diethyl carbamate as a directing group for D*o*M. Although much work has been done to develop the D*o*M reaction there has been little application of the phenol carbamate directing group in synthesis, possibly due to this difficulty in transforming the carbamate under functional group tolerant conditions.[97]

In general, rates of hydrolysis of carbamates are heavily influenced by the extent of *N*-susbstitution.[130] While both *N*-monosubstituted and *N,N*,-disubstituted carbamates can hydrolyse through a $B_{AC}2$ mechanism, only an *N*-monosubstitued carbamate can also hydrolyse through an $E1_{CB}$ mechanism, which proceeds at a considerably higher rate. However, for the purposes of D*o*M

a fully *N*-substituted carbamate is required. With this in mind, an ideal directing group would be fully substituted but easily converted to an *N*-monosubstitued carbamate.



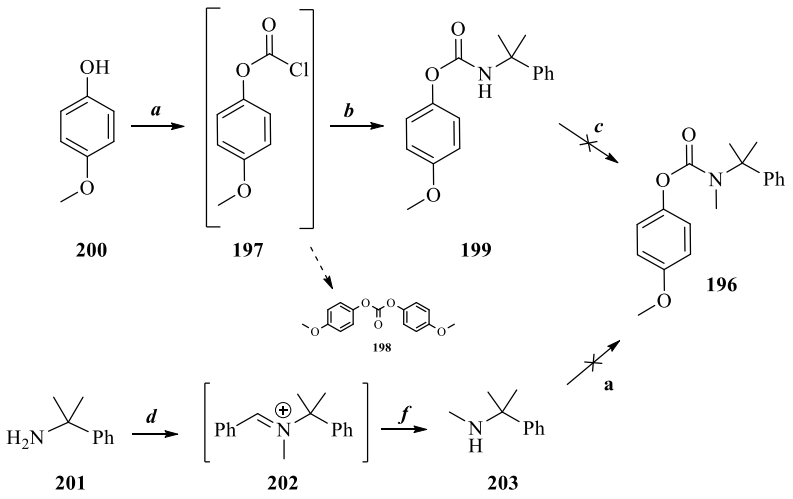
193 **194** **195**

Scheme 3.5: The cumyl carbamate D*o*M group.[131] Reagents and conditions: a) TFA, rt, 10 min; (b) 10% NaOH/EtOH/4 h.

The Snieckus group had developed such D*o*M groups and the cumyl directing group (**193**) (Scheme 3.5) was identified as the most suited to our synthesis; the fully substituted carbamate can be readily converted to methyl carbamate **194** under acidic conditions before hydrolysis with NaOH in EtOH to phenol **195**.[131-132]

However (and surprisingly), the synthesis of this cumyl carbamate group has not been definitively described in the literature and work had to be first directed towards preparing the cumyl carbamate **196** (Scheme 3.6). It was thought that this could be done *via* acyl chloride **197**, however this reaction was troubled by the formation of side product diphenyl carbonate **198**. To prevent this, triphosgene had to be used in excess, the base added dropwise, and the reaction quenched before amine addition.

Disappointingly, methylation of carbamate **199** only resulted in hydrolysis and subsequent phenol methylation yielded dimethoxybenzene. A brief survey of basic conditions were trialed but isocyanate formation from the deprotonated carbamate could not be prevented. Instead, it was decided that mono-methylation of cumyl amine **201** should be attempted, followed by condensation with acyl chloride **197**.

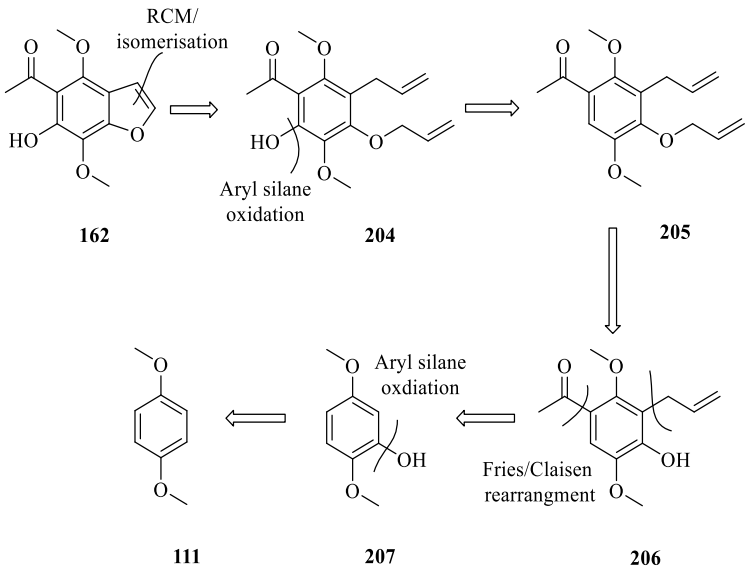


Scheme 3.6: Cumyl D*o*M carbamate synthesis. Reagents and conditions: (a) triphosgene (0.5 eq), 0 °C, DCM, DIPEA (0.75 eq) added dropwise; (b) cumyl amine (0.5 eq), DCM, rt, 2 h, 73%; (c) MeI (excess), Cs_2CO_3 (2.0 eq), 60 °C, 30 min; (d) Benzaldehyde (1.25 eq), toluene, Dean Stark apparatus, 2 h followed by Me_2SO_4 (1.05 eq), reflux, 1h; (f) H_2O, 80 °C, 30 min, 54%.

Unsurprisingly, monomethylation of the primary amine was not trivial, and could only be achieved *via* initial imine formation and Me_2SO_4 mediated methylation (**202**) and subsequent hydrolysis. However, under the optimised conditions, the carbamate could not be prepared, most likely due to the increased steric bulk of the secondary amine **203**.

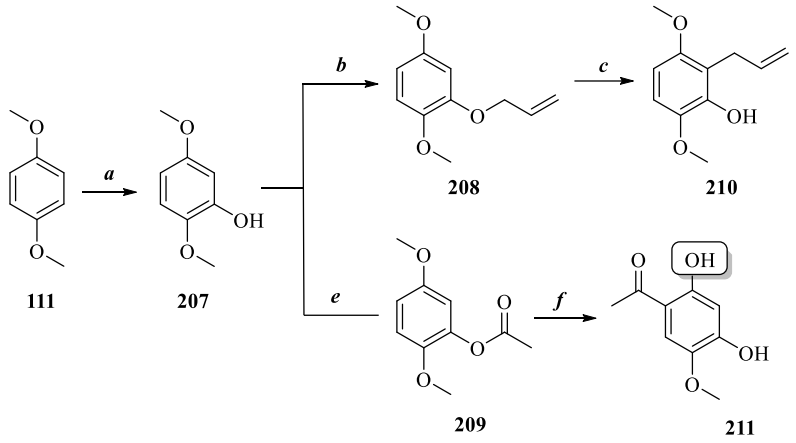
3.1.2. Synthesis of khellinone; revised approach

At this point we began to revise our synthetic strategy and developed a new route to khellinone which would circumvent the problematic carbamate D*o*M group (Scheme 3.7). We hoped to employ a method developed by Otterlo *et al*. whereby a ruthenium catalysed isomerisation and subsequent ring closing metathesis of phenol **204** would construct the benzofuran motif of khellinone **162**.[133] We had learnt from ongoing Fries and Claisen rearrangement investigations that the *para* Fries rearrangement was highly favoured over the *ortho* product at temperatures below 100 °C. With this information we envisaged the two aromatic carbon substitutions of khellinone could be made before the final phenolation of intermediate **205**. We believed phenol **206** could be prepared from consecutive *ortho* Claisen and *para* Fries rearrangements, and phenol **207** could be readily prepared from a one pot, desymmetrizing phenolation of paramethoxybenzene **111**.



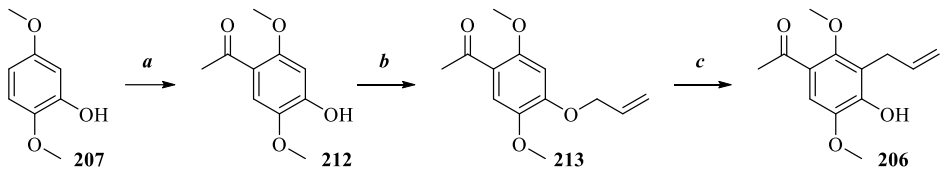
Scheme 3.7: Second retrosynthetic plan.

Although this route provided fewer opportunities to exploit the aryl silane motif as a latent phenol carried through several steps, the synthesis did rely on a key late stage hydroxylation. Pleasingly, phenol **207** was readily prepared from dimethoxybenzene in good yield (82%, Scheme 3.8). Both the Claisen and Fries rearrangements were attempted after allylation (**208**) and acetylation (**209**) respectively. The Claisen rearrangement reproduced literature results in both yield and *ortho*/*para* selectivity (**210**, 78%, ~3:1) under microwave irradiation. However, attempts to bring about a Fries rearrangement only brought formation of demethylated product **211**. Although there is strong precedent for differentiation between a hydrogen bonded phenol and free phenol, this route would contradict the initial aims of our synthetic strategy, hence, conditions of the Fries rearrangement had to be found that did not result in demethylation. The Lewis acids $AlCl_3$ and $BF_3.Et_2O$ were tested with a range of solvents and temperatures, yet only demethylated **211** continued to form.



Scheme 3.8: Synthetic progress II. Reagents and conditions: (a) *s*- BuLi (1.3 eq), TMEDA (1.3 eq), THF, –78 °C, 1.5 h then **72** (1.5 eq), –78 °C, 2 hr and finally $KHCO_3$ (2.0 eq), TBAF (0.1eq), H_2O_2 (6.0 eq), 1:1 MeOH/THF, rt, 16 hr, 82%; (b) K_2CO_3 (3.0 eq), allyl bromide (1.5 eq), acetone, reflux, 16 h, 52%; (c) DMF, 200 °C (microwave), 1 h, 60% (18% *para* product); (e) Ac_2O (5.0 eq), pyridine (5.0 eq) rt, 1 h, 95%; (f) $BF_3.OEt_2$ (3.0 eq), 70 °C, 2 h. 31%.

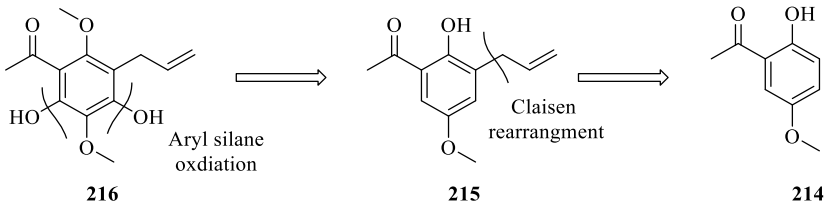
Suspecting that the demethylation was activated by heat, a low temperature Friedel-Crafts acylation was proposed as a viable alternative. Hence, allyl ether **208** was treated with AcCl and $AlCl_3$ at 0 °C, but this only afforded a complex mixture of products, including the *ortho* and *para* rearranged Claisen products. Finally, free phenol **207** was treated to the same conditions and pleasingly the required ketone **212** was acquired (Scheme 3.9). Despite the highly activated aromatic **207** showing very good regioselectivity for *para*-acylation, the yield was quite poor. The subsequent allylation and Claisen reaction were successful but also disappointing in yield.



Scheme 3.9: Synthetic progress III. Reagents and conditions: (a) $AlCl_3$ (1.0 eq), AcCl (1.05 eq), DCM, 0 °C, 16 h, 39%; (b) allyl bromide (1.5 eq), K_2CO_3 (2.0 eq), DMF, 60 °C, 30 min 72%; (c) DMF, 200 °C, 1 h, 35%.

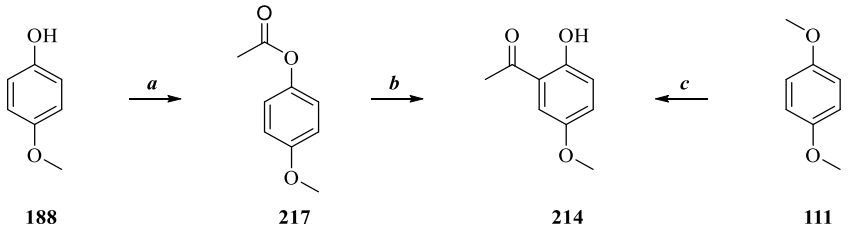
Although the sequential acylation and allylation of the aromatic ring had been successful, the low yielding nature of acylation was considered unacceptable at such an early stage of the synthesis. Thus we adapted our synthetic strategy once more, with the hope of acylating the ring in a more efficient manner (Scheme 3.10). If acylated aromatic **214** could be prepared in good yield, then it

was also envisaged that a more efficient Claisen rearrangement could be carried out, as the *para* position to the allyl ether was blocked and only an *ortho* rearranged product could be produced.



Scheme 3.10: Retrosynthesis adaptation

The synthesis of aceylated aromatic **214** was first attempted *via* Fries rearrangement of phenyl acetate **217** (Table 3.2).



Entry	Reaction	Conditions	Result
1	**a**	Ac_2O (5.0 equiv), Pyridine (5.0 equiv), RT, 16 h	91% **217**
2	**b**	$AlCl_3$ (1.3 equiv), 130 ^oC, 1 h	mixture of products, including demethylated **217** (16%)
3	**b**	$TiCl_4$ (1.4 equiv), toluene, 100 ^oC, 1 h	complex mixture of products
4	**b**	$BF_3.Et_2O$ (3.0 equiv)	partial cleavage of acetate group and demethylation
5	**c**	AcCl (1.05), $AlCl_3$ (1.0 equiv), DCM, 0 ^oC, 40 min	**217** formed only (<89%)
6	**c**	$BF_3.2CH_3CO_2H$	43%, **214**

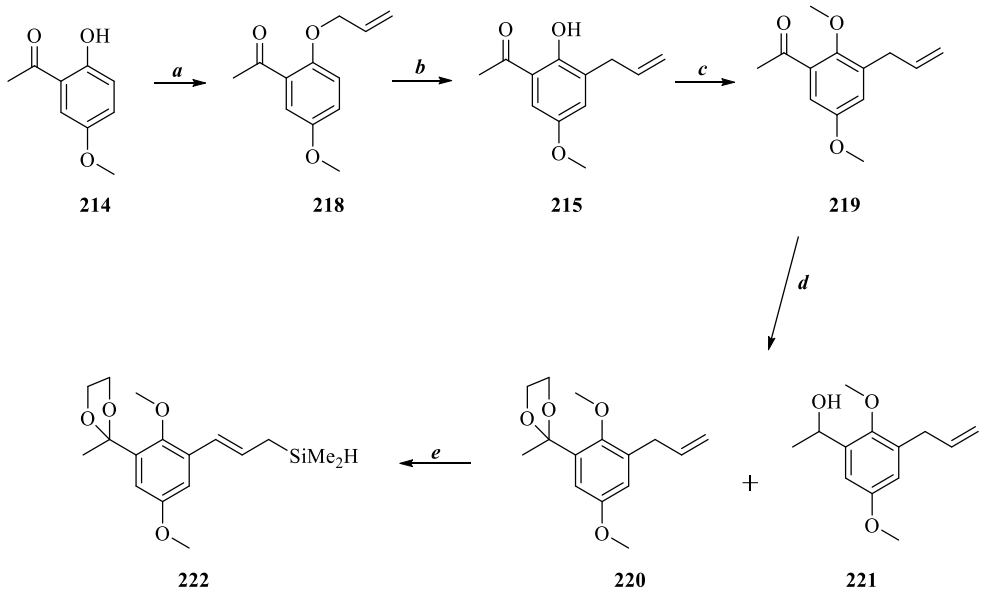
Table 3.2: Optimisation of acylated intermediate synthesis

Although acyl ester formation was facile (Entry 1) the subsequent rearrangement could not be successfully carried out (Entry 2-4). Instead, demethylation often occurred, as well as acetate group cleavage and decomposition of material. A direct transformation from phenol **111** to

intermediate **214** was attempted instead, which finally afforded the target compound in reasonable yield. Pleasingly, this reaction was reliable on a large scale, which was of great importance at this early stage in the synthesis.

With phenol **214** in hand, we were able to carrying out an allylation and subsequent aromatic Claisen rearrangement with pleasing efficiency (Scheme 3.11). With only one position available for the allyl group to migrate to, the 74% yield of phenol **215** was higher than previously observed for the ortho product (60%). Additionally 22% of the starting material was recovered from the reaction and could be resubmitted to the rearrangement. Despite our hopes to limit the use of these synthetic tools, we decided that ketal protection of ketone **219** would quickly provide a substrate suitable for lithiation *via* directed ortho lithiation.

Protection of ketone **219** under Dean Stark conditions was partially successful. Although 90% conversion was achieved after heating at reflux for 18 h, starting material **219** could not be separated from ketal **220** by column chromatography. Instead, the mixture of ketal **220** and ketone **219** was submitted to reductive conditions ($NaBH_4$) which afforded alcohol **221** and untouched ketal **220** in 10% and 77% overall yield respectively. At this point in our synthetic study, the development of an improved method of arylsilane synthesis (see Chapter 2) was reaching completion. Following the observation that *hydro*silanes serve as useful intermediates, an attempt to silylate aromatic **220** was made with dimethylchlorosilane instead of chloroaminosilane **72**. Disappointingly, deprotonation took place at the benzylic position of the allyl group instead of on the aromatic ring. It was thought likely that subsequent silylation took place *via* an allylic anion rearrangement to produce the more substituted alkene product.



Scheme 3.11: Limited synthetic success. Reagents and conditions; (a) allyl bromide (1.3equiv), K_2CO_3 (2.0 equiv), DMF, 60 °C, 5 h, 79%; (b) 190 °C, 6 h, 74%; (c) MeI (4.0 equiv), K_2CO_3 (4.0 equiv), acetone, reflux, 24 h, 75%; (d.i) TsOH (0.01 equiv), ethylene glycol (2.0 equiv), toluene, reflux, 18 h; (d.ii) $NaBH_4$ (1.0 equiv), ethanol, 0 °C, 90 min, 77% **220**, 10% **221**; (e.i) *s*BuLi (1.3 equiv), TMEDA (1.3 equiv), THF, −78 °C, 2 h; (e.ii) $ClSiMe_2H$ (1.5 equiv), −78 °C to RT, 16 h, 65%.

Following this result, efforts towards the synthesis of khellinone were temporarily halted. The arylsilane methodology had been extremely reliable during these studies and the difficulties faced were related to limitations in synthetic methods beyond the scope of our methodology. With this in mind, two relatively simple and, we hoped, accessible compounds were newly identified as realistic targets for the methodology (Figure 3.2).[134-135]

3.1.3. New synthetic targets

Phenylpropanoid **223** was recently isolated from the bark of *Pachypodanthium confine*, some time after closely related benzyl phenol **224** had shown hypolipidemic bioactivity.[134-135] We hoped these simple but significant compounds would be good alternative targets for an efficient total synthesis using our arylsilane oxidation methodology.

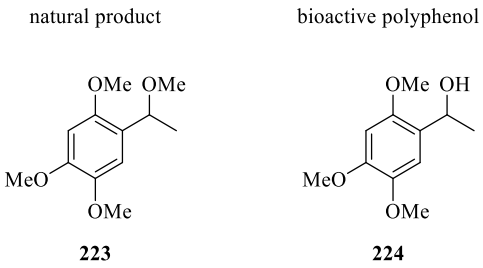
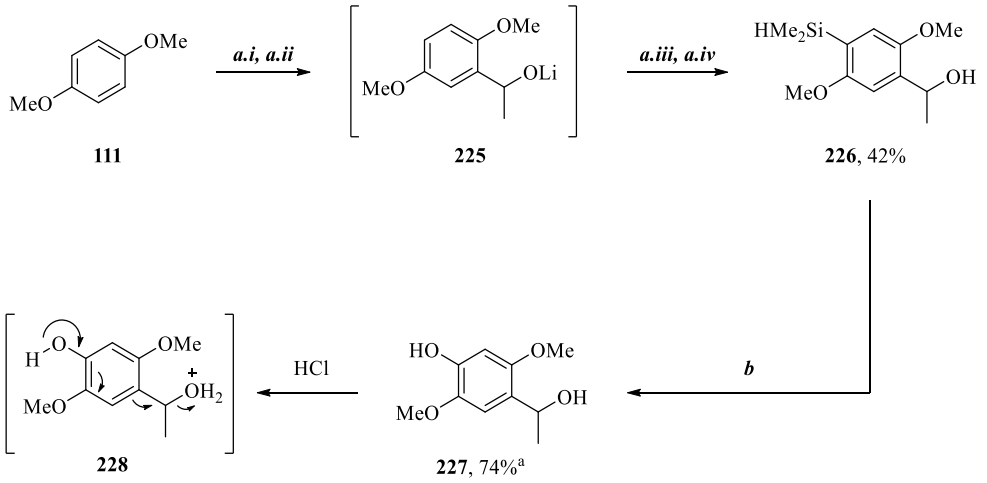


Figure 3.2: New synthetic targets

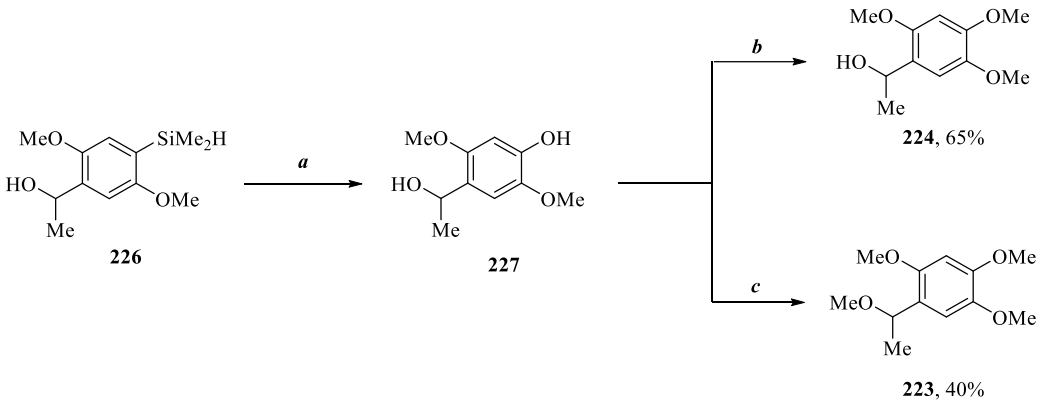
Inspired by the double bromine/lithiation reactions that had previously been used for the synthesis of sensitive arylhydrosilanes (Scheme 2.6), we found that it was possible to carry out two sequential directed *ortho* lithiations of 1,4-dimethoxybenzene (Scheme 3.12). This desymmetrization reaction provided an extremely efficient route to our most complex arylhydrosilane substrate **226** to date.



Scheme 3.12: Synthetic progress IV. Reagents and Conditions: **(**a.i) *s*-BuLi (1.2 equiv), TMEDA (1.2 equiv) 2 h, −78 °C; (a.ii) Acetaldehyde (1.5 equiv); (a.iii) *s*-BuLi (1.3 equiv), TMEDA (1.3 equiv), 4 h; (a.iv) $ClSiMe_2H$ (1.0 equiv), −78 °C to RT, 42%; (b.i) Ru cat.**83** (0.5 mol%), MeOH (5 M), RT, 5 min; (b.ii) $KHCO_3$ (0.5 equiv), TBAF (0.5 equiv), H_2O_2 (6.0 equiv), MeOH/THF, RT, 3 h, 74%; [a]Reaction quenched with aq. $Na_2S_2O_3$.

The arylhydrosilane was successfully oxidised through both our ruthenium catalysed and Pd/C/oxidation procedure, although it was necessary to adapt the work-up procedure slightly: in the presence of 1N HCl, phenol **227** would decompose, presumably *via* protonation of the benzyl alcohol (intermediate **228**). A sodium thiosulphate solution however, was capable of removing any excess hydrogen peroxide without disturbing polyphenol **227**.

Following the successful synthesis of phenol **227**, efforts were made to synthesise the target natural and bioactive compounds **223** and **224** (Scheme 3.13).

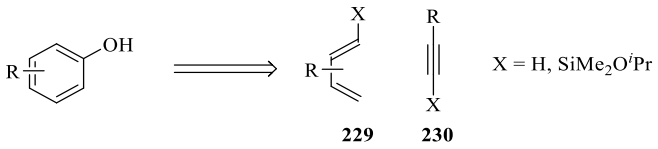


Scheme 3.13: Natural product synthesis: (a.i) 10% Pd/C (0.5 mol%), MeOH (5 M), RT, air, 5 min; (a.ii) H_2O_2 (30% aq., 6 equiv), TBAF (1 M in THF, 0.1 equiv), $KHCO_3$ (0.5 equiv), THF/MeOH (1:1, 0.3 M), air, RT; (b) K_2CO_3 (4.0 equiv), MeI (1.0 equiv), (KI, catalytic), MeCN (0.25 M), 80 °C, 3 h; (c) NaH (4.0 equiv), MeI (6.0 equiv), THF (0.1 M), 0 °C to RT, 1 h.

Following sequenced Pd/C silyl ether formation and oxidation, crude phenol **227** was immediately converted to methylated derivatives **224** and **223**, to avoid substrate decomposition (which would occur rapidly after isolation). By harnessing the acidic nature of phenolic hydroxyl groups, we were able to selectively methylate phenol **227** to form bioactive polyphenol **224**. Alternatively, a global methylation of phenol **227** provided natural product **223** in an overall yield of 40% from hydrosilane **226**. With this short and effective synthesis, we felt that the utility of arylsilane oxidations for the synthesis of natural polyphenols had been well demonstrated.

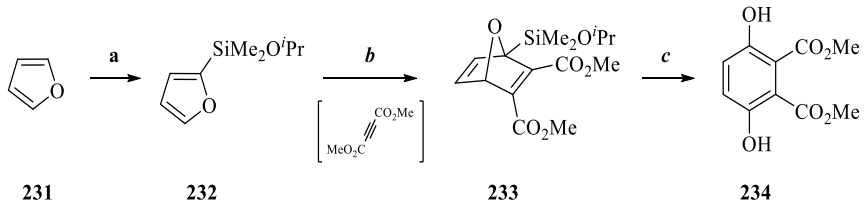
3.2. Cycloaddition routes to phenols

As an extension to the use of directed phenolation in natural product synthesis, alternative methods of phenol preparation *via* silicon oxidation were of interest to us. In particular, we hoped to regioselectively prepare organosilicon intermediates through cycloaddition reactions. The oxidation of these products would allow access to phenols in high regioselectivity, with greater scope for varying the additional substitution of the aromatic (Scheme 3.14)



Scheme 3.14: Phenols *via* cycloadditions reactions.

The Diels Alder (DA) reaction of furans and alkynes looked well suited to our study, as the resulting cycloadducts could be readily converted to phenols. With this in mind, furyl silane **232** (Scheme 3.15) was prepared *via* chloroaminosilane (**72**) quench of lithiated furan. Pleasingly, furan **232** successfully produced cyclo-adduct **233** on heating with dimethyl acetylenedicarboxylate (DMAD), which was then readily transformed to diphenol **234** with only sub-stoichiometric addition of TBAF.

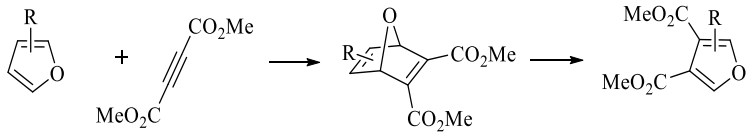


Scheme 3.15: Cycloaddition and oxidation sequence. Reagents and conditions: (a) *n*-BuLi (1.4 eq), 0 °C, 90 min followed by **72** (1.5 eq), 0 °C, 90 min before *i*-PrOH (excess) and DMAP (cat.), rt, 16 h 76%; (b) DMAD (1.3 eq), toluene, 110 °C, 16 h, 46%; (b) $KHCO_3$ (2.0 eq), H_2O_2 (6 eq), TBAF (0.1 eq), MeOH/THF, rt, 5 h, 71%.

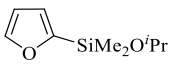
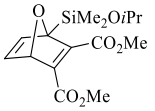
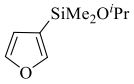
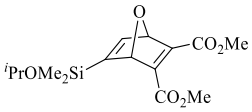
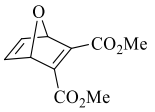
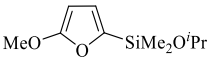
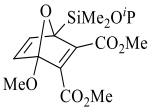
After this initial promising result, efforts to improve the conditions of the reaction were tested, along with an exploration of other substrates. Given its synthetic utility, there have been many attempts to improve the practicalities of the DA reaction, including heterogeneous catalysis, Lewis acid catalysis and microwave irradiation.[136-140] Of these methods, only microwave irradiation improved on our more conventional heating conditions; Lewis acids either could not activate the reaction at a lower temperature or were too harsh for the silicon moiety. However, the microwave reaction, though much more efficient, gave retro-DA products as well as the cycloadduct (Entry 1, Table 3.3). Tuning the reaction to avoid these undesired side products was quite challenging, and the best conditions were found to be 3 h at 120 °C at a 200 mg/ml concentration. The retro–DA

reaction was favoured at higher concentrations and temperatures, while 3 h was necessary for the reaction to go to completion.

Further silicon substrates were subsequently prepared (Table 3.3). Interestingly, attempts to trap the cycloadduct (**CA**) of 3-furyl derivative **235** were unproductive. Although conversion of starting material was rapid, surprisingly so was formation of the retro-DA product (**RDAP**).



CA **RDAP**

Entry	Furan		Cycloadduct		CA : RDAP ratio[a]	cycloadduct yield (%)
1		**232**		**233**	3:1	63
2		**235**		**236**	0:1[b]	-[b]
3		**237**		**238**	1:0	21
4		**239**		**240**	1:0	14

[a]Conditions - toluene, microwave irradiation 120 °C, 3 h; [b]cycloadduct was not isolated.

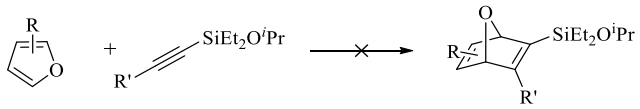
Table 3.3: Microwave assisted DA reactions

A control experiment was conducted with furan and DMAD and although complete conversion of starting material was observed, the retro Diels Alder product was not (Entry 3). However, the isolated yield of the cycloadduct was very low, suggesting there was residual furan starting material which could have been lost when removing the solvent *in vacuo*. From these results it appears that silicon substitution of the furan ring activates it towards both the DA and retro-DA

reactions. 3-Furylsilane **235** is more reactive towards the DA cycloaddition than 2-furlysilane **232**, presumably due to steric issues. However 3-furylsilane cycloadduct **236** is less stable than 2-furylsilane cycloadduct **233**. This surprising result can possibly be explained by a thermodynamic preference for the silyl alkyne "leaving group".

Methoxy-furyl silane **239** was hoped to be highly activated towards the DA reaction, and indeed cycloadduct **240** was isolated (Entry 4), although much material was lost through decomposition during column chromatography; subsequent attempts to oxidise the compound yielded a complex mixture of products. As a result, the substrate was abandoned as we believed the ability of the methoxy group to destabilise the bridgehead carbon-oxygen bond and ring open the cycloadduct, rendered it an unpractical substrate.

Silyl alkynes **241** and **242** were also prepared (Scheme 3.16) in the hope of affecting cycloaddition reactions with furan and 2-methoxy furan. Disappointingly no addition was observed, even with large excess of the furans and higher temperatures.



R' = H, **241**
R' = CO_2Me, **242**

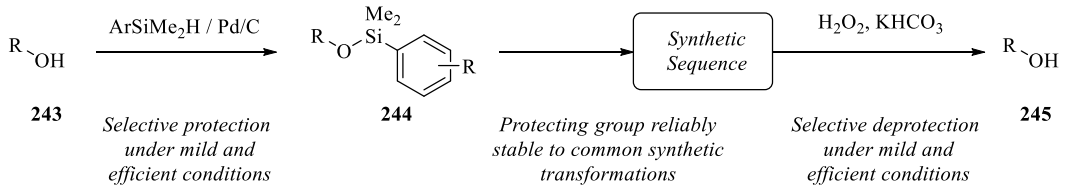
Scheme 3.16: Further cycloaddition attempts.

At this point, given the disappointing results of our investigation into furan cycloadditions, we decided to put the work to one side. The aromaticity of furan rendered the DA reaction too problematic for our substrates and future studies would look towards cycloadditions of less restrictive silicon containing compounds.

3.3. Controlled cleavage of Si–O bonds

After obtaining greater knowledge of the reactivity of arylsilanes towards oxidation, we hoped to shift the focus of the methodology to the cleavage of Si–O bonds within alkoxysilanes. If cleavage of this bond could be initiated under the oxidative conditions just developed, it was envisaged that arylsilanes could serve as novel protecting groups with orthogonal reactivity to other available silyl protecting groups.

Protecting groups have been essential to the synthesis of many complex natural products and pharmaceuticals for their ability to "protect" sensitive moieties of intermediate compounds from chemical conditions required for transformations elsewhere in molecule.[141-142] An ideal protecting group can be easily and selectively introduced to a compound, is stable to a variety of chemical conditions and can be finally selectively removed under mild conditions. A number of silicon protecting groups have developed for the protection of hydroxyl groups.[143] Often, more than one of these may be used during a multi-step synthesis to differentiate hydroxyl groups and orthogonal reactivity between these silyl ethers is thus essential.[141] The Pd/C dehydrogenative silyl ether formation and arylsilane oxidation reactions that had been developed were believed to hold the potential to fulfil the requirements of an ideal protecting group (Scheme 3.17).

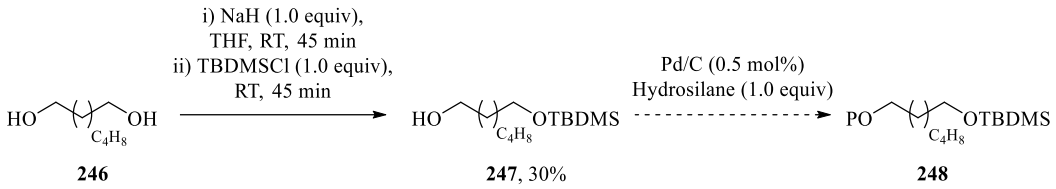


Scheme 3.17 Protecting group outline

Of particular interest was the possibility that the conditions described would be orthogonal to common methods of arylsilane cleavage, the addition of TBAF in particular.

3.3.1. Synthesis and stability of arylsilane protecting groups

It was hoped that a range of arylsilane substrates could be tested for their stability to our oxidative conditions as well as to common silicon deprotection conditions. Thus, hexane-1,6-diol was monosilylated with *tert*-butyldimethylsilylchloride (TBDMSCl) to form silyl ether **247**. Hexane-1,6-diol was chosen so that the six carbon chain, separating the silyl ethers, would lessen the risk of migration of silicon groups between the two alcohols.



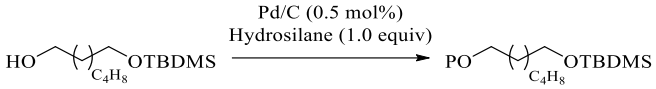
Scheme 3.18 Synthesis of arylsilane protected alcohols

Subsequent silylation of alcohol **247** *via* the Pd/C dehydrogenation reaction could hopefully be carried out with just an equimolar equivalent of hydrosilane and without the need for a solvent (Scheme 3.18).

Four hydrosilanes were prepared and tested for their suitability as protecting groups (Table 3.4). Silane **96** had already been prepared in the development of our arylsilane methodology and silanes **249** and **250** were synthesised in a similar manner; following bromine/lithium exchange the intermediates were quenched with dimethylchlorosilane and diethylchlorosilane respectively. Diethylchlorosilane was prepared in house *via* ethyl magnesium chloride addition to trichlorosilane. This reaction was partially successful as the target compound was the main product, however it was not possible to isolate it from the secondary products dichloroethylsilane and triethylsilane instead the mixture was used to successfully prepare arylhydrosilane **250**. The Pd/C silyl ether formation of these compounds was reliable, although the poor quality of diethylchlorosilane preared caused a low isolated yield of silyl ether **253**.

Arylhydrosilane **254** was prepared by quenching lithiated 1-bromo-4-(trifluoromethyl)benzene with 0.5 equivalents of dichloromethylsilane. This reaction produced a disappointing yield of 36%, and

a product which could not be isolated a side-product hydrosilane **255**, nevertheless the silane could also be used to prepare silyl ether **256** which was successfully purified.



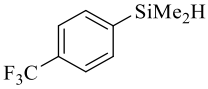
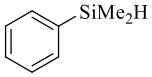
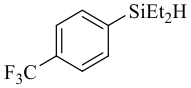
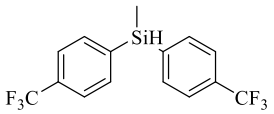
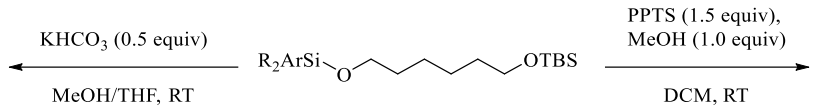
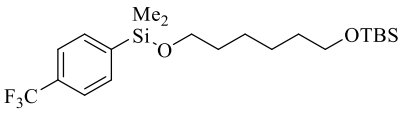
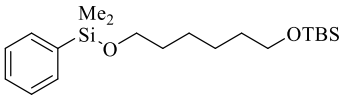
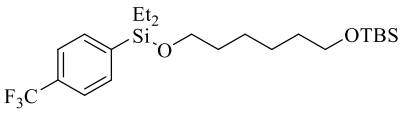
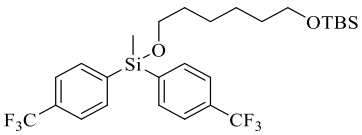
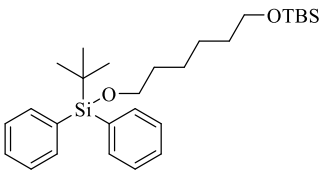
Entry	Hydrosilane		Protected alcohol / Yield (%)
1		**96**	**251** / 90
2		**249**	**252** / 97
3		**250**	**253** / 64
4		**254**	**256** / 29

Table 3.4: Synthesis of arylsilane protecting group substrates

To begin with, a mild method of TBS removal was sought to allow selective removal of this protecting group in the presence of our arylsilylethers. Previously, mildly acidic conditions have been used to selectively remove a TBS group in the presence of other silyl ethers, and these conditions were therefore thought to be a good starting point for our investigation.[144-145] Subsequently, all silyl ethers were subjected to treatment with both basic MeOH/THF and acidic PPTS with MeOH in dichloromethane. To our disappointment, none of the silyl ethers prepared showed stability to these conditions. In fact, all arylsilyl ethers were cleaved to some degree with no more forcing conditions than basic MeOH/THF. The TBS protecting group showed much greater stability, although the extent of cleavage under acidic conditions was a little unpredictable. The popular *t*-butyldiphenylsilyl (TBDPS) group was used to protect alcohol **247** and the product (**257**) also tested for comparison. This arylsilyl ether proved to be far more stable than our arylsilanes towards deprotection. It appeared that the most important factor in achieving silyl ether stability was in increasing steric strain around the silicon centre.



Entry	Protected alcohol		$KHCO_3$	PPTS/MeOH
1		**251**	Full deprotection of arylsilane after 1 h	after 1 h : 48% arylsilane deprotection and 43% TBS group deprotection
2		**252**	Full deprotection of arylsilane after 15 h	after 15 h: 86% arylsilane deprotection and 21% TBS group deprotection
3		**253**	10% arylsilane cleavage after 45 min	No deprotection observed within 45 min
4		**256**	71% deprotection of arylsilane after 16 h	after 16 h: 72% arylsilane group deprotection 45% TBS group deprotection
5		**257**	No deprotection observed even after addition of H_2O_2 (1.0 equiv)	n.d.

It was felt at this point in our study that our arylsilane groups were too inferior to protecting groups already in use to warrant further development. It is possible that a derivative of the TBDPS group, which contains electron deficient arenes, may hold the same stability as the TBDPS group but may also be cleaved under our oxidative conditions. This would be a likely focus of future work.

3.4. Development of a flow reactor

3.4.1. The Principles of Green Chemistry

Although enormous advances have been made in the selectivity of organic reactions, current organic chemistry laboratory techniques have changed little over the last century and are very labour and resource intensive.[146] Through batch and iterative processes, waste is often produced in large quantities, especially when each intermediate is isolated and purified.[147] To improve this seemingly inefficient process and reduce the environmental impact of organic synthesis and chemistry in general, green chemistry has emerged as an important new area of research. The 12 Principles of Green Chemistry (Figure 3.3) are now established as guidelines for the development of environmentally benign chemical products and processes.[148]

1. *It is better to prevent waste than to treat or clean up waste after it is formed.*
2. *Synthetic methods should be designed to maximize the incorporation of all materials used in the process into the final product.*
3. *Wherever practical, synthetic methodologies should be designed to use and generate substances that possess little or no toxicity to human health and the environment.*
4. *Chemical products should be designed to preserve efficacy of function while reducing toxicity.*
5. *The use of auxiliary substances (e.g. solvents, separation agents, etc.) should be made unnecessary wherever possible and innocuous when used.*
6. *Energy requirements should be recognized for their environmental and economic impacts and should be minimized. Synthetic methods should be conducted at ambient temperature and pressure.*
7. *A raw material of feedstock should be renewable rather thatn depleting wherever technically and economically practical.*
8. *Unnecessary derivatization (blocking group, protection/deprotection temporary modification of physical/chemical processes) should be avoided wherever possible.*
9. *Catalytic reagents (as selective as possible) are superior to stoichiometric reagents.*
10. *Chemical products should be designed so that at the end of their function they do not persist in the environment and break down into innocuous degradation products.*
11. *Analytical methodologies need to be further developed to allow for real-time, in process monitoring and control prior to the formation of hazardous substances.*
12. *Substances and the form of a substance used in a chemical process should be chosen so as to minimize the potential for chemical accidents, including releases, explosions and fires.*

Figure 3.3: The 12 Principles of Green Chemistry

Our Pd/C activation/oxidation sequence had already satisfied some of the principles of green chemistry. Methoxysilane formation was an atom economical process, with environmentally

benign hydrogen the only side product (Figure 3.3, Principle 2 and 3). It must be acknowledged that the oxidation of arylsilanes itself is not an atom economical process! However the benign nature of silicon does improve the methodology's "green" credentials (Principle 3). In agreement with Principle 6, all oxidative reactions developed in this Chapter are carried out at room temperature and under atmospheric pressure.

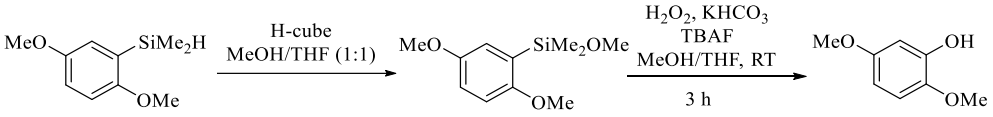
During the development of a heterogeneous catalyst for oxidation, we had hoped to produce methoxysilane in a state which could be taken directly onto arylsilane oxidation, which would satisfy Principle 5. This was not possible in the batch process, as the necessary rinse of Celite® with methanol reduced the concentration of arylmethoxysilane to an extent that would have dramatically lowered the rate of oxidation. It was still thought however, that a convenient route into one-flow, multi-step synthesis may exist.[147] We hoped that the automated H-Cube® system, designed for hydrogenation reactions, could convert our hydrosilane solution to a methoxysilane solution through its Pd/C catalytic cells.[149] Although our oxidative process is essential the reverse of hydrogenation, we envisaged that the H-cube might still suit our needs, as the system was developed with the safe handling of hydrogen gas in mind.

3.4.2. Optimisation of the H-cube® hydrosilane oxidation

Optimisation with the H-cube® began under the manufacturer's recommended conditions where concentration and flow rate were kept below 0.1 M and 1 mL/min respectively. We chose a challenging substrate from our library of hydrosilanes, so we could be confident that less hindered arylsilanes would perform well under the same reaction conditions. We were pleased to observe full conversion to methoxysilane under these conditions but hoped to increase the concentration to allow for product solutions to be used directly in an oxidation (the oxidation was optimised at 0.3 M concentration). Although full conversion was still observed at 0.33 M concentration, the H-cube® flow began to slow down (Entry 2). The flow rate was increased to 2 mL/min, but still a gas appeared to be blocking the system, and the actual rate of flow was much slower. The gas was presumed to be hydrogen. The concentration of starting material solution was reduced to avoid this

blockage, and although this stabilised the system, the pump would still occasionally stop working. Nevertheless, the reaction was found to be high yielding up to a concentration of 0.2 M (Entry 4).

We attempted the reaction at 0.33 M concentration again but hoped that, by reducing the flow rate, the H-cube® would not block. The pump did not function well, and after rinsing the machine to extract any residual product, the concentration was lowered to 0.25 M. This product was taken on to oxidation, but a disappointing 35% yield of phenol was isolated (Entry 5). It was surprising that the automated system was disrupted by the formation of hydrogen, considering the original purpose of the system.



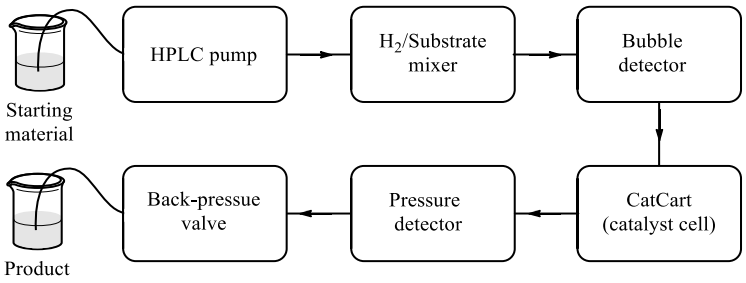
111 **130** **147**

Entry	Concentration	Flow rate (mL/min)	Scale (mmol)	Conversion (%) / Yield (%)	Comments
1	0.03 M	1	0.5	100 / -	-
2	0.33 M	1-2	0.5	100 / 87	Blocked pump
3	0.1 M	1	0.5	100 / 97	Stop/Start pump.
4	0.2 M	1	1.0	100 / 92	Stop/Start pump
5	0.33 M	0.5	1.0	100/-	Final molarity 0.25 M Stop/start pump oxidation yield 35%
6	0.2 M	1	2.0	100/-	Final molarity 0.16 M Oxidation 64%
7	0.1 M	1	1.0	100	Final molarity 0.05 M Oxidation 80%

Table: 3.5 Optimisation of oxidation in the H-Cube® microreactor

Only by considering the design of the H-cube® were we able to suggest an explanation for the problem. Of the stages in the system shown in Scheme 3.19, the bubble detector is normally relied on to maintain a free flowing solution. The hydrogen formed in the catalyst cell in our reaction may

well remain unobserved, as it arises after this detector, and the cause of blockage is thus beyond the control of the system.



Scheme 3.19: Flow diagram of H-Cube® microreactor

We settled on a dilute solution of starting material, followed by a generous rinse of the H-Cube® to ensure that no product was left in the microreactor (Entry 7, Table: 3.5). The dilute solution of product then had to be concentrated before the final oxidation could be enacted. Although the H-Cube® was reliable in converting hydrosilane **111** to methoxysilane **130**, this limit in concentration restricted the continuous flow of the procedure.

We believed we could improve on this process by building a flow set-up ourselves. When carrying out the reaction in batch, the catalyst was removed from the product by filtration through a Celite® plug, and it was thought that a flow system could be developed from this. If the Pd/C catalyst could simply be mixed with Celite®, and packed into a flash chromatography column above a packed layer of pure Celite®, then it seemed possible that the reaction and subsequent filtration could both occur within this column.

3.4.3. Optimisation of flow cell

The design of our first flow system is represented in Figure 3.4. Celite was packed into a flash chromatography column, before a mixture of Pd/C in Celite was packed above. Finally another layer of Celite® was added and packed down. It was thought that this set-up would allow us to control the moment that hydrosilane starting material would come into contact with Pd/C, and that

once this solution had passed by the catalyst, the bottom layer of Celite would prevent Pd/C from travelling any further down the column and into the product solution.

Our first attempt at methoxysilane **130** formation with this apparatus showed a great improvement on the H-cube®. A solution of hydrosilane could be eluted through the column with concentration 1.0 M. By submitting the hydrosilane to the column in such high concentration, we were able to subsequently rinse the system and dilute the product to a concentration of 0.3 M; the target final concentration.

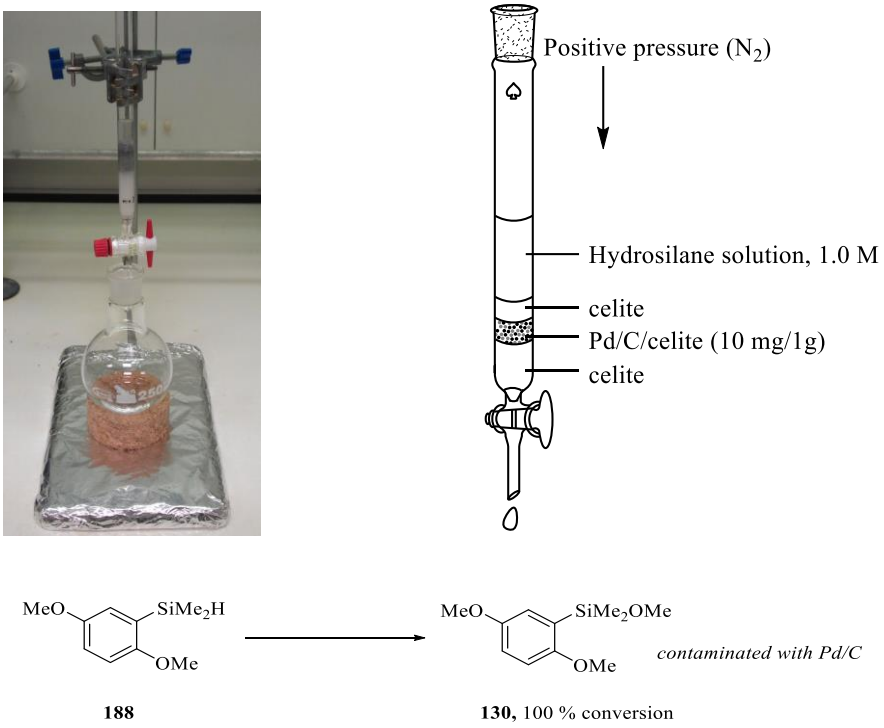
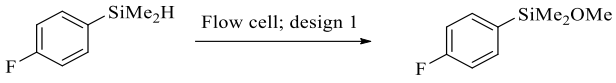


Figure 3.4: Flow cell; design 1

1.0 mol% of catalyst was used for this 1.0 mmol scale reaction but we were confident that a greater volume of solution could pass through the column and thus the catalyst equivalents could be dramatically reduced. Unfortunately, we found that under these conditions Pd/C leached through the column. This was an unacceptable result, as the hydrogen peroxide due to be added in the following oxidation had been found to decompose in the presence of Pd/C. The more readily available substrate **99** was tested until this issue could be overcome, where we soon discovered that leaching could be prevented by eluting methanol through the system before adding hydrosilane **99**.

Additionally, the catalyst loading could be lowered to 2.5 mg and the reaction scaled up 10-fold (Entry 2, Table 3.6). This brought full conversion on a 10 mmol scale with only 0.025 mol% loading of catalyst.



99 **126**

Entry	Mass Pd/C (mg)/Mass Celite (g)	Hydrosilane Concentration (M)	Scale (mmol)	Conversion (%) / Yield (%)	Comments
1	2.5 / 0.5	1.0	1.0	100 / 79	Pre-elution with MeOH
2	2.5 / 0.5	1.0	10	100 / 65	

Table 3.6 Flow cell optimisation I

We hoped to gain similar success with dimethoxyarylsilane **130**. Disappointingly, under the same conditions as described above, only 63% conversion was observed (Entry 1, Table 3.7). It became clear that the steric hindrance around the Si–H bond of substrate **111** inhibited the reaction and the conditions would have to be optimised again for this substrate. We hoped that, by increasing the catalyst loading, the percentage conversion could be improved. To our surprise, the conversion was poorer when 5 mg of Pd/C were added to the system. We concluded that the concentration of Pd/C in the cell was not inhibiting the reaction and thought instead that the length of the cell may be too short. Pleasingly the conversion did improve when the path length was increased, and finally we observed full conversion with 10 mg Pd/C in 2 g of Celite (Entry 4, Table 3.7) although this result was tainted by the resurgence of Pd/C in the product. We repeated the reaction on a large scale, but were again disappointed to obtain only 65% conversion. We had reduced the flow rate to improve the chance of full conversion so we were surprised by this poor result and decided to rethink our column set-up.



111 **130**

Entry	Mass Pd/C (mg)/Mass Celite (g)	Flow rate (mL/min)	Concentration (mol dm^{-3})	Scale (mmol)	Conversion (%)	Comments
1	2.5 / 0.5	8	1.0	10	65	
2	5 / 0.5	8	1.0	2.5	30	
3	5 / 1	8	1.0	2.5	70	
4	10 / 2	8	1.0	2.5	100	Slight Pd/C leaching
5	10 / 2	5	1.0	10	65	

Table 3.7 Flow cell optimisation II

The layer of Celite above the Pd/C prevented us from knowing when exactly the hydrosilane solution came into contact with Pd/C. We therefore decided to replace this layer of Celite with Pd/C in Celite, so that the oxidation would begin as soon as the hydrosilane solution was added to the flow cell (Figure 3.5). Additionally, the flow rate was reduced to increase the amount of time the hydrosilane was in contact with Pd/C.

The new procedure initially produced very good results (Entry 1, Table 3.8) and full conversion was observed on a 2.5 mmol scale. The product was collected in fractions so that any episodes of incomplete conversion could be identified more accurately. After scaling up the reaction however, the percentage conversion dropped during the experiment. During the batch process previously described, hydrogen was rapidly released from the system. In our flow-procedure, it was possible that hydrogen was not being released quickly enough from the flow cell (and perhaps the active palladium site) to allow further dehydrogenation to occur. A sacrificial alkene is commonly used in dehydrogenative process to remove hydrogen from the catalyst; however we hoped to overcome the issue by optimising the flow cell.[150]

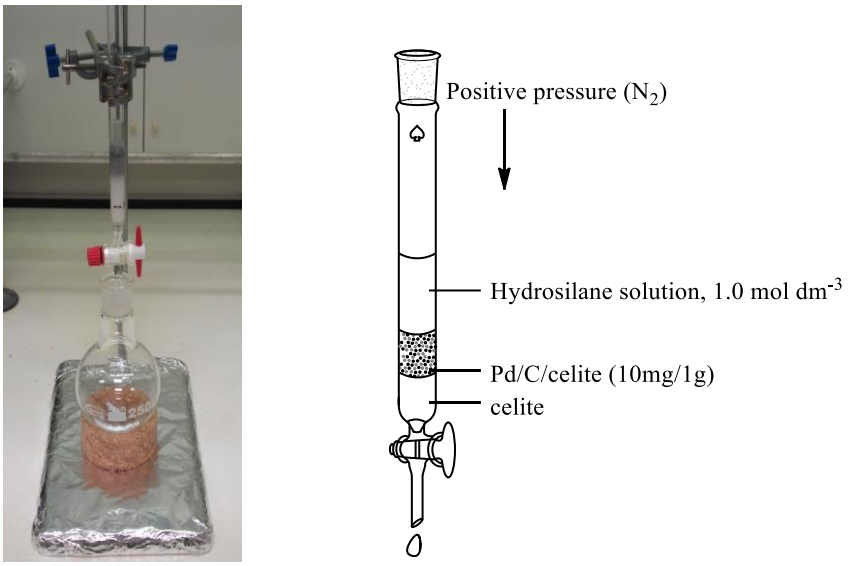
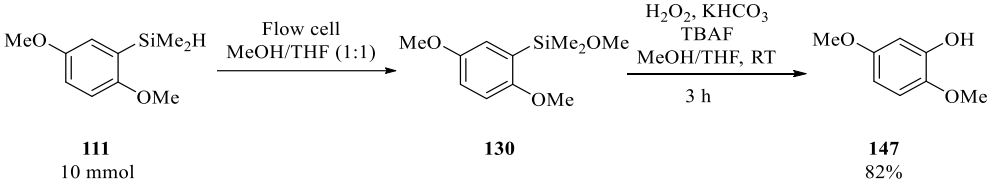


Figure 3.5: Flow cell; design 2

Entry	Mass Pd/C (mg) / Mass Celite (g)	Flow rate (mL/min)	Concentration (mol dm^{-3})	Scale (mmol)	Conversion (%)					
					F1	F2	F3	F4	F5	F6
1	10 / 1	5	1.0	2.5	-	100	100	100	100	-
2	10 / 1	5	1.0	10	100	50	30	95	-	-
3	10 / 1	5	0.5	10	100% conversion					

Table 3.8 Flow cell optimisation 3

Indeed this was possible and we were finally able to achieve full conversion on a 10 mmol scale by decreasing the concentration of the hydrosilane solution (Entry 3, Table 3.8). After rinsing the column, the product was diluted to 0.3 M and taken onto an oxidation reaction.



111
10 mmol

130

147
82%

Figure 3.6: Large scale flow cell/oxidation sequence

The final phenolic product **147** was isolated in 82% overall yield from hydrosilane **111** in multigram quantity. This corresponded to an extremely practical method of conversion to phenol, with 0.1 mol% of Pd/C.

3.5. Conclusions and future work

During attempts to prepare natural product khellinone **162**, the oxidation of arylsilanes was reliable, although further transformations of the aromatic ring were found to be challenging. After shifting the focus of this work to simpler target compounds, the strength of the methodology was proven in the rapid synthesis of natural and bioactive polyphenols. Despite some initial success, our investigation into cycloaddition reactions was limited by the propensity of silicon containing cycloadducts to collapse *via* retro-DA reactions. Futhermore, attempts to prepare novel protecting groups, based on our arylsilane methodology were heavily restricted by the reactivity of alkoxysilanes. More successfully, through the development of a flow-chemistry procedure, the synthetic utility and environmentally favourable nature of the arylsilane oxidation were greatly improved, allowing phenols to be prepared on a large scale with ease.

Since this work, the arylsilane oxidation has been applied in our group to the synthesis of natural product scaffolds.[151] Following the preparation of tricyclic arylsilanes through cyclotrimerisation of triynes, a number of oxidations were carried out.

4. A mechanistic study of arylsilane oxidation

4.1. Introduction

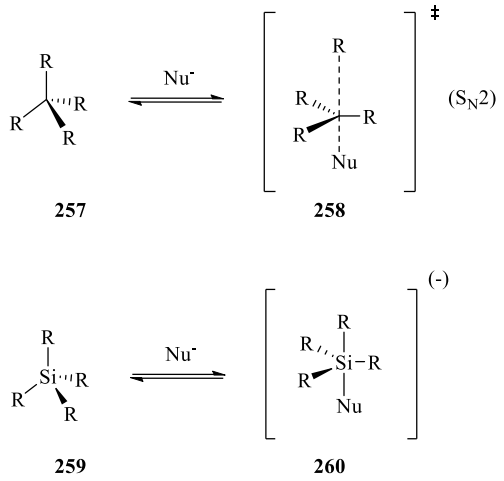
4.1.1. Overview

Throughout the methodology development described in Chapter 2, interesting variations in the selectivity and reactivity of arylsilane substrates towards oxidation were observed. The ability of the substrates to undergo fluoride-free oxidation was of particular interest and contradicted the general consensus of the literature.[69, 98, 152] Through the identification of silanol intermediates, we had discovered that multiple mechanistic pathways were likely to be present in the course of the oxidation and hoped to gain further insights through mechanistic experiments.

4.1.2. Chemistry of silicon

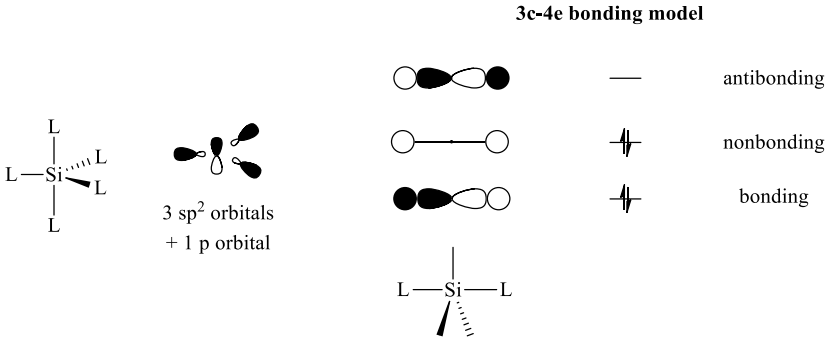
Before examining the mechanism of arylsilane oxidation, some characteristics of the organic reactivity of silicon are worth considering. Silicon's ability to form pentavalent structures explains much of its characteristic reactivity. Although carbon and silicon share the same valence electron configuration, they form very different structures when attacked by an anionic nucleophile (Scheme 4.1). The nucleophilic substitution of tetrahedral carbon centres is well studied, and an S_N2 transition state (**258**) generally accepted. A carbon pentavalent intermediate has never been observed; instead concomitant bond formation and dissociation takes place. In contrast, pentavalent silicon compounds (**260**) have been successfully isolated and characterised.[68, 153-154]

The traditional theory to explain this relied on low energy d atomic orbitals to form hybrid dsp^3 and d^2sp^3 orbitals. These d orbitals are only available to third-row elements or heavier, which conveniently explains why silicon can form more than four bonds while carbon cannot.[155]



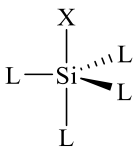
Scheme 4.1: Hypervalency of silicon

Later studies found this theory to be invalid and a more accurate bonding model is becoming accepted.[156] The d orbitals are believed to be at too high an energy to significantly contribute to bonding, and instead are thought to be limited in role to acceptor orbitals for back donation from ligands. Instead, the 3-centre-4-electron (3c-4e) bonding model has more recently been employed.[157-159] By considering the equatorial bonds, in a trigonal bipyramidal structure, to be bonded through 3 sp^2 orbitals, the remaining p orbital is left to form a linear 3c-4e bond. The linear combination of one p orbital and two ligand bonding orbitals results in a bonding, non-bonding and antibonding set of orbitals (Scheme 4.2). The stability of hexacoordinate silicon species has been studied, and the effect of silicon substituents found to be extremely important.[160-161] Chuit and co-workers found that only with predominantly electronegative substituents are stable hexacoordinate silane structures possible. This can be explained by the hexavalent bonding model involving three 3c-4e bonds, the electron density will be spread over all the substituents equally, thus electronegative substituents are necessary to stabilise this charge.



Scheme 4.2: Bonding theory of hypervalent silicon

The four electrons fill the bonding and non-bonding orbitals. Consequently, significant electron density is held on the axial (or apical) ligands. It is not surprising then that hypervalent silicon is most commonly observed with electronegative ligands, which stabilize this extra electron density and favour an apical position. Steric effects also contribute to apicolphilicity (Figure 4.1); small ligands, such as hydride, take the sterically most hindered apical position despite unfavourable electronic considerations.[162]



261

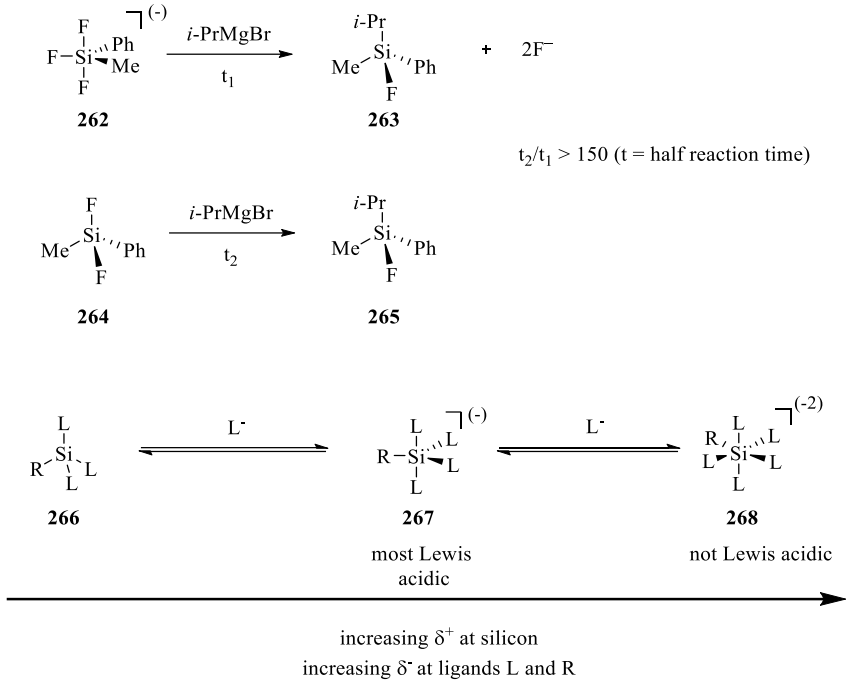
Preference for apical position

F > H > OH (OR) ~Cl > NR_2 > Ph > Me

Figure 4.1: Apicophilicity

Theoretical calculations show that despite the increase in negative charge on the whole system when an anionic ligand coordinates to tetravalent silicon, there is no significant change in charge on silicon. Some anionic ligands can in fact increase the degree of positive charge at a silicon centre, such as F^- coordinating to SiF_4.[163-164] This counterintuitive electronic effect can be used to explain the striking difference in reactivity of tetravalent and pentavalent silicon observed by Corriu and co-workers (Scheme 4.3).[165] Grignard addition to pentavalent silicon compound **262** was found to be over 150

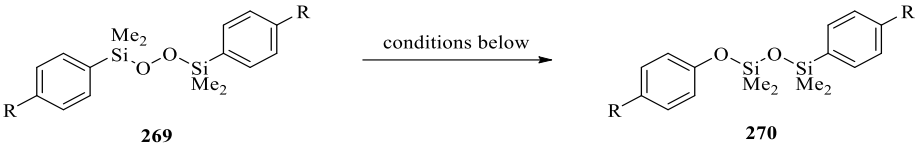
times faster than tetrahedral **264**, testament to the increased electrophilicity of silicon when coordinated to electronegative ligands. It is thus thought that many substitution reactions of silicon involve two nucleophiles. The first nucleophile acts as a catalyst by forming a reactive pentavalent intermediate, which is primed for displacement by a second nucleophile.[163] Hexacoordinate silicon **268** however is less reactive as silicon is unable to coordinate more than six ligands.



Scheme 4.3: Relative reactivity of tetravalent and pentavalent silicon

4.1.3. Current understanding of the mechanism of oxidative migration around silicon

The first report of a 1,2-migration from silicon to oxygen of silicon peroxides, by Davies and co-workers, included the observation that a phenyl group migrated more readily than a methyl group (Scheme 1.8).[56] A Hammett study of this reaction by Razuvaev and co-workers revealed that the thermal rearrangement exhibited a negative linear free energy relationship (LFER) with the electron density of the aryl ring (Scheme 4.4). However, with the addition of a nucleophile (KCN, KF or CsF), the opposite dependence was observed, signifying a change in mechanism.[166]

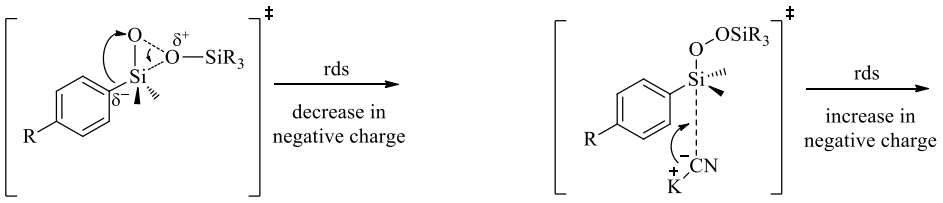


269 **270**

Conditions	ρ value / *p*-substituent rate dependence
Anisole, 100 °C	-0.88 / Br < H < Me < MeO
KCN (7.5 mol%), IPA, 50 °C	+2.04 / MeO < Me < H < Cl

Scheme 4.4: Thermal rearrangement of silicon peroxides

The thermal rearrangement was observed to show first order reaction kinetics while the catalysed process exhibited second order kinetics, with first order dependence on both the catalyst and peroxide. These findings suggest that the thermal rearrangement proceeds *via* nucleophilic attack of β-oxygen onto the silicon centre, with a build up of negative charge on the silicon substituents, including the aromatic ring (Scheme 4.5, mechanism 1). The following rate-determining migration of the aryl group would produce a decrease in negative charge on the aromatic ring. Conversely, a build up of negative charge on the aromatic ring would be expected from the nucleophilic attack of the KCN catalyst onto the silicon centre (Scheme 4.5, mechanism 2), correlating with a positive LFER and reaction order of two.



1st order TS
mechanism 1

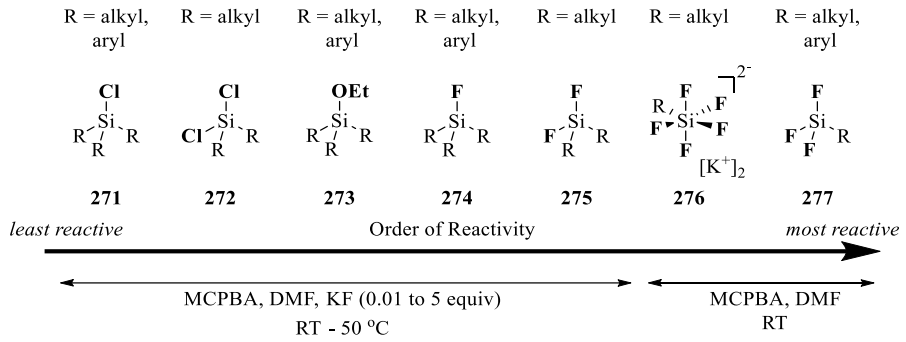
2nd order TS
mechanism 2

Scheme 4.5: Comparison of the transition states of thermal and catalytic rearrangements

Although full conversion was observed under thermal and catalytic activation conditions, significant solvolysis of the peroxide to form silanol, isopropoxysilane and molecular oxygen was observed when the catalyst concentration was increased. The ease of nucleophilic displacement of labile silicon

substituents is a central theme to our mechanistic work, and will be highlighted whenever mentioned in the literature.

Some twenty years later, the *m*CPBA oxidation of a number of organosilanes was reported in multiple publications, predominantly by Tamao and Kumada (See Chapter 1).[57-60] Over the course of this work, many species were found to undergo oxidation (Scheme 4.6).[60] In tetracoordinate silanes, the reactivity increased with fluoride substitution. Although pentafluorosilanate anion **276** also displayed high reactivity, it was less reactive than trifluorosilane **277**. As previously discussed, hexacoordinate **276** is no longer Lewis acidic as no further coordination is possible, therefore reactivity is inhibited. This was found to be the case for hydrogen peroxide oxidation of pentavalent silicon, later studied by Tamao and co-workers.[68] Although the diorganodifluorosilane **275** could undergo oxidation, the addition of KF dramatically increased the reaction rate. Substrates less reactive than **275** required super-stoichiometric KF to promote complete oxidation of all R substituents to alcohols. The reaction was found to be very sensitive to the nature of solvent used, specifically by the Lewis basicity of the solvent. High yields were reported for oxidations in DMF, *N*-methylpyrrolidone and HMPA: solvents that are strongly Lewis basic. Indeed, solvents that were unfavourable for oxidation such as diethyl ether and THF could be employed if accompanied by just one equivalent of HMPA.



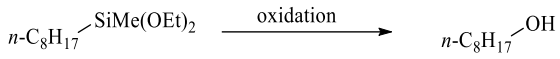
Scheme 4.6: Reactivity of halosilanes to *m*CPBA oxidation

These effects suggested to the authors that solvent coordination to the silicon centre must play an important role in the mechanism of the oxidation. Solvent coordination to the silanes was then

confirmed spectroscopically by apparent scrambling of the ^{19}F spectra of fluorosilanes in the presence of DMF or HMPA.

Shortly after the discovery of these findings, Tamao and co-workers found that 30% aqueous hydrogen peroxide could bring about similar results and optimised the process using dialkoxysilanes. With water as a by-product, and at a lower cost than *m*CPBA, the oxidation with hydrogen peroxide was an improvement.[63-65] Selected examples from their oxidation optimisation are shown in Table 4.1. Of note is the discovery that weak alkaline conditions, albeit with heating, can replace the need for fluoride to promote the reaction (Entry 6).

By varying the alkoxy substituent on the silane, the effect of sterics on the reaction rate were observed. As the size of alkoxy group increased, the oxidation became less favourable; although an ethoxysilane would oxidise under fluoride or base activated conditions (Table 4.1, entry 3 and 4 respectively), more forcing conditions were required for *iso*-propoxy- and *tert*-butoxy-silane oxidation (not shown).



278 **279**

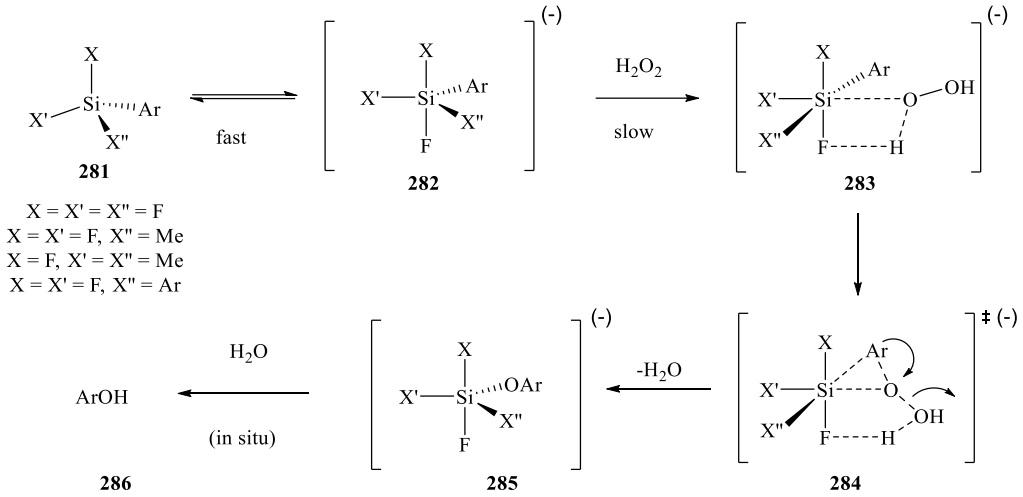
Entry	Oxidant (equiv)	Additive (equiv)	Solvent	Temperature, °C (time, h)	Yield, %
1	*m*CPBA (2.5)	KHF_2 (2)	DMF	RT (2)	91
2	30 % H2O2 (12)	KHF2 (2)	DMF	60 (7)	82
3	30 % H2O2 (12)	KHF2 (2)	MeOH/THF (1:1)	60 (7)	83
54	30 % H2O2 (12)	KHCO3 (1)	MeOH/THF (1:1)	reflux (3)	96

Table 4.1: Optimisation of Tamao-Kumada H_2O_2 oxidation

Tamao and co-workers were able to confirm through competition experiments that aromatic groups migrate from a silicon centre in preference to other alkyl groups. Significantly, the methyl group was rarely found to oxidise, and this allowed all further discussion of the mechanism to take place with confidence that the migration of methyl substituents around silicon need not be considered. In all

future discussion of the mechanism of arylsilane oxidation, the assumption will be made that the rate of methyl migration around silicon is negligible.

The effect of functional groups on silicon was then studied, and the relative rates of oxidation observed are shown in Scheme 4.7. A positive effect of fluorine substitution to the silane was observed for the *m*CBPA oxidation of silanes (Scheme 4.6) and this trend is partially mirrored under H_2O_2 conditions. However, the slow reactivity of $PhSiF_3$ does not follow the trend (Scheme 4.7).



Relative rate of oxidation: $PhMeSiF_3^-$ > $PhMeSiF_2$ >> $PhMe_2SiF$ > $PhSiF_3$
(reaction conditions: H_2O_2 (1 equiv), TBAF (1 equiv), THF, 10 °C)

Scheme 4.7: Tamao mechanism of H_2O_2 oxidation

Of the pentavalent precursors to migration shown in Figure 4.2, the silicon centre in silane **288** will hold a greater positive charge than the silicon centre in silane **287** due to the extra electronegative fluorine substituent. This extra positive charge may actually result in a stronger Si–C bond: as the silicon atomic orbitals contract, they may overlap better with the carbon atomic orbitals (both in size and energy). The paradoxical low reactivity of $PhSiF_3$ may be a result of this strong Si–C bond which would limit the rate of migration to the extent that it becomes the rate determining step. Additionally, the formation of hexacoordinate silane **289** from $PhSiF_3$ can be envisaged, as the species is highly stabilised with five fluorine substituents. Species **289** however, may inhibit the reaction as it is less

susceptible to further nucleophilic attack; only by fluoride dissociation can hydrogen peroxide coordinate.

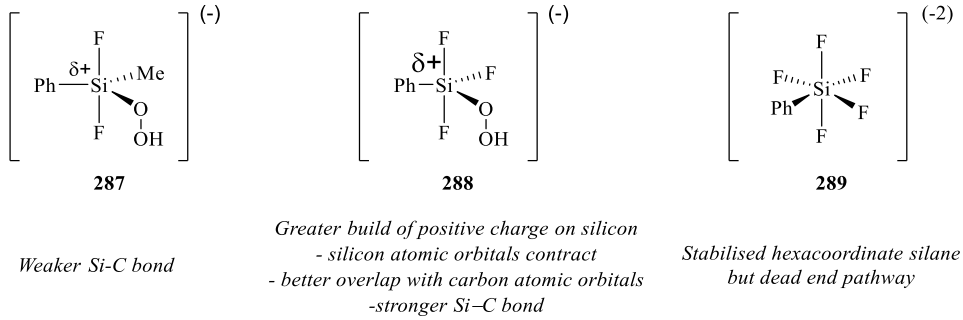
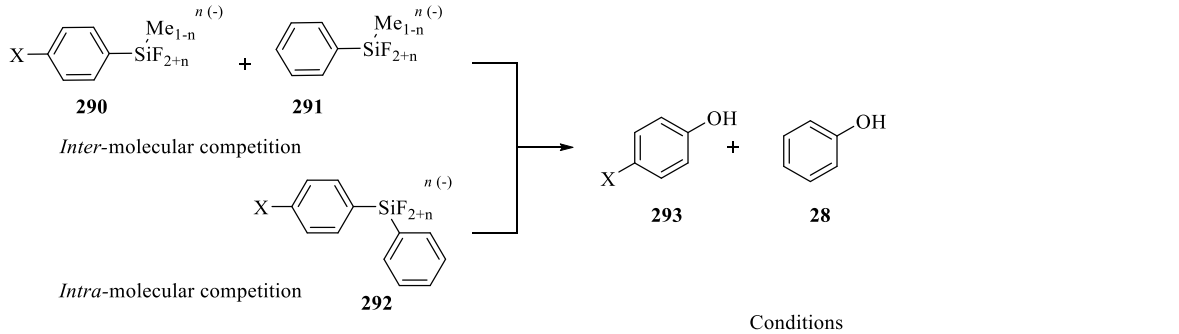


Figure 4.2: Reactivity of Tamao arylfluorosilanes

The phenylsilane oxidation reactions studied by Tamao were found to be heavily affected by the presence of a fluoride source; $PhMeSiF_2$ did not react at all without the addition of TBAF. By preparing a pentavalent species $[PhMeSiF_3]^-$ the authors were able to conduct the oxidation without a fluoride source (although fluoride is likely to be released following oxidation). Notably, no other substrates were tested without TBAF. Tamao therefore proposed that the oxidation would begin with a rapid equilibrium between starting material **281** and fluorinated pentavalent intermediate **282** (Scheme 4.7). Subsequently, slow hydrogen peroxide coordination to silicon, encouraged by hydrogen bonding with a fluorine substituent, would determine the rate of the oxidation. Hexacoordinate intermediate **283** would rearrange through transition state **284** with concomitant loss of water.

A study on the electronic effects of the migrating aromatic group revealed a LFER in the oxidation, with a positive ρ value, which is consistent with our own Hammett study (Chapter 2). As the aromatic ring increases in electron density, the rate of conversion decreases. This reflects a developing negative charge in the transition state of the rate determining step of the reaction during hydrogen peroxide coordination to the silicon centre.

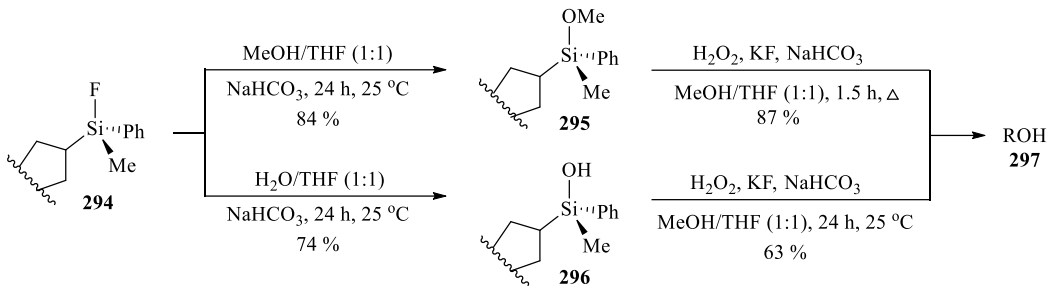


Intermolecular competition		**Intramolecular competition**	
$n = 0$	$n = 1$	$n = 0$	$n = 1$
$\rho = +1.1$	$\rho = +1.1$	$\rho = +0.5$	$\rho = +0.6$

Scheme 4.8: Competition experiments of H_2O_2 oxidation

Tamao explained the ρ-value for the intramolecular competition by considering the relative ease of aryl group migration, this would require the migration to be the rate limiting step. The intermolecular competition results were thought to express the relative rate of hydrogen peroxide addition to silicon. It is possible however that the smaller intramolecular ρ-values are actually a result of the moderating effect of an additional phenyl group substituted on silicon: as **292** varies, the subsequent variation in electron density at silicon may be limited by the constant phenyl substituent.[56, 166]

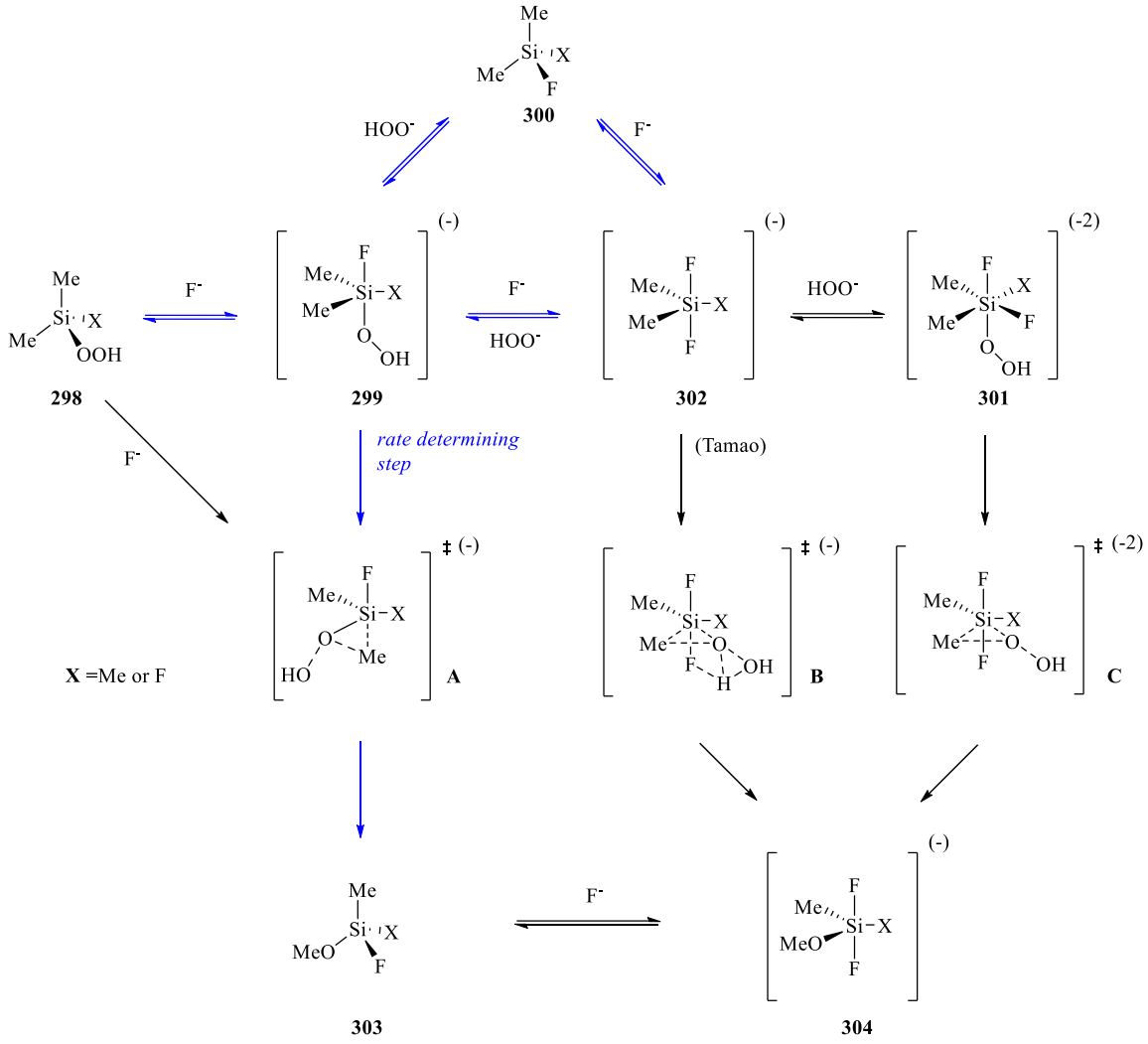
During the methodology development described previously (Chapter 2), the most intriguing results obtained were the observation and isolation of side products. Similar observations have been found in the oxidation work of Knölker and co-workers.[167] Under Tamao oxidation conditions, fluorosilane **294** was shown to undergo partial conversion to alcohol **297** as well as intermediates methoxysilane **295** and silanol **296**. It was possible for the authors to synthesise these intermediates selectively by simply omitting the oxidising agent from the reaction to form methoxysilane **295**, or replacing methanol with water to form silanol **296**. These findings correlate with our own, and also support our theory that fluoride displacement is favoured under these conditions, despite the well known strength of the Si–F bond .



Scheme 4.9: Isolation of oxidation intermediates

The most recent additions to the discussion of the Tamao-Kumada oxidation mechanism were two theoretical studies contributed by Mader and Norrby (Scheme 4.10). Formation of an anionic pentavalent intermediate was assumed to be the first step in any oxidative pathway. Within this condition two possible nucleophiles (HOO^- and F^-), and the following possible mechanisms were compared.[168] The authors highlighted in this work that the thermodynamic driving force for the reaction is the simultaneous breaking of the weak O–O bond and formation of strong Si–O and C–O bonds. The rate determining step was presumed to be breaking of the O–O bond, simultaneous with migration of the alkyl substituent. This is in contrast to the hypothesis of Tamao.

Transitions states **A**, **B**, and **C,** shown in Scheme 4.10, were considered. Silane **298** was found to be a stable intermediate in solution, however a direct S_N2 route to its formation was calculated as unlikely; the pentavalent intermediate **299** would be formed in preference to **298**. Although a stable intermediate, silane **298** cannot be considered as part of the major reaction pathway, as fluoride attack is only likely to result in formation of intermediate **299**, and not direct alkyl migration through transition state A. In general, pentavalent intermediate **299** was found to be low in energy, and nearly isoenergetic with fluorosilane **300** in methanol. Transition state **B** (Tamao mechanism Scheme 4.7) was calculated to be at a much higher energy than transition state **A**. Formation of hexacoordinate intermediate **301** was also found to be disfavoured in solution, again with higher energy than transition state **A**. Pathways through this intermediate were therefore deemed unlikely.

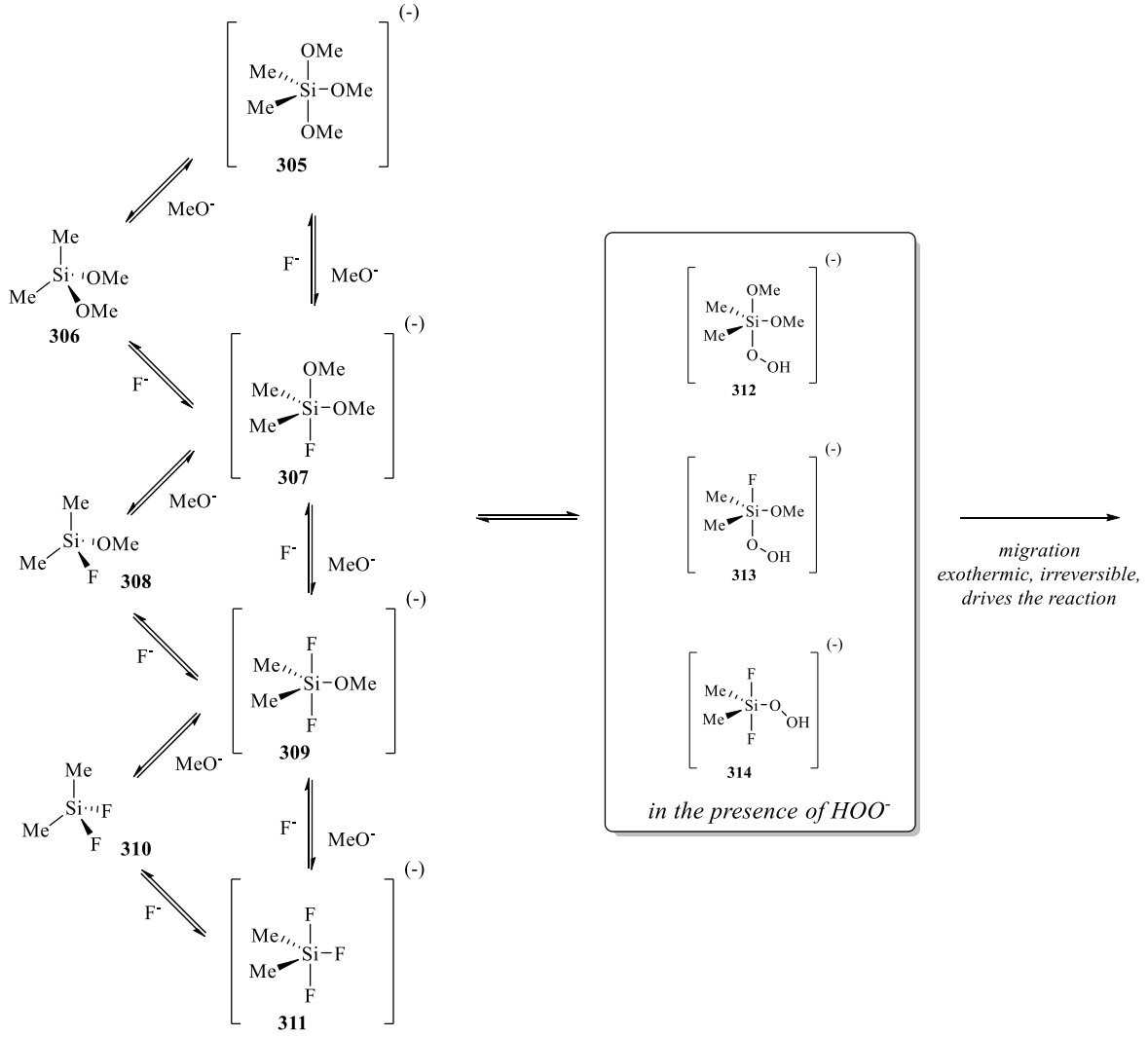


Scheme 4.10: Mader and Norrby mechanistic work

The geometries of the transition states were also considered; as previously highlighted, the hydroperoxide anion would add at the axial position and generally occupy axial positions (see previous discussion). To facilitate alkyl migration, the peroxide substituent would then rotate to an equatorial position.

Overall, formation of transition state **A** from silane **300** was determined to be the most favourable mechanistic pathway. Although this system was not identical to our system, it seemed possible that the results may be extended to our reactions. The anionic pentavalent intermediate was therefore regarded as the most likely precursor in the oxidation.

It was not until the second study was published by Mader and Norrby, which focused on the effect of fluoride on the oxidation of alkoxysilanes, that methoxide and hydroxide anions were identified as competitive nucleophiles to fluoride and hydroperoxide anions. Under standard Tamao conditions of mildly basic MeOH/THF and aqueous hydrogen peroxide, all these nucleophilic species should be expected to be present (Scheme 4.11).[152]



Scheme 4.11: Background equilibria and oxidation in the Tamao-Kumada oxidation

In the presence of an excess of fluoride source, the authors believed that alkoxysilane **306** would slowly, through a series of equilibria, convert to the more stable fluorinated intermediate **310**. These equilibria would form in the absence of hydrogen peroxide, and are represented by the transformations shown outside of the box in Scheme 4.11. As previously found, migration around a

pentavalent anionic transition state, with loss of hydroxide, was assumed to be the most favoured mechanistic pathway. With the addition of hydrogen peroxide, intermediates **306** to **311** would still be rapidly interconverting, but intermediate **312**, or its fluorinated equivalents **313** and **314**, can now also form at any moment by hydrogen peroxide anion attack. The migration transitions states of lowest energy were formed from fluorinated intermediates **313** and **314**. The major pathway can therefore be considered to travel through these species in accord with the Curtin-Hammett principle.

Fluoride free conditions were also discussed: tetravalent starting material **306** has the lowest energy, however the two pentavalent intermediates **305** and **312** are of comparable, and relatively low, energy. The actual migration is exothermic, and should drive the reaction through the transition state formed from intermediate **312**. The advantage but not dependence of adding a fluoride source to the oxidation can be explained by this mechanism. By converting the starting material to its fluorinated derivative through a series of equilibria, more reactive substrates for oxidation are formed.

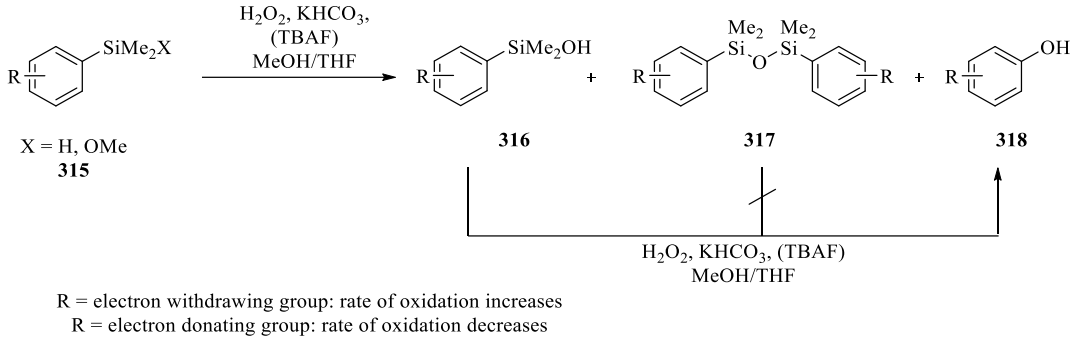
The geometry of the transition state was also considered. Again, although a hydroperoxide ion prefers an axial position in the pentavalent intermediate, the preferred geometry of the transition state involves an axial methyl group and equatorial hydroperoxide group. Fortunately the low barrier to Berry pseudorotation allows this arrangement to form with ease.

Although these studies give greater theoretical insight into the ease of nucleophilic substitution at silicon centres under Tamao-Kumada conditions, the formation of silanol intermediates was not predicted by Mader and Norrby.

4.2. Summary of previous observations

The most striking observation throughout our methodology development was the variation in reaction times for substrates of differing aromatic electron density. This was quantified during the Hammett study described in Chapter 2. A positive LFER was observed which corresponds to a build up in negative charge, proximal to the aromatic ring, in the transition state of the rate determining step of

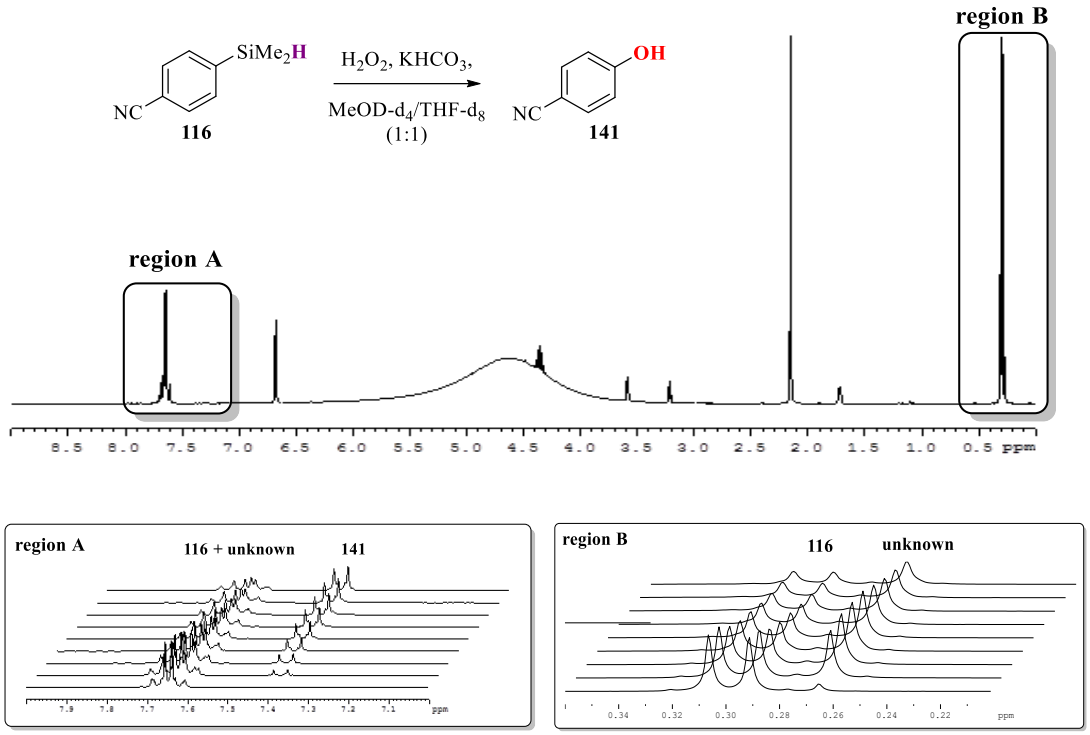
the reaction. We had found that complete conversion of arylsilanes (all methoxysilanes and all but electron rich hydrosilanes) to phenols was possible without TBAF, but that just 0.1 equivalents of TBAF could significantly decrease the time needed for full conversion. Through TLC experiments and NMR aliquots we were able to identify two side products of the fluoride free oxidation; silanol **316** and disiloxane **317**. After isolating and submitting these compounds to the reaction conditions, it was observed that silanols **316** would undergo oxidation, but disiloxanes **317** would not (Scheme 4.12).



Scheme 4.12: Summary of empirical mechanistic observations

4.3. Preliminary investigation

As discussed in our methodology development, quantification of the composition of the oxidation reaction mixture through aliquots was not possible as the work-up procedures appeared to cause further transformations of the intermediates. To overcome this we hoped it would be possible to observe the reaction *in situ* with NMR spectroscopic experiments. Our investigation began by following the oxidation through ^{1}H NMR spectroscopy. Unfortunately, this was limited by the high concentration of water in the reaction, which brought about a broad peak in the ^{1}H NMR spectra and over-integration of other overlapping resonances within it (Figure 4.3). To limit this problem, we chose our most electron deficient, 4-(dimethylsilyl)benzonitrile (**116**) to begin our study. The aromatic peaks were at as great a distance as possible from the distorting effect of the water peak.



^{1}H NMR spectra of arylsilane oxidation in 1:1 MeOH-d_4/THF-d_8

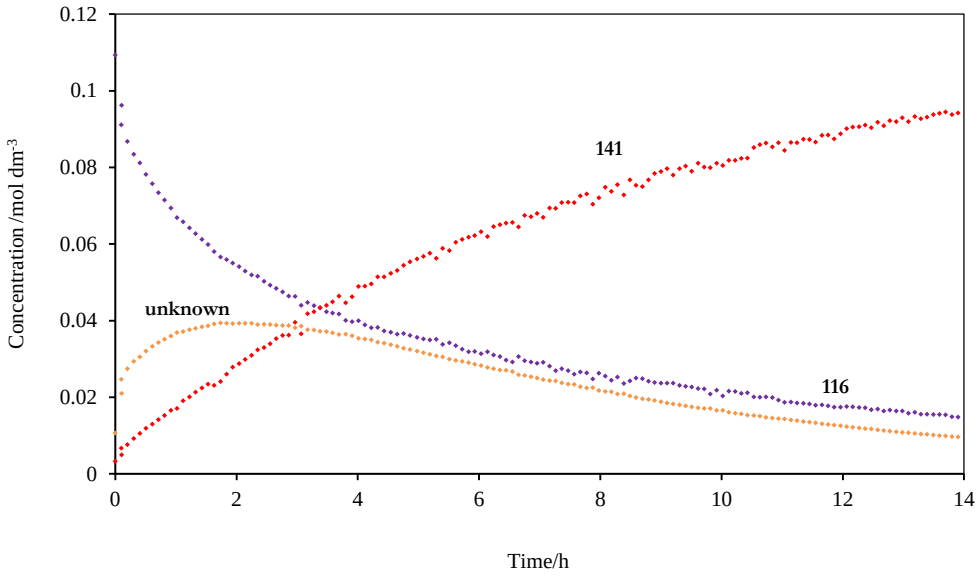


Figure 4.3: ^{1}H NMR spectroscopic observation of 4-(dimethylsilyl)benzonitrile oxidation in 1:1 MeOH-d_4/THF-d_8

The concentration of the reaction was lowered to 0.1 M (from 0.3 M) to slow the rate of reaction and allow accurate profiling of changing concentrations (Figure 4.3). Reaction progress was followed by focusing particularly on the two regions in the spectra highlighted (A and B, Figure 4.3). In the

aromatic region, we were able to observe phenol formation, however it was not found to be a suitable region to observe other arylsilane intermediate transformations as the aromatic resonances of these compounds frequently overlapped. As the reaction progressed, sharp arylhydrosilane signals were transformed into indecipherable multiplets. Fortunately, region B was much more informative. Alongside steady consumption of arylhydrosilane **116**, rapid formation of an intermediate, with a singlet at approximately 0.27 ppm, was also observed. This intermediate, which was itself consumed as the reaction progressed, was assigned as silanol **117**, as had commonly been found in our other work. The lack of coupling to other protons of this resonance also supported a silanol structure. It was still not possible however, to compare directly the chemical shifts of our experiment to the data we had obtained to characterise silanol **117**, as the mixed solvent system of the oxidation affected ^{1}H NMR chemical shift values. Instead, to confirm the silanol assignment, we submitted an authentuc mixture of silanol **117** and hydrosilane **116** to the same conditions, and observed identical ^{1}H NMR chemical shifts of these compounds to the intermediates of the previous experiment as well as a very similar concentration profile (Figure 4.4). This was felt to be indisputable evidence of the silanol assignment

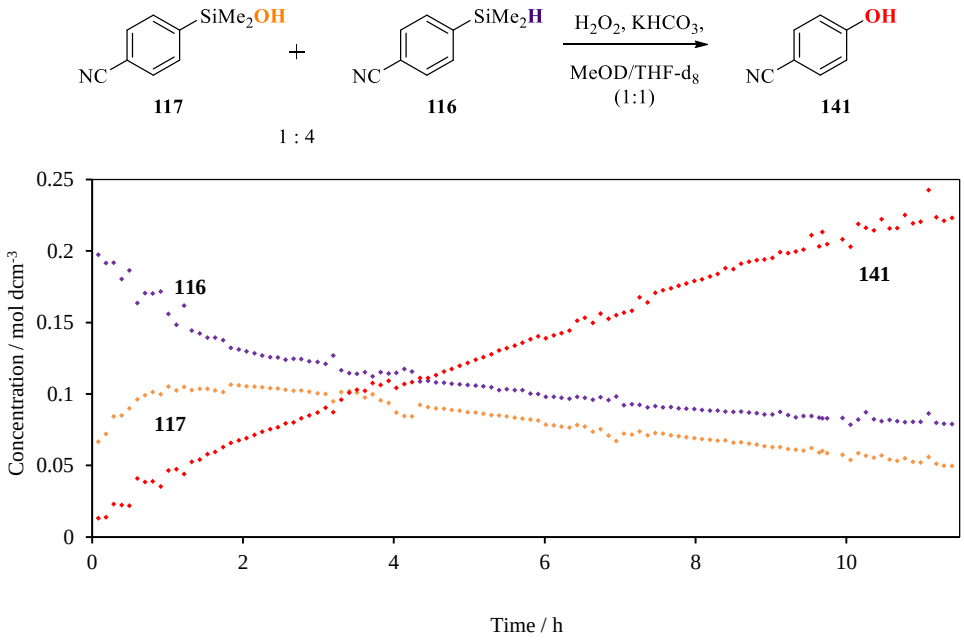
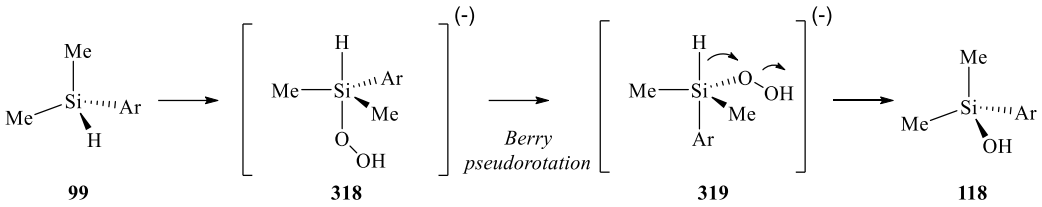


Figure 4.4: ^{1}H NMR spectroscopic profiling of silanol/hydrosilane oxidation reaction in 1:1 MeOH-d$_4$/THF-d$_8$

We were very interested to see the true extent of silanol formation during the oxidation of arylhydrosilanes. We had previously thought that the supposedly inert hydrosilane would most likely react *via* this intermediate, itself formed from a 1,2-hydride shift (Scheme 4.13), before oxidation to phenol was possible, but had not anticipated the extent if its build up during an oxidation. Arylhydrosilane **99** holds no electronegative heteroatom substituents, as are believed to be required for arylsilane oxidation, and we therefore believed the silanol to be a true intermediate and not a side product in the reaction. The geometry of pentavalent silicon in the transition state can be envisaged to follow the predictions made by Mader and Norrby (Scheme 4.10).



Scheme 4.13: Hydrosilane semi-oxidation mechanism

Initial hydroperoxide attack of silane **99** would form intermediate **318** with diaxial hydrogen and hydroperoxide. Following a Berry pseudorotation to pentavalent intermediate **319**, an axial to equatorial migration may occur. The aromatic group in intermediate **319** is also aligned in the correct geometry to migrate, thus the initial formation of silanol before phenol is a testament to the higher migratory aptitude of hydride compared to aryl groups.

We were disappointed with the quality of the data shown in Figure 4.4; although the essential trends could be observed, the method was not consistent and the individual data points often appeared inaccurate. The problem was likely to be a result of the broad water peak (seen in the NMR spectrum, Figure 4.3) so we looked towards other NMR-active nuclei which could be observed spectroscopically. With fluorinated substrate **99** already in hand, it seemed most convenient to move to ^{19}F NMR spectroscopy as a suitable method of observing the reaction. Fluorine nuclei would only be found on the silicon substrates under investigation; the solvent and other reagents would no longer be able to distort the observation of the oxidation. The synthesis of all but one fluorine containing

species has been described in the previous chapters (Figure 4.5), and fluorosilane **322** was prepared *via* a copper mediated process.[169]

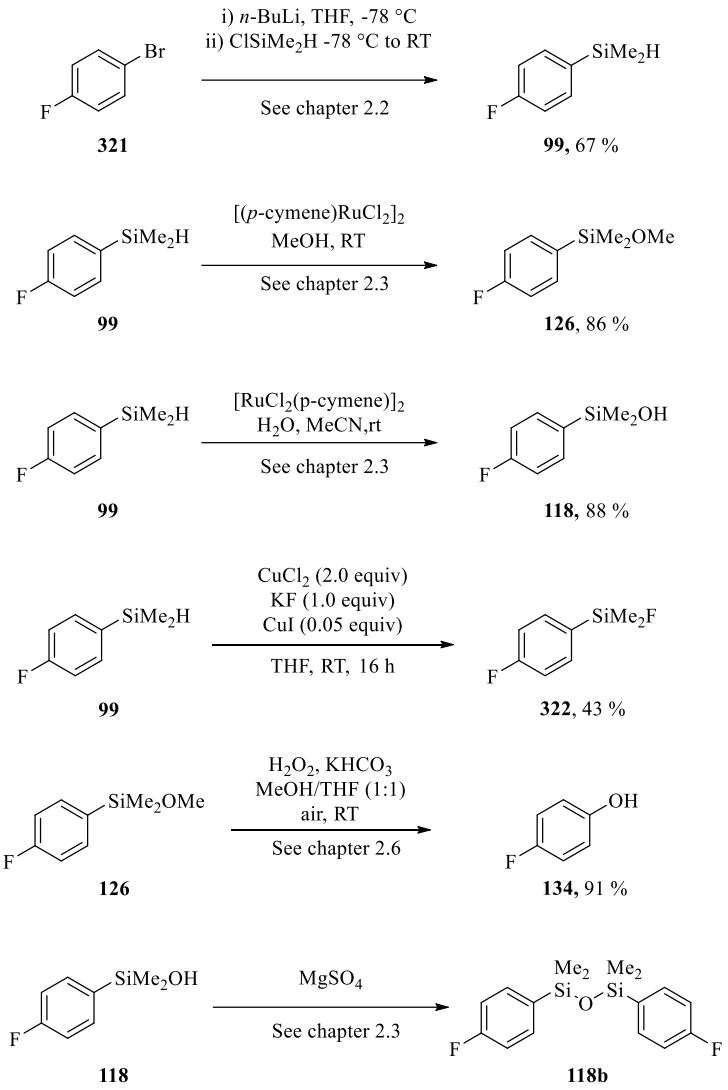


Figure 4.5: Synthesis of 4-fluorophenylsilanes and 4-fluorophenol

4.4. Observing the oxidation by ^{19}F NMR spectroscopy

The advantages of ^{19}F NMR over ^{1}H NMR spectroscopy were obvious from our first experiment. Far clearer spectra were obtained when the oxidation of fluorosilane **99** was monitored. The intermediates were found to have distinct chemical shifts, allowing us to follow their individual concentrations with accuracy (Figure 4.6). Hexafluorobenzene was added to the reaction to act as an

internal standard, under the assumption it would behave as a spectator, and therefore that its concentration would remain constant. We used a solvent mixture of 1:1 MeOD/THF-d_8 with the magnetic field "locked" onto THF-d_8. A spectrum taken during the oxidation of hydrosilane **99** is shown in Figure 4.6.

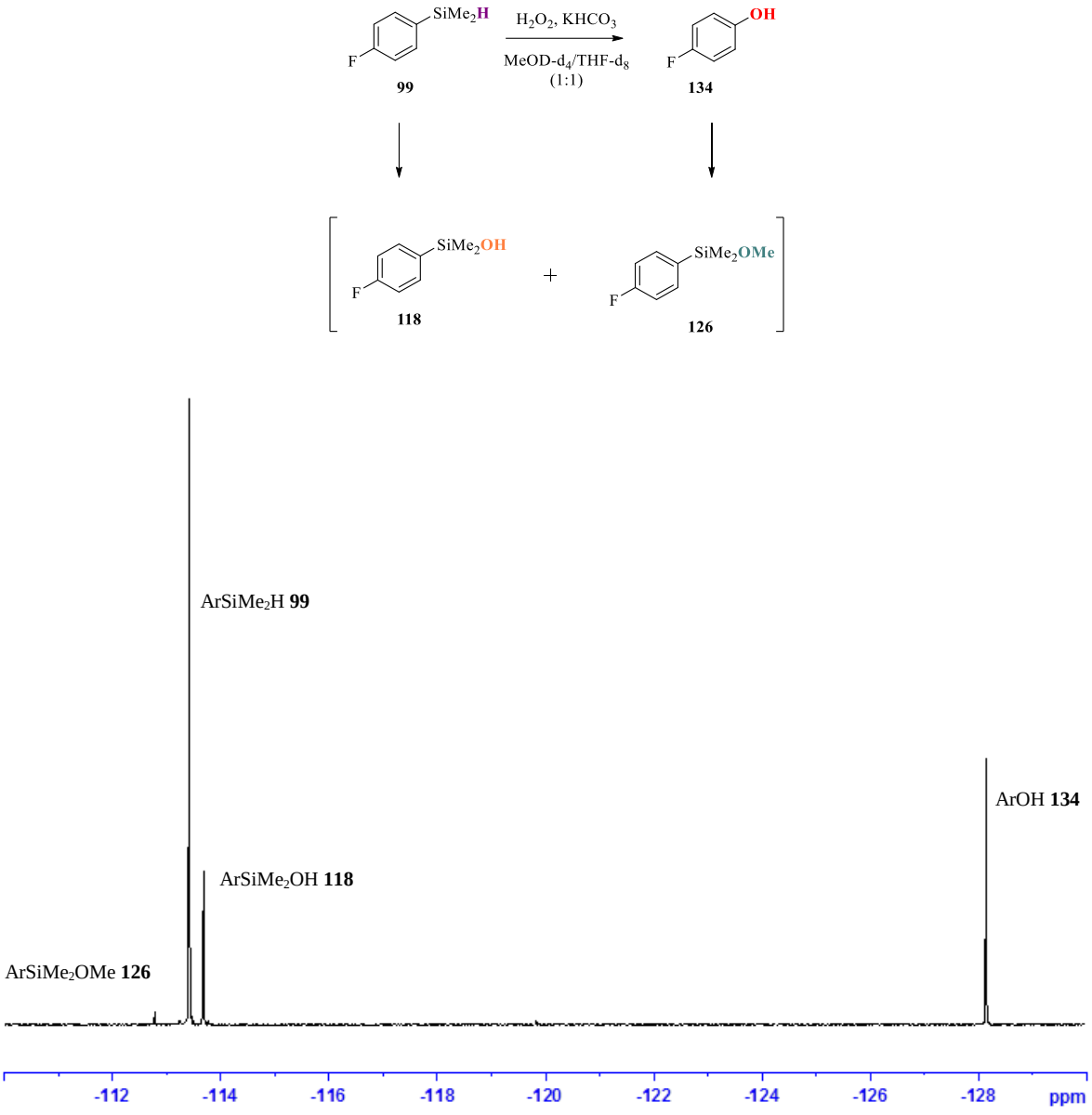


Figure 4.6: ^{19}F spectrum mid-arylsilane oxidation in 1:1 MeOH-d_4/THF-d_8

The absolute resonances observed in the reaction were very sensitive to changes in solvent (see Table 4.2) and could only be assigned by comparison with other NMR spectroscopy experiments, or by doping the reaction once it was complete, and observing an increase in concentration of a species at a

particular chemical shift. It was also interesting to note that the *relative* chemical shift of silanol and methoxysilane varied with solvent. Most arylsilane species shifted by approximately 1.7 ppm when measured in the polar reaction solvent mixture instead of non-polar $CDCl_3$. However, silanol **118** and phenol **134** are seen to shift by greater values. It was thought this could be explained by the ability of these two hydroxyl containing compounds to form hydrogen bonds in the polar solvent. This bonding interaction polarises the O–H bond which results in a build up in negative charge on the oxygen. Increased electron shielding of the fluorine nucleus can therefore be understood through the distribution of this charge onto the aromatic ring.

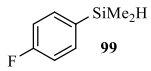
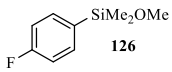
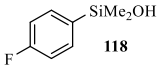
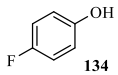
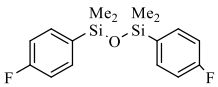
Fluorosilane	^{19}F NMR chemical shift (δ) relative to C_6F_6 in $CDCl_3$ (ppm)	^{19}F NMR chemical shift relative (δ) to C_6F_6 in THF/MeOH/H_2O (ppm)	Δδ
 **99**	53.1	51.4	1.7
 **126**	53.6	52.0	1.6
 **118**	53.9	51.1	2.8
 **134**	40.7	36.7	4.0
 **118b**	53.4	51.7	1.7

Table 4.2: ^{19}F NMR chemical shift values of arylsilane intermediates

By integrating the spectra over time, the concentration profile shown in Figure 4.7 was obtained. As a result of the increased electron density at silicon of fluorinated substrate **99**, the overall rate of oxidation was slower than that of nitrile containing substrate **116**.

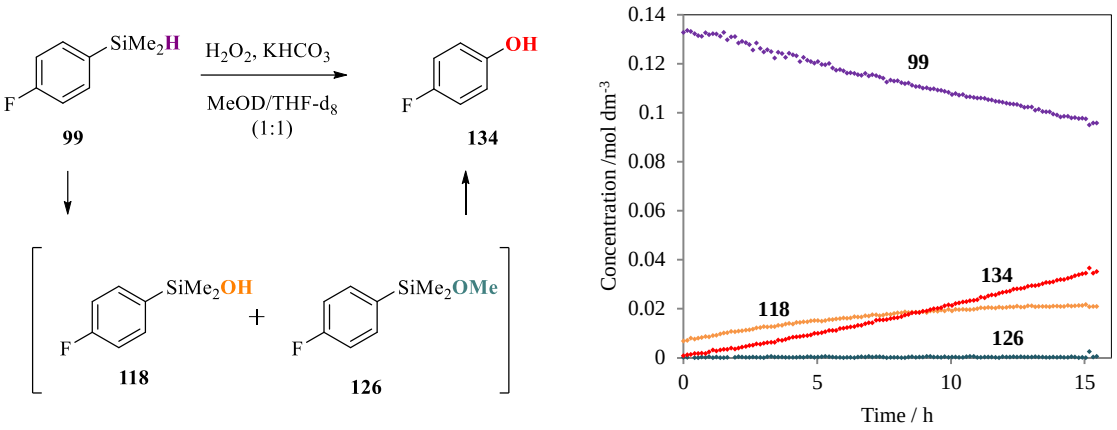
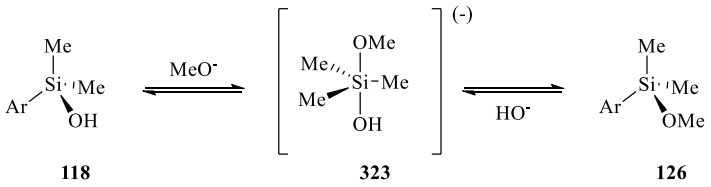


Figure 4.7: ^{19}F observation of the oxidation of hydrosilane in 1:1 MeOH-d$_4$/THF-d$_8$

This experiment enabled us to observe more subtle details of the early phase of the oxidation. The slow rate of formation of silanol intermediate **118** appears to significantly affect the formation of phenol; there is a considerable lag in the production of phenol until after a certain amount of silanol has formed, which also provided further strong evidence that hydrosilane **99** itself would not undergo arene oxidation. There was an additional small resonance observed in the ^{19}F NMR spectra which we were able to identify as methoxysilane **126**. This intermediate is well precedented; the attack of methoxide anions was predicted by Mader and Norrby and the methoxysilane intermediate isolated by others (Scheme 4.14).[98, 152, 167]



Scheme 4.14: Equilibrium of methoxysilane and silanol

We were now confident that all intermediates or side products, that build up to a significant concentration during oxidation, had been identified, and were anxious to understand the role of these species in the oxidation. We hoped to discover which of these species was most reactive, and from that develop a stronger understanding of the mechanism of oxidation, and potentially improve our conditions for the reaction. We had already learnt that the oxidation of silanol is slower than the

oxidation of methoxysilane. This strongly indicates that methoxysilanes are more reactive than silanols towards oxidation, which in turn implies that formation of methoxysilane **126** in the oxidation shown above (Figure 4.7) could provide the most favourable pathway to oxidation.

4.4.1. Experimental conditions

In the following NMR spectroscopic studies, we continued to use a 1:1 solvent mixture unless otherwise stated. Towards the end of the work, h_8-THF was used instead of d_8-THF to reduce the cost of the study. The magnetic field was locked on to MeOD, which had no noticeable effect on the results obtained. As before, hexafluorobenzene was used as an internal standard in all ^{19}F experiments.

It was not possible to run the experiments with sufficient delay between pulses to avoid saturation of the signal. Although this led to a small inaccuracy in the integration of our spectra, the delay required would have significantly restricted our ability to observe the reaction through its most dynamic initial phase. The spin lattice relaxation constants (T_1) of the reactive components were approximated using the inversion recovery method.[170] A T_1 value of 3.6 was obtained for both methoxysilane **126** and 4-fluorophenol **134** while perfluorobenzene held a T_1 value of 2.2. We were then able to carry out NMR experiments to calculate any error which may occur during out experiments (see experimental details). When spectra were collected with a relaxation time of 5.5s the error was found never to rise above 5%. Nevertheless, the crude integration values obtained during our spectroscopic experiments were corrected and thus the accuracy of integration of our NMR spectra was believed to be sound.

Unfortunately a limitation of the experimental method remained. Typically for ^{19}F NMR spectroscopy, the automatic phasing parameters were often incorrect and resulted in spectra that were not set for reliable integration. Instead, the phasing had to be corrected manually for each spectrum. This was, unfortunately, a laborious process; however the informative nature of the concentration profiles obtained motivated us to continue with this method.

4.4.2. Concentration profiles of fluoride free oxidation

The concentration profiles of silanol **118** and methoxysilane **126** were required to compare the reactivity of these two species. The oxidation of silanol proceeded with a faster rate of phenol formation than that observed for hydrosilane **99** (Figure 4.8). This can be understood if the formation of silanol in the oxidation of hydrosilane **99** is rate determining. During the oxidation, methoxysilane **126** was also observed in low concentrations.

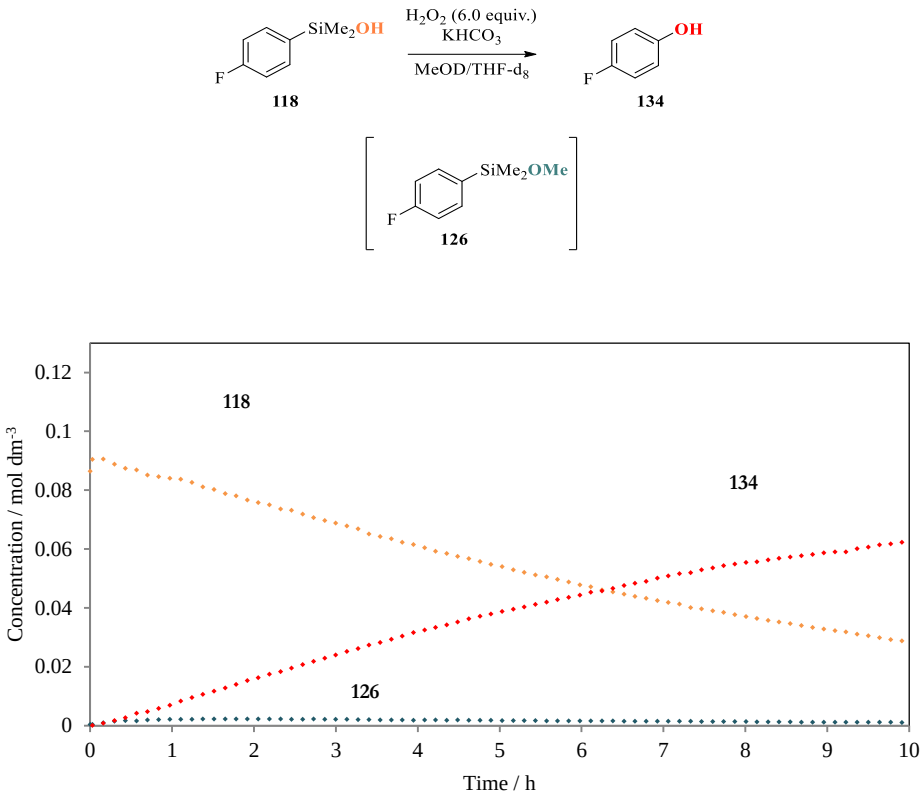


Figure 4.8 ^{19}F NMR spectroscopic observation of the oxidation of silanol X in 1:1 MeOH-d_4/THF-d_8

A repeat of this oxidation at a higher concentration of starting material and oxidant provided a more informative view of the oxidation (Figure 4.9). Again, we observed the formation of methoxysilane **126** in these reactions. After an initial small increase in concentration at the beginning of the reaction, a gradual consumption was observed, common to both experiments.

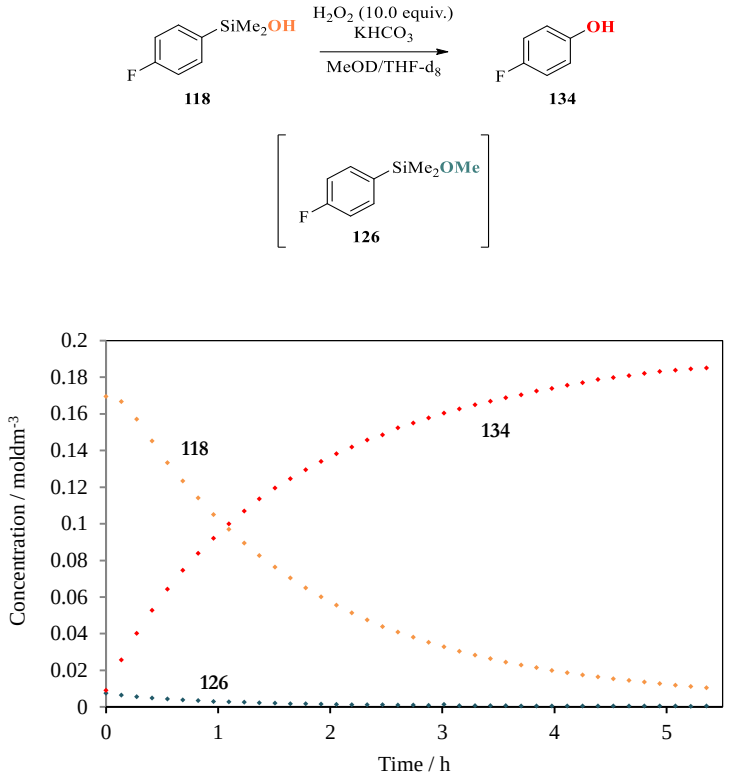
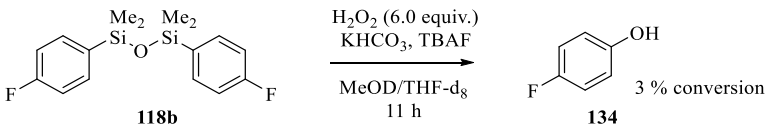


Figure 4.9: ^{19}F NMR spectroscopic observation of the oxidation of silanol in 1:1 MeOH-d_4/THF-d_8. Reaction carried at 0.18 M concentration.

The lack of reactivity of disiloxanes was confirmed when a solution of disiloxane **118b** was submitted to the standard hydrogen peroxide conditions and the reaction observed by ^{19}F NMR spectroscopy (Scheme 4.15). We were curious to see if any transformations took place, in particular whether the disiloxane would be in equilibrium with silanol as observed under Denmark's basic cross-coupling conditions.[171] All that was observed was a very small amount of phenol formation, most likely the result of oxidation of residual silanol from the previous step.



Scheme 4.15: Attempted oxidation of disiloxane 118b

By observing the oxidation of methoxysilane **126**, we found the highest reaction rate of all the substrates so far examined (Figure 4.10), in agreement with our previous methodology results. In the

course of the oxidation however, a significant amount of silanol formed, indicating that silanol **118** and methoxysilane **126** are in equilibrium under our oxidation conditions, and that silanol **118** is thermodynamically favoured. When the faster rate of oxidation of methoxysilane **126** compared to silanol **118** was considered, this concentration profile also implied that the formation of silanol during the reaction inhibited the rate of formation of phenol. Conversely, the formation of methoxysilane **126** in previous concentration profiles may present part of a rate enhancing mechanistic pathway. The low concentration of methoxysilane **126** seen previously may only reflect the far greater rate of oxidation of methoxysilane **126** compared to formation from silanol **118**.

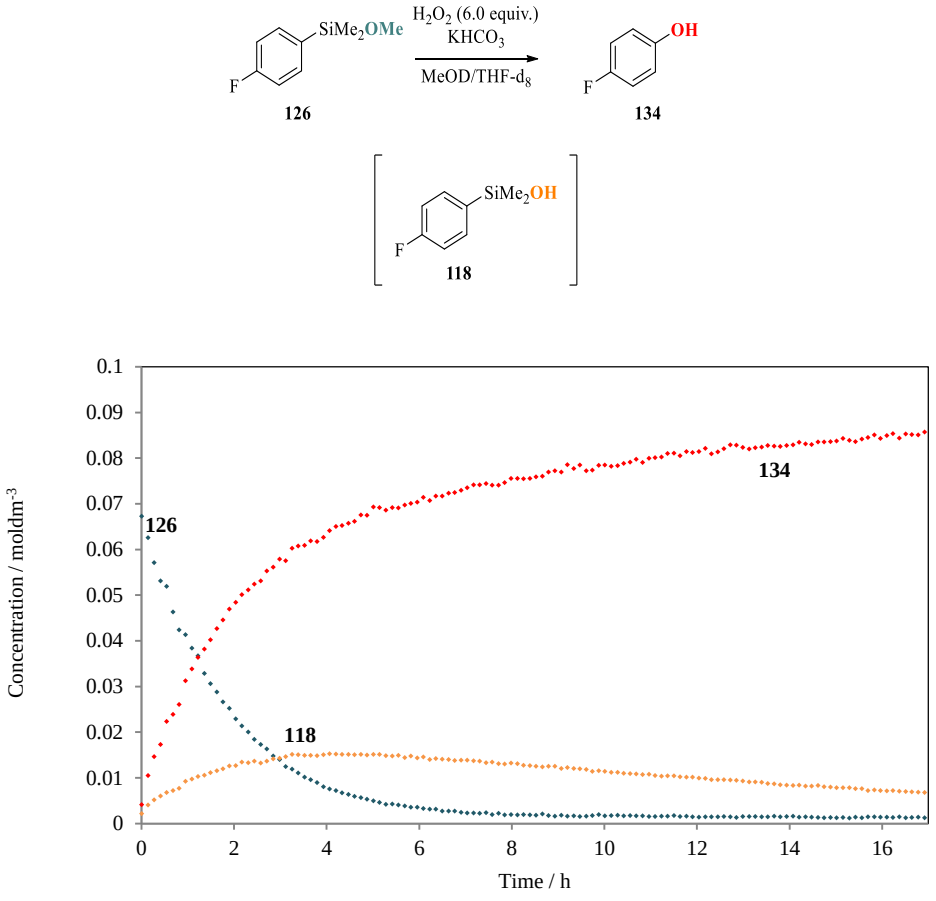


Figure 4.10: ^{19}F NMR spectroscopic observation of the oxidation of methoxysilane in 1:1 MeOH-d$_4$/THF-d$_8$

In light of this, we sought to examine the equilibrium between the two species in detail to support these hypotheses.

4.5. Equilibrium experiments

During the mechanistic studies previously discussed, nucleophilic displacement of anions at silicon centres was shown to be reversible. This is in agreement with the equilibrium observed between silanol **118** and methoxysilane **126** during our oxidations. In order to characterise this equilibrium in more detail, methoxysilane **126** was submitted to conditions designed to mimic the oxidation in the absence of hydrogen peroxide (Figure 4.11). This corresponded to approximately 25 equivalents of water in a basic methanol/THF mixture.

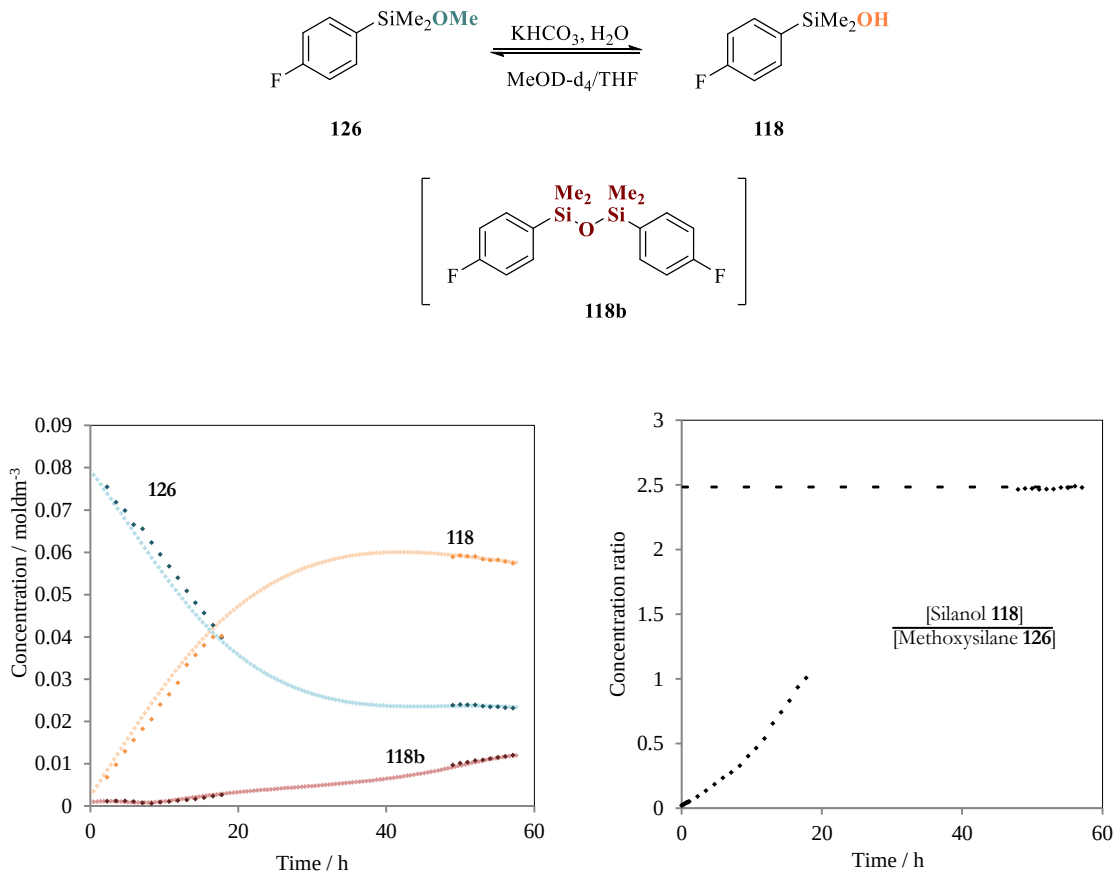


Figure 4.11: ^{19}F NMR spectroscopic observation of equilibrium formation between methoxysilane and silanol in 1:1 MeOH-d$_4$/THF

The system did equilibrate, but due to the length of time required for the system to stabilise, it was not possible to observe this process in full. However, we were able to insert a spline interpolation of the data between 18 and 48 hours using OriginPro graphical software.[172] During the reaction we were

also able to see that a very slow formation of disiloxane. It was reassuring to see that formation of this dead-end side product was far from rapid under these conditions, although it is possible that disiloxane formation would be catalysed by hydroperoxide anion addition. An additional graph of the ratio of silanol to methoxysilane is shown (Figure 4.11). It can be estimated from this plot that the equilibrium stabilised after approximately 50 hours with $K_{obs} = 2.49$.

It was thought that the position of the equilibrium was likely to have evolved from a number of factors, beyond the intrinsic stability of the two arylsilanes. The effect of solvents on chemical equilibria is well studied and the composition of basic alcohol/water solvent mixtures has been shown to be particularly influential.[173-177] Equilibrium 4.1, shown in Scheme 4.16, can be assumed to be present in any reaction involving some alcohol/water solvent composition with base. It can also be assumed that since the reaction involves rapid proton transfer, the equilibrium is attained almost instantaneously and remains constant. Additionally, the sum of hydroxide and alkoxide concentrations can be assumed to be constant, as the rate of proton transfer should be much faster than any other process in the reaction.[173] The position of equilibrium 4.1, however, has shown extreme sensitivity to methanol/water solvent composition, and as such the relative acidities of hydroxide and methoxide are difficult to quantify. Previous efforts to identify K_{mh} have produced values between 0.1 and 1.31.[178]

$$MeO^- + H_2O \overset{K_{mh}}{\rightleftharpoons} HO^- + MeOH \qquad (4.1)$$

$$HO^- + ArSiMe_2OMe \overset{K_{obs}}{\rightleftharpoons} MeO^- + ArSiMe_2OH \qquad (4.2)$$

Scheme 4.16: Contributing equilibria

The preference for silanol in equilibrium 4.2 is likely to result from a combination of equilibrium 4.1, the stability of the arylsilanes, and the relative stabilising solvent effects of the methanol/THF/water mixture. Solvent effects may be most significant in this system as silanols are known to hold strong hydrogen bonds.[179] In a polar solvent, silanol **118** will therefore be stabilised relative to methoxysilane **126**.

Although equilibration was slow under these conditions, it could be seen in the oxidation of methoxysilane (Figure 4.10) that the rate of silanol formation was much faster under oxidative conditions, suggesting that hydroperoxide anions catalyse this equilibration. It could also be concluded that the low concentration of methoxysilane observed in silanol **118** or arylhydrosilane **99** oxidations reflected the rate of its oxidation outpacing the rate of its formation from silanol **118**. Likewise, the formation of significant amounts of silanol reflected its dominance at equilibrium, and its lack of reactivity towards oxidation (Figure 4.12).

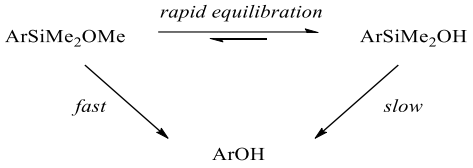
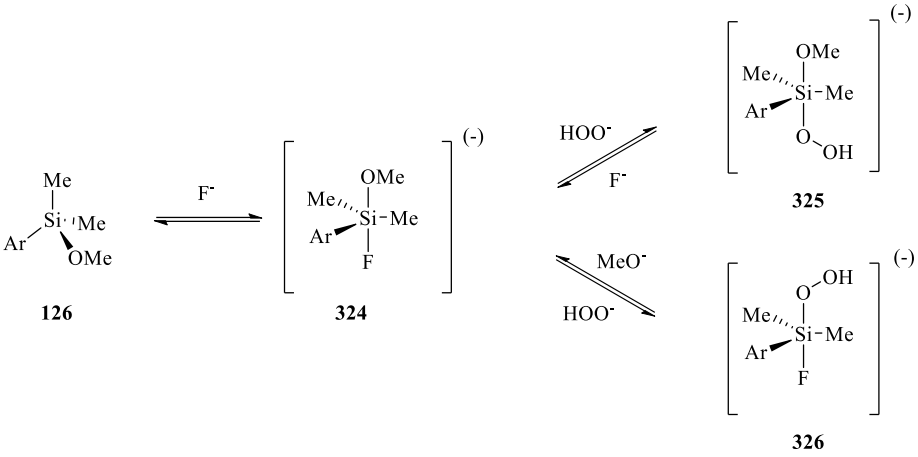


Figure 4.12: Qualitative rates of reaction in an arylsilane oxidation

4.6. The addition of TBAF

In previous Tamao oxidations, stoichiometric amounts of TBAF, KF, or KHF_2 were required to bring about full conversion of alkylsilanes. In contrast, most of our substrates could undergo full oxidation without a fluoride activating agent. Additionally, in this work, and previous work within the group, only 0.1 equivalents of TBAF were needed to reduce the time needed for full conversion. In the work of Mader and Norrby, discussed in chapter 4.1.3, it was thought that fluoride sources increase the rate of oxidation by reacting with the alkylsilicon compounds to form fluorosilanes, which oxidise at a faster rate.[152] For TBAF to act catalytically, fluoride would have to be released back into the reaction at some point. We considered whether the formation of pentavalent fluorosilane **324**, may be sufficient to catalyse the reaction (Scheme 4.17).



Scheme 4.17: Mechanism of fluoride catalytic action I

From pentacoordinate fluorosilane **324**, a peroxide anion may add to form either of the two intermediates **325** or **326**. As discussed in Chapter 4.1.2, pentavalent silicon compounds are more electrophilic than their tetrahedral equivalent, and are activated towards nucleophilic substitution in this state. Thus fluoride coordination to methoxysilane **126** is likely to increase the rate of hydroperoxide substitution at silicon, and thereby increase the overall rate of oxidation.

We returned to our most unreactive fluorinated substrate, hydrosilane **99**, to observe the effect of 0.1 equivalents of TBAF by ^{19}F NMR spectroscopy (Figure 4.13). The formation of silanol, and therefore the overall oxidation, proceeded at a higher rate. As seen previously (Figure 4.7), a delay in the formation of phenol occurred until silanol had formed. Again, as previously observed, a small amount of methoxysilane **126** was formed in the reaction.

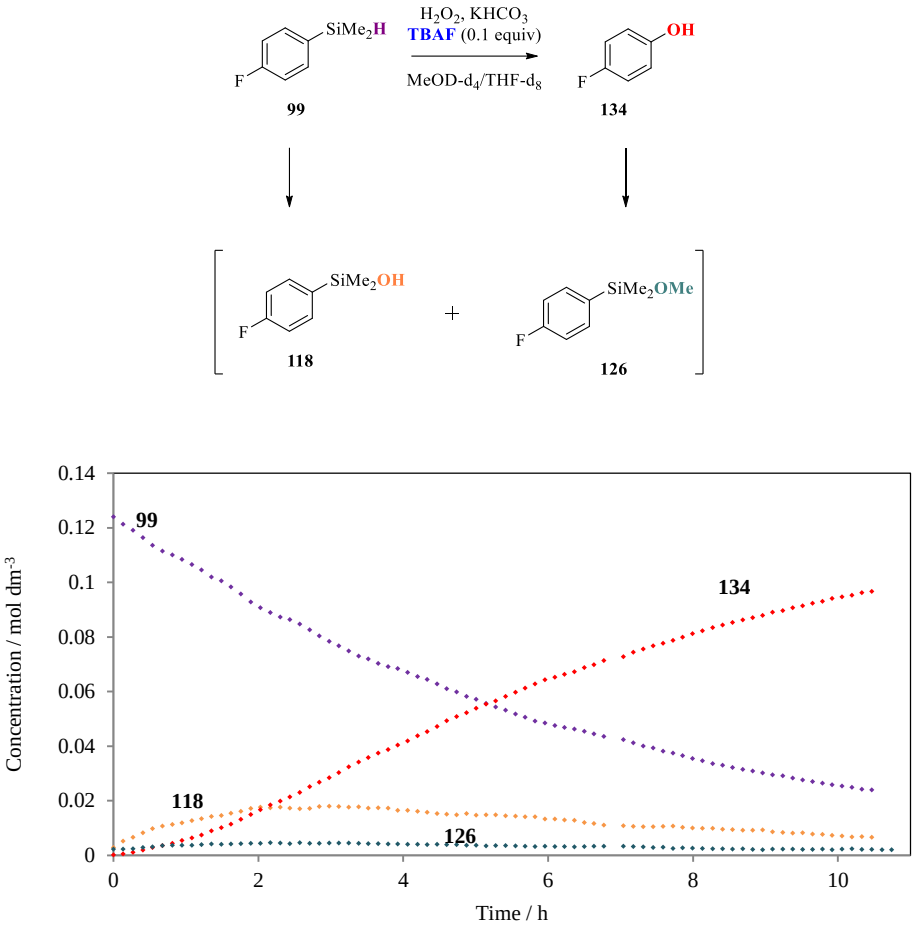
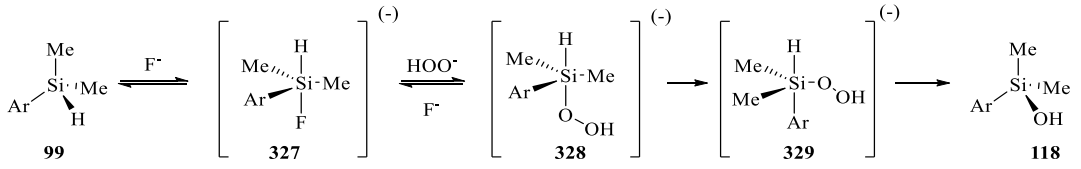


Figure 4.13: ^{19}F NMR spectroscopic observation of the oxidation of hydrosilane X with catalytic TBAF in 1:1 MeOH-d$_4$/THF-d$_8$ (normalised data)

Our proposed mechanism for fluoride activation could be extended to explain the increased rate of silanol **118** formation in the presence of TBAF, during the oxidation of hydrosilane **99** (Scheme 4.18). If formation of silanol **118** from hydrosilane **99** proceeds through a 1,2-hydride shift from silicon to oxygen, the pentavalent intermediate **328** necessary for this migration would form faster from pentavalent fluorosilane **327** than the starting material **99**.



Scheme 4.18: Mechanism of fluoride catalytic action II

The oxidation of methoxysilane was also repeated with 0.1 equivalents of TBAF (Figure 4.14). Here, it is not so clear that this oxidation proceeds at a higher rate than its uncatalysed equivalent (Figure 4.10). The rate of formation of silanol certainly increased, but as we believed silanol to be a less reactive substrate for oxidation, it could be envisaged that this would not improve the initial rate. In this oxidation, a small amount of disiloxane **118b** was observed. The higher rate of its formation than that which had been previously seen was attributed to the presence of (catalytic) TBAF.

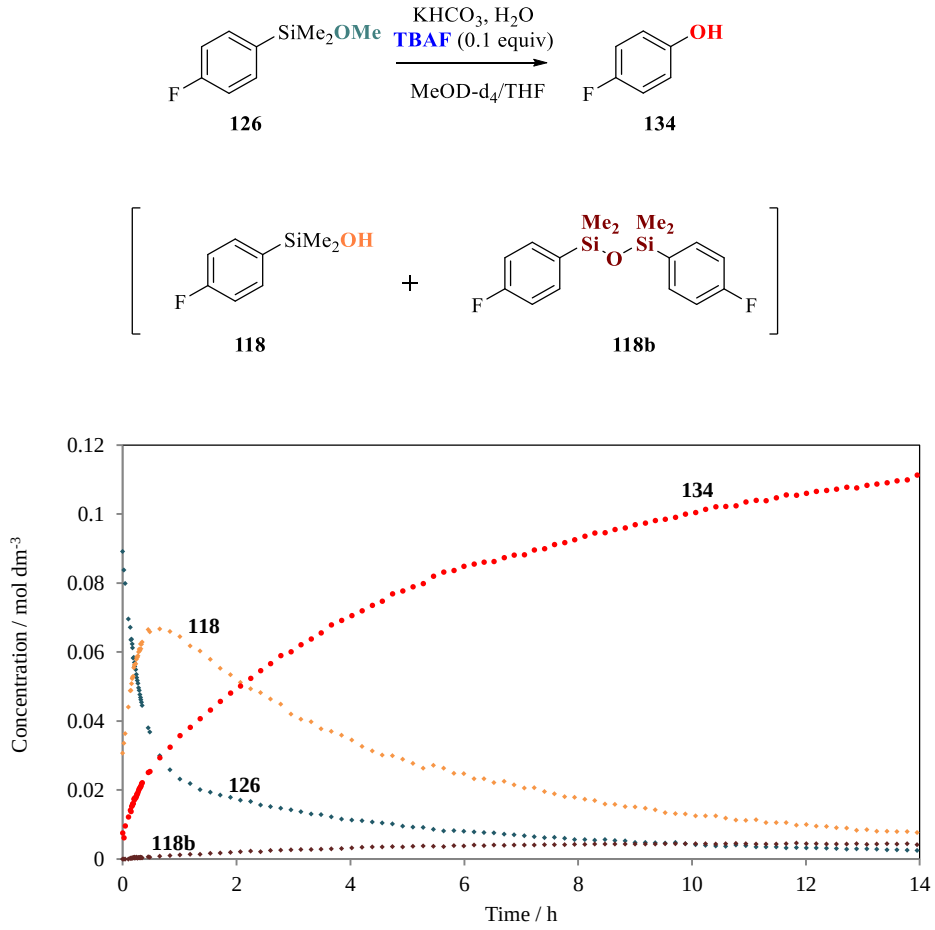
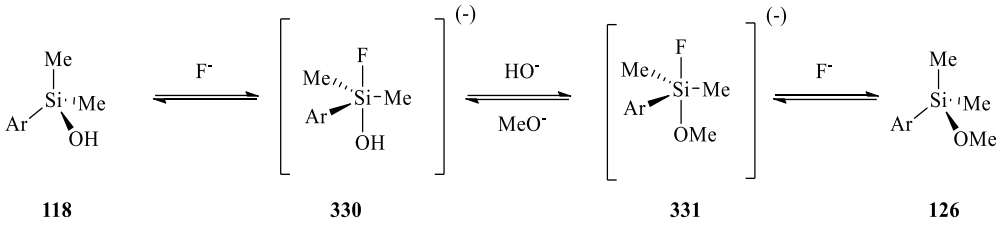


Figure 4.14: ^{19}F observation of TBAF catalysed oxidation of methoxysilane in 1:1 MeOH-d_4/THF-d_8

During our methodology development, we consistently observed that the addition of TBAF reduced the time needed for overall conversion of our arylsilanes to phenol (Chapter 2). There were also many other examples in the literature where the addition of TBAF had improved the rate of oxidation. However, it was now thought that TBAF must be capable of both accelerating and inhibiting the

reaction. The initial rate of oxidation may be reduced due to silanol formation, but it is possible that in the final stages of the oxidation, where silanol **118** is at a greater concentration than methoxysilane **126**, TBAF could then improve the rate of reaction relative to the uncatalysed oxidation. If our theory of the mechanism of fluoride catalysis is correct, the rate of exchange between silanol and methoxysilane should increase (Scheme 4.19). The rate of oxidation in the final stages of the reaction may thus depend on the rate that silanol **118** can convert to methoxysilane **126**, which is improved by the presence of TBAF. Additionally, the oxidation of methoxysilane **126** is itself likely to be improved by fluoride attack by the mechanism described in Scheme 4.17.



118 **330** **331** **126**

Scheme 4.19: Mechanism of fluoride catalytic action III

To gain further information of the effect of fluoride, the equilibrium process under fluoride-catalysed conditions was investigated: methoxysilane **126** was submitted to the previously described conditions of water, methanol and $KHCO_3$ with the addition of 0.1 equivalents of TBAF. In this study, we observed that TBAF significantly increased the rate of interconversion of silanol **118** and methoxysilane **126**. Unlike the equilibrium studied previously in Figure 4.11, in less than 5 hours the system had stabilised, with K_{obs} = 2.6. The equilibrium constant was however, very similar to that observed under fluoride-free conditions. These results supported our mechanism of fluoride catalysis described in Scheme 4.19.

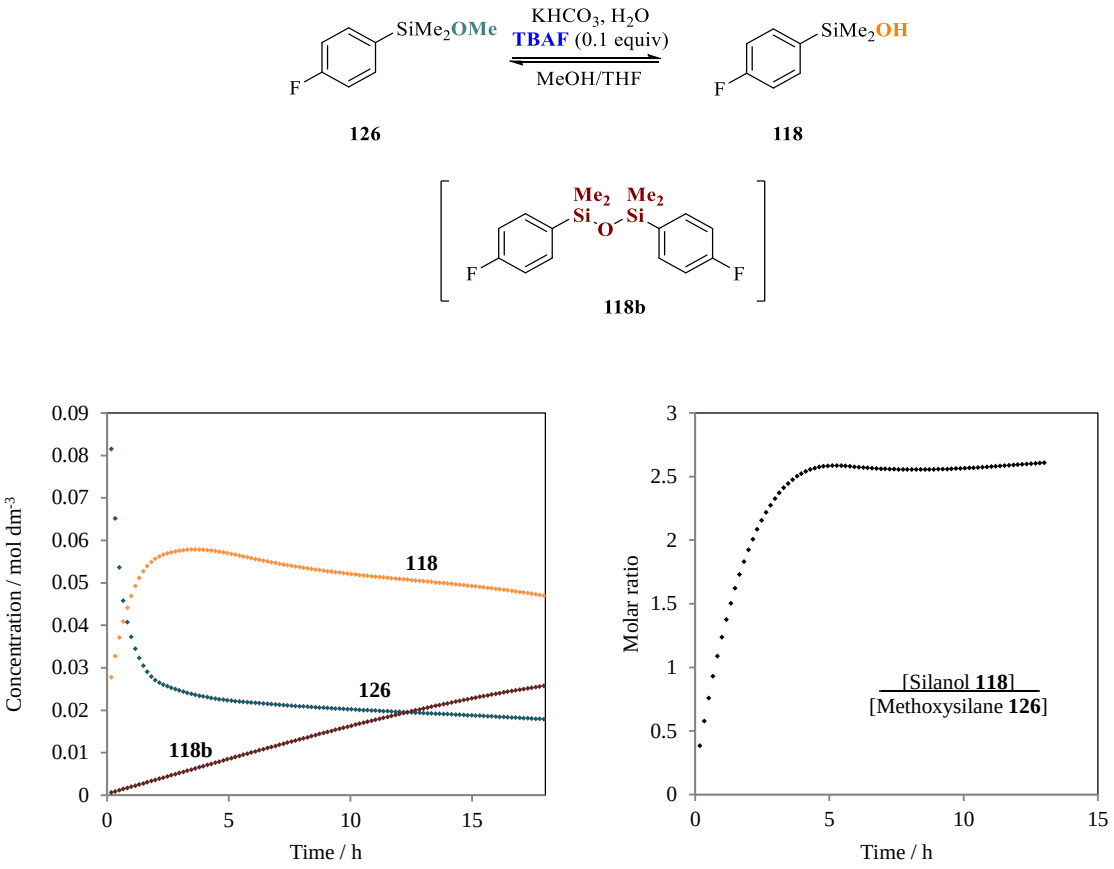
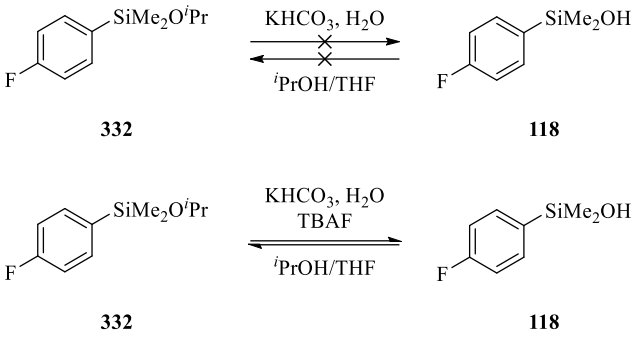


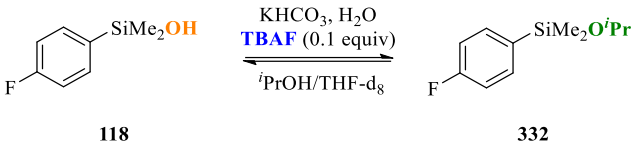
Figure 4.15: ^{19}F NMR spectroscopic observation of silanol/methoxysilane equilibrium in 1:1 MeOH-d$_4$/THF

We hoped to find conditions that would suppress this equilibrium, so that we could simplify the reaction and observe only one substrate oxidising at a time. By replacing the solvent methanol, with isopropanol, and methoxysilane **126** with isopropoxysilane **332**, we hoped that hydroxide attack would be disfavoured by the increased steric bulk around the silicon centre (Scheme 4.20). Thus the conversion of isopropoxysilane to silanol would be inhibited. Additionally we hypothesized that an isopropoxide ion would be hindered in its attack at the silicon centre due to its steric bulk, and that the silanol to alkoxysilane reaction would also diminish.



Scheme 4.20: Equilibrium of isopropoxysilane 332 and silanol 118

This was indeed the case: no conversion to silanol from isopropoxysilane **332** was observed in the absence of TBAF (Scheme 4.20). Once the fluoride catalyst was added, conversion to silanol and the reverse reaction began, but at a much slower rate compared to that of methoxysilane. Similarly, when silanol **118** was observed under the same conditions, no conversion to isopropoxysilane **332** occured until the addition of TBAF (Figure 4.16).



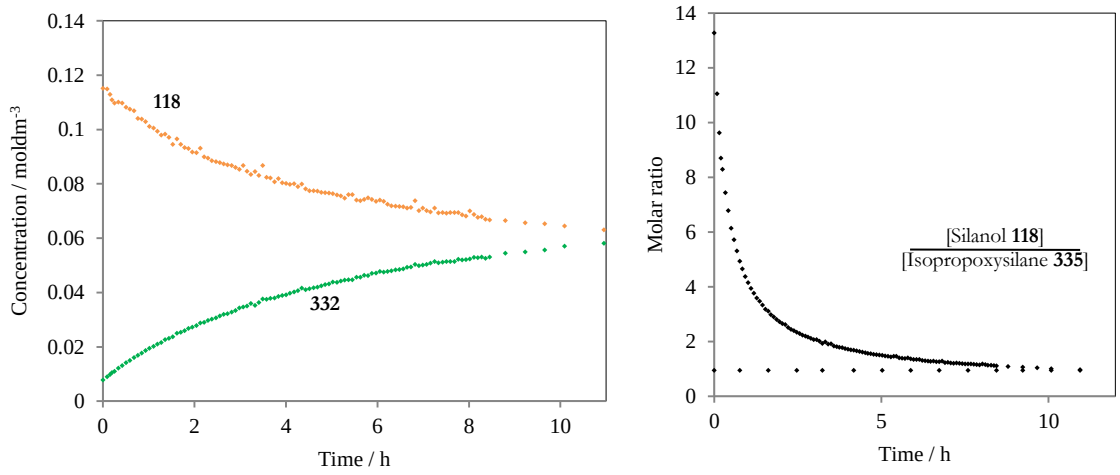


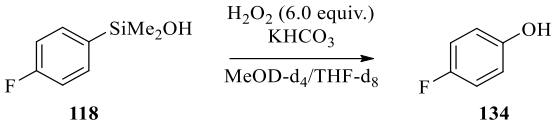
Figure 4.16: ^{19}F NMR spectroscopic observation of isopropoxysilane and silanol equilibrium in 1:1 IPA/THF-d_8

Unfortunately, the equilibrium had not completely stabilised by the end of our experiment, but an estimate of the silanol to isopropoxysilane ratio of 0.95 to 1 could be made from the graph. This equilibrium constant was lower than that previously observed in the methoxysilane system (Figure 4.11). We believed this could be explained by the relative ability of the two solvents to form hydrogen bonds with silanol, a stabilising interaction. Methanol is known to be a more polar solvent than isopropanol, with dipole moments 1.70 and 1.56, respectively, thus silanol is stabilised to a greater degree in methanol than isopropanol.

With conditions that suppressed the $ArSiMe_2OH/ArSiMe_2OMe$ equilibrium found, we hoped to compare the rates of oxidation under these conditions with the standard reactions. Ideally, the effects of the equilibria could then be differentiated from the varying rates of oxidation of silane intermediates. Unfortunately an isopropanol/THF solvent mixture was found to be insufficiently polar to be miscible with aqueous hydrogen peroxide. Several further attempts to observe the oxidation of silanol, in both isopropanol/THF mixtures and pure isopropanol, were unsuccessful. Thus, this particular line of investigation was abandoned for the time being.

4.7. Initial rate experiments

To compare the rates of silane oxidation, quantitative data on the rates of reaction were needed. Disappointingly, upon twice repeating the NMR spectroscopic observation of silanol oxidation (Figure 4.9) the data obtained had a relative standard deviation (RSD) of 11.5 %. Although the reaction profiles of arylsilane oxidations under various conditions had been highly qualitatively informative, it was not possible to analyse them quantitatively with this degree of imprecision.



118 **134**

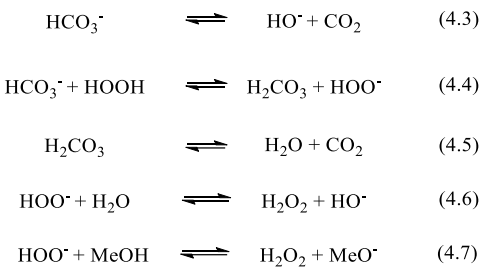
Trial	Rate constant (h^{-1}) (gradient of -ln[$ArSiMe_2OH$] graph)
1 (Figure 4.9)	0.5252
2	0.4077
3	0.5270

Table 4.3: Reproducibility of NMR spectroscopic observation

4.7.1. Development of a reproducible method

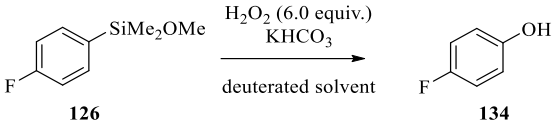
Efforts were directed towards developing a more accurate method of obtaining initial rates of phenol formation in arylsilane oxidations. The first attempt to establish a reproducible method was made by adding stock solutions of equal volume to each other to begin the experiment, thereby minimising the experimental error of measuring small volumes of liquids. Unfortunately, we found that a gel-like substance would often form during preparation of the reaction in this way (Table 4.4, entry 1). This material had been observed previously during arylsilane oxidations, and in the work of others, but only in the late stages of the oxidation. Following optimisation of solvent preparation (Entry 2 and 3), a homogenous solution could be prepared but the data were still inconsistent. We had observed that a very gentle effervescence takes place during arylsilane oxidations, and believed this was likely to be carbon dioxide, one product of potassium bicarbonate decomposition in solution. A potassium bicarbonate solution alone does not effervesce, thus equilibrium (4.3) in Scheme 4.21 was thought unlikely to be responsible for carbon dioxide formation. Instead, hydrogen peroxide may initiate bicarbonate decomposition (equation 4.4). The hydroperoxide anion produced through this equilibrium was believed to be essential to arylsilane oxidation. The loss of gaseous carbon dioxide was expected to drive equilibrium (4.5) to the right hand side, which in turn would promote formation of carbonic acid in equilibrium (4.4). Overall these transformations promote the formation of

hydroperoxide anion when carbon dioxide is removed from solution. This would explain the sensitivity of the rate of reaction to loss of carbon dioxide gas.



Scheme 4.21: Potassium bicarbonate equilibria

Any slight agitation of the solution would initiate more effervescence and it was thought that this erratic loss of carbon dioxide could explain the inconsistent results so far obtained. We attempted to regulate the agitation of the solution by using a mechanical shaker on the NMR reaction before inserting it into the spectrometer, but still the results were inconsistent (Entry 4). In an attempt to offset the production of gas and gel precipitation, the base loading was reduced to 0.1 equivalents (from 0.2). By following a similar procedure as that described in entry 1, a gel did not form. Still, the oxidation was slow and the results inconsistent. It was then thought that by degassing the solution, and removing all carbon dioxide, the concentration of hydroperoxide anions might remain constant, regardless of shaking or other forms of agitation. When we first attempted to degas a solution containing hydrogen peroxide, base, MeOH and THF, we were surprised to observe the return of the unknown gel substance (Entry 6). Whatever the identity of the substance, it added inaccuracy to the system as we were not able to know the exact concentrations of reagents if some had been used to form the gel. The THF/MeOH solvent mixture was subsequently replaced with methanol alone. Although the gel substance was no longer observed, the reaction rate had increased and phenol formation was now too fast for data collection (Entry 7).

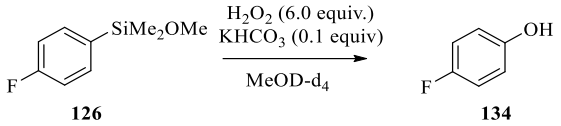


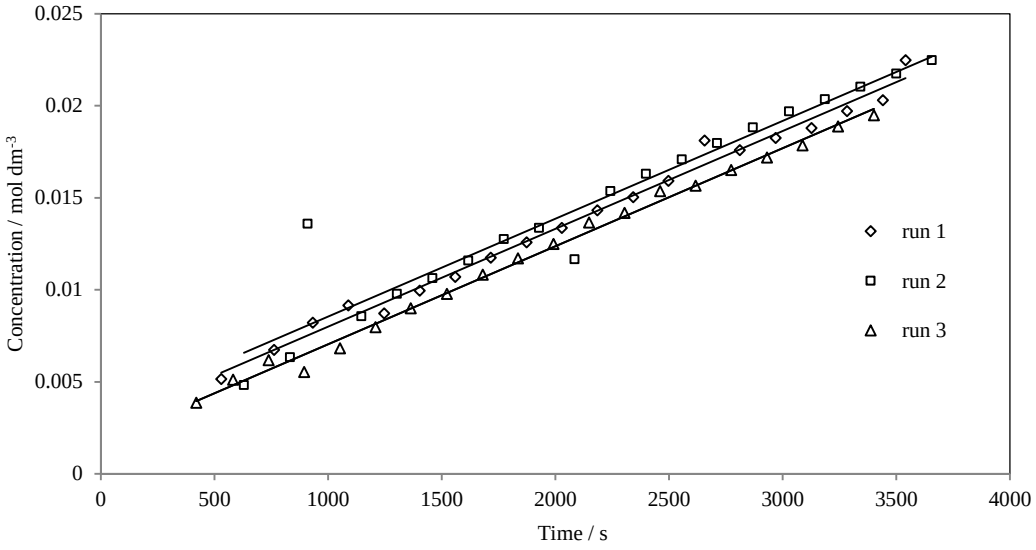
126 **134**

Entry	Method	Result
1	Addition of H_2O_2/$KHCO_3$ solution to arylsilane in MeOD/THF	A gel was formed when the mixtures met
2	Base added to MeOD/THF before H_2O_2 addition	$KHCO_3$ was incompletely dissolved
3	H_2O_2/$KHCO_3$ solution prepared and diluted with MeOD/THF, before arylsilane addition	Homogenous solution formed, but inconsistent data was obtained 6.0 equiv. H_2O_2 ; 41 % (RSD) 9.0 equiv. H_2O_2 ; 48 % (RSD)
4	Automated sample shaking	Irreproducible; effervescence of varying amounts observed despite automated sample shaking <100 % (RSD)
5	Base lowered to 0.1 equivalents, and added in H_2O_2/$KHCO_3$ solution again	Gel was not formed, but reaction slow and not reproducible
6	H_2O_2/$KHCO_3$ (0.2 equiv)/MeOH/THF solution degassed before addition to arylsilane in MeOD/THF	A gel of unknown composition was formed while degassing the solution (using both freeze-thaw or argon bubbling)
7	H_2O_2/$KHCO_3$ (0.2 equiv)/MeOH solution degassed before addition to arylsilane in MeOD	Degassing partially successful; some effervescence was still observed. Reaction inconsistent and too fast to follow
8	H_2O_2/$KHCO_3$ (0.1 equiv)/MeOH solution degassed before addition to arylsilane in MeOD	Reaction reproducible; 0.12 % (RSD)

Table 4.4: Optimisation of method for kinetic experiments

Finally, by lowering the amount of $KHCO_3$ added we were pleased to observe a stable solution which did not effervesce when struck and most pleasingly, provided consistent data over three runs (Figure 4.17). The reaction was only observed within the first 25 % of conversion, where the concentration of the reactants may be considered constant, and the concentration of phenol was calculated in reference to the internal standard (hexafluorobenzene).





Initial rate (mol dm^{-3} s^{-1})			Average	% RSD
Run 1	**Run 2**	**Run 3**		
5.3156 x 10^{-6}	5.3224 x 10^{-6}	5.3118 x 10^{-6}	5.32 x 10^{-6}	0.082
(R^2 = 0.9147)	(R^2 = 0.9946)	(R^2 = 0.9894)		

Figure 4.17: Collection of kinetic data. [a] The point at which the sample was inserted into the spectrometer is equivalent to time = 0

It is important to note that the necessary measures, taken to produce a reliable method of observing the reaction kinetics, led us away from the reaction conditions of our methodology development. However, the slight variation in the composition of the reaction mixture allowed us to make detailed observations of the oxidation. Figure 4.18 shows a trial of one set of conditions (Table 4.4, Entry 7).

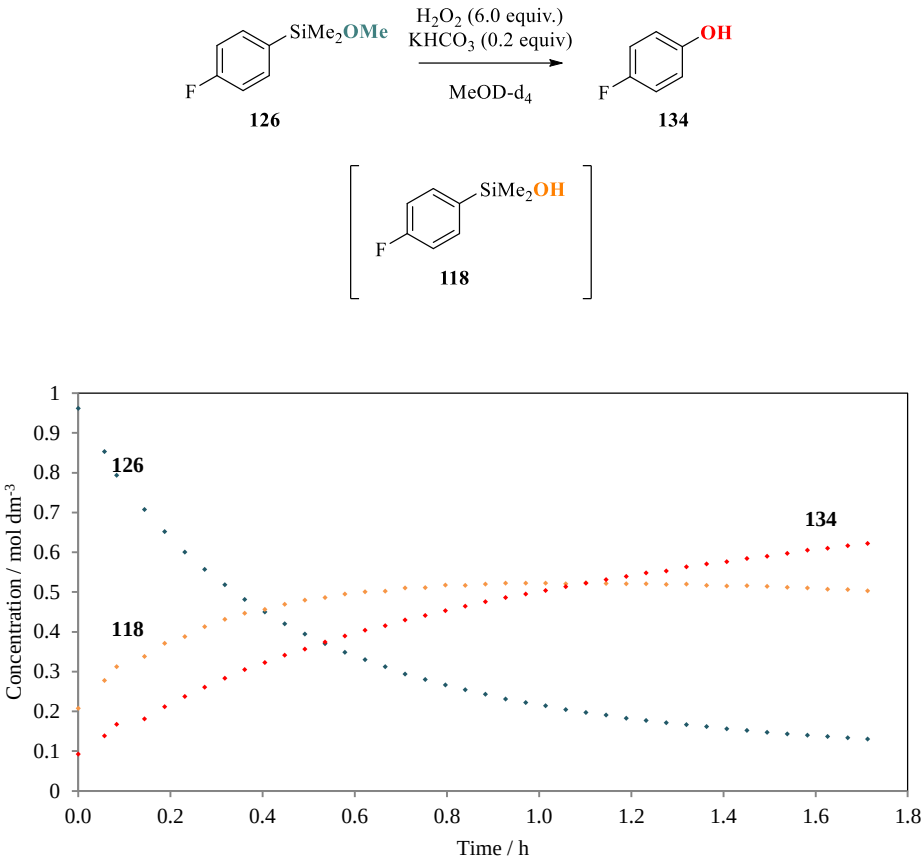


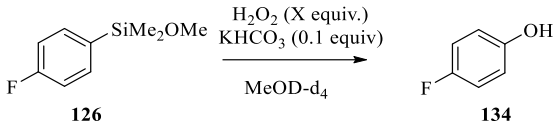
Figure 4.18: Trial of kinetic run

These conditions produced such a rapid oxidation that they could not be used for kinetic data as the first 10 % of the reaction had occurred before analysis had begun. This heightened reactivity was attributed to the degassed solution of hydrogen peroxide and potassium bicarbonate, in which the concentration of basic species was likely to be increased. Additionally, the rate of silanol/methoxysilane equilibration had significantly increased with pure methanol as solvent. Unfortunately, it had already been found that arylsilane oxidations cannot generally be carried out in pure methanol as many non-polar arylsilanes are not soluble in this solvent.

4.8. Initial rate experiment results

Effect of hydrogen peroxide concentration on the initial rate of reaction

To determine the order of reaction with respect to hydrogen peroxide, the concentration of hydrogen peroxide was varied while all other reagent concentrations were kept constant (including water). As expected, the rate increased with concentration of hydrogen peroxide. The graph in Figure 4.19 fits with a first order dependence of hydrogen peroxide concentration on the rate of reaction.



Entry	H_2O_2 concentration (mol dm^{-3})/ equiv	Initial rate of phenol formation (mol dm^{-3} s^{-1})	% RSD (over 3 runs)
1	0.6 / 6.0	5.32 x 10^{-6}	0.082
2	0.3 / 3.0	3.96 x 10^{-6}	2.97
3	0.2 / 2.0	2.52 x 10^{-6}	1.34
4	0.1 / 1.0	1.59 x 10^{-6}	3.61

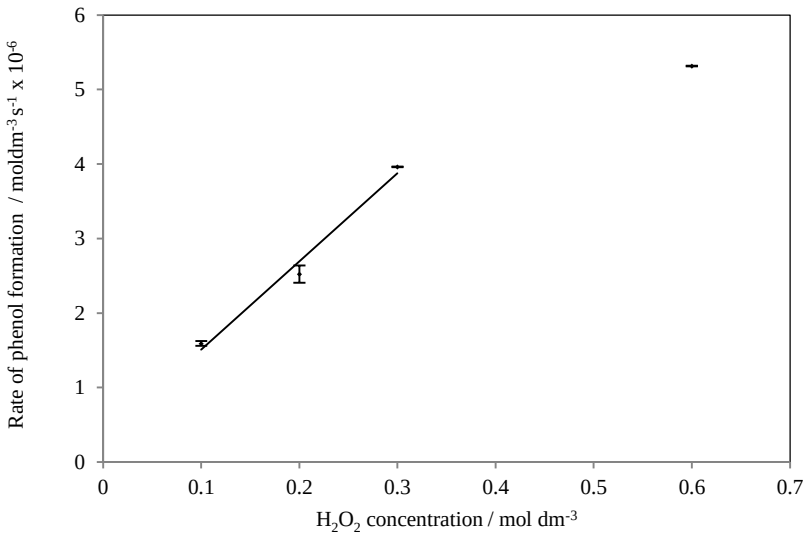


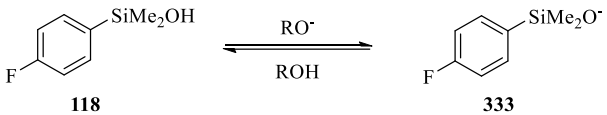
Figure 4.19: Effect of hydrogen peroxide concentration on the rate of reaction

The increase in reaction rate did appear to "taper off" as the equivalents of hydrogen peroxide were increased above 6.0. This was not thought to be an indication of a reaction order smaller than one, instead it was thought that other factors may become rate limiting at very high concentrations of hydrogen peroxide.

We had hoped to observe the reaction when hydrogen peroxide, not base, was the limiting reagent. Unfortunately this was not possible as we discovered that no more than 0.3 equivalents of $KHCO_3$ would dissolve in the reaction medium, regardless of the length of time the stock solution was left to degas. Neither could we lower the oxidant concentration below that of base (lower than 0.3 equiv) as the reactions became extremely slow: although formation of phenol could be seen, it was occurring in such small concentrations that the signal to noise ratio of the ^{19}F NMR spectra heavily distorted the data.

Effect of $KHCO_3$ concentration on the initial rate of reaction

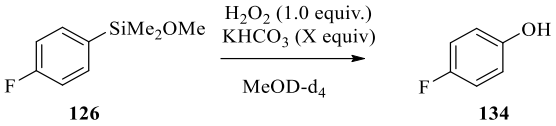
We continued with our investigation by varying the concentration of $KHCO_3$ in the reaction. Although only a small variation in concentration was possible, we were able to see a positive effect on the rate of phenol formation (Figure 4.20) as the amount of base increased. There also appeared to be a diminishing effect of base concentration on the rate, even though the base was not close to being in excess. This can be explained by the low solubility of $KHCO_3$ in the reaction mixture: if more base were added we would expect it to have little effect on the initial rate if it were not fully dissolved. Alternatively, it is possible that an increase in concentration of base would encourage formation of silanolate **333** (Scheme 4.22); silanols are known to be more acidic than their carbon counterparts.[180] Silanolate **333** would presumably be far less reactive to oxidation and formation of this species would therefore inhibit the otherwise rate enhancing effect of increasing $KHCO_3$ concentration.



118 **333**

Scheme 4.22: Silanolate equilibrium

Unfortunately, these experiments did little to inform us of the extent of the dependence of reaction rate on $KHCO_3$ concentration as the range of concentrations we could observe was very limited. However, the general rate dependence of both hydrogen peroxide and $KHCO_3$ can correspond to the involvement of hydroperoxide anion in either a rate limiting step of the oxidation, or a step preceding this.



126 **134**

Entry	$KHCO_3$ concentration (mol dm^{-3})	Initial rate of phenol formation (mol dm^{-3} s^{-1})	% RSD (over 3 runs)
1	0.01	1.59 x 10^{-6}	3.61
2	0.02	2.35 x 10^{-6}	2.16
3	0.03	2.44 x 10^{-6}	4.31

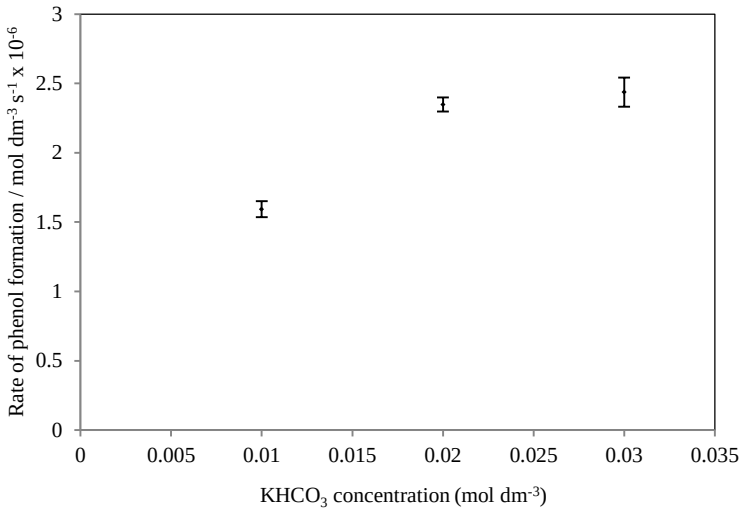


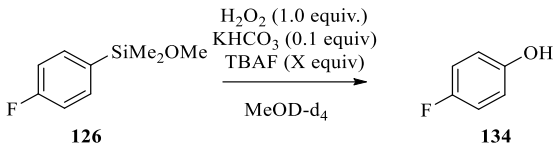
Figure 4.20: Effect of $KHCO_3$ concentration on the rate of reaction

Effect of TBAF concentration on the initial rate of reaction

We were very interested to learn the effect that TBAF would have on the initial rate of the reaction due to the conflicting observations we had made in our previous work. We knew that the addition of

TBAF reduces the overall time needed for full conversion of an arylsilane to phenol, however we had also seen that in the presence of TBAF, a greater amount of silanol formation takes place.

We had come to believe that silanol formation was an unfavourable process, and may well have a negative effect on the rate of reaction. As shown in Figure 4.21, the initial rate was indeed found to decrease with increasing TBAF concentration. Although this result was in agreement with our previous observations, it was still intriguing to see that a catalyst could hinder reaction rate in the initial phase, but nevertheless improve the rate of reaction overall.



126 **134**

Entry	TBAF concentration (mol dm^{-3})	Initial rate of phenol formation (mol dm^{-3} s^{-1})	% RSD (over 3 runs)
1	0	1.59×10^{-6}	3.61
2	0.005	1.34×10^{-6}	6.48
3	0.01	0.821×10^{-6}	2.07

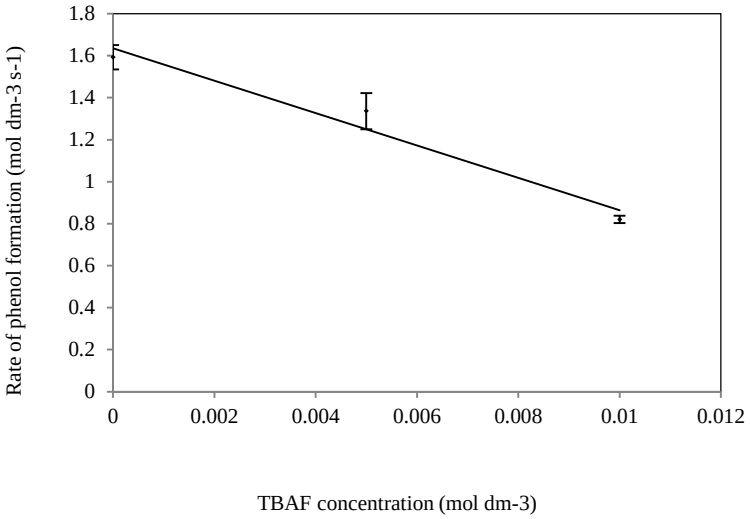
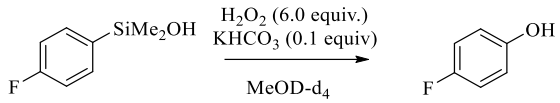


Figure 4.21: Effect of TBAF concentration on the rate of reaction

It is important to note however that the addition of TBAF can be expected to increase the pH of the reaction mixture. It is thought that this would be a rate enhancing effect, as the concentration of hydroperoxide anions should increase. However, it is also possible that greater silanol deprotonation could occur when the concentration of basic species is increased.

Silanol oxidation

The role of silanol in the oxidation has been repeatedly discussed in this chapter. We thought it important to directly compare the oxidation of methoxysilane and silanol to quantify finally the reactivity (or unreactivity) of silanol. The instability of silanol towards disiloxane formation made this substrate a more challenging compound to test. It was essential that stock solutions of silanol were prepared immediately before conducting NMR spectroscopic experiments to produce the most accurate results possible. After careful experimentation it was indeed discovered that the oxidation of silanol proceeds at a slower rate than the oxidation of methoxysilane.



118 **134**

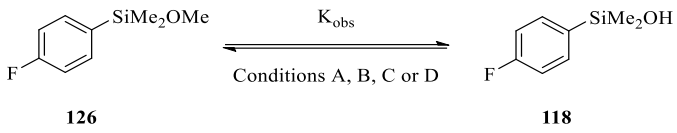
Entry	Oxidation substrate	Initial rate of phenol formation (mol dm^{-3} s^{-1})	% RSD (over 3 runs)
1	$ArSiMe_2OMe$	5.32×10^{-6}	0.082
2	$ArSiMe_2OH$	4.56×10^{-6}	3.58

Figure 4.22: Initial rates of $ArSiM_2OMe$ and $ArSiMe_2OH$ oxidation

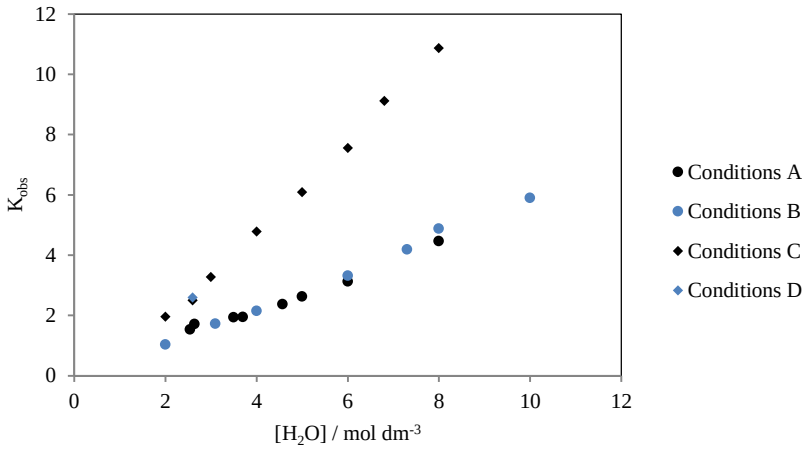
The rapid equilibration between methoxysilane and silanol did seriously limit this experiment. This result however gave us greater confidence in our theory that the fastest pathway of arylsilane oxidation, under Tamao conditions, occurs from a methoxysilane intermediate.

4.9. Further equilibrium experiments

After learning the significance of the equilibrium between silanol **118** and methoxysilane **126** on the rate of arylsilane oxidation, we chose to investigate further factors which may affect this equilibrium. NMR experiments were carried out over a range of solvent compositions. The resulting observed equilibrium constants are displayed in Figure 4.23. Through this study we found that increasing the water content increased the concentration of silanol at equilibrium. The addition of TBAF did not effect the position of equilibrium although it did increase the speed with which equilibrium was reached, suggesting that the fluoride source catalyses the reaction in both directions equally.



126 **118**



Conditions A: $KHCO_3$ (0.1 equiv), H_2O (x M), MeOH
Conditions B: $KHCO_3$ (0.1 equiv), TBAF (0.1 equiv), H_2O (x M), MeOH
Conditions C: $KHCO_3$ (0.1 equiv), H_2O (x M), MeOH/THF (1:1)
Conditions D: $KHCO_3$ (0.1 equiv), TBAF (0.1 equiv), H_2O (x M), MeOH/THF (1:1).

Figure 4.23: K_{obs} with various solvent composition.

The trends shown in Figure 4.23 can be explained in terms of the background equilibria shown in Scheme 4.23. If K_{mh}, K_{SiOR} (equilibria 4.1 and 4.2) and the concentration of methanol are assumed to be constant, K_{obs} can be shown to depend on water concentration alone (Scheme 4.23). Previous work

however, in methanol/water systems, has shown that K_{mh} is not constant. Instead it was observed to decrease slightly with the addition of water.[173, 181-182] This can explain why K_{obs} does not increase proportionally with water concentration, especially in our methanol/water system.

This study confirmed that increasing water content in a Tamao oxidation reaction will encourage the formation of silanol, and therefore is likely to inhibit the reaction. A suitably polar solvent is necessary however, to allow full solvation of hydrogen peroxide. Ideal conditions would strike a balance between these two factors.

$$MeO^- + H_2O \overset{K_{mh}}{\rightleftharpoons} HO^- + MeOH \qquad (4.1)$$

$$HO^- + ArSiMe_2OMe \overset{K_{SiOR}}{\rightleftharpoons} MeO^- + ArSiMe_2OH \qquad (4.2)$$

$$K_{mh} = \frac{[HO^-][MeOH]}{[MeO^-][H_2O]} \propto \frac{[HO\text{-}]}{[MeO\text{-}][H_2O]} \qquad K_{SiOR} = \frac{[ArSiMe_2OH][MeO^-]}{[ArSiMe_2OMe][HO^-]}$$

$$K_{obs} = \frac{[ArSiMe_2OH]}{[ArSiMe_2OMe]} \propto K_{SiOR}.K_{mh}.[H_2O]$$

Scheme 4.23: Factors affecting K_{obs}

4.10. Modelling the oxidation

Having identified factors which affect the position and speed at equilibration between silanol **118** and methoxysilane **126**, we looked towards modelling the reaction to gain a better understanding of the relative rates of oxidation of these arylsilanes.

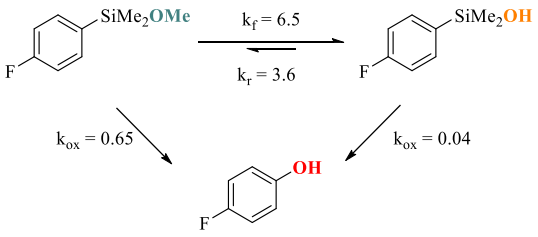
Concentration profiles of the oxidation of methoxysilane **126** (Graph A) and silanol **118** (Graph B) in methanol were obtained, using the conditions optimised above for accuracy (Figure 4.24). In methanol, rapid equilibration between silanol and methoxysilane was observed; by the time the spectroscopic observation had begun, equilibrium between silanol and methoxysilane had already

been attained. Using Berkeley Madonna™ software, we then investigated models to fit our experimental data and provide further insight into the reaction.[183]

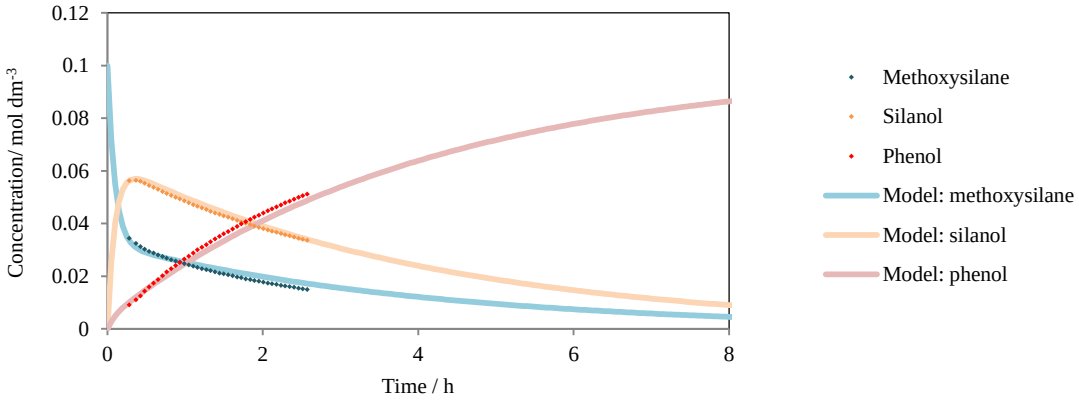
The intricate equilibria previously discussed (Scheme 4.23) prevented us from establishing the concentrations of hydroperoxide, methoxide and hydroxide ions in the system, let alone how they would change during the oxidation. As the oxidations of silanol and methoxysilane share a common dependence on hydroperoxide concentration, it was felt that informative models could still be made without taking the concentrations of the ions into account. We also assumed that the concentration of hydroperoxide ions would not change significantly in the first 50% of conversion to phenol and therefore used experimental data within this range only.

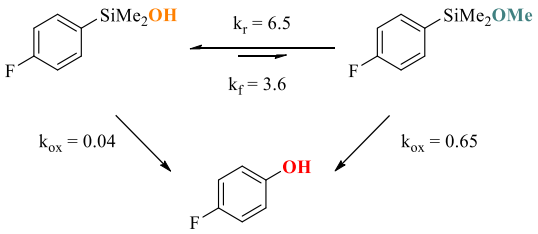
Pleasingly, we were able to find a model that supported our understanding of the mechanism of arylsilane oxidation, and had a good fit with the experimental data. This model relied on a markedly faster rate of methoxysilane than silanol oxidation, confirming our suspicion that the difference in reactivity between these species was much greater than we were able to identify through our experiments. To explain this variation in reactivity, the polar O–H bond was considered. A build up of negative charge can be expected on oxygen in silanol, an effect that would be enhanced by hydrogen bonding in suitable solvents. The silanol's silicon centre can therefore be considered to hold slightly more electron density than that in methoxysilane **126**, which in turn would inhibit its electrophilicity and rate of attack from hydroperoxide anions.

The models highlighted the rapid anionic substitution of arylsilanes. The relative rate constants indicate that silanol **118** and methoxysilane **126** interconversion is approximately ten times faster than the oxidation of methoxysilane. Hydroperoxide is a stronger nucleophile than methoxide or hydroxide, in accordance with the "alpha effect", and it must therefore be concluded that hydroperoxide addition to arylsilanes would proceed at an even faster rate.[184] Attack of hydroperoxide at silicon can thus not be considered as the rate limiting step in this oxidation.



Graph A: Fluoride free methoxysilane oxidation in methanol





Graph B: Fluoride free silanol oxidation in methanol

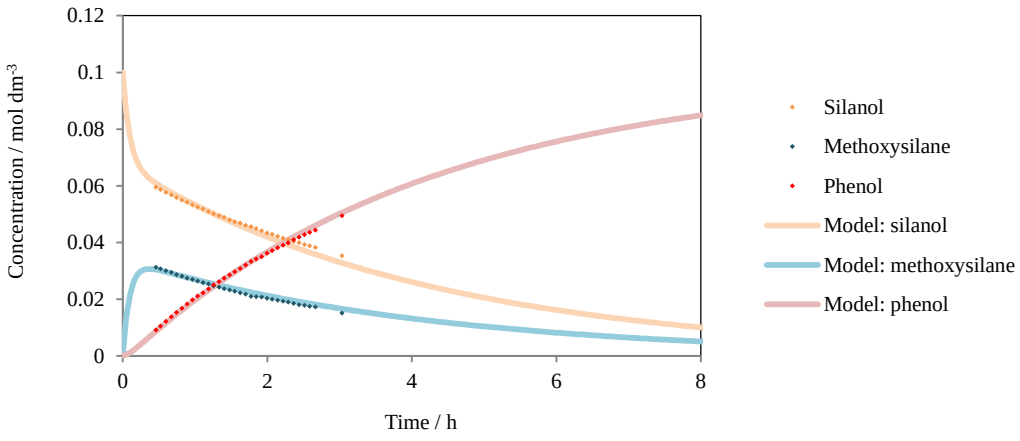
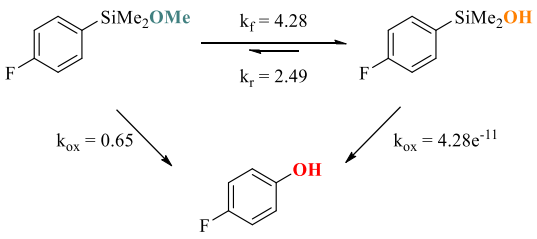


Figure 4.24: A common model to fit ^{19}F NMR spectroscopic observation of the oxidation of methoxysilane 126 and silanol 118 in MeOH

An oxidation of methoxysilane **126** was carried out in methanol with the addition of 0.1 equivalents of TBAF (Figure 4.25). Interestingly, the fluoride catalyst appeared to have little effect on this reaction, which is reflected in the relative rate constants of the model shown. It appears that in the polar methanol solvent, the rate of methoxide and hydroxide addition to silicon proceeds at such a rapid rate that TBAF addition has little effect on the rate of silanol and methoxysilane interconversion.



Fluoride catalysed oxidation of methoxysilane in methanol

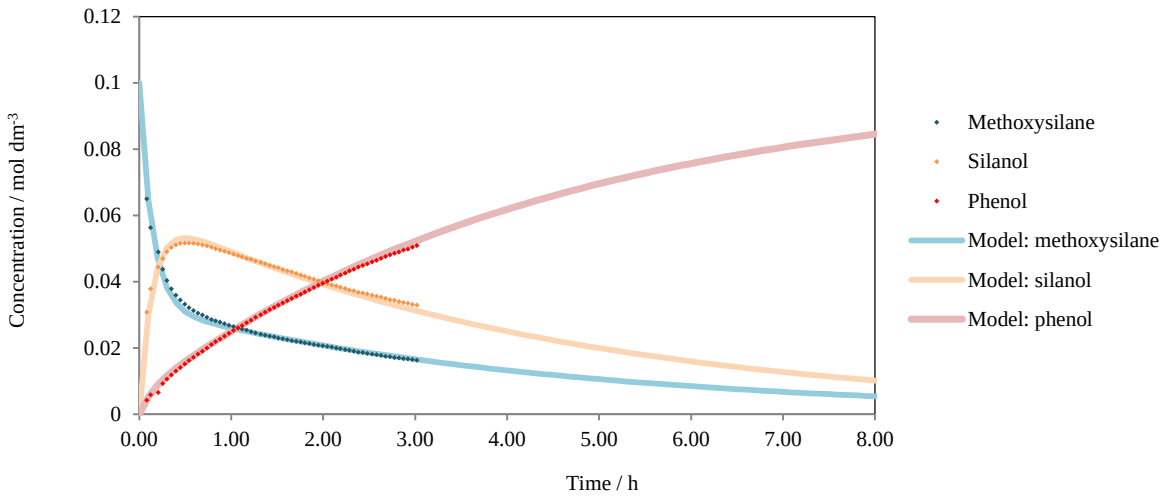
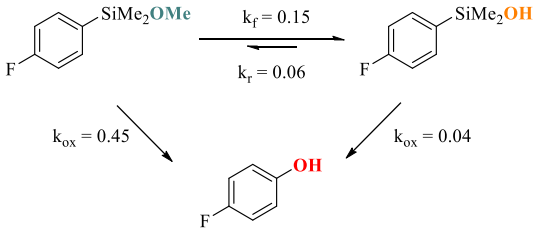
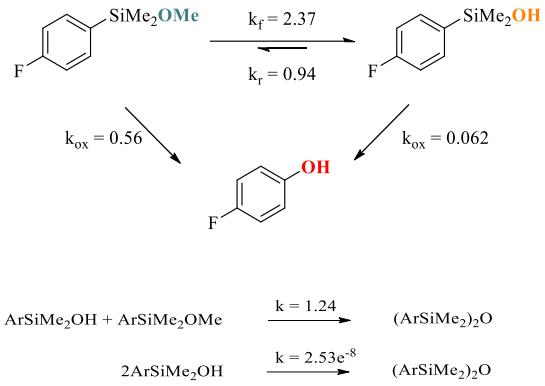


Figure 4.25: A model combined with ^{19}F NMR spectroscopic observation of the oxidation of methoxysilane in MeOH with the addition of 0.1 equivalents of TBAF

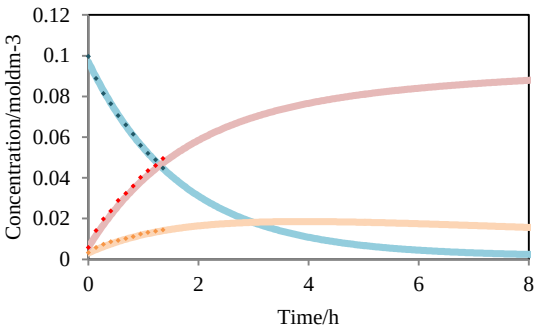
This result contrasts strongly with the effects of TBAF addition to the oxidation of methoxysilane in methanol/THF (Figure 4.14). In this system, a drastic increase in the rate of silanol formation was observed. To aid comparison, the oxidations of methoxysilane with (Graph D) and without TBAF (Graph C) were also modelled; using the same assumptions as previously described (Figure 4.25). In these models, the rate enhancing impact of fluoride on the methoxysilane/silanol equilibrium can be clearly seen. In methanol/THF the rate of anionic addition to silicon has proven to be much lower

than in pure methanol and the addition of TBAF to this mixed solvent system therefore can have a drastic effect. From these models, methoxysilane **126** was again shown to oxidise at a much faster rate than silanol **118**.





Graph C: Fluoride free methoxysilane oxidation in MeOH/THF (1:1)



Graph D: Fluoride catalysed methoxysilane oxidation in MeOH/THF (1:1)

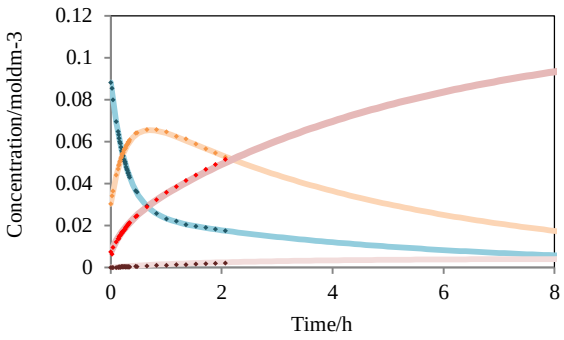


Figure 4.26: Models combined with ^{19}F NMR spectroscopic observation of the oxidation of methoxysilane 126 in MeOH/THF with and without the addition of 0.1 equivalents of TBAF

The overall rate of oxidation appears to be faster in the absence of TBAF. This can be attributed to the lack of silanol **118** formed during the reaction, leaving methoxysilane **126** free to oxidise at a faster rate. The position of equilibrium between silanol and methoxysilane predicted by the models, can be seen to sit fairly close to the equilibrium observed in the absence of hydrogen peroxide. As such, it can be understood that hydrogen peroxide improves the rate of silanol/methoxysilane equilibration but does not affect the equilibrium position.

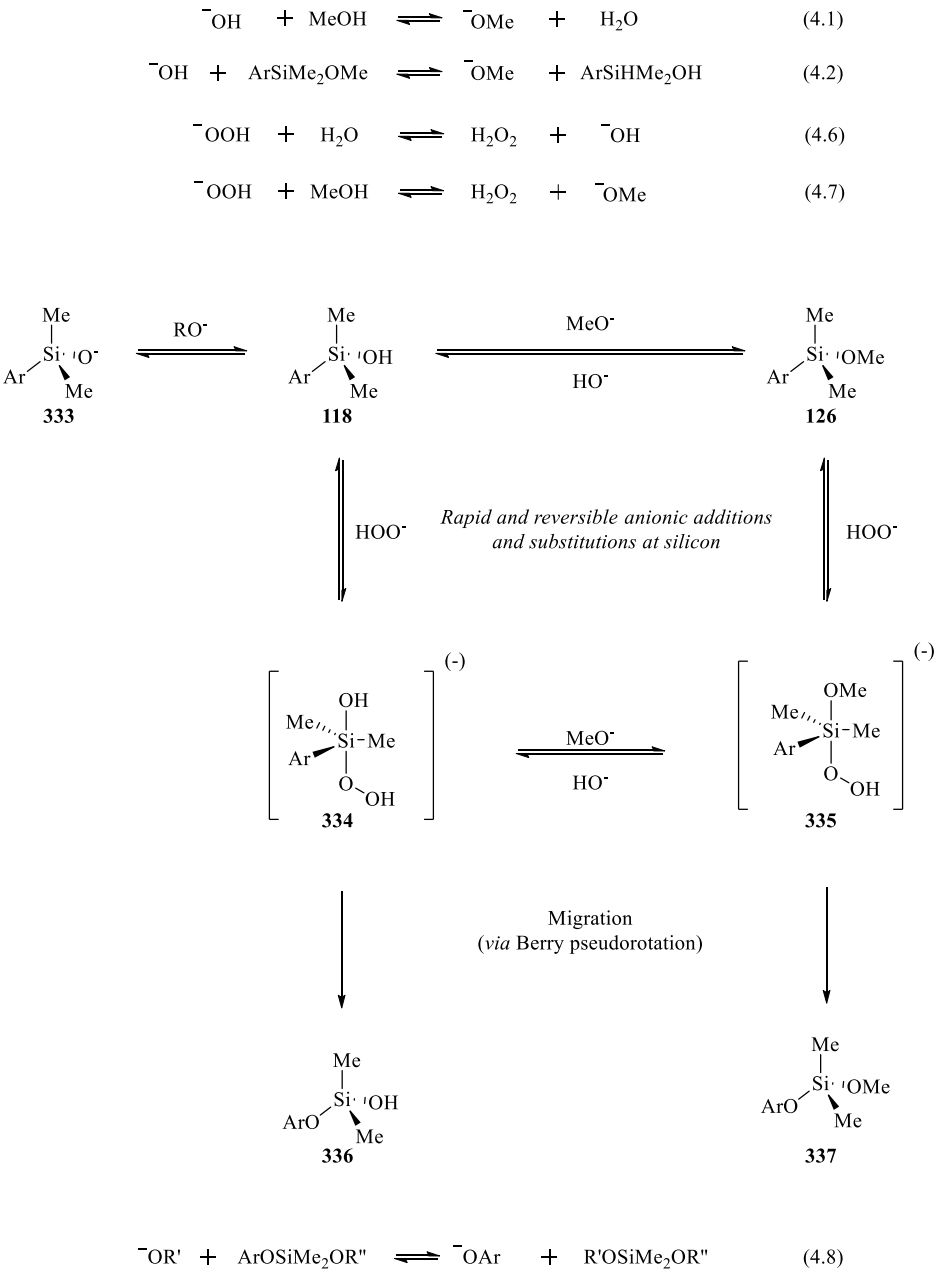
4.11. Conclusions and future work

By collecting concentration profiles of arylsilane oxidations, we have learnt that a background equilibrium between silanol **118** and methoxysilane **126** occurs in all systems studied (equilibrium 4.2). This equilibrium was found to shift with solvent composition, a feature of the system that was attributed to a further background reaction between hydroxide and methoxide ions (equilibrium 4.1). Silanol **118** was always found to hold a greater concentration than methoxysilane **126** at equilibrium, but it was also thought to oxidise at a slower rate than methoxysilane **126**, and formation of this species during oxidation was therefore a rate lowering process. The apparent unreactivity of silanol **118** can be attributed to either hydrogen bonding of silanol **118**, or full deprotonation of silanol to the unreactive silanolate **333**. Through hydrogen bonding, the electron density of silicon in silanol can be expected to increase, and its electrophilicity would therefore decrease. Alternatively, if significant deprotonation of silanol **118** occurs, the overall rate of oxidation would decrease as the concentration of both silanol **118** and hydroperoxide anions would be lower.

Within this work, we observed the rate enhancing effects of increasing hydrogen peroxide and $KHCO_3$ concentration. However, the rapid rate of substitution at silicon, and the strength of hydroperoxide as a nucleophile, strongly indicate that hydroperoxide addition to silicon is a rapid process and unlikely to be rate limiting. Instead, aryl migration is thought to be the rate determining step. In this case, hydroperoxide concentration enhances the rate of oxidation by increasing the concentration of pentavalent intermediates such as **334** and **335**. This contradicts the hypothesis of Tamao and co-workers, but is in agreement with Mader and Norrby.[68, 168] Release of free phenol following migration will depend upon equilibrium (4.8). Bearing in mind the acidity of phenol, this equilibrium is likely to favour the dissociated phenoxide anion.

Finally, we found that addition of TBAF to the oxidation of arylsilanes was not always rate enhancing, but that its likely mode of action in the oxidation was through formation of pentavalent intermediates, which are more susceptible to nucleophilic attack by hydroperoxide, methoxide and hydroxide anions. The utility of TBAF was particularly clear in equilibrium experiments of

isopropoxysilane **332**. In these reactions, nucleophilic substitution only occurred in the presence of TBAF, indicating that less reactive arylsilanes may benefit greatly from the addition of TBAF. However, the basicity of TBAF was thought to increase the complexity of this reaction. Although a greater concentration of hydroperoxide anions is expected as the pH of the reaction mixture increases, a greater concentration of silanolate anions (**333**) may also be formed under these conditions.



Scheme 4.24: Mechanistic conclusions

An interesting question that remains, and that is likely to be the focus of future work, is the appearance of the aryl migration transition state. Our Hammett study (and Tamao's) indicated that within this transition state, a negative charge is built up on the aromatic ring. Within the studies of Mader and Norrby, the geometry of the transition state was carefully considered, but electronic effects were not.

Ideal conditions for methoxysilane oxidation would inhibit the formation of silanol (and consequently silanolate). Our equilibrium studies indicate that decreasing the concentration of water in the system would achieve this. However, a polar solvent system is highly advantages to the reaction as it increases the rate of nucleophilic attack at silicon, to the extent that TBAF did little to enhance the rate of reaction. Future work to optimise the reaction will attempt to find a beneficial balance between these factors.

5. Experimental

5.1. General Experimental

Chromotography: Thin layer chromatography was performed using Merck DC Kieselgel 60 F_{254} plates. Product spots were visualised by the quenching of UV fluorescence (λ_{max} 254 nm) then stained and heated using anisaldehyde, ammonium molybdate or potassium manganate as appropriate. Retention factors (R_f) are reported with the solvent system used in parentheses. Flash column chromatography was carried out on Macherey-Nagel Kieselgel 60M (230 – 400 mesh) under positive pressure, and the solvent system used in parentheses.

Melting points: Melting points were determined using a Griffin melting point apparatus and are uncorrected.

Infrared Spectra: Infrared spectra were recorded on a Bruker Tensor 27 Fourier Transform spectrometer, and samples were prepared as a thin film between NaCl plates. Absorption maxima (ν_{max}) are quoted in wavenumbers (cm^{-1}) and are described as s (strong), m (medium), w (weak) or br (broad). Only selected, characteristic IR absorption data are provided for each compound.

NMR Spectra: Proton (^{1}H) and carbon (^{13}C) spectra were recorded on a Bruker DPX200 (200/50 MHz), Bruker DQX400 (400/125 MHz), Bruker DRX500 (500/125 MHz) or a Bruker ACV500 (500/125 MHz) spectrometer. Fluorine (^{19}F) spectra were recorded on a Bruker AVB500. Data are presented in the order: chemical shift, integration, multiplicity (br, broad; s, singlet; d, doublet; dd doublet of doublets; dt, doublet of triplets; t, triplet; q, quartet; sept, septet; m, multiplet), coupling

constant and proton assignment. Chemical shifts (δ_H or δ_C) are quoted in ppm downfield of $SiMe_4$ with residual solvent as the internal standard. ^{19}F chemical shifts are quoted in ppm downfield of $CFCl_3$. Assignments were made on the basis of chemical shifts and coupling constants. Coupling constants (*J*) are given in Hz and are rounded to the nearest 0.5 Hz.

Mass Spectra: High resolution mass spectra (HRMS) were recorded using a Bruker Daltronics microTOF spectrometer by Robin Procter at the Chemistry Research Laboratory. High resolution values are calculated to four decimal places from the molecular formula and all obtained values are within a tolerance of 5 ppm.

Solvents and Reagents: Solvents and commercially available reagents were dried and purified before use where appropriate using standard procedures. THF, diethyl ether, dichloromethane and methanol were obtained dry and oxygen free from solvent dispenser units having been passed through an activated alumina column under argon. DIPEA, TMEDA, DMSO and MeCN were distilled over CaH_2 under reduced pressure and stored over CaH_2 and under N_2. Petroleum ether refers to the fraction of light petroleum ether which boils in the range 40-60 °C.

Reactions: For reactions requiring anhydrous conditions, experiments were carried out in oven-dried glassware. Unless otherwise stated, all reactions were carried out under argon.

5.2. Methodology development

General procedure I for butyl lithium exchange and silylation

To a stirred solution of bromo arene at –78 °C in anhydrous THF, was added *n*- (1.1 to 1.2 equiv) or *t*- (2.0 to 2.4 equiv) BuLi (2.5 M n-BuLi in hexanes, 1.6 M t-BuLi in hexanes). The resulting mixture was stirred for 1 to 3 h at –78 °C before addition of chlorodimethylsilane (1.0 to 1.5 equiv), and the reaction mixture allowed to warm to RT overnight. The crude reaction mixture was diluted in petrol and filtered to remove lithium salts. Purification was conducted by column chromatography or vacuum distillation.

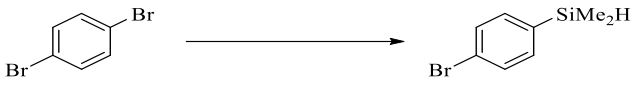
Dimethyl(4-(trifluoromethyl)phenyl)silane (96)



According to the general procedure **I**, 4.27 mL (10.7 mmol, 1.2 equiv) of *n*-BuLi was added to 2.0 g (8.89 mmol, 1.0 equiv) of 1-bromo-4-(trifluoromethyl)benzene in anhydrous THF (50 mL). The resulting mixture was stirred for 2 h at –78 °C before 1.26 mL (11.6 mmol, 1.3 equiv) of chlorodimethylsilane was added and the reaction stirred overnight. The product was purified by vacuum distillation (60-64 °C at 20 mbar) to afford the title compound as a colourless oil (943 mg, 52%); $\mathbf{R_f}$ 0.59 (petroleum ether); **^{1}H NMR** (500 MHz, $CDCl_3$) δ_H 0.38 (6H, d, *J* 4.0, Si(C*H*$_3$)$_2$), 4.46 (1H, sept, *J* 4.0, Si*H*), 7.61 (2H, d, *J* 8.0, Ar*H*), 7.67 (2H, d, *J*, 8.0, Ar*H*); **^{13}C NMR** (125 MHz, $CDCl_3$) δ_C –4.00, 124.1 (q, *J* 272.0), 124.3 (q, *J* 3.5), 131.1 (q, *J* 32.0), 134.3, 142.4.

The spectroscopic data was found to be in agreement with that reported by Kira and co-workers.[185]

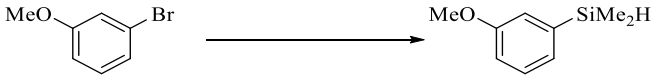
(4-Bromophenyl)dimethylsilane (97)



According to the general procedure **I**, 5.59 mL (14.0 mmol, 1.1 equiv) of *n*-BuLi was added to 3.0 g (12.7 mmol, 1.0 equiv) of 1,4-dibromobenzene in anhydrous THF (30 mL). The resulting mixture was stirred for 3 h at –78 °C before 1.69 mL (18.5 mmol, 1.2 equiv) of chlorodimethylsilane was added and the reaction stirred overnight. The product was purified by vacuum distillation (70-72 °C at 10 mbar) to afford the title compound as a colourless oil (2.41 g, 89%); $\mathbf{R_f}$ 0.76 (petroleum ether); **^{1}H NMR** (400 MHz, $CDCl_3$) δ_H 0.35 (6H, d, *J* 3.5, Si(C*H*$_3$)$_2$), 4.41 (1H, sept, *J* 3.5, Si*H*), 7.41 (2H, d, *J* 8.0 Ar*H*), 7.51 (2H, d, *J* 8.0, Ar*H*); **^{13}C NMR** (100 MHz, $CDCl_3$) δ_C) –3.87, 124.0, 131.0, 135.6, 136.2.

The spectroscopic data was found to be in agreement with that reported by Ishikawa and co-workers.[186]

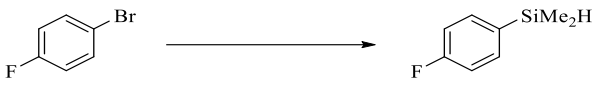
(3-Methoxyphenyl)dimethylsilane (98)



To a solution of 3-bromoanisole (1.0 g, 5.35 mmol, 1.0 equiv) in THF (20 mL) at −78 °C was added *t*-BuLi (6.7 mL, 10. 7 mmol, 2.0 equiv). The reaction mixture was stirred fro 30 min at −78 °C before the addition chlorodimethylsilane (655 μL, 5.88 mmol, 1.1 equiv), after which the reaction was allowed to warm to RT overnight. Methanol (2 mL) was added, and the crude mixture concentrated *in vacuo* before purification *via* silica plug (diethyl ether) to afford a colourless oil (724 mg, 81%); $\mathbf{R_f}$ 0.67 (petroleum ether / Et_2O (9:1)); **^{1}H NMR** (400 MHz, $CDCl_3$) δ_H 0.36 (6H, d, *J* 4.0, SiH(C*H*$_3$)$_2$), 3.84 (3H, s, OC*H*$_3$), 4.43 (1H, sep, *J* 4.0, Si*H*), 6.93 (1H, dd, *J* 7.5, 2.5, Ar*H*), 7.10 (1H, d, *J* 2.5, Ar*H*), 7.14 (1H, d, *J* 7.5, Ar*H*), 7.32 (1H, d, *J* 7.5, Ar*H*); **^{13}C NMR** (100 MHz, $CDCl_3$) δ_C –3.79, 55.1, 114.5, 119.4, 126.2, 129.1, 139.1, 159.0.

The spectroscopic data was found to be in agreement with that reported by Pitt and co-workers.[187]

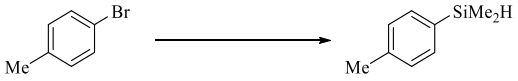
(4-Fluorophenyl)dimethylsilane (99)



According to the general procedure **I**, 8.23 mL (20.6 mmol, 1.2 equiv) of *n*-BuLi was added to 3.0 g (17.1 mmol, 1.0 equiv) of 1-bromo-4-fluorobenzene in anhydrous THF (60 mL). The resulting mixture was stirred for 3 h at –78 °C before 2.86 mL (25.7 mmol, 1.5 equiv) of chlorodimethylsilane was added and the reaction stirred overnight. The product was purified by vacuum distillation (52 °C at 20 mbar) to afford the title compound as a colourless oil (1.78, 67%); **R_f** 0.78 (petroleum ether); **IR** (thin film, ν_{max} / cm^{-1}) 2120m, 1589m, 1499m, 1231m, 1106m, 877s; **^{1}H NMR** (500 MHz, $CDCl_3$) δ_H 0.35 (6H, d, *J* 3.5, Si(C*H*$_3$)$_2$), 4.44 (1H, sept, *J* 3.5, Si*H*), 7.07 (2H, t, *J* 8.5, Ar*H*), 7.53 (2H, dd, *J* 8.5, 6.0, Ar*H*); **^{13}C NMR** (125 MHz, $CDCl_3$) δ_C –3.68, 115.0 (d, *J* 20.0), 132.8 (d, *J* 3.5), 135.9 (d, *J* 7.0), 163.8 (d *J* 248.5); **^{19}F NMR** (377 MHz, $CDCl_3$) δ_F -111.8; **HRMS** (FI^+) calc. for $C_8H_{11}FSi$ $[M]^+$ 154.0614, found 154.0615.

Compound previously reported by Lipowitz and co-workers.[188]

Dimethyl(p-tolyl)silane (100)



According to the general procedure **I**, 5.6 mL (14.0 mmol, 1.2 equiv) of *n*-BuLi was added to 2.0 g (11.7 mmol, 1.0 equiv) of *para*-bromotoluene in anhydrous THF (40 mL). The resulting mixture was stirred for 2 h at –78 °C before 1.69 mL (15.2 mmol, 1.3 equiv) of chlorodimethylsilane was added and the reaction stirred overnight. The product was purified by column chromatography (petroleum ether) to afford the title compound as a colourless oil (1.41 g, 80%); **R_f** 0.66 (petroleum ether); **^{1}H NMR** (400 MHz, $CDCl_3$) δ_H 0.35 (6H, d, *J* 3.5, Si(C*H*$_3$)$_2$), 2.38 (3H, s, ArC*H*$_3$), 4.43 (1H, sept, *J* 3.5,

Si*H*), 7.21 (2H, d, *J* 7.5, Ar*H*), 7.47 (2H, d, *J* 7.5, Ar*H*); **^{13}C NMR** (100 MHz, $CDCl_3$) δ_C –3.69, 21.5, 128.7, 133.8, 134.0, 139.0.

The spectroscopic data was found to be in agreement with that reported by Hevesi and co-workers.[189]

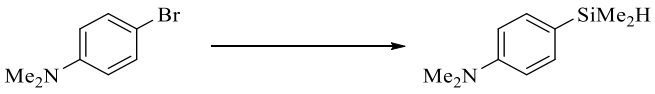
(4-Methoxyphenyl)dimethylsilane (101)



According to the general procedure **I**, 8.0 mL (12.8 mmol, 2.2 equiv) of *t*-BuLi was added to 1.0 g (1.49 mmol, 1.0 equiv) of *para*-bromotoluene in anhydrous THF (20 mL). The resulting mixture was stirred for 40 min at –78 °C before 1.42 mL (12.8 mmol, 1.0 equiv) of chlorodimethylsilane was added and the reaction stirred overnight. The product was purified by column chromatography (petroleum ether) to afford the title compound as a colourless oil (758 mg, 85%); **R_f** 0.69 (petroleum ether); **^{1}H NMR** (400 MHz, $CDCl_3$) δ_H 0.34 (6H, d, *J* 3.5, Si(C*H*$_3$)$_2$), 3.84 (3H, s, OC*H*$_3$), 4.43 (1H, sept, *J* 3.5, Si*H*), 6.94 (2H, d, *J* 8.5, Ar*H*), 7.49 (2H, d, *J* 8.5, Ar*H*); **^{13}C NMR** (100 MHz, $CDCl_3$) δ_C –3.54, 55.0, 113.7, 115.3, 135.4, 160.6.

The spectroscopic data was found to be in agreement with that reported by Hevesi and co-workers.[189]

4-(Dimethylsilyl)-N,N-dimethylaniline (102)

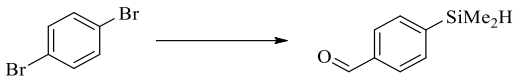


According to the general procedure **I**, 3.45 mL (5.50 mmol, 2.0 equiv) of *t*-BuLi was added to 500 mg (2.5 mmol, 1.0 equiv) of 4-bromo-N,N-dimethylaniline in anhydrous THF (10 mL). The resulting mixture was stirred for 2 h at –78 °C before 335 μL (3.0 mmol, 1.2 equiv) of chlorodimethylsilane was added and the reaction stirred overnight. The product was purified by column chromatography (petroleum ether) to afford the title compound as a yellow oil (378 mg, 84%); **R_f** 0.79 (petroleum ether / Et_2O (4:1)); **^{1}H NMR** (400 MHz, $CDCl_3$) δ_H 0.32 (6H, d, *J* 3.5, Si(C*H*$_3$)$_2$), 2.98 (6H, s,

N(CH_3)$_2$), 4.42 (1H, sep, *J* 3.5, Si*H*), 6.76 (2H, t, *J* 8.5, Ar*H*), 7.43 (2H, d, *J* 8.5, Ar*H*); **^{13}C NMR** (100 MHz, $CDCl_3$) δ_C -3.42, 40.2, 112.0, 122.3, 135.1, 151.2.

The spectroscopic data was found to be in agreement with that reported by Laszlo and co-workers.[189]

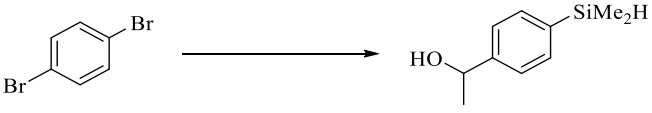
4-(Dimethylsilyl)benzaldehyde (105)



To a stirred solution of 1,4 dibromobenzene (1.5 g, 6.36 mmol, 1.0 equiv) at −78 °C in anhydrous THF (40 mL), was slowly added *t*-BuLi (7.92 mL of a 1.6 M solution in hexanes, 12.7 mmol, 2.0 equiv). The resulting mixture was stirred for 1 h at −78 °C before the addition of DMF (540 μL, 7.0 mmol, 1.2 equiv). The reaction mixture was stirred for another 15 min, after which *t*-BuLi (7.92 mL of a 1.6 M solution in hexanes, 12.7 mmol, 2.0 equiv) was added and stirring continued for 20 min. $ClSiMe_2H$ (777 μL, 7.0 mmol, 1.1 equiv) was finally added and the reaction allowed to warm to RT. After 16 h the reaction mixture was quenched with sat. aq. NH_4Cl (10 mL) and the mixture extracted with Et_2O (3 × 20 mL). The combined organic layers were dried ($MgSO_4$) and concentrated *in vacuo* to afford a yellow oil which was purified by column chromatography (petroleum ether → petroleum ether / Et_2O (9:1)) to a colourless oil (620 mg, 59%); **R_f** 0.51 (petroleum ether / Et_2O (9:1)); **^{1}H NMR** (400 MHz, $CDCl_3$) δ_H 0.39 (6H, d, *J* 4.0, Si(C*H*$_3$)$_2$), 4.47 (1H, sep, *J* 4.0, Si*H*), 7.72 (2H, d, *J* 8.0, Ar*H*), 7.89 (2H, d, *J* 8.0, Ar*H*), 10.0 (1H, s, C*H*O).

The spectroscopic data was found to be in agreement with that reported by Burnell and co-workers.[190]

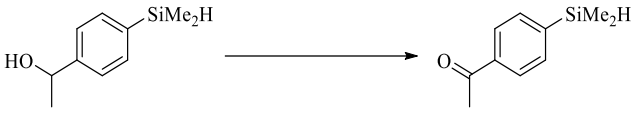
1-(4-(Dimethylsilyl)phenyl)ethanol (106)



This procedure was developed from that reported by Kim *et al*;[95] To a solution of 1,4 dibromobenzene (1.5 g, 6.36 mmol, 1.0 equiv) in anhydrous THF (40 mL) at –78 °C was added *t*-

BuLi (7.95 mL of a 1.6 M solution in hexanes, 12.7 mmol, 2.0 equiv) and the reaction stirred for 1 h at –78 °C. Acetaldehyde (395 μL, 7.00 mmol, 1.1 equiv) was added and the reaction warmed to 0 °C over 30 min. The reaction was then cooled to –78 °C before the addition of *t*-BuLi (8.74 mL of a 1.6 M solution, 14.0 mmol, 2.2 equiv) and continued stirring at –78 °C for 1 h. Finally, dimethylchlorosilane (920 μL, 8.27 mmol, 1.3 equiv) was added and the reaction allowed to warm to RT over 2 h. The reaction was quenched with NH_4Cl (20 mL, sat., aq.), the mixture extracted with EtOAc (3 x 20 mL) and the combined organic layers dried ($MgSO_4$) and concentrated *in vacuo* to a red oil, before purification by column chromatography (petroleum ether → petroleum ether / EtOAc (4:1)) afforded the title compound as a colourless oil (899 mg, 78%); **R_f** 0.31 (petroleum ether / Et_2O (4:1)); **IR** (thin film, ν_{max} / cm^{-1}) 2970w, 2117m, 1249w, 1083w, 878s; **^{1}H NMR** (400 MHz, $CDCl_3$) δ_H 0.36 (6H, d, *J* 3.5, Si(C*H*$_3$)$_2$H), 1.51 (3H, d, *J* 6.5, CH(OH)C*H*$_3$), 1.82 (1H, br s, CH(O*H*)), 4.44 (1H, sept, *J* 3.5, Si(CH$_3$)$_2$*H*), 4.91 (1H, q, *J* 6.5, C*H*(OH)CH$_3$), 7.39 (2H, d, *J* 7.5, Ar*H*), 7.55 (2H, d, *J* 7.5, Ar*H*); **^{13}C NMR** (100 MHz, $CDCl_3$) δ_C –3.76, 25.1, 70.4, 124.9, 134.3, 136.6, 146.8; **HRMS** (FI^+) calc. for $C_{10}H_{16}OSi$ $[M]^+$ 180.0970, found 180.0969.

1-(4-(Dimethylsilyl)phenyl)ethanone (107)



SO_3·pyridine (1.67 g, 10.5 mmol, 3.0 equiv) and anhydrous DMSO (2.48 mL, 30.5 mmol, 10.0 equiv) were stirred at RT for 15 min before a solution of 1-(4-(dimethylsilyl)phenyl)ethanol (630 mg, 3.49 mmol, 1.0 equiv) and DIPEA (3.04 mL, 17.5, 5.0 equiv) in dichloromethane (15 mL) was added. The reaction mixture was stirred at RT for 1 h by which time the reaction was observed to be complete by TLC. The reaction mixture was diluted with dichloromethane (10 mL), quenched with HCl (10 mL, 1 N aqueous solution) and stirred vigorously for 15 min at RT. The biphasic mixture was separated, and the aqueous phase washed with dichloromethane (3 x 10 mL). The combined organic phases were washed with $NaHCO_3$ (2 x 20 mL, sat., aq.), dried ($MgSO_4$) and concentrated *in vacuo* to a yellow oil which was purified by column chromatography (petroleum ether → petroleum ether / Et_2O

(9:1)) to afford the title compound as a colourless oil (605 mg, 97%); **R_f** 0.51 (petroleum ether / Et_2O (9:1)); **IR** (thin film, ν_{max} / cm^{-1}) 2120m, 1684s, 1251m, 875s, 820m; **^{1}H NMR** (500 MHz, $CDCl_3$) δ_H 0.38 (6H, d, *J* 3.5, Si(C*H*$_3$)$_2$), 2.61(3H, s, COC*H*$_3$), 4.46 (1H, sept, *J* 3.5, Si*H*), 7.65 (2H, d, *J* 8.0, Ar*H*), 7.93 (2H, d, *J* 8.0, Ar*H*); **^{13}C NMR** (125 MHz, $CDCl_3$) δ_C –4.03, 26.6, 127.3, 134.2, 137.5, 144.2, 198.3; **HRMS** (ES^+) calc. for $C_{10}H_{14}NaOSi$ $[M+Na]^+$ 201.0708, found 201.0708.

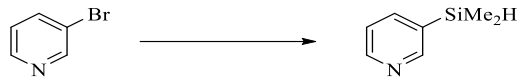
Compound previously reported by Schott and co-workers without full characterisation.[191]

(2,5-Dimethoxyphenyl)dimethylsilane (111)



To a stirred solution of 1,4 dimethoxybenzene (8.29 g, 60.0 mmol, 1.0 equiv) and TMEDA (10.8 mL, 72.0 mmol, 1.2 equiv) in anhydrous THF (150 mL) at –78 °C, was added *s*-BuLi (52.0 mL of a 1.3 M solution in hexanes, 72.0 mmol, 1.2 equiv). The resulting mixture was stirred for 2 h at –78 °C before addition of chlorodimethylsilane (8.66 mL, 78.0 mmol, 1.3 equiv), and the reaction mixture allowed to warm to RT overnight. The reaction mixture was quenched with NH_4Cl (50 mL, sat., aq.), the phases separated and the aqueous phase extracted with dichloromethane (3 x 50 mL). The combined organic phases were dried ($MgSO_4$) and concentrated *in vacuo* before purification by column chromatography (petroleum ether) afforded the title compound as a colourless oil (11.5 g, 98%); **R_f** 0.73 (petroleum ether); **IR** (thin film, ν_{max} / cm^{-1}) 3424br, 2120w, 1643m 1272m, 892s; **^{1}H NMR** (400 MHz, $CDCl_3$) δ_H 0.34 (6H, s, SiC*H*$_3$), 3.79 (6H, s, OC*H*$_3$), 4.39 (1H, sept, *J* 3.5, Si*H*), 6.79 (1H, d, *J* 9.0, Ar*H*), 6.89 (1H, dd, *J* 9.0, 3.0, Ar*H*), 7.00 (1H, d, *J* 3.0, Ar*H*); **^{13}C NMR** (100 MHz, $CDCl_3$) δ_C –3.86, 55.8, 55.9, 110.5, 115.3, 121.5, 126.8, 153.5, 158.1; **HRMS** (FI^+) calc. for $C_{10}H_{16}O_2Si$ $[M]^+$ 196.0920, found 196.0919.

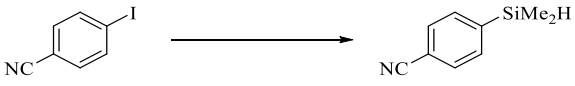
3-(Dimethylsilyl)pyridine (114)



The procedure of Kung *et al*[16] was followed. *i*-PrMgCl (8.35 mL of a 2 M solution in THF, 16.7 mmol, 1.0 equiv) was added slowly to a solution of 3-bromopyridine (2.60 mL, 16.7 mmol, 1.0 equiv) in anhydrous THF (30 mL) at RT. After 1 h the solution was cooled to 0 °C and chlorodimethylsilane (2.15 mL, 19.24 mmol, 1.15 equiv) was added. The reaction mixture was allowed to warm to RT. The reaction was then diluted in ether (30 mL) and washed with water (3 x 20 mL) and brine (2 x 30 mL). The combined organic phases were dried ($MgSO_4$) and concentrated *in vacuo* to a yellow oil which was purified by column chromatography ($CHCl_3$) to afford a slightly yellow oil (1.17 g, 51%); R_f 0.32 ($CHCl_3$); ^{1}H NMR (400 MHz, $CDCl_3$) δ_H 0.38 (6H, d, *J* 4.0, SiC*H*$_3$), 4.46 (1H, sept, *J* 4.0, Si*H*), 7.27 (1H, dd, *J* 7.5, 5.0, Ar*H*), 7.81 (1H, dt, *J* 7.5, 1.5, Ar*H*), 8.60 (1H, dd, *J* 5.0, 1.5, Ar*H*), 8.71 (1H, t, *J* 1.5, Ar*H*); ^{13}C NMR (100 MHz, $CDCl_3$) δ_C –4.10, 123.3, 132.4, 141.7, 150.2, 154.3.

The spectroscopic data was found to be in agreement with that reported by Itami and co-workers.[192]

***4*-(Dimethylsilyl)benzonitrile (116)**

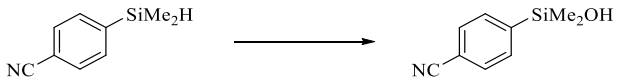


The following procedure was developed from that reported by Wood *et al*;[100] *i*-PrMgCl (4.25 mL of a 2 M solution in THF, 8.52 mmol, 1.3 equiv) was slowly added to a cooled solution (ice/salt bath, –20 °C) of 4-iodobenzonitrile (1.5 g, 6.55 mmol, 1.0 equiv) in anhydrous THF (15 mL). After 30 min the solution was transferred slowly *via* cannular to a cooled (ice/salt bath –20 °C) solution of chlorodimethylsilane (1.10 mL, 9.82 mmol, 1.5 equiv) in anhydrous THF (15 mL). The reaction mixture was allowed to warm to RT over 4 h. The reaction was then quenched with NH_4Cl (10 mL, sat., aq.), the phases separated and the aqueous phase extracted with dichloromethane (3 x 10 mL). The combined organic layers were dried ($MgSO_4$) and concentrated *in vacuo* to afford a colourless oil (950 mg, 90%) without the need for further purification; **R_f** 0.71 (petroleum ether); **^{1}H NMR** (400

MHz, $(CD_3)_2CO$) δ_H 0.40 (6H, d, *J* 3.5, Si(C*H*$_3$)$_2$), 4.45 (1H, sept, *J* 3.5, Si*H*), 7.76 (2H, d, *J* 8.0, Ar*H*), 7.79 (2H, d, *J* 8.0, Ar*H*); **^{13}C NMR** (100 MHz, $(CD_3)_2CO$) δ_C –4.66, 113.2, 118.9, 131.5, 134.2, 144.5.

The spectroscopic data was found to be in agreement with that reported by Rich and co-workers.[190]

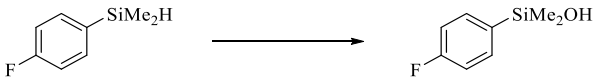
4-(Hydroxydimethylsilyl)benzonitrile (117)



To a solution of silane **116** (200 mg, 1.24 mmol, 1.0 equiv) and water (41 μL) in MeCN (4 ml), under air, was added $[RuCl_2(p\text{-cymene})]_2$ (15 mg, 0.025 mmol, 2 mol%). After 2/3 seconds of effervescence the reaction was seen to be complete by TLC. The reaction was diluted with petrol (2 mL) and eluted through a silica plug (petroleum ether / Et_2O (9:1)) to afford the title compound as a colourless liquid (223 mg, 100%); **R$_f$** 0.71 (petroleum ether); **^{1}H NMR** (250 MHz, (CD_3OD) δ_H 0.39 (6H, s, Si(C*H*$_3$)$_2$), 1.51 (1H, br s, O*H*), 7.76 (4H, d, *J* 3.0, Ar*H*).

The spectroscopic data was found to be in agreement with that reported by Denmark and co-workers.[193]

(4-Fluorophenyl)dimethylsilanol (118)



To a solution of silane **99** (100 mg, 0.648 mmol, 1.0 equiv) and water (23 μL, 1.30 mmol, 2.0 equiv) in MeCN (2 mL), under air, was added $[RuCl_2(p\text{-cymene})]_2$ (8.0 mg, 0.013 mmol, 2 mol%). After 2/3 seconds of effervescence the reaction was seen to be complete by TLC. The reaction was diluted with petrol (2 mL) and eluted through a silica plug (petroleum ether / Et_2O (9:1)) to afford the title compound as a colourless liquid (97.3 mg, 88%); **R$_f$** 0.41 (petroleum ether / Et_2O (9:1)); **^{1}H NMR** (200 MHz, $CDCl_3$) δ_H 0.41 (6H, s, Si(C*H*$_3$)$_2$), 1.87 (1H, br s, SiO*H*), 7.09 (2H, dd, *J* 9.5, 8.5, Ar*H*), 7.58 (2H, dd, *J* 8.5, 6.0, Ar*H*); **^{19}F NMR** (470 MHz, $CDCl_3$) δ_F -111.0.

Data in agreement with that reported by Yoshida *et al*[194]

Dimethyl(p-tolyl)silanol (119)



To a solution of silane **100** (50 mg, 0.33 mmol, 1.0 equiv) and water (10 μL, 0.66 mmol, 2.0 equiv) in MeCN (1 mL), under air, was added $[RuCl_2(p\text{-cymene})]_2$ (4.1 mg, 0.007 mmol, 2 mol%). After 2/3 seconds of effervescence the reaction was seen to be complete by TLC. The reaction was diluted with petrol (2 mL) and eluted through a silica plug (petroleum ether / Et_2O (9:1)) to afford the title compound as a colourless liquid (46 mg, 84%); $\mathbf{R_f}$ 0.19 (petroleum ether / Et_2O (9:1)); **^{1}H NMR** (400 MHz, $CDCl_3$) δ_H 0.41 (6H, s, Si(C*H*$_3$)$_2$), 1.79 (1H, br s, O*H*), 2.37 (1H, s, ArC*H*$_3$), 7.18-7.26 (2H, m, Ar*H*), 7.47-7.56 (2H, m, Ar*H*); **^{13}C NMR** (100 MHz, $CDCl_3$) δ_C 0.02, 21.5, 128.7, 133.1, 135.6, 139.6.

The spectroscopic data was found to be in agreement with that reported by Hirabayashi and co-workers.[195]

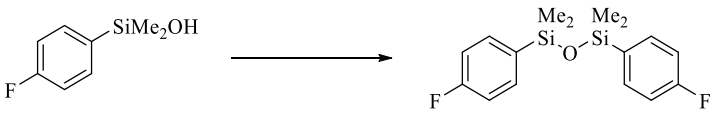
Methoxy(4-methoxyphenyl)dimethylsilane (120)



To a solution of silane **101** (250 mg, 1.50 mmol, 1.0 equiv) and water (500 μL, 30 mmol, 20 equiv) in MeCN (5 mL), under air, was added $[RuCl_2(p\text{-cymene})]_2$ (18 mg, 0.03 mmol, 2 mol%). After 2/3 seconds of effervescence the reaction was seen to be complete by TLC. The reaction was diluted with petrol (2 mL) and eluted through a silica plug (petroleum ether / Et_2O (9:1)) to afford the title compound as a colourless liquid (270 mg, 92%); $\mathbf{R_f}$ 0.21 (petroleum ether / Et_2O (85:15)); **^{1}H NMR** (400 MHz, $CDCl_3$) δ_H 0.39 (6H, s, Si(C*H*$_3$)$_2$), 2.10 (1H, s, SiO*H*), 3.83 (3H, s, OC*H*$_3$), 6.94 (2H, m, Ar*H*), 7.53 (2H, m, Ar*H*); **^{13}C NMR** (100 MHz, $CDCl_3$) δ_C 0.08, 55.1, 113.6, 130.2, 134.6, 160.8.

The spectroscopic data was found to be in agreement with that reported by Denmark and co-workers.[193]

1,3-Bis(4-fluorophenyl)-1,1,3,3-tetramethyldisiloxane (118b)



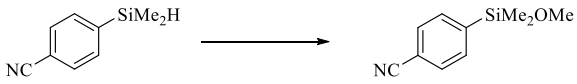
Silanol **118** was found to transform, in the presence of $MgSO_4$, to disiloxane **118b** above −20 °C. The disiloxane was purified through vacuum distillation (156 °C, 11 mbar); $\mathbf{R_f}$ 0.84 (petroleum ether); **^{1}H NMR** (400 MHz, $CDCl_3$) δ_H 0.32 (12H, s, Si(C*H*$_3$)$_2$), 7.05 (4H, t, *J* 8.5, Ar*H*), 7.49 (4H, dd, *J* 8.5, 6.5, Ar*H*); **^{19}F NMR** (377 MHz, $CDCl_3$) δ_F −111.54.

Data in agreement with that reported by Porzel *et al* [196]

General procedure II; methoxysilane formation

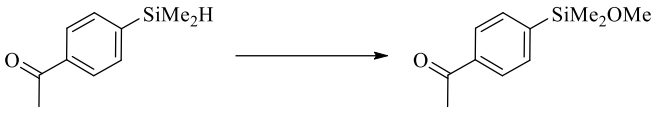
$[RuCl_2(p\text{-cymene})]_2$ (0.5 mol%) was added to the hydrosilane in MeOH (5 M), under air. After 2 to 10 seconds of effervescence the reaction was seen to be complete by TLC. The reaction mixture was diluted in Et_2O and eluted through a silica plug (Et_2O) to afford methoxy silane.

4-(Methoxydimethylsilyl)benzonitrile (121)



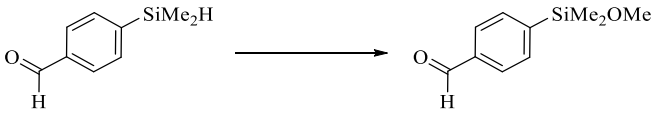
According to general procedure **II**, 50 mg (0.310 mmol) of arylhydrosilane **116** afforded the title compound as a colourless oil (56 mg, 95%); $\mathbf{R_f}$ 0.34 (petroleum ether / Et_2O (9:1)); **IR** (thin film, ν_{max} / cm^{-1}) 2960w, 2229m, 1386w, 1255m, 1083s, 823s; **^{1}H NMR** (400 MHz, $CDCl_3$) δ_H 0.40 (6H, s, Si(C*H*$_3$)$_2$), 3.46 (3H, s, SiOC*H*$_3$), 7.66 (4H, d , *J* 1.5, Ar*H*); **^{13}C NMR** (100 MHz, $CDCl_3$) δ_C –2.43, 50.8, 113.2, 118.9, 131.2, 133.9, 144.2; **HRMS** (ES$^+$) calc. for $C_{10}H_{13}NNaOSi$ $[M+Na]^+$ 214.0659, found 214.0656.

1-(4-(Methoxydimethylsilyl)phenyl)ethanone (122)



According to general procedure **II**, 286 mg (1.60 mmol) of arylhydrosilane **107** afforded the title compound as a colourless oil (320 mg, 96%); $\mathbf{R_f}$ 0.49 (petroleum ether); **IR** (thin film, ν_{max} / cm^{-1}) 1684s, 1388m, 1243s, 1081s, 820s, 785s; **^{1}H NMR** (400 MHz, $CDCl_3$) δ_H 0.41 (6H, s, Si(C*H*$_3$)$_2$), 2.62 (3H, s, COC*H*$_3$), 3.46 (3H, s, SiOC*H*$_3$), 7.68 (2H, d, *J* 8.0, Ar*H*), 7.95 (2H, d, *J* 8.0, Ar*H*); **^{13}C NMR** (100 MHz, $CDCl_3$) δ_C –2.36, 26.7, 50.8, 127.4, 133.7, 137.8, 143.9, 198.5; **HRMS** (ES^+) calc. for $C_{11}H_{16}NaO_2Si$ $[M+Na]^+$ 231.0812, found 231.0812.

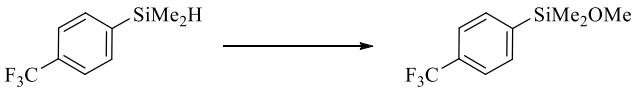
4-(Methoxydimethylsilyl)benzaldehyde (123)



According to general procedure **II**, 200 mg (1.22 mmol) of arylhydrosilane **105** afforded the title compound as a colourless oil (231 mg, 98%); $\mathbf{R_f}$ 0.27 (petroleum ether); **^{1}H NMR** (400 MHz, $CDCl_3$) δ_H 0.42 (6H, s, Si(C*H*$_3$)$_2$), 3.47 (3H, s, SiOC*H*$_3$), 7.75 (2H, d, *J* 8.0, Ar*H*), 7.89 (2H, d, *J* 8.0, Ar*H*), 10.0 (1H, s, CO*H*).

The product decomposed before further characterisation was possible.

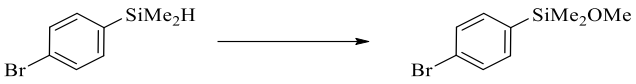
Methoxydimethyl(4-(trifluoromethyl)phenyl)silane (124)



According to general procedure **II**, 250 mg (1.22 mmol) of arylhydrosilane **96** afforded the title compound as a colourless oil (254 mg, 89%); $\mathbf{R_f}$ 0.51 (petroleum ether / Et_2O (9:1)); **IR** (thin film, ν_{max} / cm^{-1}) 1324s, 1256w, 1164m, 1124s, 1059s, 822s; **^{1}H NMR** (400 MHz, $CDCl_3$) δ_H 0.46 (6H, s, Si(C*H*$_3$)$_2$), 3.51 (3H, s, SiOC*H*$_3$), 7.69 (2H, d, *J* 8.0, Ar*H*), 7.75 (2H, d, *J* 8.0, Ar*H*); **^{13}C NMR** (100

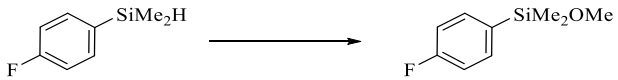
MHz, $CDCl_3$) δ_C –1.92, 51.2, 124.6 (q, *J* 272.5), 124.9 (q, *J* 3.5), 132.0 (q, *J* 32.0), 134.2, 142.8; **HRMS** (FI^+) calc. for $C_{10}H_{13}F_3OSi$ $[M]^+$ 234.0688, found 234.0687.

(4-Bromophenyl)(methoxy)dimethylsilane (125)



According to general procedure **II**, 160 mg (0.653 mmol) of arylhydrosilane **97** afforded the title compound as a colourless oil (155 mg, 85%); $\mathbf{R_f}$ 0.49 (petroleum ether); **IR** (thin film, ν_{max} / cm^{-1}) 2958w, 1575w, 1479w, 1376w, 1255m, 1066s, 1009m; **^{1}H NMR** (500 MHz, $CDCl_3$) δ_H 0.42 (6H, s, Si(C*H*$_3$)$_2$), 3.49 (3H, s, SiOC*H*$_3$), 7.49 (2H, t, *J* 8.0, Ar*H*), 7.58 (2H, d, *J* 8.0, Ar*H*); **^{13}C NMR** (100 MHz, $CDCl_3$) δ_C –1.19, 51.1, 125.0, 131.5, 135.5, 136.7; **HRMS** (FI^+) calc. for $C_9H_{13}BrOSi$ $[M]^+$ 245.9899, found 245.9918.

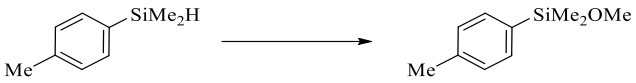
(4-Fluorophenyl)(methoxy)dimethylsilane (126)



According to general procedure **II**, 250 mg (1.62 mmol) of arylhydrosilane **99** afforded the title compound as a colourless oil (255 mg, 86%); $\mathbf{R_f}$ 0.56 (petroleum ether; **IR** (thin film, ν_{max} / cm^{-1}) 1589m, 1450w, 1252w, 1231w, 1082s; **^{1}H NMR** (500 MHz, $CDCl_3$) δ_H 0.38 (6H, s, Si(C*H*$_3$)$_2$), 3.44 (3H, s, SiOC*H*$_3$), 7.09 (2H, t, *J* 9.0, Ar*H*), 7.56 (2H, dd, *J* 9.0, 6.5, Ar*H*); **^{13}C NMR** (100 MHz, $CDCl_3$) δ_C –2.27, 50.6, 115.0 (d, *J* 19.5), 133.0 (d, *J* 4.0), 135.5 (d, *J* 7.5), 164.0 (d, *J* 248.5); **^{19}F NMR** (377 MHz, $CDCl_3$) δ_F -111.0; **HRMS** (FI^+) calc. for $C_9H_{13}FOSi$ $[M]^+$ 184.0720, found 184.0719.

Compound previously reported by Lipowitz and co-workers.[188]

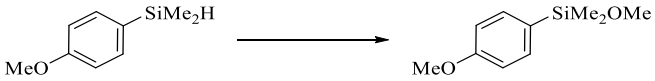
Methoxydimethyl(p-tolyl)silane (127)



According to general procedure **II**, 150 mg (0.998 mmol) of arylhydrosilane **100** afforded the title compound as a colourless oil (160 mg, 89%); $\mathbf{R_f}$ 0.53 (petroleum ether); **IR** (thin film, ν_{max} / cm^{-1}) 1604w, 1250m, 1083s, 828s, 777s; **^{1}H NMR** (400 MHz, $CDCl_3$) δ_H 0.39 (6H, s, Si(C*H*$_3$)$_2$), 2.39 (3H, s, ArC*H*$_3$), 3.46 (3H, s, SiOC*H*$_3$), 7.24 (2H, d, *J* 7.5, Ar*H*), 7.50 (2H, d, *J* 7.5 Ar*H*); **^{13}C NMR** (100 MHz, $CDCl_3$) δ_C –2.29, 21.5, 50.6, 128.7, 133.5, 133.8, 139.6; **HRMS** (FI^+) calc. for $C_{10}H_{16}OSi$ $[M]^+$ 180.0970, found 180.0969.

Previously reported by Yen and co-workers.[197]

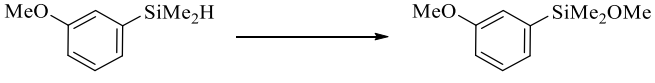
Methoxy(4-methoxyphenyl)dimethylsilane (128)



According to general procedure **II**, 100 mg (0.660 mmol) of arylhydrosilane **101** afforded the title compound as a colourless oil (122 mg, 99%); $\mathbf{R_f}$ 0.33 (petroleum ether); **^{1}H NMR** (400 MHz, $CDCl_3$) δ_H 0.38 (6H, s, Si(C*H*$_3$)$_2$), 3.44 (3H, s, SiOC*H*$_3$), 3.84 (3H, s, OC*H*$_3$), 6.95 (2H, d, *J* 8.5, Ar*H*), 7.53 (2H, d, *J* 8.5, Ar*H*); **^{13}C NMR** (100 MHz, $CDCl_3$) δ_C –1.84, 51.0, 55.5, 114, 128.8, 135, 161.3.

The spectroscopic data was found to be in agreement with that reported by Grogger and co-workers.[198]

Methoxy(3-methoxyphenyl)dimethylsilane (129)

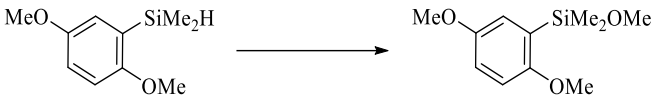


According to general procedure **II**, 100 mg (0.601 mmol) of arylhydrosilane **98** afforded the title compound as a colourless oil (117 mg, 100%); $\mathbf{R_f}$ 0.41 (petroleum ether / Et_2O (9:1)); **^{1}H NMR** (400 MHz, $CDCl_3$) δ_H 0.39 (6H, s, Si(C*H*$_3$)$_2$), 3.46 (3H, s, Si(OC*H*$_3$), 3.84 (3H, s, ArOC*H*$_3$), 6.96 (1H, dd, *J*

8.0, 2.5, Ar*H*), 7.12 (1H, d, *J* 2.5, Ar*H*), 7.16 (1H, d, *J* 8.0, Ar*H*), 7.34 (1H, t, *J* 8.0, Ar*H*); **^{13}C NMR** (100 MHz, $CDCl_3$) δ_C -2.33, 50.7, 55.1, 115.0, 118.8, 125.7, 129.1, 139.0, 159.1.

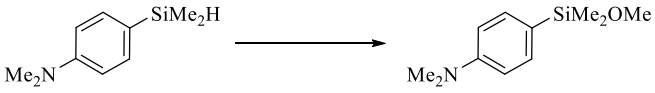
The spectroscopic data was found to be in agreement with that reported by Koehler and co-workers.[199]

(2,5-Dimethoxyphenyl)(methoxy)dimethylsilane (130)



According to general procedure **II**, 209 mg (1.06 mmol) of arylhydrosilane **111** afforded the title compound as a colourless oil (214 mg, 89%); **R_f** 0.55 (petroleum ether / Et_2O (9:1)); **IR** (thin film, ν_{max} / cm^{-1}) 2955m, 2832m, 1158w, 1481s, 1272s, 1147m; **^{1}H NMR** (400 MHz, $CDCl_3$) δ_H 0.38 (6H, s, SiC*H*$_3$), 3.53 (1H, s, SiOC*H*$_3$), 3.78 (3H, s, OC*H*$_3$), 3.80 (3H, s, OC*H*$_3$), 6.80 (1H, d, *J* 9.0, Ar*H*), 6.90 (1H, dd, *J* 9.0, 3.0, Ar*H*), 7.05 (1H, d, *J* 3.0, Ar*H*); **^{13}C NMR** (100 MHz, $CDCl_3$) δ_C –1.66, 50.9, 55.7, 55.8, 110.7, 115.7, 120.9, 126.8, 153.5, 158.3; **HRMS** (ES^+) calc. for $C_{11}H_{18}NaO_3Si$ $[M+Na]^+$ 249.0917, found 249.0920.

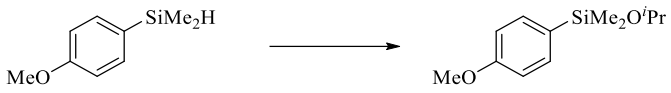
4-(Methoxydimethylsilyl)-N,N-dimethylaniline (131)



According to general procedure **II**, 200 mg (1.12 mmol) of arylhydrosilane **102** afforded the title compound as a colourless oil (176 mg, 75%); **R_f** 0.49 (petroleum ether / Et_2O (9:1)); **^{1}H NMR** (400 MHz, $CDCl_3$) δ_H) 0.36 (6H, s, Si(C*H*$_3$)$_2$), 2.99 (6H, s, N(C*H*$_3$)$_2$), 3.43 (3H, s, Si(OC*H*$_3$), 6.76 (2H, t, *J* 8.5, Ar*H*), 7.46 (2H, d, *J* 8.5, Ar*H*)**;** **^{13}C NMR** (100 MHz, $CDCl_3$) δ_C -2.26, 40.1, 50.5, 111.8, 122.4, 134.7, 151.4;

The spectroscopic data was found to be in agreement with that reported by Grogger and co-worker.[198]

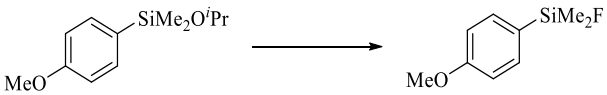
Isopropoxy(4-methoxyphenyl)dimethylsilane (136)



$[RuCl_2(p\text{-cymene})]_2$ (9.2 mg, 0.015 mmol, 0.5 mol%) was added to hydrosilane **101** (500 mg, 3.01 mmol, 1.0 equiv) and isopropanol (460 μL, 6.03 mmol, 2.0 equiv) under air. After 2/3 seconds of effervescence the reaction was seen to be complete by TLC. The reaction mixture was diluted in Et_2O and eluted through a silica plug (Et_2O) to afford isopropoxysilane **136** (617 mg, 91%); $\mathbf{R_f}$ 0.63 (Et_2O); **^{1}H NMR** (400 MHz, $CDCl_3$) δ_H 0.37 (6H, s, Si(C*H*$_3$)$_2$), 1.13 (6H, d, *J* 6.0, CH(C*H*$_3$)$_2$), 3.83 (3H, s, OC*H*$_3$), 3.98 (1H, sept, *J* 6.0, C*H*(CH$_3$)$_2$), 6.93 (2H, d, *J* 8.5, Ar*H*), 7.53 (2H, d, *J* 8.5, Ar*H*).

The spectroscopic data was found to be in agreement with that reported by Bracegirdle and co-workers.[83]

Fluoro(4-methoxyphenyl)dimethylsilane (137)

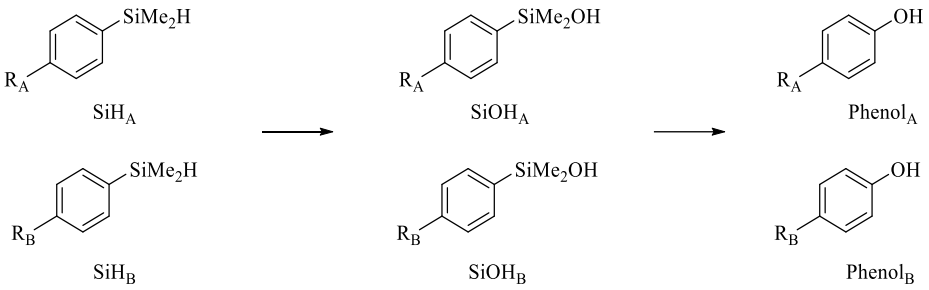


TBAF (2.23 mL of a 1 M solution in THF, 2.23 mmol, 2.0 equiv) was added to a solution of isopropoxysilane **136** (250 mg, 1.11 mmol, 1.0 equiv) and $KHCO_3$ (224 mg, 2.23 mmol, 2.0 equiv) in MeOH/THF (5 mL). The reaction was stirred for 4 h at RT, after which the starting material was observed to be complete by TLC analysis. The reaction was quenched with water (3 mL), the phases separated and the aqueous phase extracted with diethyl ether (3 x 5 mL). The combined organic phases were dried ($MgSO_4$) and concentrated *in vacuo* to a colourless oil which was purified by column chromatography (petroleum ether → petroleum ether / Et_2O (7:3)) to afford the title compound as a colourless oil with 60.4% purity (55 mg, 19%); R_f 0.51 (petroleum ether / Et_2O (4:1)); ^{1}H NMR (200 MHz, $CDCl_3$) δ_H 0.48 (6H, d, *J* 7.0, SiC*H*$_3$), 3.84 (3H, s, OC*H*$_3$), 6.96 (2H, m, Ar*H*), 7.55 (2H, m, Ar*H*).

The spectroscopic data was found to be in agreement with that reported by Lickiss and co-workers.[200]

Hammett Procedure

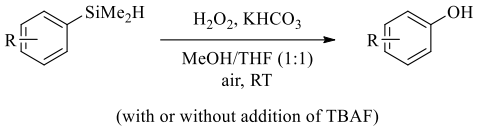
To a 1:1 mixture of silane SiH_A and SiH_B, in MeCN, was added water (1.0 equiv) and $[RuCl_2(p\text{-cymene})]_2$ (2 mol%). After 5/10 seconds of effervescence the reaction was seen to be complete by TLC. The reaction was diluted with diethyl ether (2 mL) and eluted through a silica plug (diethyl ether) to afford a 1:1 mixture of silanols $SiOH_A$ and $SiOH_B$ in diethyl ether. This solution was concentrated and MeOH was added to form a 1:1 Et_2O/MeOH, 0.2 M solution. H_2O_2 (12.0 equiv) and $KHCO_3$ were added and aliquots taken from the reaction at the times stated below. Aliquots were quenched with $Na_2S_2O_3$ (sat. aq) and extracted with EtOAc. After concentrating *in vacuo* analysis by ^1H NMR spectroscopy yielded the following relative integrations of phenol.



Mixture	Aliquot 1		Aliquot 2		Aliquot 2		Average
R_A / R_B	**Time (min)**	**[Phenol$_A$] / [Phenol$_B$]**	**Time (min)**	**[Phenol$_A$] / [Phenol$_B$]**	**Time (min)**	**[Phenol$_A$] / [Phenol$_B$]**	
Me / OMe	30	1.04	35	1.04	40	1.06	1.05
Me / OMe[a]	30	1.08	40	1.04	-	-	1.06
F / Me	20	1.21	40	1.41	60	1.25	1.33
Br / F	15	2.18	20	2.00	25	2.19	2.12
Ac / Br	10	1.40	20	1.50	25	1.54	1.52
CN / Ac	20	2.41	30	2.15	45	2.52	2.36

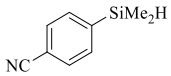
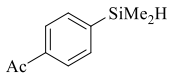
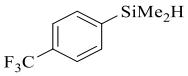
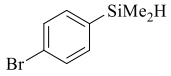
[a]Carried out at 0 °C

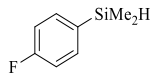
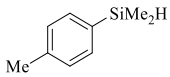
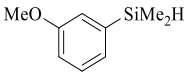
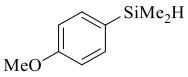
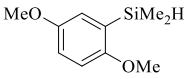
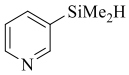
Reaction details; Table 2.7



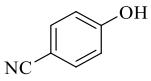
General procedure III

To a solution of hydrosilane (0.500 mmol, 1.0 equiv) in MeOH/THF (1.5 mL, 0.3 M) at RT, under air, was added $KHCO_3$ (25 mg, 0.250 mmol, 0.5 equiv), TBAF (50 μL of a 1 M solution in THF, 0.05 mmol, 0.1 equiv) and H_2O_2 (340 μL of a 30% w/w solution, 3.00 mmol, 6.0 equiv). The reaction mixture was stirred for 3 to 24 h (see table) after which HCl (1 mL, 1 N aqueous solution) was added and the monophasic mixture stirred for a further 5 min. The reaction mixture was then extracted with EtOAc (3 × 5 mL). The combined organic phases were dried ($MgSO_4$) and concentrated *in vacuo* to afford a crude phenolic product which was purified by column chromatography.

Entry	Hydrosilane	Mass of starting material/ Reaction Scale	TBAF	Reaction Length	Mass of isolated product/Yield
1		100 mg / 0.621 mmol	-	5 h	73 mg / 99%
		100 mg / 0.621 mmol	0.1 equiv	3 h	69 mg / 93%
2		89 mg / 0.500 mmol	-	7 h	50 mg/ 73%
		89 mg / 0.500 mmol	0.1 equiv	3 h	45 mg / 66%
3		102 mg / 0.500 mmol	-	7 h	74 mg / 91%
		102 mg / 0.500 mmol	0.1 equiv	5 h	59 mg / 73%
4		100 mg / 0.467 mmol	-	7 h	46 mg / 57%
		108 mg / 0.500 mmol	0.1 equiv	5 h	65 mg / 75%

Entry	Hydrosilane	Mass of starting material/ Reaction Scale	TBAF	Reaction Length	Mass of isolated product/Yield
5		150 mg / 0.972 mmol	-	12 h	77 mg / 71%
		150 mg / 0.972 mmol	0.1 equiv	7 h	70 mg / 64%
6		100 mg / 0.670 mmol	-	12 h	48 mg / 67%
		150 mg / 0.998 mmol	0.1 equiv	7 h	92 mg / 85%
7		98 mg / 0.590 mmol	-	24 h	25 mg / 40%
		98 mg / 0.590 mmol	0.1 equiv	24 h	20 mg / 32%
8		83 mg / 0.499 mmol	-	24 h	n.d (33% conversion)
		150 mg / 0.902 mmol	0.1 equiv	24 h	73 mg / 65% (80% conversion)
9		1.2 g / 6.11 mmol	0.1 equiv	24 h	n.d < 5% conversion
10		150 mg / 1.09 mmol	-	2 h	81 mg / 78%
		69 mg / 0.500 mmol	0.1 equiv	1 h	33 mg / 71%

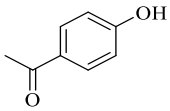
4-Hydroxybenzonitrile (141)



Purification by column chromatography (petroleum ether → petroleum ether / Et_2O 4:1)) of the crude reaction mixture afforded 4-hydroxybenzonitrile as a white solid; **R_f** 0.32 (petrolueum ether / Et_2O (4:1)); **mp** 114-116 °C (Lit. 108-109 °C)[28]; **^{1}H NMR** (500 MHz, $CDCl_3$) δ_H 6.33 (1H, br s, O*H*), 6.98 (2H, d, *J* 9.0, Ar*H*), 7.61 (2H, d, *J* 9.0 Ar*H*); **^{13}C NMR** (125 MHz, $CDCl_3$) δ_C 103.9, 116.9, 119.6, 134.8, 160.4.

The spectroscopic data was found to be in agreement with that reported by Sergeev and co-workers.[28]

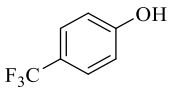
1-(4-Hydroxyphenyl)ethanone (142)



Purification by column chromatography (petroleum ether → petroleum ether / Et_2O (4:1)) of the crude reaction mixture afforded 1-(4-hydroxyphenyl)ethanone as a white solid; **R_f** 0.23 (petrolueum ether / Et_2O (1:1)); **mp** 109-111°C (Lit. 107-109 °C)[201]; **^{1}H NMR** (400 MHz, $CDCl_3$) δ_H 2.58 (3H, s, COC*H*$_3$), 6.92 (2H, d, *J* 9.0, Ar*H*), 7.92 (2H, d, *J* 9.0, Ar*H*), 8.41 (1H, br s, ArO*H*); **^{13}C NMR** (100 MHz, $CDCl_3$) δ_C 26.3, 115.4, 130.0, 131.1, 160.8, 197.8.

The spectroscopic data was found to be in agreement with that reported by Zhang and co-workers.[201]

4-(Trifluoromethyl)phenol (144)

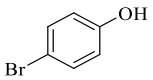


Purification by column chromatography (petroleum ether → petroleum ether / Et_2O (4:1)) of the crude reaction mixture afforded 4-(trifluoromethyl)phenol as a waxy solid; **R_f** 0.29 (petrolueum ether / Et_2O (1:1)); **^{1}H NMR** (400 MHz, $CDCl_3$) δ_H 5.62 (1H, br s , O*H*), 6.92 (2H, d *J* 8.5, Ar*H*), 7.52 (2H, d *J*

8.5, Ar*H*); **^{13}C NMR** (100 MHz, $CDCl_3$) δ_C 115.5, 123.2 (q, *J* 33.0), 124.3 (q, *J* 271.0), 127.2 (q, *J* 4.0), 158.0.

The spectroscopic data was found to be in agreement with that reported by Sergeev and co-workers.[28]

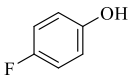
4-Bromophenol (145)



Purification by column chromatography (petroleum ether → petroleum ether / Et_2O (4:1)) of the crude reaction mixture afforded 4-bromophenol as an off white solid; **R_f** 0.42 (petrolueum ether / Et_2O (4:1)); **mp** 56-59 °C (Lit. 54-68 °C)[202]; **^{1}H NMR** (400 MHz, $CDCl_3$) δ_H 5.17 (1H, br s, O*H*), 6.73 (2H, d, *J* 9.0, Ar*H*), 7.34 (2H, d, *J* 9.0, Ar*H*); **^{13}C NMR** (100 MHz, $CDCl_3$) δ_C 113.0, 117.2, 132.5, 154.4.

The spectroscopic data was found to be in agreement with that reported by Magano and co-workers.[202]

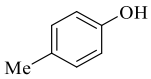
4-Fluorophenol (134)



Purification by column chromatography (petroleum ether → petroleum ether / Et_2O (9:1)) of the crude reaction mixture afforded 4-fluorophenol as a white waxy solid; **R_f** 0.32 (petrolueum ether / Et_2O (9:1)); **^{1}H NMR** (500 MHz, $CDCl_3$) δ_H 4.85 (1H, br s, O*H*), 6.81 –6.85 (2H, m, Ar*H*), 6.99 (2H, t, *J* 8.5, Ar*H*); **^{13}C NMR** (125 MHz, $CDCl_3$) δ_C 116.4 (d, *J* 23.5), 116.7 (d, *J* 7.5), 151.9, 157.7 (d, *J* 237.5); **^{19}F NMR** (377 MHz, $CDCl_3$) δ_F −124.4.

The spectroscopic data was found to be in agreement with that reported by Inamoto and co-workers.[203]

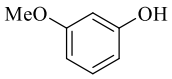
p-Cresol (133)



Purification by column chromatography (petroleum ether → petroleum ether / Et_2O (9:1)) of the crude reaction mixture afforded *p*-cresol as a pale yellow waxy solid; **R_f** 0.39 (petrolueum ether / Et_2O (9:1)); **^{1}H NMR** (500 MHz, $CDCl_3$) δ_H 2.28 (3H, s, ArC*H*$_3$), 4.57 (1H, br s, O*H*), 6.74 (2H, d *J* 8.5 Ar*H*), 7.05 (2H, d *J* 8.5 Ar*H*); **^{13}C NMR** (125 MHz, $CDCl_3$) δ_C 20.4, 115.0, 129.9, 130.0, 153.2.

The spectroscopic data was found to be in agreement with that reported by Inamoto and co-workers.[203]

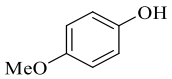
3-Methoxyphenol (146)



Purification by column chromatography (petroleum ether → petroleum ether / Et_2O (9:1)) of the crude reaction mixture afforded 4-methoxyphenol as a light yellow oil; **R_f** 0.39 (petrolueum ether / Et_2O (9:1)); **^{1}H NMR** (200 MHz, $CDCl_3$) δ_H 3.79 (3H, s, OC*H*$_3$), 4.88 (1H, br s, O*H*), 6.40 – 6.51 (3H, m, Ar*H*), 7.15 (1H, t, *J* 8.5, Ar*H*)

The spectroscopic data was found to be in agreement with that reported by Molander and co-workers.[53]

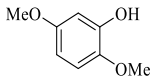
4-Methoxyphenol (135)



Purification by column chromatography (petroleum ether → petroleum ether / Et_2O (9:1)) of the crude reaction mixture afforded 4-methoxyphenol as a white solid; **R_f** 0.39 (petrolueum ether / Et_2O (9:1)); **mp** 49 – 52 °C (Lit. 49-51 °C)[204]; **^{1}H NMR** (400 MHz, $CDCl_3$) δ_H 3.78 (3H, s, OC*H*$_3$), 4.77 (1H, br s, O*H*), 6.76 – 6.82 (4H, m, Ar*H*); **^{13}C NMR** (100 MHz, $CDCl_3$) δ_C 55.8, 114.9, 116.0, 149.4, 153.7.

The spectroscopic data was found to be in agreement with that reported by Chan and co-workers.[204]

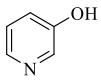
2,5-Dimethoxyphenol (147)



Purification by column chromatography (petroleum ether → petroleum ether / Et_2O 4:1)) of the crude reaction mixture afforded 2,5-dimethoxyphenol as a very pale yellow liquid; **R_f** 0.36 (petrolueum ether / Et_2O (9:1)); **^{1}H NMR** (400 MHz, $CDCl_3$) δ_H 3.76 (3H, s, OC*H*$_3$), 3.86 (3H, s, OC*H*$_3$), 5,73 (1H, br s, O*H*), 6.39 (1H, dd, *J* 9.0, 3.0, Ar*H*), 6.57 (1H, d, *J* 3.0, Ar*H*), 6.79 (1H, d, *J* 9.0, Ar*H*); **^{13}C NMR** (100 MHz, $CDCl_3$) δ_C 55.6, 56.6, 101.7, 104.2, 111.5, 140.9, 146.4, 154.6.

The spectroscopic data was found to be in agreement with that reported by Bjørsvik and co-workers.[205]

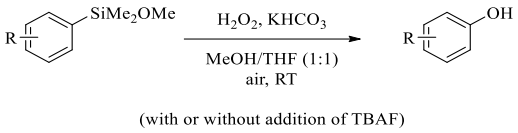
Pyridin-3-ol (149)



Purification by column chromatography ($CHCl_3$ → $CHCl_3$ / MeOH (9:1)) of the crude reaction mixture afforded pyridine-3-ol as a white solid; **R_f** 0.25 ($CHCl_3$ / MeOH (9:1)); **mp** 123 – 125 °C (Lit. 127 – 129 °C)[206]; **^{1}H NMR** (500 MHz, DMSO–*d*$_6$) 7.14 – 7.16 (1H, m, Ar*H*), 7.20 (1H, dd, *J* 8.0, 4.5, Ar*H*), 8.03 (1H, dd, *J* 4.5, 1.5, Ar*H*), 8.13 (1H, d, *J* 2.5 Ar*H*), 9.86 (1H, br s, O*H*); **^{13}C NMR** (125 MHz, DMSO–*d*$_6$)) δ_C 122.0, 124.1, 138.0, 140.2, 153.6.

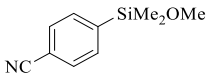
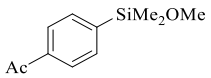
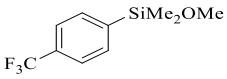
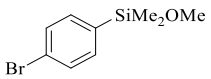
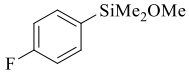
The spectroscopic data was found to be in agreement with that reported by Jing and co-workers.[34]

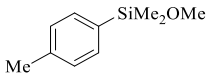
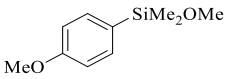
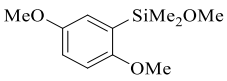
Reaction details; Table 2.8



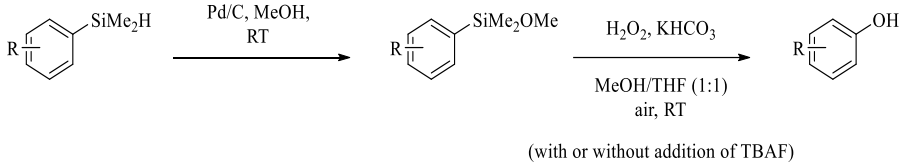
General procedure IV

To a solution of methoxysilane (0.500 mmol, 1.0 equiv) in MeOH/THF (1.5 mL, 0.3 M) at RT, under air, was added $KHCO_3$ (25 mg, 0.250 mmol, 0.5 equiv), TBAF (50 μL of a 1 M solution in THF, 0.05 mmol, 0.1 equiv) and H_2O_2 (340 μL of a 30% w/w solution, 3.00 mmol, 6.0 equiv). The reaction mixture was stirred for 30 min to 4.5 h (see table) after which HCl (1 mL, 1 N aqueous solution) was added and the monophasic mixture stirred for a further 5 min. The reaction mixture was then extracted with EtOAc (3 × 5 mL). The combined organic phases were dried ($MgSO_4$) and concentrated *in vacuo* to afford a crude phenolic product which was purified by column chromatography.

Entry	Methoxysilane	Mass of starting material/ Reaction Scale	TBAF	Reaction Length	Mass of isolated product/Yield
1		100 mg / 0.523 mmol	-	45 min	55 mg / 89%
		100 mg / 0.523 mmol	0.1 equiv	30 min	58 mg / 93%
2		104 mg / 0.500 mmol	-	45 min	55 mg/ 81%
		104 mg / 0.500 mmol	0.1 equiv	30 min	60 mg / 87%
3		117 mg / 0.500 mmol	-	60 min	59 mg / 73%
		117 mg / 0.500 mmol	0.1 equiv	30 min	62 mg / 76%
4		102 mg / 0.416 mmol	-	90 min	62 mg / 86%
		119 mg / 0.485 mmol	0.1 equiv	60 min	72 mg / 86%
5		127 mg / 0.689 mmol	-	90 min	70 mg / 91%
		93 mg / 0.505 mmol	0.1 equiv	60 min	49 mg / 87%

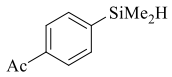
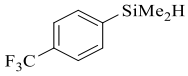
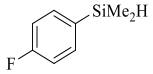
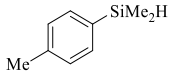
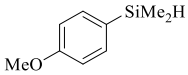
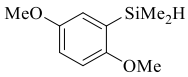
Entry	Methoxysilane	Mass of starting material/ Reaction Scale	TBAF	Reaction Length	Mass of isolated product/Yield
6		90 mg / 0.500 mmol	-	3 h	43 mg / 79%
		79 mg / 0.438 mmol	0.1 equiv	90 min	38 mg / 80%
7		126 mg, 0.644 mmol	-	3 h	70 mg / 88%
		151 mg, 0.769 mmol	0.1 equiv	2 h	89 mg / 93%
8		109 mg / 0.482 mmol	-	4.5 h	58 mg / 78%
		105 mg / 0.464 mmol	0.1 equiv	3 h	65 mg / 91%

Reaction details; Table 2.10

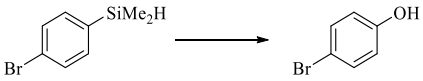


General procedure V

To a vial containing aryl hydrosilane (0.500 mmol, 1.0 equiv) was added MeOH (200 μL). The vial was purged with argon before the addition of Pd/C (2.6 mg, 10 wt.% loading, 0.0025 mmol, 5 mol%). After 2/3 seconds – 5 minutes of effervescence the reaction was seen to be complete by TLC. The resulting solution was filtered through a celite plug, eluted with Et_2O, and concentrated *in vacuo*. To this crude product was added MeOH/THF (1.5 mL), $KHCO_3$ (25 mg, 0.250 mmol, 0.5 equiv), TBAF (50 μL of a 1 M solution in THF, 0.050 mmol, 0.10 equiv) and H_2O_2 (340 μL of a 30% w/w solution, 3.00 mmol, 6.0 equiv) and the reaction mixture stirred for 30 min to 3 h (see table). Upon completion, the reaction was quenched with HCl (1 mL, 1 N aqueous solution) and the monophasic mixture stirred for a further 5 min. The reaction mixture was then extracted with EtOAc (3 x 5 mL). The combined organic phases were dried ($MgSO_4$) and concentrated *in vacuo* to afford a crude phenolic product which was purified by column chromatography.

Entry	Hydrosilane	Mass of starting material/ Reaction Scale	TBAF	Reaction Length	Mass of isolated product/Yield
1		89 mg / 0.500 mmol	0.1 equiv	30 min	49 mg / 72%
2		102 mg / 0.500 mmol	0.1equiv	30 min	72 mg / 89%
3		77 mg / 0.500 mmol	0.1 equiv	60 min	49 mg / 88%
4		75 mg / 0.500 mmol	0.1 equiv	90 min	50 mg / 92%
5		75 mg / 0.451 mmol	0.1 equiv	3 h	45 mg / 80%
6		98 mg / 0.500 mmol	0.1 equiv	3 h	60 mg / 79%

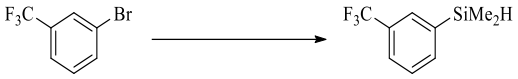
4-Bromophenol (145, Table 2.10)



To a vial containing (4-bromophenyl)dimethylsilane (108 mg, 0.500 mmol, 1.0 equiv) in Et_2O (2 mL) was added MeOH (200 μL). The vial was purged with argon before the addition of Pd/C (2.6 mg, 10 wt.% loading, 0.0025 mmol, 5 mol%). After 15 minutes of effervescence the reaction was seen to be complete by TLC. The resulting solution was filtered through a celite plug, eluted with Et_2O, and concentrated *in vacuo*. To this crude product was added MeOH/THF (1.5 mL), $KHCO_3$ (25 mg, 0.250 mmol, 0.5 equiv), TBAF (50 μL of a 1 M solution in THF, 0.050 mmol, 0.10 equiv) and H_2O_2 (340 μL of a 30% w/w solution, 3.00, 6.0 equiv) and the reaction mixture stirred for 30 min. Upon completion, the reaction was quenched with HCl (1 mL, 1 N aqueous solution) and the monophasic

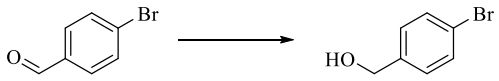
mixture stirred for a further 5 min. The reaction mixture was then extracted with EtOAc (3 x 5 mL). The combined organic phases were dried ($MgSO_4$) and concentrated *in vacuo* to afford a crude phenolic product which was purified by column chromatography to afford the title compound as a yellow solid (74 mg, 85%).

Dimethyl(3-(trifluoromethyl)phenyl)silane (152)



According to the general procedure **I**, 4.27 mL (10.7 mmol, 1.2 equiv) of *n*-BuLi was added to 2.0 g (8.89 mmol, 1.0 equiv) of 1-bromo-3-(trifluoromethyl)benzene in anhydrous THF (50 mL). The resulting mixture was stirred for 2 h at –78 °C before 1.26 mL (11.6 mmol, 1.3 equiv) of chlorodimethylsilane was added and the reaction stirred overnight. NH_4Cl (15 mL) was added to the reaction, the phases separated and the aqueous phase extracted with CH_2Cl_2 (3 x 15 mL). The combined organic phases were dried ($MgSO_4$) and concentrated *in vacuo* to a colourless oil which was purified by vacuum distillation (66 ^oC at 32 mbar) to afford the title compound as a colourless oil (1.31 g, 72%); $\mathbf{R_f}$ 0.55 (petroleum ether); **IR** (thin film, ν_{max} / cm^{-1}) 2786w, 2801w, 2118w, 1115w, 1077m, 850s; **^{1}H NMR** (500 MHz, $CDCl_3$) δ_H 0.39 (6H, d, *J* 4.0, Si(C*H*$_3$)$_2$), 4.47 (1H, sept, *J* 4.0, Si*H*), 7.49 (1H, t, *J* 7.5, ArH), 7.63 (1H, d, *J* 7.5, ArH), 7.73 (1H, d, *J* 7.5, ArH), 7.78 (1H, s, ArH); **^{13}C NMR** (125 MHz, $CDCl_3$) δ_C –3.60, 124.6 *(*q, *J* 269.0*)*, 126.3 (q, *J* 4.0), 128.4, 130.4 (q, *J* 32.0), 130.8 (q, *J* 4.0) 137.7, 139.2; **^{19}F NMR** (377 MHz, $CDCl_3$) δ_F –62.6 (1F); **HRMS** (FI^+) calc. for $C_9H_{11}SiF_3$ $[M]^+$ 204.0582, found 204.0580.

(4-Bromophenyl)methanol (153a)

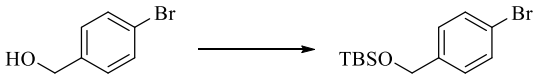


To a suspension of $NaBH_4$ (307 mg, 8.11 mmol, 0.5 equiv) in methanol (30 mL) was added a solution of 4-bromobenzaldehyde (3.0 g, 16.2 mmol, 1.0 equiv) in methanol (30 mL). The reaction was stirred

at RT for 15 min until it was observed to be complete by TLC. The reaction was quenched with aq. NH_4Cl (2 ml), dried ($MgSO_4$) and eluted through a silica plug (diethyl ether) to afford a white solid (2.83 g, 94%); δ_H (200 MHz, $CDCl_3$) 1.73 (1H, br s, O*H*), 4.67 (2H, s, ArC*H*$_2$), 7.25 (2H, d, *J* 8.5, Ar*H*), 7.50 (2H, d, *J* 8.5, Ar*H*).

The spectroscopic data was found to be in agreement with that reported by Jiang and co-workers.[207]

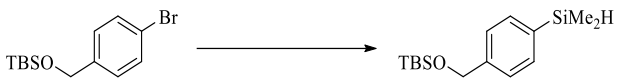
((4-Bromobenzyl)oxy)(tert-butyl)dimethylsilane (153b)



To a solution of 4-bromobenyl alcohol (1 g, 5.35 mmol, 1.0 equiv) in DCM (10 ml) was added TBDMSCl (967 mg, 6.42 mmol, 1.2 equiv) and imidazole (910 mg, 13.4 mmol, 2.5 equiv). The reaction was stirred for 16 h at room temperature before quenching with NH_4Cl (aqueous solution, 10 ml). The biphasic mixture was separated, and the aqueous phase extracted with DCM, before the combined organic phases were dried ($MgSO_4$) and concentrated *in vacuo* to a colourless oil without the need for further purification; (1.59 g, 99 %); δ_H (400 MHz, $CDCl_3$) 0.10 (6H, s, Si(C*H*$_3$)$_2$C(CH$_3$)$_3$), 0.94 (9H, s, Si(CH$_3$)$_2$C(C*H*$_3$)$_3$), 4.69 (2H, s, ArC*H*$_2$), 7.21 (2H, d, *J* 8.5, Ar*H*), 7.46 (2H, d, *J* 8.5, Ar*H*).

The spectroscopic data was found to be in agreement with that reported by Bracegirdle and co-workers.[83]

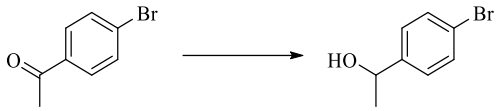
tert-Butyl((4-(dimethylsilyl)benzyl)oxy)dimethylsilane (153)



According to the general procedure **I**, 0.71 mL (1.78 mmol, 1.2 equiv) of *n*-BuLi was added to 446 mg (1.48 mmol, 1.0 equiv) of ((4-bromobenzyl)oxy)(tert-butyl)dimethylsilane in anhydrous THF (10 mL). The resulting mixture was stirred for 2 h at –78 °C before 197 μL (1.78 mmol, 1.2 equiv) of

chlorodimethylsilane was added and the reaction stirred overnight. The product was purified by by passage through a silica plug (Et_2O) to afford the title compound as a colourless oil (282 mg, 68%); **R_f** 0.81 (petroleum ether); **IR** (thin film, ν_{max} / cm^{-1}) 2956w, 2857w, 2118w, 1250m, 1087m, 834s; **^{1}H NMR** (500 MHz, $CDCl_3$) δ_H 0.11 (6H, s, Si(C*H*$_3$)$_2$C(CH$_3$)$_3$), 0.35 (6H, d, *J* 3.5, Si(C*H*$_3$)$_2$H), 0.96 (9H, s, Si(CH$_3$)$_2$C(C*H*$_3$)$_3$), 4.43 (1H, sept, *J* 3.5, Si*H*), 4.76 (2H, s, ArC*H*$_2$), 7.34 (2H, d, *J* 7.5, Ar*H*), 7.52 (2H, d, *J* 7.5, Ar*H*); **^{13}C NMR** (125 MHz, $CDCl_3$) δ_C –5.27, –3.72, 18.4, 25.9, 64.9, 125.5, 133.9, 135.7, 142.5; **HRMS** (ES^+) calc. for $C_{15}H_{28}NaOSi_2$ $[M+Na]^+$ 303.1571, found 303.1571.

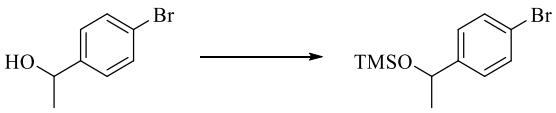
1-(4-Bromophenyl)ethan-1-ol (154a)



To a suspension of $NaBH_4$ (285 mg, 7.54 mmol, 0.5 equiv) in methanol (30 mL) was added a solution of 4'-bromoacetophenone (3 g, 15.07 mmol, 1.0 equiv) in methanol (30 mL). The reaction mixture was stirred at room temperature for 40 minutes before sat. aq. NH_4Cl (2 mL) was added. The solution was dried with $MgSO_4$, filtered, and concentrated *in vacuo* to afford a white solid of 92% purity (2.89 g, 87%); **R_f** 0.21 (petroleum ether / Et_2O (4:1)); **^{1}H NMR** (400 MHz, $CDCl_3$) δ_H 1.47 (3H, d *J* 6.5, CH(OH)C*H*$_3$), 1.97 (1H, br s, O*H*), 4.87 (1H, quartet, *J* 6.5, C*H*(OH)CH$_3$), 7.25 (2H, d, *J* 8.5, Ar*H*), 7.47 (2H, d, *J* 8.5, Ar*H*).

The spectroscopic data was found to be in agreement with that reported by Bracegirdle and co-workers.[83]

(1-(4-Bromophenyl)ethoxy)trimethylsilane (154b)

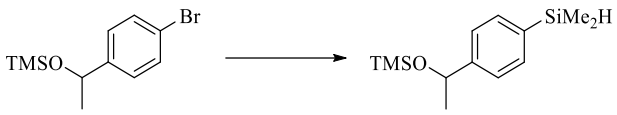


Benzyl alcohol **154a** (2.0 g, 92% purity, 10.0 mmol, 1.0 equiv) was dissolved in THF (20 mL) and triethylamine added (2.10 mL, 15.0 mmol, 1.5 equiv). To the stirred solution was then added

trimethylchlorosilane (1.90 mL, 15.0 mmol, 1.5 equiv) and the reaction stirred at RT for 24 h. The reaction mixture was then concentrated *in vacuo* to remove excess triethylamine, trimethylchlorosilane and THF. The resulting mixture was diluted with diethyl ether, filtered and concentrated *in vacuo* to afford a yellow oil which was purified by vacuum distillation (112 °C, 13 mbar) to afford the title compound as a colourless oil of 92% purity (2.22g, 81%); **^{1}H NMR** (400 MHz, $CDCl_3$) δ_H 0.00 (9H, s, Si(C*H*$_3$)$_3$), 1.32 (3H, d, *J* 6.5, CH(OTMS)C*H*$_3$), 4.73 (1H, quartet, *J* 6.5, C*H*(OTMS)CH_3), 7.13 (2H, d, *J* 8.5, Ar*H*), 7.36 (2H, d, *J* 8.5, Ar*H*).

The spectroscopic data was found to be in agreement with that reported by Rajagopal and co-workers.[208]

(1-(4-(Dimethylsilyl)phenyl)ethoxy)trimethylsilane (154)



Protected alcohol **154b** (1.53 g, 5.61 mmol, 1.0 equiv) was diluted in THF (30 mL) and cooled to −78 °C before *t*-BuLi (7.00 mL of a 1.6 M solution in hexanes, 1.22 mmol, 2.0 equiv) was added. The reaction was stirred at −78 °C for 2 h before the addition of dimethylchlorosilane (750 μL, 6.73 mmol, 1.2 equiv) and the reaction allowed to warm to RT overnight. Methanol (2 mL) was added to the reaction mixture before the crude solution was concentrated *in vacuo*. The resulting mixture was diluted with petrol, filtered, and concentrated *in vacuo* before purification by vacuum distillation (110-112 °C, 14 mbar) to afford a colourless oil of 79% purity (843 mg, 42%); **IR** (thin film, ν_{max} / cm^{-1}) 2959w, 2119w, 1250m, 1090m, 881s, 839s; **^{1}H NMR** (400 MHz, $CDCl_3$) δ_H 0.10 (9H, s, Si(C*H*$_3$)$_3$), 0.35 (6H, d, *J* 3.5, Si(C*H*$_3$)$_2$H), 1.45 (3H, d, *J* 6.5, CH(OTMS)C*H*$_3$), 4.43 (1H, sep, *J* 3.5, Si*H*), 4.87 (1H, quartet, *J* 6.5, C*H*(OTMS)CH_3), 7.35 (2H, d, *J* 7.5, Ar*H*), 7.51 (2H, d, *J* 7.5, Ar*H*); **^{13}C NMR** (125 MHz, $CDCl_3$) δ_C −3.74, 0.10, 26.8, 70.49, 124.86, 133.2, 133.9, 135.6; ***m/z*** (ESI^+) 275.12 (MNa^+, 60%); **HRMS** (EI+) not found.

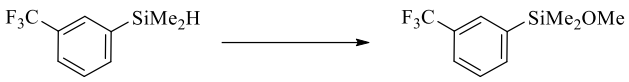
(2,6-Dimethylphenyl)dimethylsilane (155)



According to the general procedure **I**, 16.2 mL (25.9 mmol, 2.4 equiv) of *t*-BuLi was added to 2.0 g (10.8 mmol, 1.0 equiv) of 2-bromo-1,3-dimethylbenzene in anhydrous THF (50 mL). The resulting mixture was stirred for 1 h at –78 °C before 1.56 mL (14.0 mmol, 1.3 equiv) of chlorodimethylsilane was added and the reaction stirred overnight. The product was purified by column chromatography (petroleum ether) to afford the title compound as a colourless oil (1.05 g, 59%); $\mathbf{R_f}$ 0.79 (petroleum ether); **^{1}H NMR** (500 MHz, $CDCl_3$) δ_H 0.46-0.48 (6H, m, Si(C*H*$_3$)$_2$), 2.53-2.54 (3H, m, OC*H*$_3$), 4.79-4.84 (1H, m, Si*H*), 7.06 (2H, d, *J* 7.5, Ar*H*), 7.21-7.25 (1H, m, Ar*H*); **^{13}C NMR** (100 MHz, $CDCl_3$) δ_C –2.45, 24.0, 127.6, 129.2, 134.9, 144.2.

The spectroscopic data was found to be in agreement with that reported by Hevesi and co-workers.[189]

Methoxydimethyl(3-(trifluoromethyl)phenyl)silane (157)



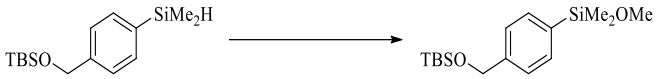
According to general procedure **II**, 105 mg (0.514 mmol) of dimethyl(3-(trifluoromethyl)phenyl)silane afforded the title compound as a colourless oil (100 mg, 83%); $\mathbf{R_f}$ 0.21 (petroleum ether / Et_2O (9:1)); **IR** (thin film, ν_{max} / cm^{-1}) 2961br, 1410w, 1326s, 1165m, 1118s, 839m; **^{1}H NMR** (400 MHz, $CDCl_3$) δ_H 0.42 (6H, s, Si(C*H*$_3$)$_2$), 3.47 (3H, s, SiOC*H*$_3$), 7.51 (1H, t, *J* 7.5, Ar*H*), 7.66 (1H, d, *J* 7.5, Ar*H*), 7.76 (1H, d, *J* 7.5, Ar*H*), 7.81 (1H, s, Ar*H*); **^{13}C NMR** (100 MHz, $CDCl_3$) δ_C –2.00, 51.2, 124.7 (q, *J* 271.5), 126.7 (q, *J* 3.5), 128.5, 132.2 (q, *J* 4.0), 130.4 (q, *J* 31.5), 137.1, 139.3; **^{19}F NMR** (377 MHz, $CDCl_3$) δ_F –62.6 (1F); **HRMS** (FI^+) calc. for $C_{10}H_{13}F_3OSi$ $[M]^+$ 234.0688, found 234.0690;

(2,6-Dimethylphenyl)(methoxy)dimethylsilane (159)



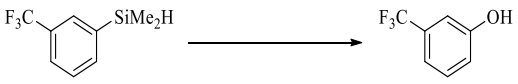
According to general procedure **II**, 105 mg (0.640 mmol) of (2,6-dimethylphenyl)dimethylsilane afforded the title compound as a colourless oil (105 mg, 84%); $\mathbf{R_f}$ 0.39 (petroleum ether / Et_2O (9:1)); **IR** (thin film, ν_{max} / cm^{-1}) 2970br, 1739s,1445w, 1368m, 1216m, 1090w, 830w; **^{1}H NMR** (400 MHz, $CDCl_3$) δ_H 0.49 (6H, s, SiC*H*$_3$), 2.49 (6H, s, ArC*H*$_3$), 3.44 (1H, s, SiOC*H*$_3$), 7.00 (2H, d, *J* 7.5, Ar*H*), 7.17 (1H, t, *J* 7.5, Ar*H*); **^{13}C NMR** (100 MHz, $CDCl_3$) δ_C 2.17, 24.3, 50.3, 128.5, 129.7, 134.9, 144.6; **HRMS** (FI^+) calc. for $C_{11}H_{18}OSi$ $[M]^+$ 194.1127, found 194.1120.

tert-Butyl((4-(methoxydimethylsilyl)benzyl)oxy)dimethylsilane (161)



Application of general procedure **II** above to hydrosilane **153** (300 mg, 1.07 mmol) afforded methoxysilane **161** (320 mg, 96%); $\mathbf{R_f}$ 0.62 (petroleum ether) **IR** (thin film, ν_{max} / cm^{-1}) 2956w, 1857w, 1471w, 1252m, 1085s, 834s; **^{1}H NMR** (400 MHz, $CDCl_3$) δ_H 0.11 (6H, s, Si(C*H*$_3$)$_2$C(CH$_3$)$_3$), 0.38 (6H, d, *J* 3.5, Si(C*H*$_3$)$_2$OCH$_3$), 0.96 (9H, s, Si(CH$_3$)$_2$C(C*H*$_3$)$_3$), 3,44 (3H, s, Si(CH$_3$)$_2$OC*H*$_3$), 4.77 (2H, s, ArC*H*$_2$), 7.36 (2H, d, *J* 8.0, Ar*H*), 7.56 (2H, d, *J* 8.0, Ar*H*); **^{13}C NMR** (100 MHz, $CDCl_3$) δ_C -5.28, -2.30, 18.4, 25.9, 50.6, 64.8, 125.5, 133.5, 133.7, 143.0; **MS** (ES^+) 293.09 (MNa^+, 100%); **HRMS** (EI+) calc. for $C_{16}H_{30}NaO_2Si_2$ $[M+Na]^+$ 333.1677, found 333.1679.

Dimethyl(3-(trifluoromethyl)phenyl)silane (156)



According to general procedure **V**, 102 mg (0.50 mmol) of silane **152** afforded the title compound as a colourless oil (55 mg, 68%); $\mathbf{R_f}$ 0.12 (petrolueum ether / Et_2O (9:1)); **^{1}H NMR** (500 MHz, $CDCl_3$) δ_H 5.67 (1H, br s, O*H*), 6.98-721 (3H, m, Ar*H*), 7.36 (1H, t, *J* 8.0, Ar*H*).

The spectroscopic data was found to be in agreement with that reported by Liu and co-workers.[209]

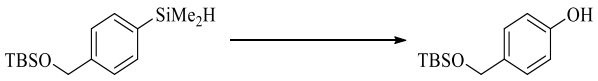
(2,6-Dimethylphenyl)dimethylsilane (158)



According to general procedure **V**, 89 mg (0.50 mmol) of (2,6-dimethylphenyl)dimethylsilane afforded the title compound as a yellow waxy solid (54 mg, 88%); $\mathbf{R_f}$ 0.21 (petrolueum ether / Et_2O (9:1)); **^{1}H NMR** (500 MHz, $CDCl_3$) δ_H 2.32 (6H, s, ArC*H*$_3$), 4.67 (1H, br s, O*H*), 6.83 (1H, t, *J* 7.5, Ar*H*), 7.05 (2H, d, *J* 7.5, Ar*H*); **^{13}C NMR** (125 MHz, $CDCl_3$) δ_C 16.3, 120.7, 123.4, 129.0, 152.6.

The spectroscopic data was found to be in agreement with that reported by Jing and co-workers.[34]

4-(((tert-Butyldimethylsilyl)oxy)methyl)phenol (160)



To a vial containing *t*-Butyl((4-(dimethylsilyl)benzyl)oxy)dimethylsilane **153** (140 mg, 0.500 mmol, 1.0 equiv) was added MeOH (200 μL). The vial was purged with argon before the addition of Pd/C (2.6 mg, 10 wt.% loading, 0.0025 mmol, 5 mol%). After 2/3 seconds of effervescence the reaction was seen to be complete by TLC. The resulting solution was filtered through a celite plug, eluted with Et_2O, and concentrated *in vacuo*. To this crude product was added MeOH/THF (1.5 mL), $KHCO_3$ (25 mg, 0.250 mmol, 0.5 equiv) and H_2O_2 (340 μL of a 30% w/w solution, 3.00 mmol, 6.0 equiv) and the reaction mixture stirred for 3 h. Upon completion, the reaction was quenched with NH_4Cl (1 mL, sat., aq.) and the monophasic mixture stirred for a further 5 min. The reaction mixture was then extracted with EtOAc (3 x 5 mL). The combined organic phases were dried ($MgSO_4$) and concentrated *in vacuo* to afford a crude phenolic product which was purified by column chromatography (petroleum ether + 1% Et_3N → petroleum ether / Et_2O (1:1) + 1% Et_3N) to afford 4-(((tert-butyldimethylsilyl)oxy)methyl)phenol as a colourless oil (88 mg, 74%); $\mathbf{R_f}$ 0.45 (petrolueum ether / Et_2O (9:1)); **^{1}H NMR** (400 MHz, $CDCl_3$) δ_H 0.94 (6H, s, Si(C*H*$_3$)$_2$(C(CH$_3$)$_3$)), 0.94 (9H, s,

$Si(CH_3)_2(C(CH_3)_3)$), 4.66 (2H, s, ArCH_2), 5.26 (1H, br s, O*H*), 6.81 (2H, d, *J* 7.5, Ar*H*), 7.18 (2H, d, *J* 7.5, Ar*H*); **^{13}C NMR** (100 MHz, $CDCl_3$) δ_C –5.17, 18.44, 26.0, 64.8, 115.2, 127.8, 133.1, 155.1.

The spectroscopic data was found to be in agreement with that reported by Bracegirdle and co-workers.[83]

5.3. Applications of the arylsilane oxidation

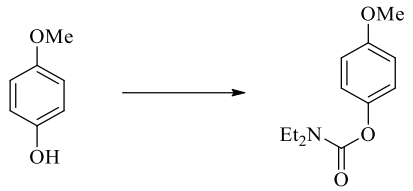
1-Chloro-N,N-diethyl-1,1-dimethylsilanamine (72)



To a stirred solution of dichlorodimethylsilane (30 ml, 249 mmol, 1.0 equiv) and Et_3N (38.1 ml, 274 mmol, 1.1 equiv) in THF (100 ml) at 0 °C was added distilled Et_2NH (25.7 ml, 249 mmol, 1.0 equiv) over a period of 2 h. Following addition the reaction was stirred overnight at rt. The reaction was diluted with pentane (50 ml), filtered over celite and concentrated *in vacuo* to yield the crude product which was purified by vacuum distillation to afford amino silane **4** as a colourless liquid (20.2 g, 49%); bp 85 °C, 100 mbar; **^{1}H NMR** (400 MHz, C_6D_6) δ_H 0.32 (6H, s, SiCH_3), 0.89 (6H, t, *J* 7.0, $N(CH_2CH_3)_2$), 2.69 (4H, q, *J* 7.0, $N(CH_2CH_3)_2$).

The spectroscopic data was found to be in agreement with that reported previously in the group.[83]

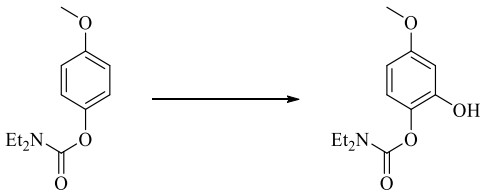
4-Methoxyphenyl diethylcarbamate (187)



To a suspension of sodium hydride (9.92 g, 248 mmol, 3.0 equiv) in anhydrous THF (200 ml), 4-methoxyphenol (10.0 g, 82.5 mmol, 1.0 equiv) was added. After stirring the reaction mixture for 2 h, diethylcarbamic chloride (22.4 ml, 165 mmol, 2.0 equiv) was added and stirring continued for another 16 hours. THF was removed *in vacuo* and the residue diluted with ethyl acetate (100 ml). The solution was washed with water (3 × 75 ml) and brine (3 × 75 ml), dried over anhydrous $MgSO_4$ and concentrated *in vacuo*. Purification by vacuum distillation (175 ^{0}C, 1.5 mmHg) afforded the title compound as a colourless oil (17.3 g, 94%); **R_f** 0.45 (petrolueum ether / EtOAc (1:1)); **^{1}H NMR** (400 MHz, $CDCl_3$) δ_H 1.17-1.29 (6H, m, rotamer A, $N(CH_2C\mathit{H}_3)_2$ overlays rotamer B, $N(CH_2C\mathit{H}_3)_2$)), 3.34 – 3.46 (4H, m, rotamer A, $N(C\mathit{H}_2CH_3)_2$ overlays rotamer B, $N(C\mathit{H}_2CH_3)_2$)), 3.80 (3H, s, $OC\mathit{H}_3$), 6.87 (2H, d, *J* 9.0, Ar*H*), 7.04 (2H, d *J* 9.0, Ar*H*); **^{13}C NMR** (100 MHz, $CDCl_3$) δ_C 13.4, 14.2, 41.8, 42.2, 55.6, 114.2, 122.6, 145.1, 154.6, 156.7.

The observed data is in agreement with that reported by J. Clayden *et al.*[210]

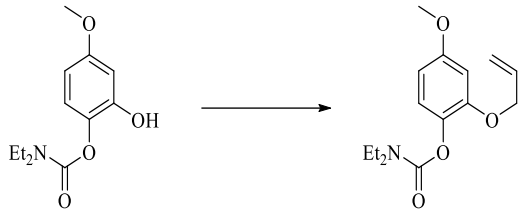
2-Hydroxy-4-methoxyphenyl diethylcarbamate (189)



To a stirred solution of phenyl diethylcarbamate **187** (1.40 g, 6.27 mmol, 1.0 equiv) and TMEDA (1.4 ml, 9.41 mmol, 1.5 equiv) at −78 ^{o}C in anhydrous THF (30 ml), was added *s*-BuLi (7.2 ml of a 1.3 M solution in hexanes, 9.41 mmol, 1.5 equiv). The resulting mixture was stirred for 1 h before addition of $ClSiMe_2(NEt_2)$ **72** (1.9 ml, 9.41 mmol, 1.5 equiv), and stirring continued at −78 ^{o}C for another 2 h. The reaction mixture was concentrated *in vacuo* and MeOH/THF (1:1) was added (16 ml) followed by

$KHCO_3$ (1.26 g, 12.5 mmol, 2.0 equiv), TBAF (630 μL of a 1 M solution in THF, 0.63 mmol, 0.1 equiv) and H_2O_2 (3.9 ml, 35% w/w, 37.6 mmol, 6.0 equiv). The reaction mixture was stirred at room temperature for 16 hours before quenching with HCl (10 ml of a 1 N aqueous solution). The phases were separated, the aqueous phases extracted with ethyl acetate (3 × 30 ml) and the combined organic extracts dried ($MgSO_4$) and concentrated *in vacuo*. Purification by flash column chromatography (petroleum ether → petroleum ether / EtOAc (4:1)) afforded the title compound as a colourless oil (1.15 g, 77%); **R_f** 0.21 (petroleum ether / EtOAc (4:1)); **^{1}H NMR** (400 MHz, $CDCl_3$) δ_H 1.20-1.30 (6H, m, $N(CH_2CH_3)_2$), 3.38-3.50 (4H, m, $N(CH_2CH_3)_2$), 3.76 (3H, s, OCH_3), 6.43 (1H, dd *J* 9.0, 3.0, Ar*H*), 6.57 (1H, d, *J* 3.0, Ar*H*), 6.92 (1H, d, *J* 9.0, Ar*H*), 7.49 (1H, s O*H*); **^{13}C NMR** (100 MHz, $CDCl_3$) δ_C 13.3, 14.1, 42.3, 42.6, 55.5, 104.5, 106.5, 122.2, 134.2, 148.5, 155.1, 158.0; **HRMS** (ES^+) calc. for $C_{12}H_{17}NNaO_4$ $[M+Na]^+$ 262.1050, found 262.1048.

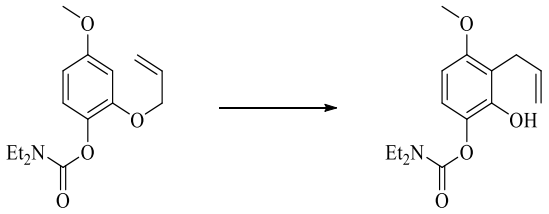
2-(Allyloxy)-4-methoxyphenyl diethylcarbamate (185)



To a stirred solution of phenol **189** (100 mg, 0.42 mmol, 1.0 equiv) in acetone (2 ml) was added K_2CO_3 (173 mg, 1.25 mmol, 3.0 equiv) and allyl bromide (40 μL, 0.46 mmol, 1.1 equiv). The mixture was heated at reflux and stirred for 16 h. After cooling to room temperature the mixture was filtered and the filtrate concentrated *in vacuo*. The resulting oil was dissolved in DCM (10 ml) and washed with 1 N NaOH (3 × 10 ml) and brine (3 × 10 ml), dried over anhydrous $MgSO_4$ and concentrated *in vacuo*. Purification by flash column chromatography (petroleum ether → petroleum ether / EtOAc (4:1)) afforded the title compound as a colourless oil (63 mg, 54%); **R_f** 0.41 (petroleum ether / EtOAc (7:3)); **IR** (thin film, ν_{max} / cm^{-1}) 2976br 1719s, 1611m, 1513m, 1421m, 1312w, 1205s, 1157m, 1045w, 932w; **^{1}H NMR** (400 MHz, $CDCl_3$) δ_H 1.15 – 1.30 (6H, m, $N(CH_2CH_3)_2$), 3.30 – 3.51 (4H, m, $N(CH_2CH_3)_2$), 3.78 (3H, s, OCH_3), 4.52 (2H, d, *J* 5.5, $CH_2CH{=}CH_2$), 5.24 (1H, dd, *J* 10.5, 1.0,

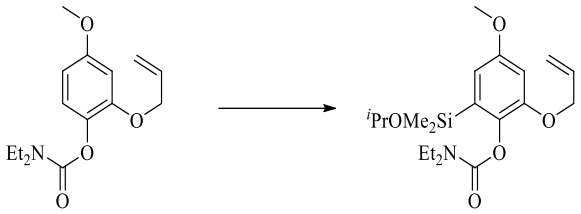
CH=C*H*H'), 5.40 (1H, dd, *J* 17.5, 1.0, CH=CH*H'*), 5.96–6.05 (1H, m, C*H*=CHH'), 6.45 (1H, dd *J* 8.5, 2.5, Ar*H*), 6.52 (1H, d, *J* 2.5, Ar*H*), 7.01 (1H, d, *J* 8.5, Ar*H*); **^{13}C NMR** (100 MHz, $CDCl_3$) δ_C 13.4, 14.1, 41.9, 42.2, 55.6, 69.3, 101.5, 104.2, 117.2, 123.3, 133.0, 134.9, 151.2, 154.4, 157.7; **HRMS** (ES^+) calc. for $C_{15}H_{21}NNaO_4$ $[M+Na]^+$ 302.1363, found 302.1364.

3-Allyl-2-hydroxy-4-methoxyphenyl diethylcarbamate (191)



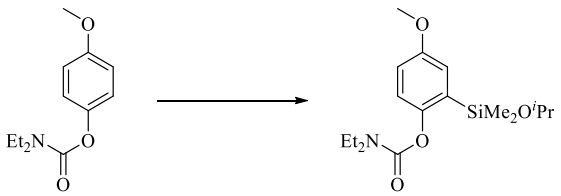
Allyl ether **185** (50 mg, 0.179 mmol) was dissolved in *N, N*- dimethylalanine (0.50 ml) and heated at 170 °C for 2 h. After cooling to room temperature, the reaction mixture was diluted with diethyl ether (5 ml), washed with 1 N HCl solution (3 × 5 ml), dried ($MgSO_4$) and concentrated *in vacuo*. The resulting crude mixture was purified by flash column chromatography (petroleum ether → petroleum ether / EtOAc (4:1)) to afford the title compound as a colourless oil (15 mg, 30%); **R_f** 0.36 (petroleum ether / EtOAc (4:1)); **^{1}H NMR** (400 MHz, $CDCl_3$) δ_H 1.20 – 1.29 (6H, m, $N(CH_2CH_3)_2$), 3.38 – 3.50 (6H, m, ArCH_2 overlays $N(CH_2CH_3)_2$), 3.80 (3H, s, OCH_3), 4.96-5.06 (2H, m, CH=C*H*H' overlays CH=CH*H'*), 5.94 – 6.04 (1H, m, C*H*=CH_2), 6.44 (1H, d, *J* 9.0, Ar*H*), 6.88 (1H, *J* 9.0, Ar*H*) 6.95 (1H, s, ArO*H*); **^{13}C NMR** (100 MHz, $CDCl_3$) δ_C 13.3, 14.2, 27.8, 42.3, 42.6, 56.0, 102.7, 114.5, 118.0, 119.3, 134.7, 136.4, 146.7, 155.0, 155.7.

2-(Allyloxy)-6-(isopropoxydimethylsilyl)-4-methoxyphenyl diethylcarbamate (184)



To a stirred solution of allyl ether **185** (350 mg, 1.25 mmol, 1.0 equiv) and TMEDA (280 μL, 1.88 mmol, 1.5 equiv) in THF (7 ml) at −78 °C was added *s*-BuLi (1.45 ml 1.3 M solution in hexanes, 1.88 mmol, 1.5 equiv). The resulting mixture was stirred for 1 h before addition of $ClSiMe_2(NEt_2)$ **72** (430 μL, 2.13 mmol, 1.7 equiv), then stirring was continued at −78 °C for another 2 h. Upon warming to RT, *i*-PrOH (1.4 ml) and DMAP (crystal) were added before stirring overnight. The reaction mixture was concentrated *in vacuo* and the resulting crude mixture was purified by flash column chromatography (petroleum ether → petroleum ether / EtOAc (9:1)) to afford the title compound as a colourless oil (80 mg, 23%); $\mathbf{R_f}$ 0.58 (petroleum ether / EtOAc (4:1)); **^{1}H NMR** (200 MHz, $CDCl_3$) δ_H 0.37 (6H, s, $Si(CH_3)_2$), 1.11-1.31 (12H, m, $OCH(CH_3)_2$ overlays $N(CH_2CH_3)_2$), 3.28-3.55 (4H, m, $N(CH_2CH_3)_2$), 3.81 (3H, s, OCH_3), 4.05 (1H, sept, *J* 6.0 ($OCH(CH_3)_2$), 4.51 (2H, dt, *J* 5.0, 1.5, $CH_2CH{=}CH_2$) 5.22 (1H, dq, *J* 10.5, 1.5 CH=C*H*H'), 5.39 (1H, dq, *J* 17.5, 1.5, CH=C*H*H'), 5.89-6.09 (1H, m, C*H*=CHH'), 6.55 (1H, d, *J* 3.0, Ar*H*), 6.67 (1H, d, *J* 3.0, Ar*H*); **HRMS** (EI+) calc. for $C_{20}H_{33}NNaO_5$ $[M+Na]^+$ 418.2020, found 418.2021.

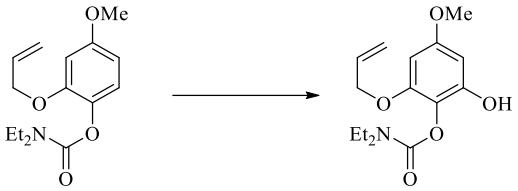
2-(Isopropoxydimethylsilyl)-4-methoxyphenyl diethylcarbamate (186)



To a stirred solution of phenyl diethylcarbamate **187** (1.00 g, 4.48 mmol, 1.0 equiv) and TMEDA (0.80 ml, 5.37 mmol, 1.2 equiv) at −78 °C in anhydrous THF (20 ml), was added *s*-BuLi (4.0 ml of a 1.3 M solution in hexanes, 5.37 mmol, 1.2 equiv). The resulting mixture was stirred for 1 h before addition of $ClSiMe_2(NEt_2)$ **72** (0.63 ml, 6.27 mmol, 1.4 equiv), then stirring was continued at −78 °C for another 2 h. Upon warming to RT, *i*-PrOH (4 ml) and DMAP (crystal) were added before stirring overnight. The reaction mixture was concentrated *in vacuo* and the resulting crude mixture was purified by flash column chromatography (petroleum ether → petroleum ether / EtOAc (9:1)) to afford the title compound (450 mg, 30%); $\mathbf{R_f}$ 0.51 (petroleum ether / EtOAc (9:1)); **IR** (thin film, ν_{max}

/ cm^{-1}) 2972s, 1718s, 1579w, 1420m, 1191s, 1028m, 961w, 784m; **^{1}H NMR** (400 MHz, $CDCl_3$) δ_H 0.37 (6H, s, $Si(CH_3)_2(OCH(CH_3)_2)$, 1.15 (6H, d, *J* 6.0, $Si(CH_3)_2(OCH(CH_3)_2)$, 1.19 (3H, t, *J* 7.0, rotamer A $N(CH_2CH_3)_2$), 1.25 (3H, t, *J* 7.0, rotamer B $N(CH_2CH_3)_2$), 3.39 (2H, q, *J* 7.0, rotamer A $N(CH_2CH_3)_2$), 3.49 (2H, q, *J* 7.0, rotamer B $N(CH_2CH_3)_2$), 3.80 (3H, s, OCH_3), 4.02 (1H, sept, *J* 6.0 $Si(CH_3)_2(OCH(CH_3)_2)$, 6.92 (1H, dd, *J* 8.5, 3.0, Ar*H*), 7.01 (1H, d, *J* 8.5, Ar*H*), 7.09 (1H, d, *J* 3.0, Ar*H*); **^{13}C NMR** (100 MHz, $CDCl_3$) δ_C −0.55, 13.3, 14.1, 25.7, 41.5, 41.9, 55.5, 65.4, 115.8, 120.0, 123.3, 131.1, 149.5, 154.6, 156.3; **MS** (ES^+) 362.16 (MNa^+, 100%), 701.28 (M_2Na^+, 100%).

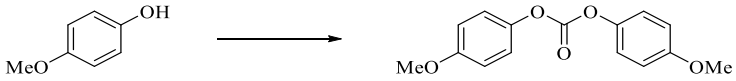
2-(Allyloxy)-6-hydroxy-4-methoxyphenyl diethylcarbamate (190)



To a stirred solution of phenyl diethylcarbamate **185** (350 mg, 1.25 mmol, 1.0 equiv) and TMEDA (250 μL, 1.63 mmol, 1.3 equiv) at −78 °C in anhydrous THF (7 ml), was added *s*-BuLi (1.25 ml of a 1.3 M solution in hexanes, 1.63 mmol, 1.3 equiv). The resulting mixture was stirred for 2 h before addition of $ClSiMe_2(NEt_2)$ **72** (375 μL, 1.88 mmol, 1.5 equiv), and stirring continued at −78 °C for 30 min, before warming to RT over 1 h. The reaction mixture was concentrated *in vacuo* and MeOH/THF (1:1) was added (2 ml) followed by $KHCO_3$ (250 mg, 2.50 mmol, 2.0 equiv), TBAF (125 μL of a 1 M solution in THF, 0.125 mmol, 0.1 equiv) and H_2O_2 (760 μL, 35% w/w, 7.50 mmol, 6.0 equiv). The reaction mixture was stirred at room temperature for 16 hours before quenching with HCl (7 ml of a 1 N aqueous solution). The phases were separated, the aqueous phases extracted with ethyl acetate (3 × 10 ml) and the combined organic extracts dried ($MgSO_4$) and concentrated *in vacuo*. Purification by flash column chromatography (petroleum ether → petroleum ether / EtOAc (85:15)) afforded the title compound as a colourless oil (134 mg, 36%); **R_f** 0.19 (petroleum ether / EtOAc (85:15)); **IR** (thin film, ν_{max} / cm^{-1}) 3418br, 2976m, 2251w, 1682m, 1524w, 1427m, 1278m, 1079m; **^{1}H NMR** (400 MHz, $CDCl_3$) δ_H 1.21 (3H, t, *J* 7.0, rotamer A, $N(CH_2CH_3)_2$), 1.28 (3H, t, *J* 7.0, rotamer B, $N(CH_2CH_3)_2$), 3.39 (2H, q, *J* 7.0, rotamer A, $N(CH_2CH_3)_2$), 3.52 (2H, q, *J* 7.0, rotamer B,

N(C*H*$_2$CH$_3$)$_2$), 3.73 (3H, s, OC*H*$_3$), 4.48 (2H, d, *J* 5.5, C*H*$_2$CH=CH$_2$), 5.25 (1H, dd, *J* 10.5, 1.5, CH=C*H*H'), 5.38 (1H, dd, *J* 17.5, 1.5, CH=CH*H'*), 5.96–6.05 (1H, m, C*H*=CHH'), 6.09 (1H, d, *J* 3.0, Ar*H*), 6.17 (1H, d, *J* 3.0, Ar*H*); **^{13}C NMR** (100 MHz, $CDCl_3$) δ_C 13.3, 14.0, 42.3, 42.5, 55.7, 69.5, 93.2, 95.3, 117.5, 118.3, 133.1, 150.4, 151.5, 155.0, 157.7; **MS** (ES^+) 318.12 (MNa^+, 100%), 613.26 (M_2Na^+, 85%); **HRMS** (EI+) calc. for $C_{15}H_{21}NNaO_5$ $[M+Na]^+$ 318.1312, found 318.1313.

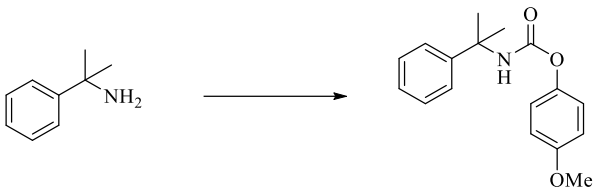
Bis(4-methoxyphenyl) carbonate (198)



A solution of *para*-methoxy phenol **200** (125 mg, 1.03 mmol, 1.5 equiv) and Hunig's base (*N*,*N*-Diisopropylethylamine) (180 μL, 1.03 mmol, 1.5 equiv) in dichloromethane (3 ml) was added dropwise to a solution of triphosgene (102 mg, 0.35 mmol, 0.5 equiv) in dichloromethane (1.5 ml) at 0 °C. The reaction mixture was stirred for 5 minutes at 0 °C after which the reaction mixture was quenched with sat. aq. $NaHCO_3$ (5 ml). The biphasic mixture was separated, and the aqueous layer extracted with dichloromethane (3 × 50 ml), the combined organic layers dried over $MgSO_2$ and concentrated *in vacuo* to afford a yellow solid which was purified by column chromatography (petroleum ether → petroleum ether / EtOAc (4:1)) to afford the title compound as a white solid (95 mg, 67%); $\mathbf{R}_f$ 0.58 (50% ether/petrol); **^{1}H NMR** (400 MHz, $CDCl_3$) δ_H 3.82 (6H, s, OC*H*$_3$), 6.92 (2H, d, *J* 9.0, Ar*H*), 7.19 (2H, d, *J* 9.0, Ar*H*); **^{13}C NMR** (100 MHz, $CDCl_3$) δ_C 55.6, 114.5, 121.8, 144.6, 152.8, 157.5.

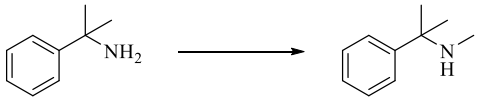
The spectroscopic data was found to be in agreement with that reported by Itami and co-workers.[211]

4-Methoxyphenyl 2-phenylpropan-2-ylcarbamate (199)



A solution of *para*-methoxy phenol **200** (125 mg, 1.03 mmol, 2.0 equiv) in dichloromethane (3 ml) was treated with triphosgene (153 mg, 0.52 mmol, 1.0 equiv) followed by the dropwise addition of a solution of Hunig's base (*N*,*N*-Diisopropylethylamine) (180 μL, 1.03 mmol, 2.0 equiv) in dichloromethane (1.5 ml) at 0 ^{o}C. The reaction mixture was allowed to warm to RT and stirred for a further 1 h after which the reaction was quenched with sat. aq. $NaHCO_3$. The biphasic mixture was separated, the aqueous layer extracted with dichloromethane (3 ×10 ml) and the combined organic layers dried over $MgSO_4$. The organic solution was added dropwise to a solution of cumyl amine (70 μL, 0.48 mmol, 1.0 equiv) and Hunig's base (100 μL, 0.58 mmol, 1.2 equiv) in dichloromethane (1.5 ml) at RT. After stirring for 1 h the reaction was quenched with water (10 mL) the layers separated and the aqueous layer extracted with dichloromethane (3 x 10 mL). The combined organic layers were dried over $MgSO_4$ and concentrated *in vacuo* to afford an off white solid which was purified by column chromatography (petroleum ether → petroleum ether / EtOAc (4:1)) to afford carbamate **24** as a white solid (100 mg, 73%); **Mp**, 117 ^{o}C; $\mathbf{R_f}$ 0.44 (petroleum ether / EtOAc (1:1)); **IR** (thin film, ν_{max} / cm^{-1}) 3322 m, 1718s, 1615w, 1605s, 1451s; **^{1}H NMR** (500 MHz, $CDCl_3$) δ_H 1.75 (s, 6H, PhC(C*H*$_3$)$_2$), 3.77 (s, 3H, OC*H*$_3$)), 5.41 (s, 1H, N*H*)), 6.84 (d, *J* 8.0, 2H, Ar*H*), 7.03 (d, *J* 8.0, 2H, Ar*H*), 7.26 (t, *J* 7.5, 1H, Ar*H*), 7.37 (t, *J* 7.5, 2H, Ar*H*), 7.48 (d, *J* 8.0, 2H, Ar*H*); **^{13}C NMR** (125 MHz, $CDCl_3$) δ_C 29.0, 55.6, 114.2, 122.5, 124.8. 126.9, 128.4, 144.4, 146.6, 153.0, 156.8 (2C); **MS** (ES^+) 308.12 (MNa^+, 97%), 593.23 (M_2Na^+, 100%); **HRMS** (EI+) calc. for $C_{17}H_{19}NNaO_3$ $[M+Na]^+$ 308.1257, found 308.1256.

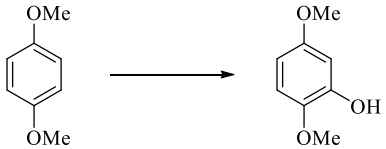
N-methyl-2-phenylpropan-2-amine (203)



Benzaldehyde (95 μL, 0.92 mmol, 1.25 equiv) was added to a stirred solution of cumyl amine (100 μL, 0.74 mmol, 1.0 equiv) in toluene (0.25 mL) and heated at reflux with a Dean Stark trap and condenser attached. The reaction was heated for 3 h at which point no more water was being collected. The reaction mixture was cooled to RT before the addition of dimethyl sulphate (75 μL, 0.77 mmol, 1.05 equiv) in toluene (0.15 mL) dropwise. Once addition was complete the mixture was again heated at reflux for 2 h before cooling to RT, water (0.25 mL) was added and the mixture heated at 80 °C for 30 min. After cooling to RT, the reaction mixture was diluted in DCM (5 mL), transferred to a separating funnel and extracted with water (3 × 5 mL). The combined aqueous layers were then basified with NaOH (10 mL, 1N aq. solution) and extracted with DCM (3 × 5 mL). The combined organic layers were dried ($MgSO_4$) and concentrated *in vacuo* to afford an inseparable mixture of mono – methylated amine (**203**) and starting material (63 mg, 1.5 : 1 respectively); **^{1}H NMR** (200 MHz, $CDCl_3$) δ_H 1.39 (6H, s, C(C*H*$_3$)$_2$), 1.98 (1H, br s, N*H*), 2.18 (3H, s, NHC*H*$_3$), 7.17 – 7.56 (5H, m, Ar*H*).

The spectroscopic data was found to be in agreement with that reported by Viallon and co-workers.[212]

2,5-Dimethoxyphenol (207)

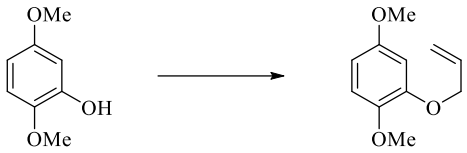


To a stirred solution of 1,4 dimethoxybenzene (2.50 g, 18.1 mmol, 1.0 equiv) and TMEDA (3.5 mL, 23.5 mmol, 1.3 equiv) at −78 °C in anhydrous THF (50 mL), was added *s*-BuLi (18.0 mL of a 1.3 M solution in hexanes, 23.5 mmol, 1.3 equiv). The resulting mixture was stirred for 2 h before addition of $ClSiMe_2(NEt_2)$ **72** (5.40 mL, 27.1 mmol, 1.5 equiv), after 1 h at −78 °C the reaction was allowed to warm to RT over 1 h. The reaction mixture was concentrated *in vacuo* and MeOH/THF (1:1) was

added (30 mL) followed by $KHCO_3$ (3.60 g, 36.2 mmol, 2.0 equiv), TBAF (1.81 mL of a 1 M solution in THF, 1.81 mmol, 0.1 equiv) and H_2O_2 (11 mL, 35% w/w, 109 mmol, 6.0 equiv). The reaction mixture was stirred at RT for 16 hours before quenching with HCl (25 mL of a 1 N aqueous solution). The phases were separated, the aqueous phases extracted with ethyl acetate (3 × 25 mL) and the combined organic extracts dried ($MgSO_4$) and concentrated *in vacuo*. Purification by flash column chromatography chromatography (petroleum ether → petroleum ether / EtOAc (9:1)) afforded the title compound as a colourless oil (2.31 g, 82%); **R_f** 0.61 (petroleum ether / EtOAc (1:1)); **^{1}H NMR** (400 MHz, $CDCl_3$) δ_H 3.76 (3H, s, OC*H*$_3$), 3.86 (3H, s, OC*H*$_3$), 6.39 (1H, dd, *J* 9.0, 3.0, Ar*H*), 6.57 (1H, d, *J* 3.0, Ar*H*), 6.79 (1H, d, *J* 9.0, Ar*H*); **^{13}C NMR** (100 MHz, $CDCl_3$) δ_C 55.6, 56.6, 101.7, 104.2, 111.5, 140.9, 146.4, 154.6;

The spectroscopic data was found to be in agreement with that reported by Bjørsvik and co-workers.[205]

2-(Allyloxy)-1,4-dimethoxybenzene (208)

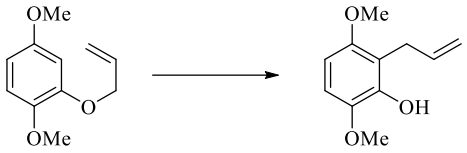


Phenol **212** (1.00 g, 6.45 mmol, 1.0 equiv), allyl bromide (840 μL, 9.68 mmol, 1.5 equiv), and K_2CO_3 (2.68 g, 19.4 mmol, 3.0 equiv) were dissolved in acetone (30 mL) and the reaction mixture heated at reflux overnight. The resulting suspension was filtered and the filtrate concentrated *in vacuo* to afford a yellow oil which was dissolved in EtOAc (30 mL) and washed with NaOH (1N aq solution, 3 × 30 mL). The organic layer was dried ($MgSO_4$) and concentrated *in vacuo* to afford a yellow oil which was purified by column chromatography (petroleum ether → petroleum ether / Et_2O (9:1) to afford the title compound as a colourless oil (649 mg, 52%); **R_f** 0.36 (petroleum ether / $E_{t2}O$ (9:1)); **^{1}H NMR** (400 MHz, $CDCl_3$) δ_H 3.77 (3H, s, OC*H*$_3$), 3.84 (3H, s, OC*H*$_3$), 4.60 (2H, d, *J* 5.5, C*H*$_2$CH=CH$_2$), 5.29 (1H, d, *J* 10.5, CH=C*H*H'), 5.42 (1H, d, *J* 17.0, CH=CH*H'*), 6.04-6.14 (1H, m, C*H*=CHH'), 6.42 (1H,

dd, *J* 9.0, 3.0 Ar*H*), 6.53 (1H, d, *J* 3.0, Ar*H*), 6.81 (1H, d, *J* 9.0, Ar*H*); **^{13}C NMR** (100 MHz, $CDCl_3$) δ_C 55.6, 56.6, 69.8, 102.2, 103.6, 112.5, 118.0, 133.2, 143.9, 148.9, 154.1;

The spectroscopic data was found to be in agreement with that reported by Otterlo and co-workers.[133]

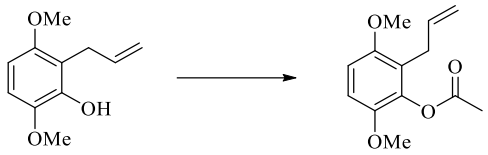
2-Allyl-3,6-dimethoxyphenol (210)



The procedure was developed from literature precedent;[133] A solution of allyl ether **208** (300 mg, 1.55 mmol) in DMF (6 mL) was heated at 200 °C under microwave irradiation for 1 h. After cooling to RT the reaction mixture was diluted with Et_2O (5 mL) and washed with water (3 × 10 mL). The combined organic layers were washed with aq. NaCl (50 mL), dried ($MgSO_4$) and concentrated *in vacuo* to afford an orange solid which was purified by column chromatography (petroleum ether → petroleum ether / Et_2O (9:1)) to afford phenols **210** and **210*p*** as white solids; ortho rearranged product **206**, (180 mg, 60%); **R_f** 0.26 (petroleum ether / $E_{t2}O$ (9:1)); **^{1}H NMR** (400 MHz, $CDCl_3$) δ_H 3.46 (2H, d, *J* 6.0, C*H*$_2$CH=CH$_2$), 3.79 (3H, s, OC*H*$_3$), 3.86 (3H, s, OC*H*$_3$), 4.94 (1H, d, *J* 10.0, CH$_2$CH=C*H*H'), 5.04 (1H, d, *J* 17.0, CH$_2$CH=CH*H'*), 5.73 (1H, s, O*H*), 6.01 (1H, ddt, *J* 17.0, 10.0, 6.0, CH$_2$C*H*=CH$_2$), 6.37 (1H, d, *J* 9.0, Ar*H*), 6.70 (1H, d, *J* 9.0, Ar*H*); **^{13}C NMR** (100 MHz, $CDCl_3$) δ_C 27.5, 56.0, 56.4, 101.1, 108.2, 114.3, 115.5, 136.4, 141.2, 144.4, 152.6; Para product (34 mg, 18%); **R_f** 0.12 (petroleum ether / $E_{t2}O$ (9:1)); **^{1}H NMR** (400 MHz, $CDCl_3$) δ_H 3.33 (2H, d, *J* 6.5, C*H*$_2$CH=CH$_2$), 3.78 (3H, s, OC*H*$_3$), 3.85 (3H, s, OC*H*$_3$), 5.03-5.07 (2H, m, CH$_2$CH=C*H*$_2$), 5.54 (1H, s, O*H*), 5.98 (1H, ddt, *J* 16.5, 10.5, 6.5, CH$_2$C*H*=CH$_2$), 6.57 (1H, s, Ar*H*), 6.68 (1H, s, Ar*H*); **^{13}C NMR** (100 MHz, $CDCl_3$) δ_C 33.7, 56.1, 56.7, 99.4, 113.0, 115.0, 119.2, 137.4, 140.1, 144.5, 151.8.

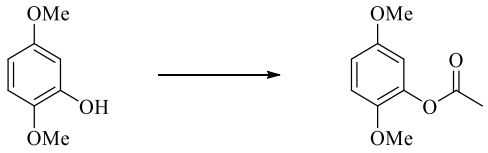
The spectroscopic data was found to be in agreement with that reported by Otterlo and co-workers.[133]

2-Allyl-3,6-dimethoxyphenyl acetate procedure (210)



The procedure was developed from literature precedent;[213] To a solution of phenol **210** (150 mg, 0.77 mmol, 1.0 equiv) in pyridine (2 mL) at RT was added acetic anhydride (365 μL, 3.86 mmol, 5.0 equiv). The solution was stirred for 3 h before addition of water (5 mL). The mixture was extracted with EtOAc (3 × 5 mL) and the combined organic layers washed with 1N HCl (3 × 5 mL). The combined organic layers were dried ($MgSO_4$) and concentrated *in vacuo* to afford an off white solid which was purified by column chromatography (petroleum ether → petroleum ether / Et_2O (9:1)) to afford the title compound as a white solid (131 mg, 72%); $\mathbf{R_f}$ 0.25 (petroleum ether / EtOAc (9:1)); **^{1}H NMR** (500 MHz, $CDCl_3$) δ_H 2.32 (3H, s, COC*H*$_3$), 3.33 (2H, d, *J* 6.0, C*H*$_2$CH=CH$_2$), 3.78 (3H, s, OC*H*$_3$), 3.79 (3H, s, OC*H*$_3$), 4.96-5.03 (2H, m, CH$_2$CH=C*H*H' overlays CH=CH*H'*), 5.82-5.90 (1H, m, CH$_2$C*H*=CH$_2$), 6.71 (1H, d, *J* 9.0, Ar*H*), 6.80 (1H, d, *J* 9.0, Ar*H*); **^{13}C NMR** (125 MHz, $CDCl_3$) δ_C 20.5, 28.5, 56.1, 56.3, 108.0, 109.9, 115.0, 122.6, 135.7, 139.2, 145.6, 151.9, 168.8; **HRMS** (EI+) calc. for $C_{13}H_{16}NaO_4$ $[M+Na]^+$ 259.0941, found 259.0941.

2,5-Dimethoxyphenyl acetate (209)

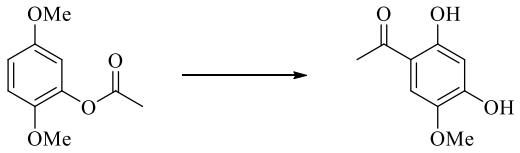


The procedure was developed from literature precedent;[214] Phenol **207** (150 mg, 0.97 mmol, 1 equiv) was dissolved in acetic anhydride (500 μL, 4.84 mmol, 5.0 equiv) and pyridine (390 μL, 4.84 mmol, 5 equiv) and stirred at RT overnight after which water (5 mL) was added to the reaction mixture before stirring for 1 h at RT. EtOAc was added (5 mL), the biphasic mixture was separated and the aqueous layer extracted with EtOAc (3 × 5 mL). The combined organic layers were washed with sat. aq. $NaHCO_3$ (3 × 10 mL), dried ($MgSO_4$), and concentrated *in vacuo* to afford the title compound as an off white solid without the need for further purification (180 mg, 95%); $\mathbf{R_f}$ 0.60 (petroleum ether /

EtOAc (1:1)); **^{1}H NMR** (400 MHz, $CDCl_3$) δ_H 2.32 (3H, s, COC*H*$_3$), 3.76 (3H, s, OC*H*$_3$), 3.79 (3H, s, OC*H*$_3$), 6.66 (1H, d, *J* 3.0, Ar*H*), 6.74 (1H, dd, *J* 9.0, 3.0, Ar*H*), 6.91 (1H, d, *J* 9.0, Ar*H*); **^{13}C NMR** (100 MHz, $CDCl_3$) δ_C 20.7, 55.8, 56.5, 109.5, 111.4, 113.3, 140.2, 145.4, 153.7, 168.9.

The spectroscopic data was found to be in agreement with that reported by Bjørsvik and co-workers.[205]

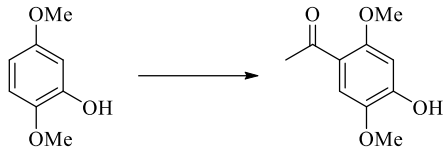
1-(2,4-Dihydroxy-5-methoxyphenyl)ethanone (211)



To a vial containing 2,5-dimethoxyphenyl acetate **209** (50 mg, 0.25 mmol, 1.0 equiv) was added neat $BF_3.Et_2O$ (100 μL, 1.53 mmol, 3.0 equiv). The reaction mixture was stirred at 70 °C for 2 h and then cooled to RT. The suspension was quenched with sat. aq NaOAc (2 mL) and then sat. aq. $NaHCO_3$ (2 mL) was added. The resulting suspension was extracted with EtOAc (3 × 5 mL) and the combined organic layers washed with brine, dried ($MgSO_4$) and concentrated *in vacuo* to afford a crude mixture which was purified by column chromatography (petroleum ether → petroleum ether / Et_2O (7:3)) to afford the *para* rearranged product as a white solid (15 mg, 31%); **R_f** 0.14 (petroleum ether / EtOAc (1:1)); **^{1}H NMR** (500 MHz, $CDCl_3$) δ_H 2.57 (3H, s, COC*H*$_3$), 3.91 (3H, s, OC*H*$_3$), 6.25 (1H, s, O*H*), 6.53 (1H, s, Ar*H*), 7.06 (1H, s, Ar*H*), 12.59 (1H, s, O*H*); **^{13}C NMR** (125 MHz, $CDCl_3$) δ_C 26.5, 56.6, 103.5, 110.6, 112.1, 139.7, 153.6, 160.4, 201.9; **HRMS** (ES^+) calc. for $C_9H_9O_4$ $[M]^+$ 181.0506, found 181.0508.

The compound was previously reported by Gable and co-workers.[215]

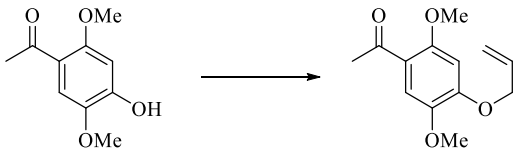
1-(4-Hydroxy-2,5-dimethoxyphenyl)ethanone (212)



To a solution of phenol **207** (100 mg, 0.65 mmol, 1.0 equiv) and AcCl (48 μL, 0.68 mmol, 1.05 equiv) in DCM (2 mL) at 0 °C was added $AlCl_3$ (87 mg, 0.65, 1.0 equiv) in small portions. The reaction mixture was allowed to warm to RT and stirred for 16 h after which 1N HCl (2 mL) was added. The biphasic mixture was separated and the aqueous layer extracted with EtOAc (3 × 5 mL). The combined organic layers were washed with sat. aq. NaCl solution (5 mL), dried ($MgSO_4$) and concentrated *in vacuo* to afford a dark yellow solid which was purified by column chromatography (petroleum ether → petroleum ether / Et_2O (65:35)) to afford the title compound as a white solid (50 mg, 39%); **R_f** 0.14 (petroleum ether / $E_{t2}O$ (1:1)); **^{1}H NMR** (400 MHz, $CDCl_3$) δ_H 2.60 (3H, s, COC*H*$_3$), 3.87 (3H, s, OC*H*$_3$), 3.90 (3H, s, OC*H*$_3$), 6.07 (1H, br s, O*H*), 6.59 (1H, s, Ar*H*), 7.45 (1H, s, Ar*H*); **^{13}C NMR** (100 MHz, $CDCl_3$) δ_C 32.1, 55.9, 56.4, 99.1, 112.2, 119.0, 140.5, 151.1, 156.1, 197.4.

The spectroscopic data was found to be in agreement with that reported by Geyer and co-workers.[216]

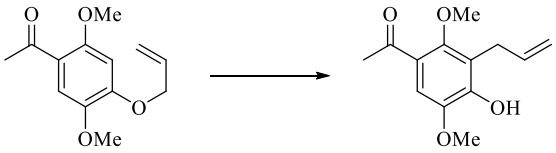
1-(4-(allyloxy)-2,5-dimethoxyphenyl)ethanone procedure (213)



The procedure was developed from literature precedent;[114] Allyl bromide (80 μL, 0.92 mmol, 1.5 equiv) was added to phenol **212** (120 mg, 0.61 mmol, 1.0 equiv) and K_2CO_3 (169 mg, 1.22 mmol, 2 equiv) in DMF (3 mL) and the reaction mixture was heated at 60 °C for 30 min. After cooling to RT the reaction mixture was diluted with Et_2O (5 mL) and extracted with water (3 × 10 mL) before the combined organic layers were washed with brine, dried and concentrated *in vauo* to afford the title compound as a colourless oil without the need for further purification (104 mg, 72%); **R_f** 0.25

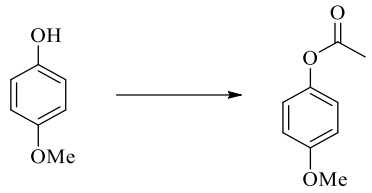
(petroleum ether / EtOAc (1:1)); **IR** (thin film, ν_{max} / cm^{-1}) 3425 br, 1649m, 1605m, 1266 m, 1214s; **^{1}H NMR** (400 MHz, $CDCl_3$) δ_H 2.59 (3H, s, COC*H*$_3$), 3.86 (3H, s, OC*H*$_3$), 3.87 (3H, s, OC*H*$_3$), 4.69 (2H, d, *J* 5.5, C*H*$_2$CH=CH$_2$), 5.34 – 5.46 (2H, m, CH$_2$CH=C*H*$_2$), 6.02-6.14 (1H, m, CH$_2$CH=C*H*$_2$), 6.52 (1H, s, Ar*H*), 7.43 (1H, s, Ar*H*); **^{13}C NMR** (100 MHz, $CDCl_3$) δ_C 32.1, 56.1, 56.3, 70.0, 98.2, 112.8, 118.6, 119.4, 132.6, 143.3, 152.9, 155.3, 197.3; **MS** (ES^+) 259.09 (MNa^+, 100%), 495.19 (M_2Na^+, 95%); **HRMS** (EI+) calc. for $C_{13}H_{16}NaO_4$ $[M+Na]^+$ 259.0941, found 259.0941.

1-(3-allyl-4-hydroxy-2,5-dimethoxyphenyl)ethanone (206)



The procedure was developed from literature precedent[133]; A solution of allyl ether **213** (100 mg, 0.42 mmol) in DMF (2 mL) was heated at 200 ºC under microwave irradiation for 1 h. After cooling to rt the reaction mixture was diluted with Et_2O (5 mL) and washed with water (3 x 10 mL). The combined organic layers were washed with NaCl (aq) (50 mL), dried ($MgSO_4$) and concentrated *in vacuo* to afford an orange solid which was purified by column chromatography (petroleum ether → petroleum ether / Et_2O (4:1)) to afford the title compound as a white solid (35 mg, 35%); **R_f** 0.26 (petroleum ether / EtOAc (9:1)); **^{1}H NMR** (200 MHz, $CDCl_3$) δ_H 2.65 (3H, s, COC*H*$_3$), 3.47 (2H, dt, *J* 6.0, 1.5, ArC*H*$_2$), 3.74 (3H, s, OC*H*$_3$), 3.90 (3H, s, OC*H*$_3$), 5.00 – 5.09 (2H, m, CH=C*H*$_2$), 6.04 (1H, ddt, *J* 17.5, 9.5, 6.0, C*H*=CH$_2$), 7.19 (1H, s, Ar*H*). **MS** (ES^+) 259.10 (MNa^+, 95%), 495.20 (M_2Na^+, 100%); **HRMS** (EI^+) calc. for $C_{13}H_{16}NaO_4$ $[M+Na]^+$ 259.0941, found 259.0939.

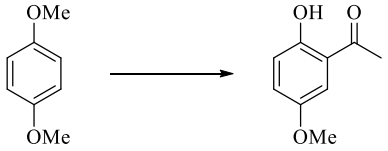
4-Methoxyphenyl acetate (217)



4-Methoxyphenol (1.0 g, 8.06 mmol, 1.0 equiv) was dissolved in acetic anhydride (3.8 mL, 40.3 mmol, 5.0 equiv) and pyridine (3.26 mL, 40.3, 5.0 equiv) and the reaction mixture was left to stir at RT for 16 h. Water (5 mL) was added and the biphasic mixture was extracted with EtOAc (3 × 10 mL). The combined organic layers were dried ($MgSO_4$) and concentrated *in vacuo* to afford the title compound as a colourless solid without the need for further purification (1.22 g, 91%); $\mathbf{R_f}$ 0.44 (petroleum ether / Et_2O (1:1)); **^{1}H NMR** (400 MHz, $CDCl_3$) δ_H 2.29 (3H, s, COC*H*$_3$), 3.81 (3H, s, OC*H*$_3$), 6.90 (2H, dt, *J* 9.0, 2.5), 7.01 (2H, dt, *J* 9.0, 2.5).

The spectroscopic data was found to be in agreement with that reported by Zhang and co-workers.[217]

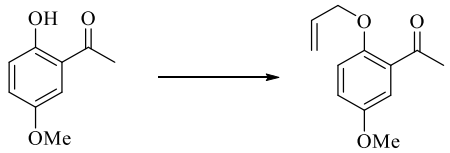
1-(2-Hydroxy-5-methoxyphenyl)ethanone (214)



1,4 Dimethoxybenzene (250 g, 1.81 mmol, 1.0 equiv) and boron trifluoride acetic acid complex (880 μL, 6.33 mmol, 3.5 equiv) were heated together in a sealed vial at 100 °C for 2 h. After cooling to RT, the reaction mixture was transferred to a 1N HCl/ice bath (20 mL) and a yellow precipitate formed. The aqueous solution was extracted with ethyl acetate (3 × 10 mL) and the combined organic layers were dried and concentrated *in vacuo* to afford a yellow oil. Purification by column chromatography (petroleum ether → petroleum ether / Et_2O (9:1)) afforded the title compound (130 mg, 43%); $\mathbf{R_f}$ 0.19 (petroleum ether / EtOAc (9:1)); **^{1}H NMR** (200 MHz, $CDCl_3$) δ_H 2.63 (3H, s, COC*H*$_3$), 3.82 (3H, s, OC*H*$_3$), 6.94 (1H, d, *J* 9.0, Ar*H*), 7.13 (1H, dd, *J* 9.0, 3.0 Ar*H*), 7.18 (1H, d, *J* 3.0 Ar*H*), 11.9 (1H, s, PhO*H*);

The spectroscopic data was found to be in agreement with that reported by Shaw and co-workers.[218]

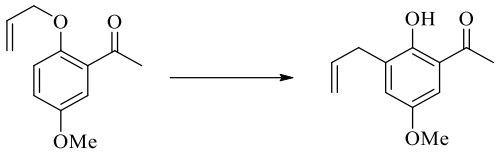
1-(2-(Allyloxy)-5-methoxyphenyl)ethanone (218)



Allyl bromide (2.30 mL, 26.8 mmol, 1.3 equiv) was added to a solution of phenol **214** (3.42 g, 20.6 mmol, 1.0 equiv) and K_2CO_3 (5.70 g, 41.2 mmol, 2.0 equiv) in dimethylformamide (24 mL). The reaction mixture was heated to 60 °C for 5 h after which it was cooled to RT and water added (200 mL). The mixture was then extracted with diethyl ether (3 × 100 mL) and the combined organic layers dried ($MgSO_4$) and concentrated *in vacuo* to afford a yellow oil. Purification by column chromatography (petroleum ether → petroleum ether / Et_2O (9:1)) afforded the title compound as a pale yellow oil which crystallised after two days to a pale yellow solid (3.35 g, 79%); $\mathbf{R_f}$ 0.15 (petroleum ether / EtOAc (9:1)); **^{1}H NMR** (500 MHz, $CDCl_3$) δ_H 2.65 (3H, s, COC*H*$_3$), 3.80 (3H, s, OC*H*$_3$), 4.60 (2H, dt, *J* 5.5, 1.5, OC*H*$_2$), 5.31 (1H, dq, *J* 10.5, 1.5, HC=C*H*H'), 5.43 (1H, dq, *J* 17.5, 1.5, HC=CH*H'*), 6.08 (1H, ddt, *J* 17.5, 10.5, 5.5, *H*C=CHH'), 6.91 (1H, d, *J* 9.0, Ar*H*), 7.01 (1H, dd, *J* 9.0, 3.0, Ar*H*), 7.29 (1H, d, *J* 3.0, Ar*H*); **^{13}C NMR** (125 MHz, $CDCl_3$) δ_C 32.0, 55.8, 70.1, 113.6, 114.6, 118.0, 120.3, 128.8, 132.9, 152.4, 153.5, 199.5.

The spectroscopic data was found to be in agreement with that reported by Reddy and co-workers.[219]

1-(3-Allyl-2-hydroxy-5-methoxyphenyl)ethanone (215)

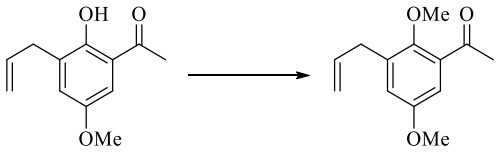


Allyl ether **218** (3.0 g, 14.6 mmol) was heated to 190 °C in a shlenk tube for 6 h. After cooling to RT the crude mixture was purified by column chromatography (petroleum ether → petroleum ether / Et_2O

(9:1)) to afford the title compound as a yellow/green oil (2.23 g, 74%) as well as starting material (650 mg, 22%) which could be resubmitted to the reaction; $\mathbf{R_f}$ 0.14 (petroleum ether / Et_2O (9:1)); **^{1}H NMR** (500 MHz, $CDCl_3$) δ_H 2.63 (3H, s, COC*H*$_3$), 3.42 (2H, d, *J* 6.5, ArC*H*$_2$), 3.80 (3H, s, OC*H*$_3$), 5.10 (2H, dt, *J* 9.5, 1.5, HC=C*H*H') overlays 5.11 (1H, dq, *J* 17.5, 1.5, HC=CH*H'*), 6.00 (1H, ddt, *J* 17.5, 9.5, 6.5, *H*C=CHH'), 7.02 (1H, d, *J* 3.0, Ar*H*), 7.06 (1H, d *J* 3.0, Ar*H*), 12.2 (1H, s, ArO*H*); **^{13}C NMR** (125 MHz, $CDCl_3$) δ_C 26.9, 33.5, 55.9, 111.1, 116.3, 118.7, 124.4, 130.7, 135.8, 151.2, 155.0, 204.2.

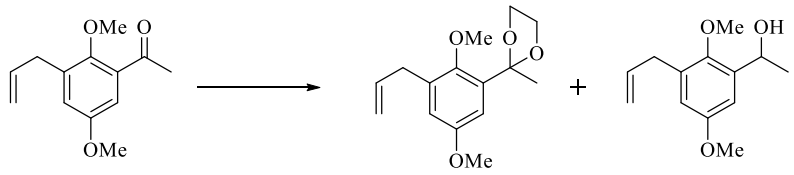
The spectroscopic data was found to be in agreement with that reported by Reddy and co-workers.[219]

1-(3-Allyl-2,5-dimethoxyphenyl)ethanone (219)



Iodomethane (2.40 mL, 38.8 mmol, 4.0 equiv) was added to a solution of phenol X (2.0 g, 9.70 mmol, 1.0 equiv) and K_2CO_3 (5.36 g, 38.8 mmol, 4.0 equiv) in acetone (40 ml) and the reaction mixture heated at reflux for 24 h. After cooling to RT, the crude mixture was diluted with cold acetone, the sediment removed by vacuum filtration and the filtrate concentrated *in vacuo*. Purification by column chromatography (petroleum ether → petroleum ether / Et_2O (95:5)) afforded dimethoxy phenol **219** as a colourless oil (1.59 g, 75%); $\mathbf{R_f}$ 0.15 (petroleum ether / Et_2O (95:5)); **IR** (thin film, ν_{max} / cm^{-1}) 3007w, 1633m, 1604m, 1462s, 1430m, 1325s, 1212s, 1050m, 985m; **^{1}H NMR** (400 MHz, $CDCl_3$) δ_H 2.65 (3H, s, COC*H*$_3$), 3.43 (2H, d, *J* 6.5, C*H*$_2$CH=CH$_2$), 3.71 (3H, s, OC*H*$_3$), 3.79 (3H, s, OC*H*$_3$), 5.08-5.15 (2H, m, CH=C*H*H' overlays CH=CH*H'*), 5.97 (1H, ddt, *J* 17.0, 10.5, 6.5, CH$_2$C*H*=CH$_2$), 6.90 (1H, d, *J* 3.0, Ar*H*), 6.98 (1H, d, *J* 3.0, Ar*H*); **^{13}C NMR** (100 MHz, $CDCl_3$) δ_C 30.4, 33.7, 55.6, 63.0, 111.3, 116.5, 120.6, 133.9, 135.4, 136.4, 151.3, 155.3, 200.9; **MS** (ES^+) 243.10 (MNa^+, 100%), 463.23 (M_2Na^+, 94%); **HRMS** (EI+) calc. for $C_{13}H_{16}NaO_3$ $[M+Na]^+$ 243.0992, found 243.0990.

2-(3-Allyl-2,5-dimethoxyphenyl)-2-methyl-1,3-dioxolane, and 1-(3-allyl-2,5-dimethoxyphenyl)ethanol (220 and 221)

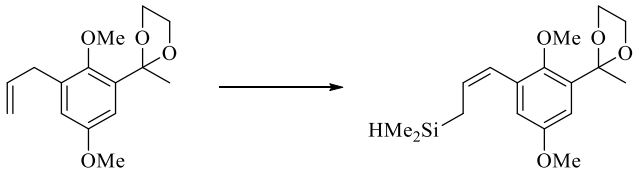


p-Toluenesulfonic acid (14 mg, 0.07 mmol, 0.01 equiv) was added to a solution of dimethoxy phenol **219** (1.59 g, 7.20 mmol, 1.0 equiv) and ethylene glycol (800 μL, 14.4 mmol, 2.0 equiv) in toluene (10 mL). The reaction mixture was heated at reflux with a Dean Stark apparatus for 18 h. After cooling to RT, the reaction mixture was diluted with diethyl ether (10 mL) and washed with 1M NaOH. The remaining organic phase was dried ($MgSO_4$) and concentrated *in vacuo* to afford a light yellow oil. The crude mixture was inseparable by column chromatography and was therefore treated with $NaBH_4$ to provide a separable mixture of ketal **220** and alcohol **221**.

$NaBH_4$ (130 mg, 3.44 mmol, 1.0 equiv) was added to the crude mixture of ketal **220** and ketone **219** (1.17 g, approximately 4.50 mmol (weighted MW), 1.0 equiv) in ethanol (2 ml) at 0 °C. The reaction mixture was stirred for 90 min at 0 °C before quenching with cold water (10 ml). The quenched solution was then extracted with ethyl acetate (3 × 10 ml) and the combined organic layers dried ($MgSO_4$) and concentrated *in vacuo* to afford a colourless oil which was purified by column chromatography (petroleum ether → petroleum ether / Et_2O (95:5)) to afford ketal **220** (804 mg, 77%) and alcohol **221** (49%, 10%); ketal **220**; $\mathbf{R_f}$ 0.21 (petroleum ether / EtOAc (9:1)); **IR** (thin film, ν_{max} / cm^{-1}) 2933br, 1739m, 1603w, 1468m, 1196s, 1110w, 1042s; **^{1}H NMR** (500 MHz, $CDCl_3$) δ_H 1.77 (3H, s, C(ketal)C*H*$_3$), 3.44 (2H, dt, *J* 6.5, 1.5, ArC*H*$_2$), 3.77 (3H, s, OC*H*$_3$), 3.78 (3H, s, OC*H*$_3$), 3.86 – 3.89 (2H, m, OC*H*H'C*H*H**'**O), 4.06 – 4.09 (2H, m, OCH*H'*CH*H'*O), 5.12 (1H, dq *J* 10.5, 1.5, HC=C*H*H') overlays 5.13 (1H, dq, *J* 16.5, 1.5, HC=CH*H'*), 5.98 (1H, ddt, *J* 16.5, 10.0, 6.5, *H*C=CHH'), 6.70 (1H, d, *J* 3.5, Ar*H*), 6.95 (1H, d, *J* 3.5, Ar*H*); **^{13}C NMR** (100 MHz, $CDCl_3$) δ_C 26.0, 34.0, 55.5, 62.4, 64.5 (2C), 108.6, 110.4, 115.3, 116.3, 135.4, 136.6, 136.9, 149.7, 155.1; **MS** (ES^+) 287.12 (MNa^+, 100%), 551.28 (M_2Na^+, 78%); **HRMS** (EI+) calc. for $C_{15}H_{20}NaO_4$ $[M+Na]^+$ 287.1254,

found 287.1250; **EA**. calc for $C_{13}H_{16}O_3$; C, 70.89; H, 7.32. Found C, 70.99; H, 7.20; alcohol **221**; $\mathbf{R_f}$ 0.08 (petroleum ether / EtOAc (9:1)); **IR** (thin film, ν_{max} / cm^{-1}) 3412be,2976w, 1604w, 1473s, 1429m, 1210m, 1052s, 1007s; **^{1}H NMR** (500 MHz, $CDCl_3$) δ_H 1.52 (3H, d, *J* 6.5, CHC*H*$_3$), 2.26 (1H, br s, O*H*), 3.41 (2H, dt *J* 6.5, 1.5, ArC*H*$_2$), 3.75 (3H, s, OC*H*$_3$), 3.79 (3H, s, OC*H*$_3$), 5.09 – 5.13 (2H, m, CH=C*H*H' overlays CH=CH*H'*), 5.20 (1H, qt, *J* 6.5, C*H*CH$_3$), 5.97 (1H, ddt, *J* 17.5, 9.5, 6.5, CH_2CH=CH_2), 6.67 (1H, d, *J* 3.0, Ar*H*), 6.86 (1H, d, *J* 3.0, Ar*H*); **^{13}C NMR** (125 MHz, $CDCl_3$) δ_C 23.9, 33.9, 55.5, 62.0, 65.1, 109.3, 114.7, 116.2, 134.0, 136.8, 139.3, 149.0, 156.1; **MS** (ES^+) 245.12 (MNa^+, 100%); **HRMS** (EI+) calc. for $C_{13}H_{18}NaO_3$ $[M+Na]^+$ 245.1148, found 245.1152;

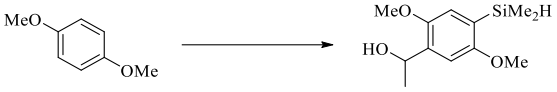
(*E*)-(3-(2,5-Dimethoxy-3-(2-methyl-1,3-dioxolan-2-yl)phenyl)prop-1-en-1-yl)dimethylsilane (222)



s-BuLi (945 μL of a 1.3 M solution in hexanes, 1.23 mmol, 1.3 equiv) was added to a solution of ketal **220** (250 mg, 0.95 mmol, 1.0 equiv) and TMEDA (185 μL, 1.23 mmol, 1.3 equiv) in THF (5 ml) at – 78 ^{o}C and the reaction mixture stirred at this temperature for 2 h. Dimethylchlorosilane (160 μL, 1.42 mmol, 1.5 equiv) was then added and the reaction mixture allowed to warm to room temperature overnight. The reaction was quenched with NH_4Cl (2 mL) and the crude mixture extracted with diethyl ether (3 x 5 mL). The combined organic layers were dried ($MgSO_4$) and concentrated *in vacuo* to afford a colourless oil which was purified by column chromatography (petroleum ether → petroleum ether / Et_2O (4:1)) to afford the title compound as a colourless oil (198 mg, 65%); $\mathbf{R_f}$ 0.19 (petroleum ether / EtOAc (4:1)); **IR** (thin film, ν_{max} / cm^{-1}) 2957w, 2114w, 1599w, 1463m, 1418m, 1197s, 1043s, 880s; **^{1}H NMR** (500 MHz, $CDCl_3$) δ_H 0.15 (6H, d, *J* 3.5, Si(C*H*$_3$)$_2$), 1.78 (3H, s, C(ketal)C*H*$_3$), 1.81 (2H, ddd, *J* 8.0, 3.0, 1.5, SiC*H*$_2$), 3.76 (3H, s, OC*H*$_3$), 3.80 (3H, s, OC*H*$_3$), 3.86 – 3.88 (2H, m, OC*H*H'C*H*H'O), 3.95 (1H, sep, *J* 3.5, Si*H*), 4.06 – 4.09 (2H, m, OCH*H'*CH*H'*O), 6.24 (1H, dt, *J* 16.0, 8.0, CH_2CH=CH), 6.53 (1H, d, *J*16.0, CH_2CH=C*H*), 6.91 (1H, d, *J* 3.0, Ar*H*), 6.94

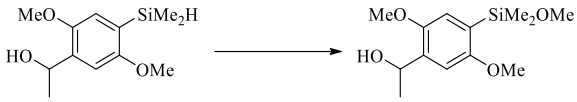
(1H, d, *J* 3.0, Ar*H*); **^{13}C NMR** (125 MHz, $CDCl_3$) δ_C –4.65, 21.5, 26.0, 55.5, 62.4, 64.5, 108.5, 110.7, 110.9, 123.6, 128.7, 133.7, 136.7, 148.7, 155.1; **MS** (ES^+) 345.16 (MNa^+, 72%), 667.13 (M_2Na^+, 100%); **HRMS** (EI+) calc. for $C_{17}H_{26}NaO_4Si$ $[M+Na]^+$ 345.1493, found 345.1480.

1-(4-(Dimethylsilyl)-2,5-dimethoxyphenyl)ethanol (226)



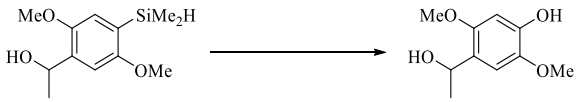
To a solution of 1,4 dimethoxybenzene (2.00 g, 14.5 mmol, 1.0 equiv) and TMEDA (2.6 mL, 17.4 mmol, 1.2 equiv) in anhydrous THF (50 mL) at –78 °C was added *s*-BuLi (13.4 mL of a 1.3 M solution in hexanes, 14.5 mmol, 1.2 equiv). The reaction mixture was stirred at –78 °C for 2 h before the addition of acetaldehyde (1.1 mL, 18.8 mmol, 1.3 equiv), after which the mixture was stirred at –78 °C for a further 40 min. TMEDA (2.81 mL, 18.8 mmol, 1.3 equiv) was added, followed quickly by *s*-BuLi (14.5 mL of a 1.3 M solution in hexanes, 18.8 mmol, 1.3 equiv) and the reaction mixture stirred at –78 °C for 4 h, before chlorodimethylsilane (2.10 mL, 18.8 mmol, 1.3 equiv) was added and the reaction allowed to warm to RT overnight. The reaction was quenched with sat. aq. NH_4Cl (20 mL), the biphasic mixture separated and the aqueous phase extracted with EtOAc (3 × 20 mL). The combined organic layers were dried ($MgSO_4$) and concentrated *in vacuo* to a yellow oil (1.46 g, 42%); **R_f** 0.19 (petroleum ether / Et_2O (9:1)); **IR** (thin film, ν_{max} / cm^{-1}) 2958w, 2840w, 2114m, 1376s, 1179s, 1043s, 889s; **^{1}H NMR** (400 MHz, $CDCl_3$) δ_H 0.34 (6H, d, *J* 3.5, Si(C*H*$_3$)$_2$), 1.51 (3H, d, *J* 6.5, CH(OH)C*H*$_3$), 2.59 –2.61 (1H, m, O*H*), 3.81 (3H, s, OC*H*$_3$), 3.85 (3H, s, OC*H*$_3$), 4.39 (1H, sept, *J* 3.5, Si*H*), 5.10 (1H, quintet, *J* 6.5, C*H*(OH)CH_3), 6.91 (1H, s, Ar*H*), 6.95 (1H, s, Ar*H*); **^{13}C NMR** (100 MHz, $CDCl_3$) δ_C –3.76, 23.2, 55.9, 56.0, 66.7, 108.3, 117.9, 124.6, 136.2, 150.2, 158.7; **HRMS** (ES^+) calc. For $C_{12}H_{20}NaO_3S$ $[M+Na]^+$ 263.1074, found 263.1072; **EA** calc. for $C_{12}H_{20}O_3Si$: C, 59.96; H, 8.39. Found: C, 59.84; H, 8.50.

1-(2,5-Dimethoxy-4-(methoxydimethylsilyl)phenyl)ethanol (226b)



Application of the general procedure above to hydrosilane **226** (200 mg, 0.83 mmol) afforded methoxysilane **226b** (233 mg, 99%); $\mathbf{R_f}$ 0.59 (petroleum ether / Et_2O (9:1)); **IR** (thin film, ν_{max} / cm^{-1}) 2957w, 2836w, 1462m, 1375s, 1203s, 1042m;; **^{1}H NMR** (400 MHz, $CDCl_3$) δ_H 0.37 (6H, s, Si(C*H*$_3$)$_2$), 1.50 (3H, d, *J* 6.5, CH(OH)C*H*$_3$), 2.68 (1H, d, *J* 5.0, O*H*), 3.53 (3H, s, Si(OC*H*$_3$)), 3.80 (3H, s, OC*H*$_3$), 3.86 (3H, s, OC*H*$_3$), 5.06-5.23(1H, m, C*H*(OH)CH_3), 6.92 (1H, s, Ar*H*), 7.00 (1H, s, Ar*H*); **^{13}C NMR** (100 MHz, $CDCl_3$) δ_C -1.60, -1.59, 23.2, 50.9. 55.8, 55.9, 66.6, 108.4, 117.2, 124.6, 136.4, 150.3, 158.5; **MS** (ES^+) 293.09 (MNa^+, 100%); **HRMS** (EI+) calc. for $C_{13}H_{22}NaO_4Si$ $[M+Na]^+$ 293.1180, found 293.1185.

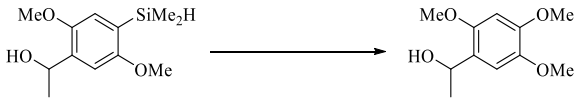
4-(1-Hydroxyethyl)-2,5-dimethoxyphenol (227)



Application of the fluoride promoted general procedure **IV** to methoxysilane **226b** (200 mg, 0.74 mmol) afforded a yellow oil. Purification by column chromatography (petroleum ether → petroleum ether / EtOAc (1:1)) afforded the title compound as a yellow waxy solid (108 mg, 74%); $\mathbf{R_f}$ 0.12 (petroleum ether / EtOAc (4:1)); **IR** (thin film, ν_{max} / cm^{-1}) 3411br, 2968w, 1509s, 1298m, 1204s, 833m; **^{1}H NMR** (400 MHz, $CDCl_3$) δ_H 1.48 (3H, d, *J* 6.5, CH(OH)C*H*$_3$), 2.51 (1H, d, *J* 6.5, $CH(CH_3)$O*H*), 3.80 (3H, s, OC*H*$_3$), 3.86 (3H, s, OC*H*$_3$), 5.02-5.13 (1H, m, C*H*(OH)CH_3), 5.68 (1H, br s, ArO*H*), 6.56 (1H, s, Ar*H*), 6.91 (1H, s, Ar*H*); **HRMS** (EI+) calc. for $C_{10}H_{14}NaO_4$ $[M+Na]^+$ 221.0784, found 221.0782.

The product decomposed before further characterisation was possible.

1-(2,4,5-Trimethoxyphenyl)ethanol (224)



Application of the general procedure above to hydrosilane **226**, without purification afforded a crude product which was dissolved in MeCN (2 mL). K_2CO_3 (276 mg, 2.0 mmol, 4.0 equiv), KI (10 mg, catalytic) and iodomethane (31 μL, 0.5 mmol, 1.0 equiv) were added and the reaction heated to 80 °C for 2 h, before being stirred at rt overnight. The reaction mixture was concentrate *in vacuo* before dilution with EtOAc (15 mL). The solution was washed with water, dried ($MgSO_4$) and concentrated to a yellow oil which was purified by column chromatography (20 – 50% EtOAc) to afford a colourless oil (69 mg, 65%); $\mathbf{R_f}$ 0.31 (petroleum ether / EtOAc (9:1)); **^{1}H NMR** (200 MHz, $CDCl_3$) δ_H 1.52 (3H, d, *J* 6.5, C(OH)C*H*$_3$), 3.88 (3H, s, OC*H*$_3$), 3.89 (3H, s, OC*H*$_3$), 3.93 (3H, s, OC*H*$_3$), 5.13 (1H, C*H*(OH)), 6.56 (1H, s, Ar*H*), 6.98 (1H, s, Ar*H*);

The spectroscopic data was found to be in agreement with that reported by Sharma and co-workers.[220]

1,2,4-Trimethoxy-5-(1-methoxyethyl)benzene (223)

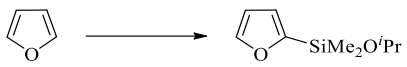


To a vial containing 1-(4-(dimethylsilyl)-2,5-dimethoxyphenyl)ethanol (120 mg, 0.500 mmol, 1.0 equiv) was added MeOH (200 μL). The vial was purged with argon before the addition of Pd/C (2.6 mg, 10 wt.% loading, 0.0025 mmol, 5 mol%). After 2/3 seconds of effervescence the reaction was seen to be complete by TLC. The resulting solution was filtered through a celite plug, eluted with Et_2O, and concentrated *in vacuo*. To this crude product was added MeOH/THF (1.5 mL), $KHCO_3$ (25 mg, 0.250 mmol, 0.5 equiv), TBAF (50 μL of a 1 M solution in THF, 0.050 mmol, 0.10 equiv) and H_2O_2 (340 μL of a 30% w/w solution, 3.00 mmol, 6.0 equiv) and the reaction mixture stirred for 3h. Upon completion, the reaction was quenched with $Na_2S_2O_3$ (1 mL, sat., aq.) and the monophasic mixture stirred for a further 5 min. The reaction mixture was then extracted with EtOAc (3 x 5 mL). The combined organic phases were dried ($MgSO_4$) and concentrated *in vacuo* to afford a crude

phenolic product which was immediately dissolved in anhydrous THF (5 mL) and cooled to 0 °C. NaH (80 mg, 2.00 mmol, 4 equiv) was added and the reaction stirred at 0 °C for 1 h before the addition of iodomethane (186 μL, 3.00 mmol, 6.0 equiv). After stirring overnight, the reaction was quenched with MeOH (1 mL) and concentrated *in vacuo*. The concentrate was dissolved in EtOAc (5 mL) and washed with water (3 x 5 mL). The organic phase was dried ($MgSO_4$) and concentrated *in vacuo* to afford a yellow oil which was purified by column chromatography (petroleum ether → petroleum ether / Et_2O (9:1)) to afford the title compound as a colourless oil (45 mg, 40%); **R_f** 0.19 (petroleum ether / Et_2O (9:1)); **^{1}H NMR** (400 MHz, $CDCl_3$) δ_H 1.38 (3H, d, *J* 6.5, CH(OMe)C*H*$_3$), 3.25 (3H, s, CH(OC*H*$_3$)CH$_3$), 3.81 (3H, s, ArOC*H*$_3$), 3.86 (3H, s, ArOC*H*$_3$), 3.90 (3H, s, ArOC*H*$_3$), 4.72 (1H, q, *J* 6.5, ArC*H*(OMe)CH$_3$), 6.52 (1H, s, Ar*H*), 6.93 (1H, s, Ar*H*); **^{13}C NMR** (100 MHz, $CDCl_3$) δ_C 22.7, 56.1, 56.4, 56.5, 56.5, 72.7, 97.5, 109.5, 123.3, 143.5, 148.4, 150.8.

The spectroscopic data was found to be in agreement with that reported by Mathouet and co-workers.[134]

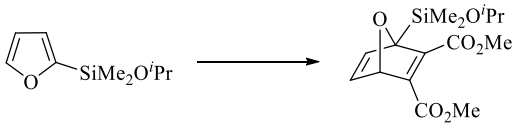
Furan-2-yl(isopropoxy)dimethylsilane (232)



The procedure was developed from literature precedent[221]; To a solution of furan (1.00 g, 14.5 mmol, 1.0 equiv) in dry THF (70 ml), was added *n*-BuLi (8.15 mL, 20.3 mmol of a 2.5 M solution in THF, 1.4 equiv) at 0 °C and the reaction mixture stirred at 0 °C for 90 min. To this solution was added $ClSiMe_2NEt_2$ **4** (4.35 mL, 21.8 mmol, 1.5 equiv) at 0 °C and the reaction mixture stirred for 90 min at RT after which IPA (15 mL) and DMAP (crystal) were added and the reaction mixture left stirring at RT overnight. The crude mixture was concentrated *in vacuo* to an orange oil which was purified by a silica plug (petroleum ether) to afford the title compound as a yellow oil (2.04 g, 76%); **R_f** 0.36 (petroleum ether / Et_2O 7:3)); **IR** (thin film, ν_{max} / cm^{-1}) 3445br, 2972s, 1739s, 1660s, 1511m, 1259s, 1030s; **^{1}H NMR** (400 MHz, $CDCl_3$) δ_H) 0.38 (6H, s, Si(C*H*$_3$)$_2$), 1.13 (6H, d, *J* 6.0, CH(C*H*$_3$)$_2$), 4.03 (1H, sept, *J* 6.0, CH(C*H*$_3$)$_2$), 6.40 (1H, dd, *J* 3.0, 1.5, Fu*H*), 6.74 (1H, d, *J* 3.0, Fu*H*), 7.67 (1H, d, *J*

1.5, Fu*H*); **^{13}C NMR** (125 MHz, $CDCl_3$) δ_C -1.57, 25.4, 30.9 65.7, 109.3, 120.6, 146.7. **HRMS** (EI+) not found.

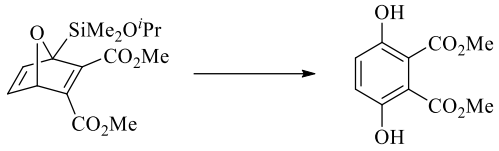
Dimethyl 1-(isopropoxydimethylsilyl)-7-oxabicyclo[2.2.1]hepta-2,5-diene-2,3-dicarboxylate (233)



Method A; 2-silyl furan (250 mg, 1.36 mmol, 1.0 equiv) and dimethylacetylene-dicarboxylate (220 μL, 1.76 mmol, 1.3 equiv) were dissolved in toluene (1.5 mL). The reaction mixture was heated at reflux for 16 h and concentrated *in vacuo* to a brown oil which was purified by column chromatography (petroleum ether → petroleum ether / EtOAc (9:1)) to afford the title compound as a yellow oil (205 mg, 46%);

Method B; 2-silyl furan (100 mg, 0.34 mmol, 1.0 equiv) and dimethylacetylene-dicarboxylate (90 μL, 0.51 mmol, 1.5 equiv) were dissolved in toluene (0.5 mL). The reaction mixture was heated under microwave irradiation at 125 °C for 3 hours and concentrated *in vacuo* to a brown oil which was purified by column chromatography (petroleum ether → petroleum ether / EtOAc (9:1)) to afford the title compound as a yellow oil (67 mg, 63%); **R_f** 0.35 (petroleum ether / EtOAc (9:1)); **IR** (thin film, ν_{max} / cm^{-1}) 2971m, 1716s, 1436w, 1255m, 1034m, 933w; **^{1}H NMR** (400 MHz, $CDCl_3$) δ_H 0.29 (3H, s, SiC*H*$_3$CH'$_3$), 0.33 (3H, s, SiCH$_3$C*H'*$_3$), 1.15 (6H, d, *J* 6.0, CH(C*H*$_3$)$_2$), 3.77 (3H, s, CO_2CH_3), 3.82 (3H, s, CO_2CH_3), 4.11 (1H, sept, *J* 6.0, C*H*(CH$_3$)$_2$), 5.74 (1H, s, C_{bh}-*H*), 7.22 (2H, s, C*H*=C*H*); **^{13}C NMR** (100 MHz, $CDCl_3$) δ_C –2.59, –2.33, 25.5, 52.1, 66.0, 85.5, 91.7, 143.2, 146.3, 149.7, 159.9, 163.1, 165.7; **MS** (ES^+) 349.10 (MNa^+, 85%), 675. 19 (M_2Na^+, 100%); **HRMS** (EI+) calc. for $C_{15}H_{22}NaO_6Si$ $[M+Na]^+$ 349.1078, found 349.1078.

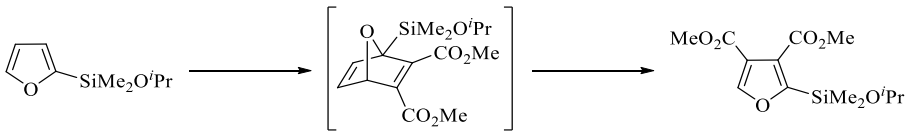
Dimethyl 3,6-dihydroxyphthalate (234)



To a stirred solution of cycloadduct **233** (90 mg, 0.28 mmol, 1.0 equiv) in MeOH/THF (1:1, 2 mL) was added $KHCO_3$ (55 mg, 0.55 mmol, 2.0 equiv), TBAF (28 μL, of a 1 M solution in THF, 0.03 mmol, 0.1 equiv) and H_2O_2 (170 μL, 35% w/w, 1.65 mmol, 6.0 equiv) before stirring for 5h at RT. The reaction was quenched with HCl (1N aq solution, 1 mL) the biphasic mixture separated and the aqueous layer extracted with EtOAc (3 × 2 mL). The combined organic layers were dried ($MgSO_4$) and concentrated *in vacuo* to afford the title compound as a yellow oil which was purified by column chromatography (petroleum ether → petroleum ether / EtOAc (3:2)) to afford a white solid (45 mg, 71%); $\mathbf{R_f}$ 0.22 (petroleum ether / EtOAc (9:1)); **^{1}H NMR** (400 MHz, $CDCl_3$) δ_H 3.91 (6H, s, CO_2CH_3), 7.10 (2H, s, Ar*H*), 8.81 (2H, s, O*H*); **^{13}C NMR** (100 MHz, $CDCl_3$) δ_C 52.7, 124.1, 152.4, 154.4, 169.39.

The spectroscopic data was found to be in agreement with that reported by Kelly and co-workers.[222]

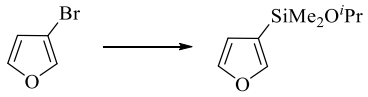
Dimethyl 2-(isopropoxydimethylsilyl)furan-3,4-dicarboxylate (233RDAP)



2-Silyl furan **232** (100 mg, 0.34 mmol, 1.0 equiv) and dimethylacetylene-dicarboxylate (90 μL, 0.51 mmol, 1.5 equiv) were dissolved in toluene (0.5 mL). The reaction mixture was heated under microwave irradiation at 125 °C for 5 h and concentrated *in vacuo* to a brown oil which was purified by column chromatography (petroleum ether → petroleum ether / EtOAc (9:1)) to afford the title compound as a yellow oil (39 mg, 38%); $\mathbf{R_f}$ 0.60 (petroleum ether / EtOAc (9:1)); **IR** (thin film, ν_{max} / cm^{-1}) 3359br, 2900s, 1715m, 1669s, 1310s, 1008s; **^{1}H NMR** (500 MHz, $CDCl_3$) δ_H 0.42 (6H, s, $Si(CH_3)_2$), 1.14 (6H, d, *J* 6.0, $CH(CH_3)_2$), 3.84 (3H, s, CO_2CH_3), 3.88 (3H, s, CO_2CH_3), 4.06 (1H, sept, *J* 6.0, $CH(CH_3)_2$), 8.09 (1H, s, Fu*H*); **^{13}C NMR** (125 MHz, $CDCl_3$) δ_C –1.36, 25.4, 51.9, 52.0,

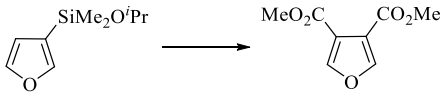
66.1, 118.4, 127.4, 151.2, 162.5, 164.0, 164.1; **MS** (ES^+) 323.08 (MNa^+, 82%), 623.14 (M_2Na^+, 100%); **HRMS** (EI+) calc. for $C_{13}H_{20}NaO_6$ $[M+Na]^+$ 323.0921, found 323.0926.

Furan-3-yl(isopropoxy)dimethylsilane (235)



This procedure was adapted from that reported by Morita *et al*[223]; 3-Bromo furan (250 mg, 1.71, 1.0 equiv) was added over 15 min to a solution of *n*-BuLi (750 μL, 1.88 mmol, 2.5 M solution in THF, 1.1 equiv) in Et_20 (14 mL) at −78 °C. The reaction was stirred for 15 min before the addition of amino silane **72** at −78 °C. The reaction was stirred for 30 min, after which *i*-PrOH (0.7 mL) and DMAP (cryst) were added. After stirring overnight at RT, the reaction was quenched with water (10 mL) and extracted with DCM (3 × 10 mL). The combined organic layers were dried ($MgSO_4$) and concentrated *in vacuo* to give a yellow oil which was purified by column chromatography (petroleum ether → petroleum ether / EtOAc (3:2)) to afford the title compound as a yellow oil (102 mg, 0.55 mmol, 32%); $\mathbf{R_f}$ 0.18 (petroleum ether / EtOAc (3:3)); **^{1}H NMR** (400 MHz, $CDCl_3$) δ_H .38 (6H, s, SiC*H*$_3$), 1.20 (6H, d, *J* 6.0, OCH(C*H*$_3$)$_2$), 4.20 (1H, sept, *J* 6.0, OC*H*$(CH_3)_2$),6.49 (1H, d, *J* 5.0, Fu*H*), 7.50 (1H, d, *J* 5.0, Fu*H*), 7.55 – 7.58 (1H, m, Fu*H*).

Dimethyl furan-3,4-dicarboxylate (236RDAP)

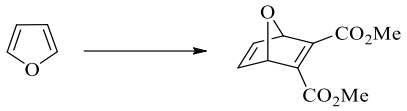


3-Silyl furan **235** (35 mg, 0.27 mmol, 1.0 equiv) and dimethylacetylene-dicarboxylate (35 μL, 0.41 mmol, 1.5 equiv) were dissolved in toluene (175 μL). The reaction mixture was heated under microwave irradiation at 125 °C for 3 h and concentrated *in vacuo* to a brown oil which was purified by column chromatography (petroleum ether → petroleum ether / EtOAc (9:1)) to afford the title compound as a yellow oil (29 mg, 60%); $\mathbf{R_f}$ 0.14 (petroleum ether / EtOAc (9:1)); **^{1}H NMR** (400

MHz, $CDCl_3$) δ_H 3.88 (6H, s, CO_2CH_3), 7.96 (2H, s, Fu*H*); **^{13}C NMR** (125 MHz, $CDCl_3$) 52.0, 148.8, 162.7, 186.8.

The spectroscopic data was found to be in agreement with that reported by Natu and co-workers.[224]

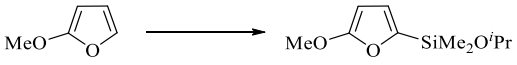
Dimethyl 7-oxabicyclo[2.2.1]hepta-2,5-diene-2,3-dicarboxylate (238)



Furan (100 mg, 1.47 mmol, 1.0 equiv) and dimethylacetylene-dicarboxylate (210 μL, 1.47 mmol, 1.0 equiv) were dissolved in toluene (0.5 mL). The reaction mixture was heated under microwave irradiation at 125 °C for 3 h and concentrated *in vacuo* to a brown oil which was purified by column chromatography (petroleum ether → petroleum ether / EtOAc (3:2)) to afford furan **238** as a yellow oil (40 mg, 21%); **R_f** 0.21 (petroleum ether / EtOAc (3:2)); **^{1}H NMR** (400 MHz, $CDCl_3$) δ_H 3.83 (6H, s, CO_2CH_3), 5.69 (2H, s, $_{bh}H$), 7.23 (2H, s, *H*C=C*H*); **^{13}C NMR** (100 MHz, $CDCl_3$) δ_C 52.4, 85.0, 143.3, 153.0, 163.2.

The spectroscopic data was found to be in agreement with that reported by Casida and co-workers.[225]

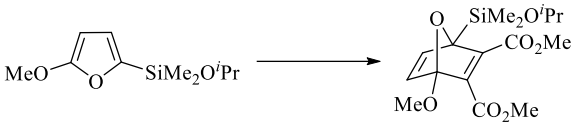
Isopropoxy(5-methoxyfuran-2-yl)dimethylsilane (239)



The procedure was developed from literature precedent;[226] To a stirred solution of 2-methoxy furan (500 mg, 5.10 mmol, 1.0 equiv), in THF (35 mL) at −20 °C was added *n*-BuLi (2.90 mL, 2.5 M solution in THF, 7.14 mmol, 1.4 equiv) dropwise and the reaction mixture stirred for 2 h. $ClSiMe_2NEt_2$ **72** (1.5 mL, 7.65 mmol, 1.5 equiv) was added to the reaction at −20 °C and the reaction allowed to warm to RT. After being stirred for 1 h, ^{i}PrOH (2.5 mL) and DMAP (crystal) were added before stirring overnight. The reaction mixture was concentrated *in vacuo,* and the resulting crude mixture was purified by flash column chromatography (petroleum ether) to afford the title compound as a yellow oil (1.05 g, 96%); **R_f** 0.53 (petroleum ether / EtOAc (3:2)); **IR** (thin film, ν_{max} / cm^{-1})

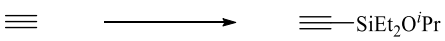
3445br, 2972s, 1739s, 1660s, 1511m, 1259s, 1030s; **^{1}H NMR** (400 MHz, $CDCl_3$) δ_H 0.33 (6H, s, Si(C*H*$_3$)$_2$), 1.14 (6H, d, *J* 6.0, OCH(C*H*$_3$)$_2$), 3.87 (3H, s, OC*H*$_3$), 4.04 (1H, sept, *J* 6.0, OCH(C*H*$_3$)$_2$), 5.16 (1H, d, *J* 3.0, Fu*H*), 6.63 (1H, d, *J* 3.0, Fu*H*); **^{13}C NMR** (100 MHz, $CDCl_3$) δ_C −1.74, 25.5, 57.7, 65.5, 79.6, 123.1, 148.4, 165.5; **MS** (ES^+) 237.10 (MNa^+, 82%); **HRMS** (EI+) calc. for $C_{10}H_{18}NaO_3Si$ $[M+Na]^+$ 237.0917, found 237.0918.

Dimethyl 1-(isopropoxydimethylsilyl)-4-methoxy-7-oxabicyclo[2.2.1]hepta-2,5-diene-2,3-dicarboxylate (240)



Methoxyfuran **239** (50 mg, 0.253 mmol 1.0 equiv), and dimethylacetylene-dicarboxylate (37 μL, 0.30 mmol, 1.3 equiv) were dissolved in toluene (0.25 mL). The reaction mixture was heated at reflux for 16 h, concentrated *in vacuo* and the resulting crude mixture was subjected to column chromatography (petroleum ether → petroleum ether / EtOAc (85:15)) to afford the title compound as a colourless oil (13 mg, 14%); **R$_f$** 0.18 (petroleum ether / EtOAc (3:2)); **^{1}H NMR** (200 MHz, $CDCl_3$) δ_H 0.34 (6H, s, Si(C*H*$_3$)$_2$), 1.15 (6H, d, *J* 6.0, OCH(C*H*$_3$)$_2$), 3.59 (3H, s, OC*H*$_3$), 3.78 (3H, s, CO_2C*H*$_3$), 3.83 (3H, s, CO_2C*H*$_3$), 4.15 (1H, sep, *J* 6.0, OC*H*$(CH_3)_2$), 7.00 (1H, d, *J* 5.0, HC=C*H*), 7.24 (1H, d, *J* 5.0, *H*C=CH); The compound decomposed before further NMR experiments were carried out; **MS** (ES^+) 379.12 (MNa^+, 100%); **HRMS** (EI+) calc. for $C_{16}H_{24}NaO_7Si$ $[M+Na]^+$ 379.1184, found 379.1182.

Diethyl(ethynyl)(isopropoxy)silane (241)

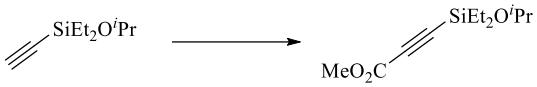


To a flask containing 1-chloro-*N*,*N*,1,1-tetraethylsilanamine (1.70 g, 8.69 mmol, 1.0 equiv) at −78 °C was added ethynylmagnesium bromide (19.5 mL, 0.5 M solution in THF, 9.6 mmol, 1.1 equiv) via cannular. The reaction was warmed to RT over 30 min and then heated at reflux for 2.5 h. After cooling to RT, *i*-PrOH (1.5 mL, 17.5 mmol, 2.0 equiv) and DMAP (crystal) were added and the

reaction mixture stirred overnight. The crude mixture was concentrated *in vacuo* and diluted in petrol before running through a celite plug. The following solution was concentrated *in vacuo* and purified by vacuum distillation (54 – 58 °C, 20 mbar) to afford the title compound as a colourless oil (590 mg, 85% pure, 33%); **^{1}H NMR** (500 MHz, $CDCl_3$) δ_H 0.68 (4H, q, *J* 7.5, Si(C*H*$_2$CH$_3$)$_2$), 1.02 (6H, t, *J* 7.5, Si(CH$_2$C*H*$_3$)$_2$), 1.21 (6H, d, *J* 6.0, OCH(C*H*$_3$)$_2$), 2.42 (1H, s, alkyne*H*), 4.18 (1H, sep, *J* 6.0, OC*H*(CH$_3$)$_2$);

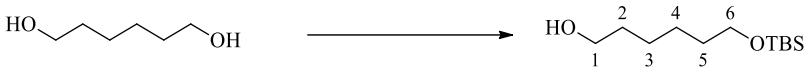
The spectroscopic data was found to be in agreement with that reported earlier within the group.[227]

Methyl 3-(diethyl(isopropoxy)silyl)propiolate procedure (242)



The procedure was adapted from literature precedent;[228] To a solution of silylacetylene (250 mg, 85% purity, 1.23 mmol, 1.0 equiv) in dry THF (3 mL), *n*-BuLi (540 μL of 1.3 M solution in hexane, 1.36 mmol, 1.1 equiv) was added dropwise at −78 °C. After stirring for 30 mins at −78 °C methyl chlorocarbonate (105 μL, 1.36 mmol, 1.1 equiv) was added and the reaction allowed to warm to RT and stirred for another 2.5 h. The mixture was poured into sat. aq. NH_4Cl (5 mL) to quench the reaction and the resulting mixture was extracted with diethyl ether (3 × 5 mL). The combined organic layers were washed with brine (3 × 10 mL), dried ($MgSO_4$) and concentrated *in vacuo* to a dark brown oil which was purified by column chromatography (petroleum ether → petroleum ether / EtOAc (95:5)) to afford the title compound as a colourless oil (230 mg, 82%); **R_f** 0.59 (petroleum ether / EtOAc (9:1)); **IR** (thin film, ν_{max} / cm^{-1}) 2962s, 2879s, 2177w, 1774m, 1720s, 1461m, 1382m, 1236s, 1035s; **^{1}H NMR** (500 MHz, $CDCl_3$) δ_H 0.74 (4H, q, *J* 8.0, Si(C*H*$_2$CH$_3$)$_2$), 1.03 (6H, t, *J* 8.0, Si(CH$_2$C*H*$_3$)$_2$), 1.21 (6H, d, *J* 6.0, OCH(C*H*$_3$)$_2$), 3.79 (3H, s, CO$_2$C*H*$_3$), 4.17 (1H, sep, *J* 6.0, OC*H*(CH$_3$)$_2$); **^{13}C NMR** (100 MHz, $CDCl_3$) δ_C 6.3 (4C), 25.4, 52.7, 66.8, 90.5, 94.5, 153.3; **MS** (ES$^+$) 251.14 (MNa$^+$, 19%).

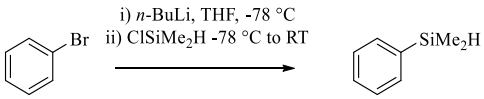
6-((*tert*-Butyldimethylsilyl)oxy)hexan-1-ol (247)



To a suspension of NaH (3.06 g, 76.2 mmol, 1.0 equiv) in THF (90 mL) at RT was added hexane-1,6-diol (9.0 g, 76.16 mmol, 1.0 equiv). The reaction was stirred at RT for 45 min after which TBDMSCl (11.5 g, 76.2 mmol, 1.0 equiv) was added and the reaction was stirred for a further 45 min at RT at which point the reaction was found to be complete by TLC analysis. The reaction mixture was diluted with diethyl ether (50 mL) and washed with K_2CO_3 (2 × 50 mL, 10% aq solution) and brine (2 × 50 mL). The organic phase was dried ($MgSO_4$) and concentrated *in vacuo* to afford a crude yellow oil which was purified by column chromatography (petroleum ether) to afford the title compound as a colourless oil (5.25 g, 30%); $\mathbf{R_f}$ 0.23 (petroleum ether); **^{1}H NMR** (400 MHz, $CDCl_3$) δ_H 0.05 (6H, s, Si(C*H*$_3$)$_2$), 0.90 (9H, s, SiC(C*H*$_3$)$_3$), 1.31-1.43 (4H, m, C(3)*H*$_2$ and C(4)*H*$_2$), 1.50-1.62 (4H, m, C(2)*H*$_2$ and C(5)*H*$_2$)), 3.63 (4H, ap q, *J* 7.0, C(1)*H*$_2$ and C(6)*H*$_2$); **^{13}C NMR** (100 MHz, $CDCl_3$) δ_C –5.28, 18.4, 25.5, 25.6, 26.0, 32.76, 32.77, 63.0, 63.2.

The spectroscopic data was found to be in agreement with that reported by Harrison and co-workers.[229]

Dimethyl(phenyl)silane (249)

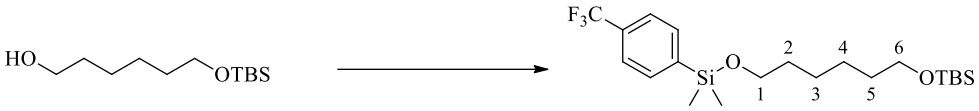


According to the general procedure **I**, 8.4 mL (21.0 mmol, 1.1 equiv) of *n*-BuLi was added to 3.0 g (19.1 mmol, 1.0 equiv) of 1,4-dibromobenzene in anhydrous THF (75 mL). The resulting mixture was stirred for 2 h at –78 °C before 2.33 mL (21.0 mmol, 1.1 equiv) of chlorodimethylsilane was added and the reaction stirred overnight. The product was purified by vacuum distillation (85-87 °C at 100 mbar) to afford the title compound as a colourless oil (1.73 g, 67%); **^{1}H NMR** (400 MHz,

$CDCl_3$) δ_H 0.38 (6H, d, *J* 3.5, Si(C*H*$_3$)$_2$), 4.46 (1H, sept, *J* 3.5, Si*H*), 7.37-7.41 (3H, m, Ar*H*), 7.56-7.59 (2H, m, Ar*H*); **^{13}C NMR** (100 MHz, $CDCl_3$) δ_C) –3.87, 127.9, 129.2, 134.0, 137.5.

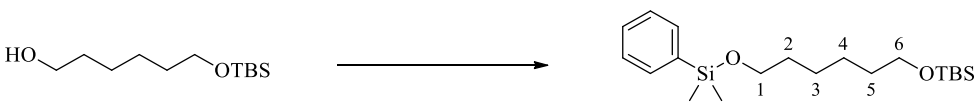
The spectroscopic data was found to be in agreement with that reported by Ishikawa and co-workers.[230]

1-(((4-Trifluoromethyl)phenyl)dimethylsilyloxy)-6-(tert-butyldimethylsilyloxy)hexane (251)



Pd/C (5.7 mg, 0.00538 mmol, 5 mol%) was added to a mixture of alcohol **247** (250 mg, 1.08 mmol, 1.0 equiv) and arylhydrosilane **96** (220 mg, 1.08 mmol, 1.0 equiv). After effervescence had subsided (10 min) the reaction was found to be complete by TLC. The reaction mixture was filtered through Celite® to afford silyl ether **251** as a colourless oil without the need for further purification (421 mg, 90%); **R$_f$** 0.73 (petroleum ether); **IR** (thin film, ν_{max} / cm^{-1}) 2932w, 2589w, 1391s, 1325m, 1165m, 1060s, 826s; **^{1}H NMR** (500 MHz, $CDCl_3$) δ_H 0.05 (6H, s, Si(C*H*$_3$)$_2$), 0.40 (6H, s, Si(C*H*$_3$)$_2$), 0.90 (9H, s, SiC(C*H*$_3$)$_3$), 1.28-1.35 (4H, m, C(3)*H*$_2$ and C(4)*H*$_2$), 1.47-1.60 (4H, m, C(2)*H*$_2$ and C(5)*H*$_2$)), 3.60 (4H, ap q, *J* 6.5, C(1)*H*$_2$ and C(6)*H*$_2$), 7.64 (2H, d, *J* 8.0, Ar*H*), 7.69 (2H, d, *J* 8.0, Ar*H*); **^{13}C NMR** (125 MHz, $CDCl_3$) δ_C –5.24, –1.78, 18.4, 25.6, 26.0, 32.6, 32.8, 63.2, 63.3, 124.2 (q, *J* 273.5), 124.4 (q, *J* 4.0), 131.4 (q, *J* 31.5), 133.8, 143.1; **HRMS** (ES$^+$) calc. for $C_{21}H_{38}F_3O_2Si_2$ [M]$^+$ 435.2357, found 435.2359.

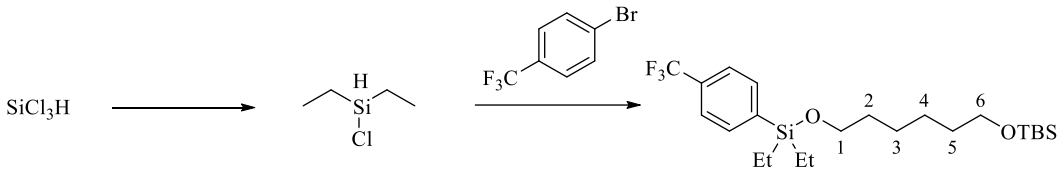
1-((Phenyl)dimethylsilyloxy)-6-(tert-butyldimethylsilyloxy)hexane (252)



Pd/C (5.7 mg, 0.00538 mmol, 5 mol%) was added to a mixture of alcohol **247** (250 mg, 1.08 mmol, 1.0 equiv) and arylhydrosilane **249** (147 mg, 1.08 mmol, 1.0 equiv). After effervescence had

subsided (10 min) the reaction was found to be complete by TLC. The reaction mixture was filtered through Celite® to afford silyl ether **252** as a colourless oil without the need for further purification (390 mg, 97%); $\mathbf{R_f}$ 0.79 (petroleum ether) **IR** (thin film, ν_{max} / cm^{-1}) 2930w, 2858w, 1471.8, 1252m, 1092s, 830s, 775s; **^{1}H NMR** (500 MHz, $CDCl_3$) δ_H 0.06 (6H, s, Si(C*H*$_3$)$_2$), 0.39 (6H, s, Si(C*H*$_3$)$_2$), 0.91 (9H, s, SiC(C*H*$_3$)$_3$), 1.31-1.41 (4H, m, C(3)*H*$_2$ and C(4)*H*$_2$), 1.48-1.61 (4H, m, C(2)*H*$_2$ and C(5)*H*$_2$)), 3.60 (4H, t, *J* 6.5, C(1)*H*$_2$ and C(6)*H*$_2$), 7.34-7.42 (3H, m, Ar*H*), 7.55-7.63 (2H, m, Ar*H*); **^{13}C NMR** (125 MHz, $CDCl_3$) δ_C –5.26, –1.78, 18.4, 25.6, 26.0, 32.6, 32.8, 63.1, 63.2, 127.8, 129.5, 133.1, 133.5, 138.4; **HRMS** (ES^+) calc. for $C_{20}H_{38}NaO_2Si_2$ $[MNa]^+$ 389.2303, found 389.2289.

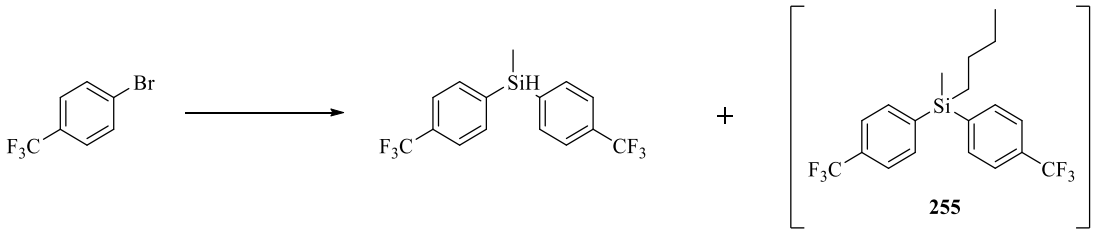
Chlorodiethylsilane (253)



To a solution of trichlorosilane (3.03 mL, 30 mmol, 1.0 equiv) in THF (20 mL) contained within a water bath at RT was added ethylmagnesium bromide (20 mL, 60 mmol, 2.0 equiv). The reaction was stirred at RT for 16 h, following which, dry pentane was added to the reaction mixture and the reaction concentrated *in vacuo*. The crude mixture was subsequently diluted with dry pentane and filtered through a plug of Celite®. The filtrate was concentrated *in vacuo* and purified by atmospheric distillation (99 °C) to afford diethylchlorosilane (708 mg, 19%) contaminated with triethylsilane; **^{1}H NMR** (400 MHz, $CDCl_3$) δ_H 0.88 (4H, m, Si(CH$_2$C*H*$_3$)$_2$), 1.03-1.09 (6H, m, Si(CH$_2$C*H*$_3$)$_2$), 4.66-4.69 (1H, m, Si*H*); **^{13}C NMR** (100 MHz, $CDCl_3$) δ_C 6.62, 7.38; The product was immediately taken on to the following reaction: *n*-BuLi (2.11 mL, 5.27 mmol, 1.2 equiv) was added to a solution of 1-bromo-4-(trifluoromethyl)benzene (988 mg, 4.39 mmol, 1.0 equiv) in THF (25 mL) at −78 °C. The solution was stirred at this temperature for 3 h before diethylchlorosilane (700 mg, 5.71 mmol, 1.3 equiv) was added and the reaction allowed to warm to RT overnight. NH_4Cl (10 mL) was added to the crude mixture, the phases were separated and the aqueous phase washed with CH_2Cl_2 (3 x 10 mL). The

combined organic phases were dried ($MgSO_4$) and concentrated *in vacuo* to a yellow oil which was purified by vacuum distillation (74 °C, 11 mbar) to afford silane **250** as a colourless oil (303 mg, 30 %); Pd/C (5.7 mg, 0.00538 mmol, 5 mol%) was added to a mixture of alcohol **247** (275 mg, 1.18 mmol, 1.1 equiv) and arylhydrosilane **250** (250 mg, 1.08 mmol, 1.0 equiv). After effervescence had subsided (10 min) the reaction was found to be complete by TLC. The reaction mixture was filtered through Celite® to afford a colourless oil. Purification by column chromatography (petroleum ether → petroleum ether / Et_2O (4:1)) afforded the title compound as a colourless oil (316 mg, 64%); $\mathbf{R_f}$ 0.11 (petroleum ether / Et_2O (9:1)); **^{1}H NMR** (500 MHz, $CDCl_3$) δ_H 0.06 (6H, s, Si(C*H*$_3$)$_2$), 0.88-0.91 (13H, m, SiC(C*H*$_3$)$_3$ overlays SiC(C*H*$_2$CH$_3$)$_2$), 0.96 – 1.02 (6 H, m, SiC(CH$_2$C*H*$_3$)$_2$), 1.30-1.39 (4H, m, C(3)*H*$_2$ and C(4)*H*$_2$), 1.49-1.61 (4H, m, C(2)*H*$_2$ and C(5)*H*$_2$)), 3.60 (2H, t, *J* 6.5, OC*H*$_2$), 3.65 (2H, t, *J* 6.5, OC*H*$_2$), 7.62 (2H, d, *J* 8.0, Ar*H*), 7.68 (2H, d, *J* 8.0, Ar*H*); **^{13}C NMR** (100 MHz, $CDCl_3$) δ_C -5.30, 4.78, 6.58, 18.4, 25.6, 26.0, 32.7, 32.8, 63.2, 63.3, 124.2 (q, *J* 272.5), 124.2 (q, *J* 4.0), 131.3 (q, *J* 32.0), 134.2, 141.4; **HRMS** (ES^+) calc. For $C_{23}H_{42}F_3O_2Si_2$ $[M]^+$ 463.2670, found 463.2683;

Methylbis(4-(trifluoromethyl)phenyl)silane (254)

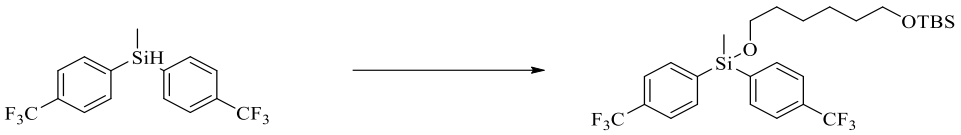


To a stirred solution of 1-bromo-4-(trifluoromethyl)benzene (4.5g, 20 mmol, 2.0 equiv) at –78 °C, in anhydrous THF (10 mL), was added *n*-BuLi (9.6 mL, 2.5 M n-BuLi in hexanes, 24 mmol, 2.4 equiv). The resulting mixture was stirred for 2 h at –78 °C before dichloromethylsilane (1.25 mL, 12 mmol, 1.2 equiv) was added and the reaction mixture allowed to warm to RT over 5 h. The crude reaction mixture was quenched with water (10 mL), the phases were separated and the organic phase was washed with water (3 × 10 mL). The combined organic layers were dried ($MgSO_4$) and concentrated *in vacuo* to a yellow oil, before purification by column chromatography (petroleum ether) afforded the title compound as a colourless oil (631 mg, 78%, 46% purity) contaminated with side product **255**; $\mathbf{R_f}$

0.11 (petroleum ether); **^{1}H NMR** (400 MHz, $CDCl_3$) δ_H 0.70 (3H, d, *J* 4.0, SiC*H*$_3$), 5.01 (1H, q, *J* 4.0, Si*H*), 7.62-7.68 (8H, m, Ar*H*);

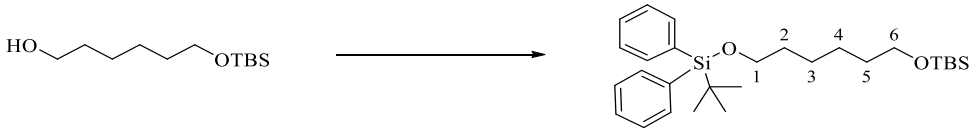
The spectroscopic data was found to be in agreement with that reported by Skrydstrup and co-workers.[231]

11,11,12,12-Tetramethyl-2,2-bis(4-(trifluoromethyl)phenyl)-3,10-dioxa-2,11-disilatridecane (256)



Pd/C (8 mg, 0.006 mmol, 5 mol%) was added to a mixture of alcohol **247** (278 mg, 1.30 mmol, 1.0 equiv) and arylhydrosilane **254** (400 mg, 1.30 mmol, 1.0 equiv). After effervescence had subsided (10 min) the reaction was found to be complete by TLC. The reaction mixture was filtered through Celite® to afford silyl ether **256** as a colourless oil. Purification by column chromatography (petroleum ether) afforded the title compound as a colourless oil (195 mg, 29%); **R_f** 0.25 (petroleum ether); **IR** (thin film, ν_{max} / cm^{-1}) 2932w, 1391w, 1324s, 1165m, 1060s, 828s; **^{1}H NMR** (500 MHz, $CDCl_3$) δ_H 0.05 (6H, s, Si(C*H*$_3$)$_2$), 0.70 (3H, s, SiC*H*$_3$), 0.90 (9H, s, SiC(C*H*$_3$)$_3$), 1.30-1.0 (4H, m, C(3)*H*$_2$ and C(4)*H*$_2$), 1.48-1.63 (4H, m, C(2)*H*$_2$ and C(5)*H*$_2$)), 3.60 (2H, t, *J* 6.5, OC*H*$_2$), 3.72 (2H, t, *J* 6.5, OC*H*$_2$), 7.64 (4H, d, *J* 8.0, Ar*H*), 7.70 (4H, d, *J* 8.0, Ar*H*); **^{13}C NMR** (125 MHz, $CDCl_3$) δ_C –4.86, –2.90, 18.8, 26.0, 26.0, 26.4, 32.9, 33.2, 63.6, 64.2, 124.1 (q, *J* 272.5), 125.0 (q, *J* 3.5), 132.4 (q, *J* 32.0), 135.0, 136.0, 140.8;

2,2,3,3,13,13-Hexamethyl-12,12-diphenyl-4,11-dioxa-3,12-disilatetradecane (257)



TBDPSCl (330 mg, 1.2 mmol, 1.0 equiv) was added to a solution of alcohol **251** (232 mg, 1 mmol, 1.0 equiv) and imidazole (89 mg, 1.3 mmol, 1.3 equiv) in dichloromethane (5 mL). The reaction mixture was stirred at RT for 16 h before dilution with dichloromethane (10 mL). The subsequent mixture was washed with NH_4Cl (3 × 10 mL) and brine (2 × 10 mL) and the final organic phase dried ($MgSO_4$) and concentrated *in vacuo* to afford a colourless oil which was purified by column chromatography (petroleum ether) to afford the title compound as a colourless oil (263 mg, 62%); $\mathbf{R_f}$ 0.41 (petroleum ether); **^{1}H NMR** (500 MHz, $CDCl_3$) δ_H 0.06 (6H, s, Si(C*H*$_3$)$_2$), 0.91 (9H, s, SiC(C*H*$_3$)$_3$), 1.06 (9H, s, SiC(C*H*$_3$)$_3$), 1.27-1.43 (4H, m, C(3)*H*$_2$ and C(4)*H*$_2$), 1.48-1.62 (4H, m, C(2)*H*$_2$ and C(5)*H*$_2$)), 3.58-3.63 (2H, m, OC*H*$_2$), 3.65-3.70 (2H, m, OC*H*$_2$), 7.36-7.45 (6H, m, Ar*H*), 7.66-7.71 (4H, m, Ar*H*); **^{13}C NMR** (125 MHz, $CDCl_3$) δ_C –5.25, 18.4, 19.2, 25.6, 25.6, 26.0, 26.9, 32.6, 32.9, 63.2, 63.9, 127.6, 129.5, 134.2, 135.6.

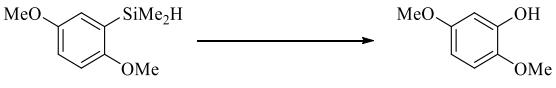
The spectroscopic data was found to be in agreement with that reported by Yeom and co-workers.[232]

Oxidation of hydrosilanes *via* filtration through Celite/Pd/C

Preparation of Celite /Pd/C column

A glass chromatography column (12.5 mm internal diameter) was packed with 1.5 g Celite (40 mm height). Pd/C (10 mg, 10 wt.% loading, 0.010 mmol) was mixed with Celite (1.0 g), loaded onto the column above the Celite and packed down (25 mm height). The column was wetted with MeOH (5 mL) under a positive pressure of N_2.

Large scale preparation of 2,5-dimethoxyphenol (147)



A solution of (2,5-dimethoxyphenyl)dimethylsilane (1.96 g, 10.0 mmol, 1.0 equiv) in MeOH/THF (1:1, 20 mL) was loaded onto the Celite/Pd/C column. The solution passed through the column at 5ml/min using a positive pressure of N_2 and was collected into a round bottomed flask equipped with a stirrer bar. The column was rinsed with MeOH/THF (1:1, 10 mL) and to the combined filtrate was

added $KHCO_3$ (500 mg, 5.00 mmol, 0.5 equiv), TBAF (1.0 mL of a 1 M solution in THF, 0.1 equiv) and H_2O_2 (6.80 mL of a 30% w/w solution, 60.0 mmol, 6.0 equiv) and the reaction mixture stirred for 3 h. Upon completion, the reaction was quenched with HCl (10 mL, 1 N aqueous solution) and the monophasic mixture stirred for a further 5 min. The reaction mixture was then extracted with EtOAc (3 x 10 mL). The combined organic phases were dried ($MgSO_4$) and concentrated *in vacuo* to afford a crude phenolic product which was purified by column chromatography (see previous procedure) to afford 2,5-dimethoxyphenol as a very pale yellow oil (1.26 g, 82%).

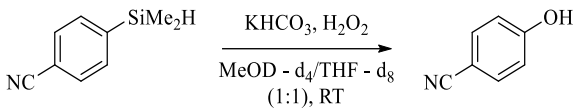
5.4. Mechanism

^{1}H NMR spectroscopic experiments

General procedure VI

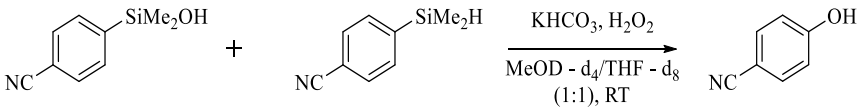
After submission to the NMR machine, spectra were collected at regular intervals to observe the variation in concentration of reactants and product. The spectra were automatically phased, corrected and integrated using the TOPSPIN multi_integ3 function.

Figure 4.3



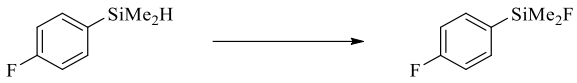
To an NMR tube containing 10 mg of $KHCO_3$ was added a solution of 4-(dimethylsilyl)benzonitrile **116** (10 mg, 0.062 mmol, 1.0 equiv) and 1,3,5-trimethylbenzene (3.7 mg, 0.031 mmol, 0.5 equiv) in a 1:1 mixture of methanol - d_4 / THF - d_8 (500 μL). H_2O_2 (42 μL, 0.37 mmol, 6.0 equiv) was added and the reaction monitored by ^{1}H NMR.

Figure 4.4



A 4:1 mixture of silanol/silane was prepared. 10 mg (0.061 mmol (weighted RMW), 1.0 equiv) of this mixture was added to an NMR tube containing 10 mg of $KHCO_3$ and a solution of 1,3,5-trimethylbenzene (3.7 mg, 0.031 mmol, 0.5 equiv) in a 1:1 mixture of methanol - d_4 / THF - d_8 (500 μL). H_2O_2 (41 μL, 0.37 mmol, 6.0 equiv) was added and the reaction monitored by ^{1}H NMR.

Fluoro(4-fluorophenyl)dimethylsilane (322)



To a pre-dried mixture of $CuCl_2$ (87 mg, 0.65 mmol, 2.0 equiv), KF (20 mg, 0.32 mmol, 1.0 equiv) and CuI (2 mg, 0.02 mmol, 0.05 equiv) was added a solution of hydrosilane **99** (50 mg, 0.32 mmol, 1.0 equiv) in THF (1 ml). The reaction was stirred at rt for 16 h, before filtration to remove the copper salts and concentration *in vacuo* to afford fluorosilane **322** (24 mg, 43%); $\mathbf{R_f}$ 0.21 (petroleum ether / Et_2O (9:1)); **^{1}H NMR** (400 MHz, $CDCl_3$) δ_H 0.50 (6H, d, *J* 7.5, Si(C*H*$_3$)$_2$), 7.12 (2H, t, *J* 8.5, Ar*H*), 7.59 (2H, dd, *J* 8.5, 6.0, Ar*H*); **^{13}C NMR** (100 MHz, $CDCl_3$) δ_C -1.11 (d, *J* 15.5), 115.3 (d, *J* 20.0), 131.8 (d, *J* 13.0), 135.2 (dd, *J* 8.0, 2.0), 164.4 (d, *J* 249.5); **^{19}F NMR** (377 MHz, $CDCl_3$) δ_F -160.8 (1F), -109.7 (1F).

Data in agreement with that reported by Lipowitz *et al*[188]

^{19}F NMR spectroscopic experiments

Spectra processing

All spectra were checked for accurate phasing, and if necessary were corrected manually. The spectra were integrated using the TOPSPIN multi_integ3 function and these values were corrected according to the values obtained from studies into the relaxation times of the reaction components.

Integration Correction values

The parameters used in the ^{19}F spectroscopic experiments were updated during the overall investigation and are listed below. To calculate correction values, a mixture of methoxysilane **126**, phenol **134** and perfluorobenzene was prepared. Their resonances were integrated from NMR experiments of varying parameters. Variation between spectra of non-ideal paramaters and ideal parameters was quantified and used to correct all spectra obtained. The correction values obtained are also shown.

Automatic ^{19}F parameters (AVB500)

D1 = 1.0, SW = 241.5717, O1P = -100. Correction factor: x1.3504 for arylsilane integration. Correction factor: x1.2846 for phenol integration.

Extended relaxation time parameters

D1 = 5.5, SW = 241.5717, O1P = -100. Correction factor: x0.97699 for arylsilane integration. Correction factor: x0.99066 for phenol integration.

Extended relaxation time and improved offset frequency

D1 = 5.5, SW = 99.6533, O1P = -150. Correction factor: x1.03488 for arylsilane integration. Correction factor: x1.05285 for phenol integration.

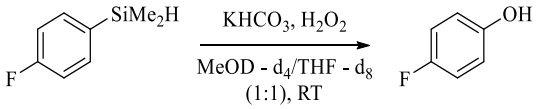
Ideal parameters

D1 = 18.0, SW = 99.6528, O1P = -145. Correction factors not necessary

Alkoxysilane peak splitting

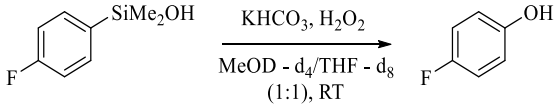
During ^{19}F spectroscopic experiments, splitting of alkoxysilane resonances were often observed. Methoxysilane **126** would split by 0.01 ppm and isopropoxysilane **332** by 0.04 ppm. This result was attributed to deuterated solvent exchange at the silicon centre, resulting in a mixture of the hydrated and partially deuterated alkoxysilanes. To confirm this, a solution of (4-fluorophenyl)(methoxy-d_3)dimethylsilane was prepared, and the ^{19}F NMR spectrum obtained before and after the addition of methoxysilane **126** where an identical peak splitting was observed. The integrations presented correspond to the sum of hydrated and partially deuterated alkoxysilane.

Figure 4.7



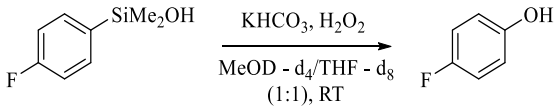
To an NMR tube containing 10 mg of $KHCO_3$ was added a solution of perfluorobenzene and (4-fluorophenyl)dimethylsilane **99** (10 mg, 0.065 mmol, 1.0 equiv) in a 1:1 mixture of methanol - d_4 / THF - d_8 (500 μL). H_2O_2 (44 μL, 0.39 mmol, 6.0 equiv) was added and the reaction monitored by ^{19}F NMR. The concentration of perfluorobenzene was determined by comparing its integration with that of (4-fluorophenyl)(methoxy)dimethylsilane at the beginning of the reaction and was subsequently used as an internal standard.

Figure 4.8



To an NMR tube containing 10 mg of $KHCO_3$, was added a solution of perfluorobenzene and (4-fluorophenyl)dimethylsilanol **118** (10 mg, 0.059 mmol, 1.0 equiv) in a 1:1 mixture of methanol - d_4 / THF - d_8 (500 μL). H_2O_2 (40 μL, 0.35 mmol, 6.0 equiv) was added and the reaction monitored by ^{19}F NMR. The concentration of perfluorobenzene was determined by comparing its integration with that of (4-fluorophenyl)(methoxy)dimethylsilane at the beginning of the reaction and was subsequently used as an internal standard.

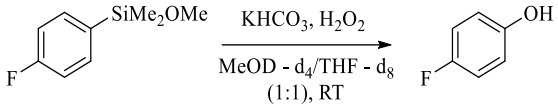
Figure 4.9



To an NMR tube containing 10 mg of $KHCO_3$, was added a solution of perfluorobenzene and (4-fluorophenyl)dimethylsilanol **118** (15 mg, 0.088 mmol, 1.0 equiv) in a 1:1 mixture of methanol - d_4 / THF - d_8 (500 μL). H_2O_2 (100 μL, 0.88 mmol, 10.0 equiv) was added and the reaction monitored by

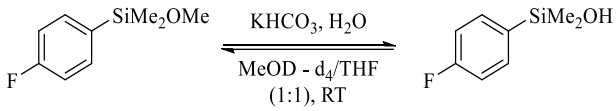
^{19}F NMR. The concentration of perfluorobenzene was determined by comparing its integration with that of (4-fluorophenyl)(methoxy)dimethylsilane at the beginning of the reaction and was subsequently used as an internal standard.

Figure 4.10



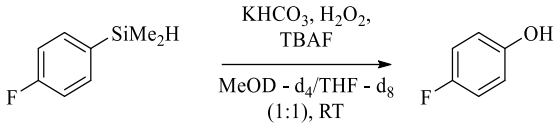
To an NMR tube containing 10 mg of $KHCO_3$, was added a solution of perfluorobenzene and (4-fluorophenyl)(methoxy)dimethylsilane **126** (10 mg, 0.054 mmol, 1.0 equiv) in a 1:1 mixture of methanol - d_4 / THF - d_8 (500 μL). H_2O_2 (37 μL, 0.32 mmol, 6.0 equiv) was added and the reaction monitored by ^{19}F NMR. The concentration of perfluorobenzene was determined by comparing its integration with that of (4-fluorophenyl)(methoxy)dimethylsilane at the beginning of the reaction and was subsequently used as an internal standard.

Figure 4.11



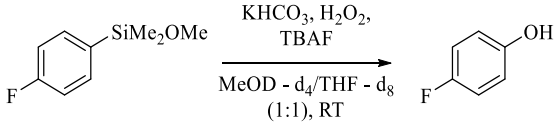
A solution of methoxysilane **126** in MeOH-d_4/THF-d_8 (0.0825 M, 500 μL) containing perfluorobenzene as an internal standard was prepared and added to an NMR tube after which water (20 μL, 1.1 mmol, 22 equiv) and $KHCO_3$ was added until the solution was saturated and the reaction monitored by ^{19}F NMR. Due to the extended length of time required to observe this equilibrium, the reaction was not monitored at all times. Instead, the data was interpolated using Origin Pro software.

Figure 4.13



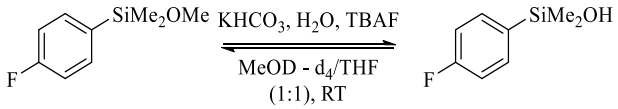
To an NMR tube containing 10 mg of $KHCO_3$, was added a solution of perfluorobenzene and (4-fluorophenyl)(methoxy)dimethylsilane **99** (10 mg, 0.065 mmol, 1.0 equiv) in methanol-d_4 (250 μL). A solution of TBAF (6.5 μL of 1M solution in THF, 0.0065 mmol, 0.1 equiv) was then added in THF (250 μL). H_2O_2 (37 μL, 0.33 mmol, 5.0 equiv) was added and the reaction monitored by ^{19}F NMR. An unknown error occurred in integration and the data was therefore normalised to a total concentration of 0.1296 M.

Figure 4.14



To an NMR tube containing 10 mg of $KHCO_3$, was added a solution of perfluorobenzene, (4-fluorophenyl)(methoxy)dimethylsilane **126** (10 mg, 0.054 mmol, 1.0 equiv) and TBAF (5 μL, 0.0054 mmol, 0.1 equiv) in a 1:1 mixture of methanol - d_4 / THF - d_8 (500 μL). H_2O_2 (37 μL, 0.33 mmol, 6.0 equiv) was added and the reaction monitored by ^{19}F NMR. The concentration of perfluorobenzene was determined by comparing its integration with that of (4-fluorophenyl)(methoxy)dimethylsilane at the beginning of the reaction and was subsequently used as an internal standard.

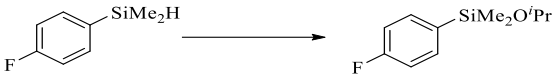
Figure 4.15



A solution of methoxysilane **126** in MeOH-d_4/THF-d_8 (0.1 M, 500 μL) containing perfluorobenzene as an internal standard was prepared and added to an NMR tube after which $KHCO_3$ (until the

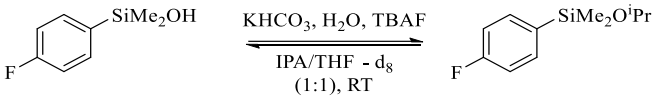
solution was saturated), TBAF (5 μL of 1 M solution in THF, 0.005 mmol, 0.1 equiv) and water (20 μL, 1.1 mmol, 22 equiv) were added and the reaction monitored by ^{19}F NMR.

(4-Fluorophenyl)(isopropoxy)dimethylsilane (332)



[$RuCl_2$(p-cymene)]$_2$ (5.0 mg, 0.0081 mmol, 0.5 mol%) was added to hydrosilane **99** (250 mg, 1.62 mmol, 1.0 equiv) and isopropanol (250 μL) under air. After 2 minutes of effervescence the reaction was seen to be complete by TLC. The reaction mixture was diluted in Et_2O and eluted through a silica plug (Et_2O) to afford the title compound (269 mg, 78%); **IR** (thin film, ν_{max} / cm^{-1}) 2972w, 1589m, 1500 m, 1384w, 1108s, 1025s, 834s; **^{1}H NMR** (400 MHz, $CDCl_3$) δ_H 0.38 (6H, s, Si(C*H*$_3$)$_2$), 1.14 (6H, d, *J* 6.0, OCH(C*H*$_3$)$_2$), 3.98 (1H, sept, *J* 6.0, OC*H*(CH$_3$)$_2$),7.07 (2H, ap t, *J* 9.0, Ar*H*), 7.57 (2H, dd, *J* 9.0, 6.0, Ar*H*); **^{13}C NMR** (100 MHz, $CDCl_3$) δ_C –1.07, 25.6, 65.3, 114.9 (d, *J* 19.5), 134.1 (d, *J* 4.0), 135.5 (d, *J* 7.5), 163.9 (d, *J* 246.6); **^{19}F NMR** (377 MHz, $CDCl_3$) δ_F -111.4 (1F); **HRMS** (ES^+) calc. for $C_{12}H_{20}OSiF$ $[M]^+$ 212.1033, found 2121029.

Figure 4.16



A solution of silanol **118** in IPA-d_7/THF-d_8 (0.083 M, 500 μL) containing perfluorobenzene as an internal standard was prepared and added to an NMR tube after which $KHCO_3$ (until the solution was saturated) and water (20 μL, 1.1 mmol, 26 equiv) were added but no change in sample composition was observed. The next day, TBAF (4 μL of 1 M solution in THF, 0.004 mmol, 0.1 equiv) was added and the reaction was monitored by ^{19}F NMR.

General Procedure VII – preparation of solution A

Arylsilane solutions were prepared at a concentration of 0.2 M and typically 0.04 M perfluorobenzene: deuterated methanol (4 mL) was added to a mixture of (4-fluorophenyl)(methoxy)dimethylsilane **126** (147.4 mg, 0.8 mmol, 1.0 equiv) and perfluorobenzene (18.5 μL, 0.16 mmol, 0.2 equiv).

General Procedure VIII

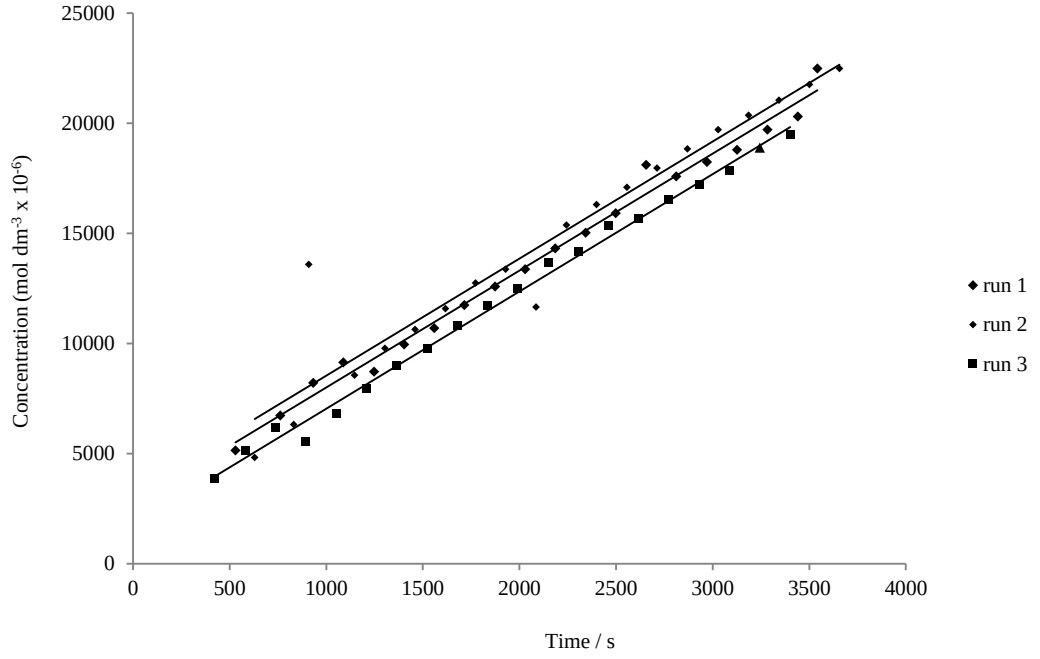
250 μL of H_2O_2 solution in methanol was added to 250 μL of a 0.2 M solution of (4-fluorophenyl)(methoxy)dimethylsilane **126** in methanol (solution A). The resulting mixture was immediately submitted to an NMR machine for spectroscopic observation. This procedure was repeated twice and the growth in phenol concentration observed by integration of the phenol's fluorine resonance (relative to the internal standard, perfluorobenzene) by ^{19}F NMR spectroscopy. The reaction was observed up to 20% completion, after which the data was discarded. The spectra were automatically integrated using the TOPSPIN multi_integ3 command. Average rate constants and R^2 values were obtained using Microsoft Excel software, and plotting concentration against time. Frequently, the phenol integration was unreliable below 2% conversion as the resonance would shift with increasing concentration. This data was therefore discarded to optimise the R^2 value. The times given for the initial data points in the plots are estimated to aid comparison of consecutive runs.

Order with respect to hydrogen peroxide

Preparation of H_2O_2 stock solution (6.0 equiv)

To a 25 mL volumetric flask was added $KHCO_3$ (50.1 mg, 0.5 mmol, 0.1 equiv) and H_2O_2 (3.4 mL, 30 mmol, 6.0 equiv). Methanol was added to the mixture until the total volume was equal to 25 mL. This solution was then degassed with a steady flow of nitrogen gas for 1 h.

Following General Procedure **VIII**, the following data and initial rates were obtained:

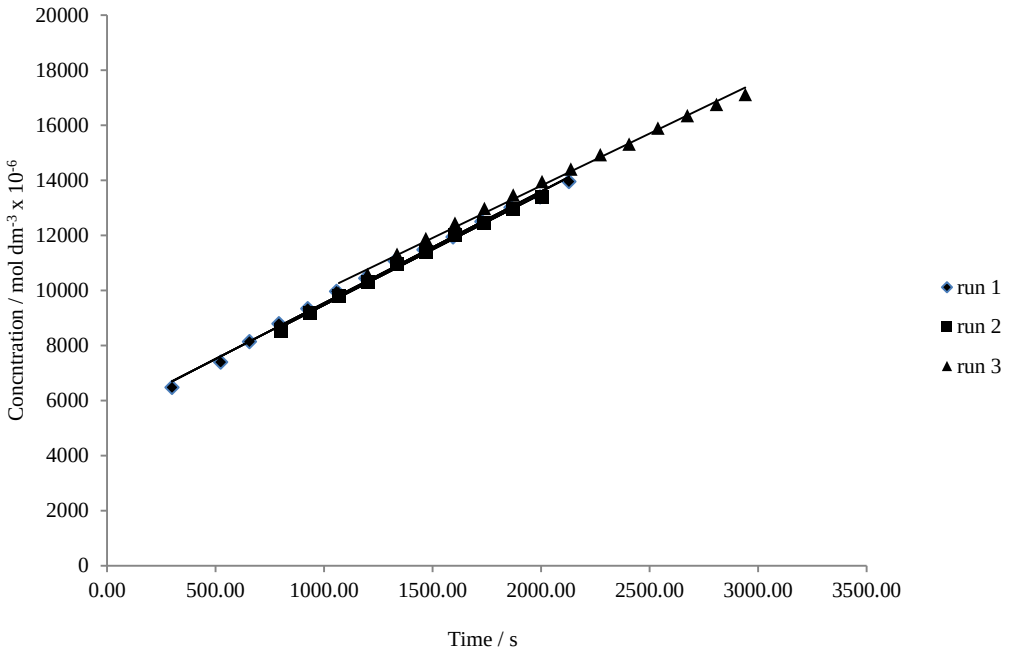


Run 1 Initial Rate / moldm^{-3}s^{-1} (R^2 value)	**Run 2 Initial Rate / moldm^{-3}s^{-1} (R^2 value)**	**Run 3 Initial Rate / moldm^{-3}s^{-1} (R^2 value)**	**Average / moldm^{-3}s^{-1}**	**% RSD**
5.3156×10^{-6} (0.9147)	5.3224×10^{-6} (0.9946)	5.3118×10^{-6} (0.9894)	5.3166×10^{-6}	0.082

Preparation of H_2O_2 stock solution (3.0 equiv)

To a 25 mL volumetric flask was added $KHCO_3$ (50.1 mg, 0.5 mmol, 0.1 equiv) and H_2O_2 (1.70 mL, 30 mmol, 3.0 equiv) and water (1.70 mL, 94.4 mmol, 18.9 equiv). Methanol was added to the mixture until the total volume was equal to 25 mL. This solution was then degassed with a steady flow of nitrogen gas for 1 h.

Following General Procedure **VIII**, the following data and initial rates were obtained:

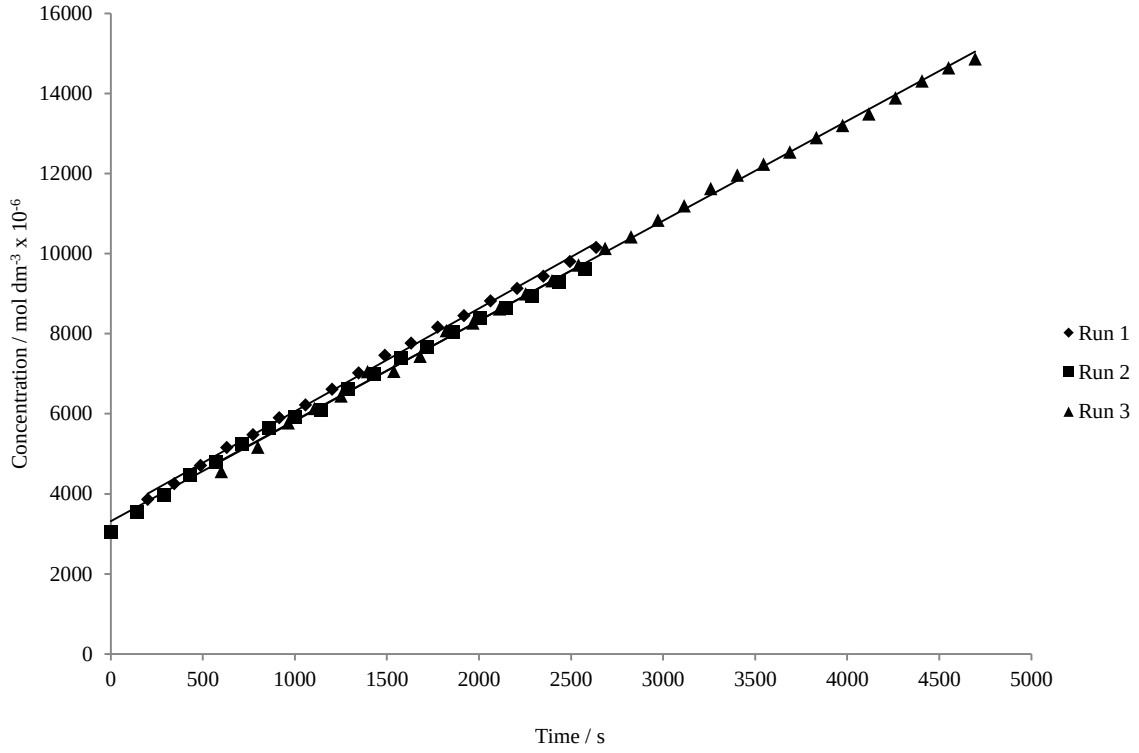


Run 1 Initial Rate / moldm^{-3}s^{-1} (R^2 value)	**Run 2 I nitial Rate / moldm^{-3}s^{-1} (R^2 value)**	**Run 3 Initial Rate / moldm^{-3}s^{-1} (R^2 value)**	**Average / moldm^{-3}s^{-1}**	**% RSD**
4.0557×10^{-6} (0.996)	4.0323×10^{-6} (0.997)	3.795×10^{-6} (0.995)	3.961×10^{-6}	2.97

Preparation of H_2O_2 stock solution (2.0 equiv)

To a 25 mL volumetric flask was added $KHCO_3$ (50.1 mg, 0.5 mmol, 0.1 equiv) and H_2O_2 (1.13 mL, 10 mmol, 2.0 equiv) and water (2.27 mL, 126 mmol, 25.2 equiv). Methanol was added to the mixture until the total volume was equal to 25 mL. This solution was then degassed with a steady flow of nitrogen gas for 1 h.

Following General Procedure **VIII**, the following data and initial rates were obtained.

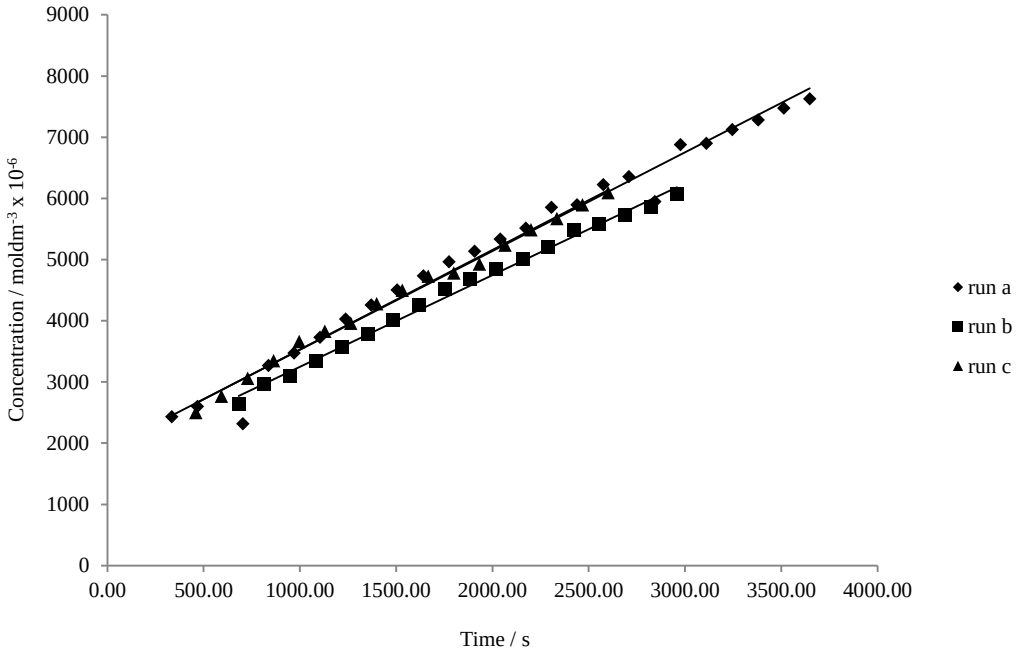


Run 1 Initial Rate / moldm^{-3}s^{-1} (R^2 value)	**Run 2 Initial Rate / moldm^{-3}s^{-1} (R^2 value)**	**Run 3 Initial Rate / moldm^{-3}s^{-1} (R^2 value)**	**Average / moldm^{-3}s^{-1}**	**% RSD**
2.4938×10^{-6} (0.999)	2.5047×10^{-6} (0.997)	2.5701×10^{-6} (0.998)	2.52×10^{-6}	1.34

Preparation of H_2O_2 stock solution (1.0 equiv)

To a 25 mL volumetric flask was added $KHCO_3$ (50.1 mg, 0.5 mmol, 0.1 equiv) and H_2O_2 (567 μL, 5.0 mmol, 1.0 equiv) and water (2.83 mL, 157 mmol, 31.4 equiv). Methanol was added to the mixture until the total volume was equal to 25 mL. This solution was then degassed with a steady flow of nitrogen gas for 1 h.

Following General Procedure **VIII**, the following data and initial rates were obtained:



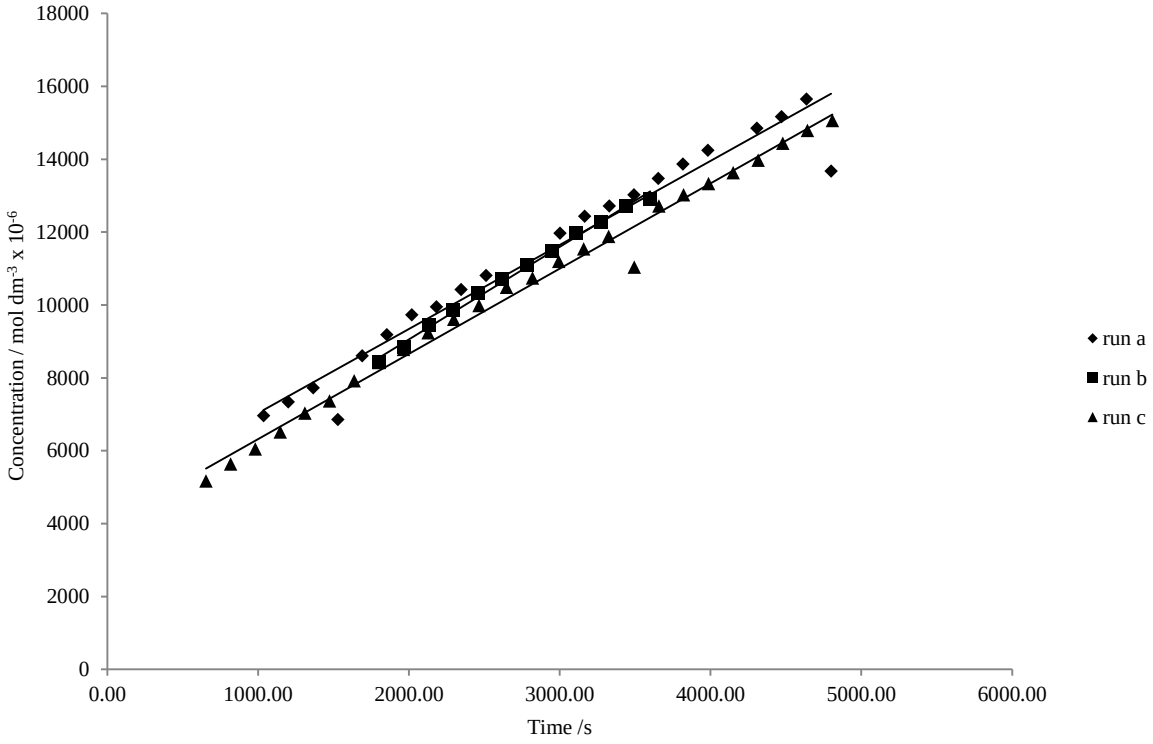
Run 1 Initial Rate / moldm^{-3}s^{-1} (R^2 value)	**Run 2 Initial Rate / moldm^{-3}s^{-1} (R^2 value)**	**Run 3 Initial Rate / moldm^{-3}s^{-1} (R^2 value)**	**Average / moldm^{-3}s^{-1}**	**% RSD**
1.6114×10^{-6} (0.979)	1.5143×10^{-6} (0.995)	1.651×10^{-6} (0.994)	1.59×10^{-6}	3.61

Order with respect to potassium bicarbonate

Preparation of H_2O_2 stock solution (0.2 equiv $KHCO_3$)

To a 25 mL volumetric flask was added $KHCO_3$ (100.1 mg, 1.0 mmol, 0.2 equiv), H_2O_2 (567 μL, 5.0 mmol, 1.0 equiv) and water (2.83 mL, 157 mmol, 31.4 equiv). Methanol was added to the mixture until the total volume was equal to 25 mL. This solution was then degassed with a steady flow of nitrogen gas for 1 h.

Following General Procedure **VIII**, the following data and initial rates were obtained:

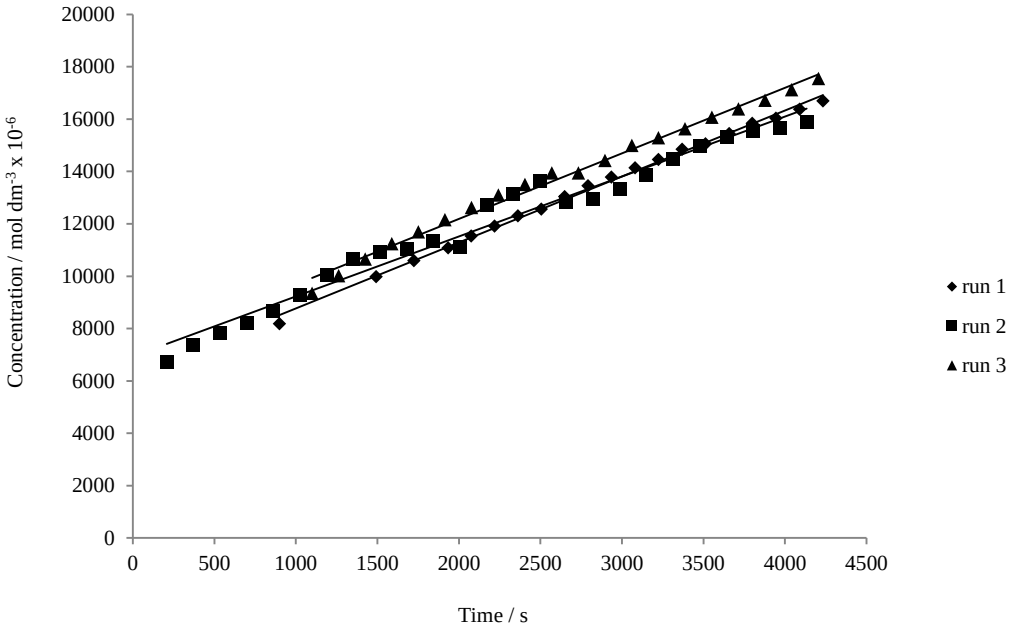


Run 1 Initial Rate / moldm^{-3}s^{-1} (R^2 value)	**Run 2 Initial Rate / moldm^{-3}s^{-1} (R^2 value)**	**Run 3 Initial Rate / moldm^{-3}s^{-1} (R^2 value)**	**Average / moldm^{-3}s^{-1}**	**% RSD**
2.3061 x 10^{-6} (0.952)	2.4193 x 10^{-6} (0.997)	2.3184 x 10^{-6} (0.990)	2.35 x 10^{-6}	2.16

Preparation of H_2O_2 stock solution (0.3 equiv $KHCO_3$)

To a 25 mL volumetric flask was added $KHCO_3$ (150.2 mg, 1.5 mmol, 0.3 equiv) and H_2O_2 (3.4 mL, 30 mmol, 6.0 equiv). Methanol was added to the mixture until the total volume was equal to 25 mL. This solution was then degassed with a steady flow of nitrogen gas for 1 h.

Following General Procedure **VIII**, the following data and initial rates were obtained:



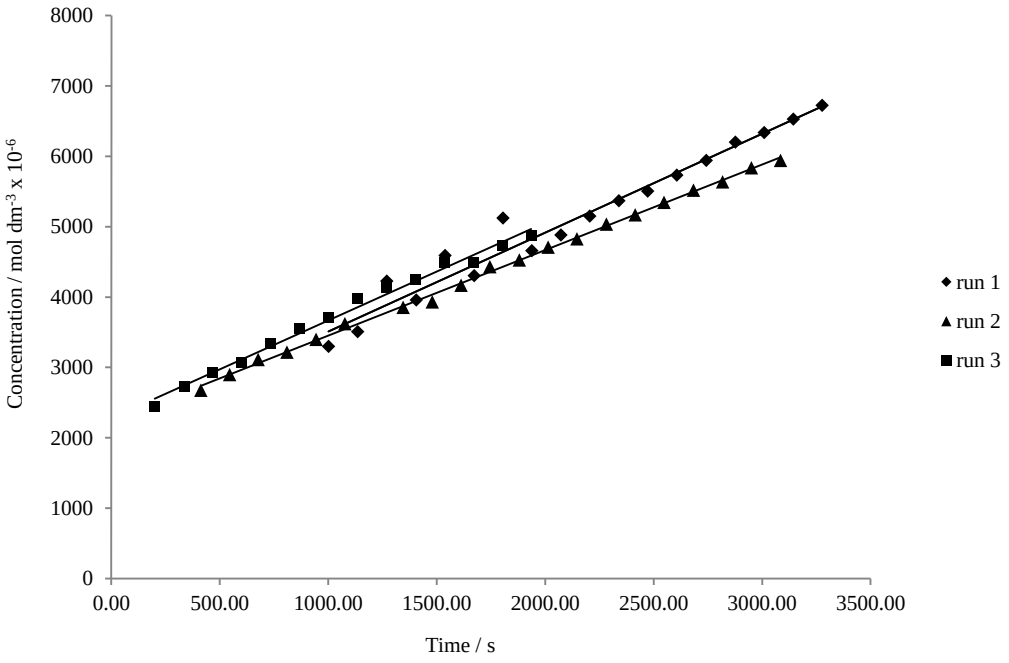
Run 1 Initial Rate / moldm^{-3}s^{-1} (R^2 value)	**Run 2 Initial Rate / moldm^{-3}s^{-1} (R^2 value)**	**Run 3 Initial Rate / moldm^{-3}s^{-1} (R^2 value)**	**Average / moldm^{-3}s^{-1}**	**% RSD**
2.5063×10^{-6} (0.991)	2.2891×10^{-6} (0.971)	2.5174×10^{-6} (0.997)	2.44×10^{-6}	4.31

Order with respect to TBAF

Preparation of H_2O_2 stock solution (0.05 equiv TBAF)

To a 25 mL volumetric flask was added $KHCO_3$ (50.1 mg, 0.5 mmol, 0.1 equiv) H_2O_2 (567 μL, 5.0 mmol, 1.0 equiv), TBAF (250 μL of a 1 M solution in THF, 0.25 mmol, 0.05 equiv) and water (2.83 mL, 157 mmol, 31.4 equiv). Methanol was added to the mixture until the total volume was equal to 25 mL. This solution was then degassed with a steady flow of nitrogen gas for 1 h.

Following General Procedure **VIII**, the following data and initial rates were obtained:

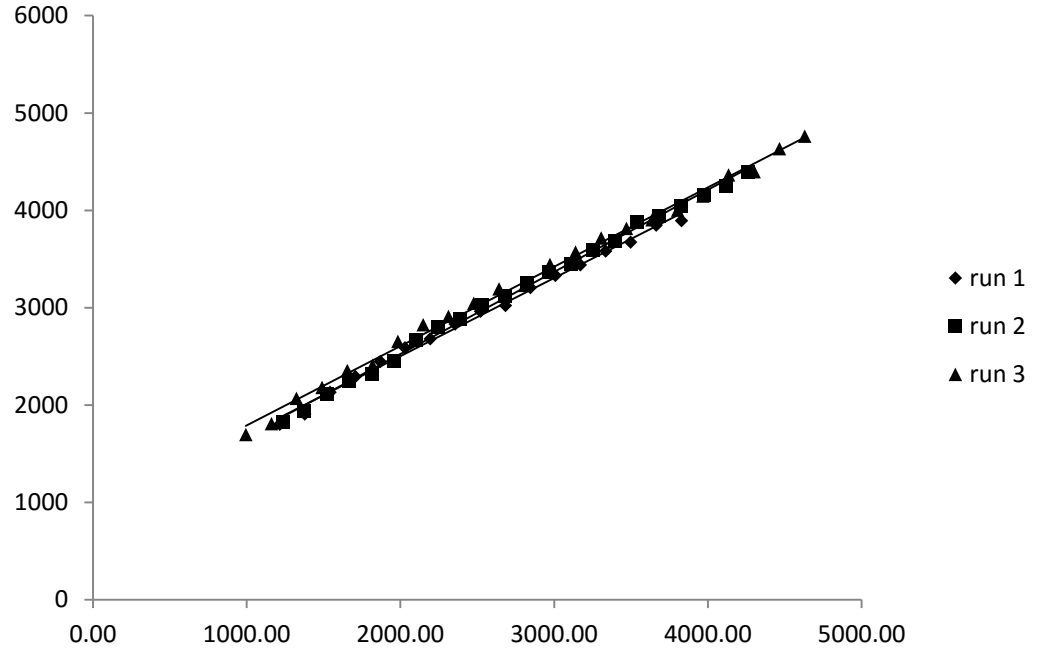


Run 1 Initial Rate / moldm^{-3}s^{-1} (R^2 value)	**Run 2 Initial Rate / moldm^{-3}s^{-1} (R^2 value)**	**Run 3 Initial Rate / moldm^{-3}s^{-1} (R^2 value)**	**Average / moldm^{-3}s^{-1}**	**% RSD**
1.4046×10^{-6} (0.964)	1.2138×10^{-6} (0.998)	1.3896×10^{-6} (0.991)	1.34×10^{-6}	6.48

Preparation of H_2O_2 stock solution (0.1 equiv TBAF)

To a 25 mL volumetric flask was added $KHCO_3$ (50.1 mg, 0.5 mmol, 0.1 equiv), H_2O_2 (567 μL, 5.0 mmol, 1.0 equiv), TBAF (500 μL of a 1 M solution in THF, 0.5 mmol, 0.1 equiv) and water (2.83 mL, 157 mmol, 31.4 equiv). Methanol was added to the mixture until the total volume was equal to 25 mL. This solution was then degassed with a steady flow of nitrogen gas for 1 h.

Following General Procedure **VIII**, the following data and initial rates were obtained:

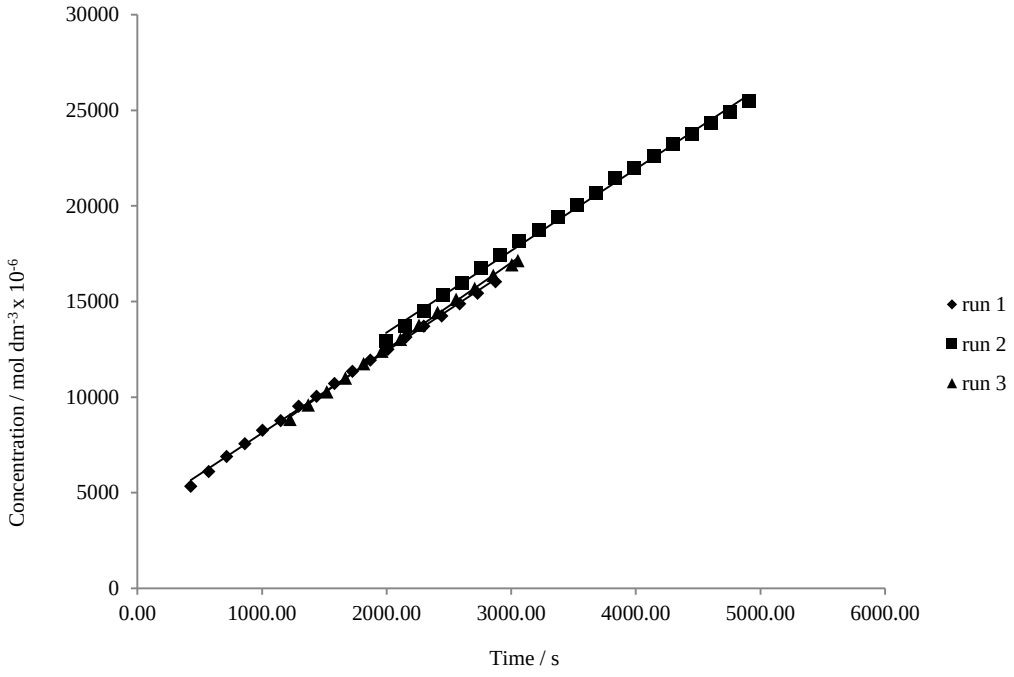


Run 1 Initial Rate / moldm^{-3}s^{-1} (R^2 value)	**Run 2 Initial Rate / moldm^{-3}s^{-1} (R^2 value)**	**Run 3 Initial Rate / moldm^{-3}s^{-1} (R^2 value)**	**Average / moldm^{-3}s^{-1}**	**% RSD**
0.8433×10^{-6} (0.997)	0.8157×10^{-6} (0.996)	0.8024×10^{-6} (0.995)	0.821×10^{-6}	2.07

Oxidation of Silanol

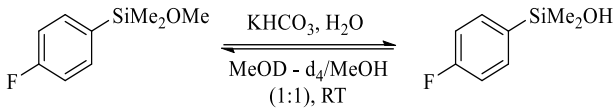
Preparation of H_2O_2 stock solution

To a 25 mL volumetric flask was added $KHCO_3$ (50.1 mg, 0.5 mmol, 0.1 equiv) and H_2O_2 (3.4 mL, 30 mmol, 6.0 equiv). Methanol was added to the mixture until the total volume was equal to 25 mL. This solution was then degassed with a steady flow of nitrogen gas for 1 h. 250 μL of H_2O_2 solution in methanol was added to 250 μL of a 0.2 M solution of (4-fluorophenyl)dimethylsilanol **X** in methanol. The resulting mixture was immediately submitted to an NMR machine for spectroscopic observation. This procedure was repeated twice and the growth in phenol concentration observed by integration of the phenol's fluorine resonance (relative to the internal standard, perfluorobenzene) by ^{19}F NMR spectroscopy. The reaction was observed up to 20% completion, after which the data was discarded. The spectra were automatically integrated using the TOPSPIN multi_integ3 command. Average rate constants and R^2 values were obtained using Microsoft Excel software, and plotting concentration against time. The times given for the initial data points in the plots are estimated to aid comparison of consecutive runs.



Run 1 Initial Rate / moldm^{-3}s^{-1} (R^2 value)	**Run 2 Initial Rate / moldm^{-3}s^{-1} (R^2 value)**	**Run 3 Initial Rate / moldm^{-3}s^{-1} (R^2 value)**	**Average / moldm^{-3}s^{-1}**	**% RSD**
4.769 x10^{-6}	4.3721 x 10^{-6}	4.5311 x 10^{-6}	4.56 x 10^{-6}	3.58
(0.999)	(0.997)	(0.999)		

Figure 4.23



Methanol/H_2O/$KHCO_3$ solutions were prepared from two stock solutions:

4 M H_2O in methanol

To a 25 mL volumetric flask was added $KHCO_3$ (50.1 mg, 0.5 mmol) and H_2O (1.80 mL, 100 mmol). Methanol was added to the mixture until the total volume was equal to 25 mL.

20 M H_2O in methanol

To a 50 mL volumetric flask was added $KHCO_3$ (100.1 mg, 1.0 mmol) and H_2O (18.0, 1.0 mol). Methanol was added to the mixture until the total volume was equal to 50 mL.

The two solutions were mixed to form solutions of molarities shown. 250 μL of H_2O_2 solution in methanol was added to 250 μL of a 0.2 M solution of (4-fluorophenyl)(methoxy)dimethylsilane **126** in methanol or THF. The resulting mixture was left to equilibrate in an NMR tube, before ^{19}F NMR spectra of the mixture were collected 24 and 48 or 64 hours later.

Equilibrium in MeOH

	[$ArSiMe_2OH$] / [$ArSiMe_2OMe$]						
[H_2O] / $moldm^{-3}$	2.54	3.5	3.7	4.57	5	6	8
24 h	1.534	1.9376	1.948	2.3804	2.6276	3.1299	4.6837
48 h			1.953				4.4678
64 h	1.581	1.967		2.360	2.586	3.071	
Average	**1.558**	**1.952**	**1.950**	**2.370**	**2.607**	**3.100**	**4.576**

Equilibrium in MeOH with 0.1 equiv TBAF

	[$ArSiMe_2OH$] / [$ArSiMe_2OMe$]						
[H_2O] / $moldm^{-3}$	2	3.1	4	6	7.3	8	10
24 h	1.042	1.7321	2.1544	3.3188	4.1955	4.665	5.8994
48 h						4.880	
64 h	1.162	1.760	2.194	2.304	4.165		5.557
Average	**1.1022**	**1.746**	**2.174**	**3.311**	**4.180**	**4.773**	**5.728**

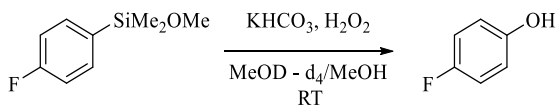
Equilibrium in MeOH/THF

	[$ArSiMe_2OH$] / [$ArSiMe_2OMe$]						
[H_2O] / $moldm^{-3}$	2	3	3.2	4	5	6	8
24 h	1.960	3.275	3.863	4.785	6.094	7.554	10.877
48 h			3.989				
64 h	2.000	3.279		4.617	5.915	7.380	10.801
Average	**1.980**	**3.277**	**3.926**	**4.701**	**6.004**	**7.467**	**10.839**

General procedure IX

Arylsilane solutions were prepared at a concentration of 0.2 M and typically 0.04 M perfluorobenzene: deuterated methanol (4 mL) was added to a mixture of (4-fluorophenyl)(methoxy)dimethylsilane **126** (147.4 mg, 0.8 mmol, 1.0 equiv) and perfluorobenzene (18.5 μL, 0.16 mmol, 0.2 equiv). 250 μL of H_2O_2 solution in methanol was added to 250 μL of a 0.2 M solution of (4-fluorophenyl)(methoxy)dimethylsilane **126** in methanol. The resulting mixture was immediately submitted to an NMR machine for spectroscopic observation. The spectra were automatically integrated using the TOPSPIN multi_integ3 command.

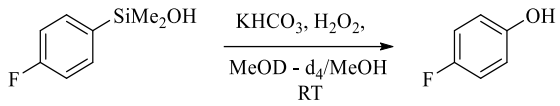
Figure 4.24, Graph A



To a 25 mL volumetric flask was added $KHCO_3$ (50.1 mg, 0.5 mmol, 0.1 equiv) and H_2O_2 (3.4 mL, 30 mmol, 6.0 equiv). Methanol was added to the mixture until the total volume was equal to 25 mL.

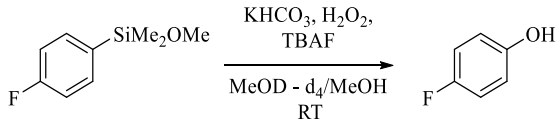
This solution was then degassed with a steady flow of nitrogen gas for 1 h. This solution was subsequently used with General Procedure **IX**.

Figure 4.24, Graph B



To a 25 mL volumetric flask was added $KHCO_3$ (50.1 mg, 0.5 mmol, 0.1 equiv) and H_2O_2 (3.4 mL, 30 mmol, 6.0 equiv). Methanol was added to the mixture until the total volume was equal to 25 mL. This solution was then degassed with a steady flow of nitrogen gas for 1 h. 250 μL of H_2O_2 solution in methanol was added to 250 μL of a 0.2 M solution of (4-fluorophenyl)dimethylsilanol **118** in methanol. The resulting mixture was immediately submitted to an NMR machine for spectroscopic observation. The spectra were automatically integrated using the TOPSPIN multi_integ3 command.

Figure 4.25



To a 25 mL volumetric flask was added $KHCO_3$ (50.1 mg, 0.5 mmol, 0.1 equiv), TBAF (500μL of a 1M solution in THF, 0.5 mmol, 0.1 equiv) and H_2O_2 (3.4 mL, 30 mmol, 6.0 equiv). Methanol was added to the mixture until the total volume was equal to 25 mL. This solution was then degassed with a steady flow of nitrogen gas for 1 h. This solution was subsequently used with General Procedure **IX**.

6. References

1) Jones, G. R.; Landais, Y., *Tetrahedron* **1996**, *52*, 7599-7662.

2) Cheynier, V. S., Quideau; Pascale, Sarni-Manchado, *Advances in Polyphenol Research*. Wiley-Blackwell: 2012; Vol. 3.

3) Adams, J.; Garcia, A., III; Foote, C., *J. Chem. Ecol.* **1978**, *4*, 17-25.

4) Quideau, S.; Deffieux, D.; Douat-Casassus, C.; Pouységu, L., *Angew. Chem. Int. Ed.* **2011**, *50*, 586-621.

5) Trevor George, R. M., Gemma Sweeney, J. B. Sweeney and Ali Tavassoli, *J. Chem. Soc., Perkin Trans. 1* **2000**, 2529-2574.

6) Tyman, J. H. P., *Synthetic and Natural Phenols*. Elsevier, New York: 1996.

7) Buchanan, B. G., Wilhelm; Jones, Russell, *Biochemistry and Molecular Biology of Plants*. Wiley-Blackwell: 2002.

8) Rappoport, Z., *The Chemistry of Phenols*. Wiley-VCH, Weinham: 2003.

9) Giguere, R., *Molecules that Matter*. Chemical Heritage Foundation: 2008.

10) Pilato, L., *Phenolic Resins: A Century of Progress*. Springer: 2010.

11) Baekeland, L. H., *J. Ind. Eng. Chem.* **1909**, *1*, 149-161.

12) Tanaka, T.; Matsuo, Y.; Kouno, I., *Int. J. Mol. Sci.* **2009**, *11*, 14-40.

13) Heldt, H.-W., *Plant Biochemistry*. Elsevier: 2005.

14) Maeda, H.; Dudareva, N., *Annu. Rev. Plant Biol.* **2012**, *63*, 73-105.

15) Patai, S., *The chemistry of the hydroxyl group*. Interscience publishers: 1971.

16) Metzler, D., *Biochemistry. The chemical reactions of living cells*. Academic Press: 2003.

17) Hock, H.; Lang, S., *Ber. Dtsch. Chem. Ges.* **1944**, *77*, 257-264.

18) Schmidt, R. J., *Appl. Catal., A* **2005**, *280*, 89-103.

19) Matsui, S.; Fujita, T., *Catal. Today* **2001**, *71*, 145-152.

20) Weissermel, K. A., Hans-Jurgen, *Industrial Organic Chemistry*. Wiley-VCH: 2003.

21) Hanson, P.; Jones, J. R.; Taylor, A. B.; Walton, P. H.; Timms, A. W., *J. Chem. Soc., Perkin Trans. 2* **2002**, 1135.

22) Krow, G. R., The Baeyer–Villiger Oxidation of Ketones and Aldehydes. In *Organic Reactions*, John Wiley & Sons, Inc.: 2004.

23) Lyttle, M. H.; Carter, T. G.; Cook, R. M., *Org. Process Res. Dev.* **2000**, *5*, 45-49.

24) Ullrich, R.; Hofrichter, M., *Cell. Mol. Life Sci.* **2007**, *64*, 271-293.

25) Enthaler, S.; Company, A., *Chem. Soc. Rev.* **2011**, *40*, 4912-4924.

26) Willis, M. C., *Ang. Chem. Int. Ed.* **2007**, *46*, 3402-3404.

27) Alonso, D.; Najera, C.; Pastor, I.; Yus, M., *Chem. Eur. J.* **2010**, 5274-5284.

28) Sergeev, A. G.; Schulz, T.; Torborg, C.; Spannenberg, A.; Neumann, H.; Beller, M., *Ang. Chem. Int. Ed.* **2009**, *48*, 7595-7599.

29) Anderson, K. W.; Ikawa, T.; Tundel, R. E.; Buchwald, S. L., *J. Am. Chem. Soc.* **2006**, *128*, 10694-10695.

30) Xu, H.-J.; Liang, Y.-F.; Cai, Z.-Y.; Qi, H.-X.; Yang, C.-Y.; Feng, Y.-S., *J. Org. Chem.* **2011**, *76*, 2296-2300.

31) Tlili, A.; Xia, N.; Monnier, F.; Taillefer, M., *Ang. Chem. Int. Ed.* **2009**, *48*, 8725-8728.

32) Zhao, D.; Wu, N.; Zhang, S.; Xi, P.; Su, X.; Lan, J.; You, J., *Ang. Chem. Int. Ed.* **2009**, *48*, 8729 - 8732.

33) Yang, D.; Fu, H., *Chem. Eur. J.* **2010**, *16*, 2366-2370.

34) Jing, L.; Wei, J.; Zhou, L.; Huang, Z.; Li, Z.; Zhou, X., *Chem. Commun. (Cambridge, U. K.)* **2010**, *46*, 4767-4769.

35) Yang, K.; Li, Z.; Wang, Z.; Yao, Z.; Jiang, S., *Org. Lett.* **2011**, *13*, 4340-4343.

36) Botteselle, G. V.; Godoi, M.; Galetto, F. Z.; Bettanin, L.; Singh, D.; Rodrigues, O. E. D.; Braga, A. L., *J. Mol. Catal. A: Chem.* **2012**, *365*, 186-193.

37) Ren, Y.; Cheng, L.; Tian, X.; Zhao, S.; Wang, J.; Hou, C., *Tetrahedron Lett.* **2010**, *51*, 43-45.

38) Huang, C.; Ghavtadze, N.; Godoi, B.; Gevorgyan, V., *Chem. Eur. J.* **2012**, *18*, 9789-9792.

39) Gulevich, A. V.; Melkonyan, F. S.; Sarkar, D.; Gevorgyan, V., *J. Am. Chem. Soc.* **2012**, *134*, 5528-5531.

40) Huang, C.; Chernyak, N.; Dudnik, A. S.; Gevorgyan, V., *Adv. Synth. Catal.* **2011**, *353*, 1285-1305.

41) Huang, C.; Ghavtadze, N.; Chattopadhyay, B.; Gevorgyan, V., *J. Am. Chem. Soc.* **2011**, *133*, 17630-17633.

42) Mo, F.; Trzepkowski, L. J.; Dong, G., *Ang. Chem. Int. Ed.* **2012**, *51*, 13075-13079.

43) Choy, P. Y.; Kwong, F. Y., *Org. Lett.* **2013**, *15*, 270-273.

44) Yang, Y.; Lin, Y.; Rao, Y., *Org. Lett.* **2012**, *14*, 2874-2877.

45) Thirunavukkarasu, V. S.; Ackermann, L., *Org. Lett.* **2012**, *14*, 6206-6209.

46) Yang, F.; Ackermann, L., *Org. Lett.* **2013**, *15*, 718-720.

47) Kuhl, N.; Hopkinson, M. N.; Wencel-Delord, J.; Glorius, F., *Ang. Chem. Int. Ed.* **2012**, *51*, 10236-10254.

48) Mkhalid, I. A. I.; Barnard, J. H.; Marder, T. B.; Murphy, J. M.; Hartwig, J. F., *Chem. Rev. (Washington, DC, U. S.)* **2010**, *110*, 890-931.

49) Maleczka, R. E.; Shi, F.; Holmes, D.; Smith, M. R., *J. Am. Chem. Soc.* **2003**, *125*, 7792-7793.

50) Zou, Y.-Q.; Chen, J.-R.; Liu, X.-P.; Lu, L.-Q.; Davis, R. L.; Jørgensen, K. A.; Xiao, W.-J., *Ang. Chem. Int. Ed.* **2012**, *51*, 784-788.

51) Jiang, H.; Lykke, L.; Uttrup Pedersen, S.; Xiao, W.-J.; Anker Jorgensen, K., *Chem. Commun. (Cambridge, U. K.)* **2012**, *48*, 7203-7205.

52) Webb, K. S.; Levy, D., *Tetrahedron Lett.* **1995**, *36*, 5117-5118.

53) Molander, G. A.; Cavalcanti, L. N., *J. Org. Chem.* **2010**, *76*, 623-630.

54) Lennox, A. J. J.; Lloyd-Jones, G. C., *Ang. Chem. Int. Ed.* **2012**, *51*, 9385-9388.

55) Zhu, C.; Wang, R.; Falck, J. R., *Org. Lett.* **2012**, *14*, 3494-3497.

56) Buncel, E.; Davies, A. G., *J. Chem. Soc. D* **1958**, 1550-1556.

57) Tamao, K.; Kakui, T.; Kumada, M., *J. Am. Chem. Soc.* **1978**, *100*, 2268-2269.

58) Hosomi, A.; Iijima, S.; Sakurai, H., *Chem. Lett.* **1981**, *10*, 243-246.

59) Kumada, M.; Tamao, K.; Yoshida, J.-I., *J. Organomet. Chem.* **1982**, *239*, 115-132.

60) Tamao, K.; Kakui, T.; Akita, M.; Iwahara, T.; Kanatani, R.; Yoshida, J.; Kumada, M., *Tetrahedron* **1983**, *39*, 983-990.

61) Tamao, K.; Ishida, N., *J. Organomet. Chem.* **1984**, *269*, c37-c39.

62) Tamao, K.; Kumada, M.; Maeda, K., *Tetrahedron Lett.* **1984**, *25*, 321-324.

63) Tamao, K.; Ishida, N.; Kumada, M., *J. Org. Chem.* **1983**, *48*, 2120-2122.

64) Tamao, K.; Ishida, N.; Tanaka, T.; Kumada, M., *Organometallics* **1983**, *2*, 1694-1696.

65) Tamao, K.; Akita, M.; Kumada, M., *J. Organomet. Chem.* **1983**, *254*, 13-22.

66) Fleming, I.; Henning, R.; Plaut, H., *J. Chem. Soc., Chem. Commun.* **1984**, 29-31.

67) Fleming, I.; Henning, R.; Parker, D. C.; Plaut, H. E.; Sanderson, P. E. J., *J. Chem. Soc., Perkin Trans. 1* **1995**, 317-337.

68) Tamao, K. H., T.; Ito, Y., *Frontiers of Organosilicon chemistry*. Royal Society of Chemistry: 1991.

69) Tamao, K., *P. Jpn. Acad. B-Phys.* **2008**, *84*, 123-133.

70) Molander, G. A.; Corrette, C. P., *Organometallics* **1998**, *17*, 5504-5512.

71) Smitrovich, J. H.; Woerpel, K. A., *J. Org. Chem.* **1996**, *61*, 6044-6046.

72) Sunderhaus, J. D.; Lam, H.; Dudley, G. B., *Org. Lett.* **2003**, *5*, 4571-4573.

73) Lam, H.; House, S. E.; Dudley, G. B., *Tetrahedron Lett.* **2005**, *46*, 3283-3285.

74) Tlais, S. F.; Lam, H.; House, S. E.; Dudley, G. B., *J. Org. Chem.* **2009**, *74*, 1876-1885.

75) Huang, C.; Gevorgyan, V., *J. Am. Chem. Soc.* **2009**, *131*, 10844-10845.

76) Bashiardes, G.; Chaussebourg, V.; Laverdan, G.; Pornet, J., *Chem. Commun. (Cambridge, U. K.)* **2004**, 122-123.

77) Angelaud, R.; Landais, Y., *Tetrahedron* **2000**, *56*, 2025-2036.

78) Ihara, H.; Suginome, M., *J. Am. Chem. Soc.* **2009**, *131*, 7502-7503.

79) Denmark, S. E.; Regens, C. S., *Acc. Chem. Res.* **2008**, *41*, 1486-1499.

80) Brough, P. A.; Fisher, S.; Zhao, B.; Thomas, R. C.; Snieckus, V., *Tetrahedron Lett.* **1996**, *37*, 2915-2918.

81) Sato, K.; Kira, M.; Sakurai, H., *Tetrahedron Lett.* **1989**, *30*, 4375-4378.

82) Cordonnier, M.-C. A.; Jennifer Kan, S. B.; Anderson, E. A., *Chem. Commun. (Cambridge, U. K.)* **2008**, 5818-5820.

83) Bracegirdle, S.; Anderson, E. A., *Chem. Commun. (Cambridge, U. K.)* **2010**, *46*, 3454-3456.

84) Simmons, E. M.; Hartwig, J. F., *J. Am. Chem. Soc.* **2010**, *132*, 17092-17095.

85) Rayment, E. J.; Summerhill, N.; Anderson, E. A., *J. Org. Chem.* **2012**, *77*, 7052-7060.

86) Lee, M.; Ko, S.; Chang, S., *J. Am. Chem. Soc.* **2000**, *122*, 12011-12012.

87) Miller, R. L.; Maifeld, S. V.; Lee, D., *Org. Lett.* **2004**, *6*, 2773-2776.

88) Jeon, M.; Han, J.; Park, J., *ACS Catalysis* **2012**, *2*, 1539-1549.

89) Ohkubo, A.; Noma, Y.; Aoki, K.; Tsunoda, H.; Seio, K.; Sekine, M., *J. Org. Chem.* **2009**, *74*, 2817-2823.

90) Beckmann, J.; Duthie, A.; Reeske, G.; Schürmann, M., *Organometallics* **2005**, *24*, 3629-3633.

91) Nakao, Y.; Imanaka, H.; Chen, J.; Yada, A.; Hiyama, T., *J. Organomet. Chem.* **2007**, *692*, 585-603.

92) Ilies, L.; Tsuji, H.; Nakamura, E., *Org. Lett.* **2009**, *11*, 3966-3968.

93) Kawachi, A.; Zaima, M.; Tani, A.; Yamamoto, Y., *Chem. Lett.* **2007**, *36*, 362-363.

94) Bonnafoux, L.; Leroux, F. R.; Colobert, F., *Beilstein J. Org. Chem.* **2011**, *7*, 1278-1287.

95) Kim, D.-S.; Bolla, K.; Lee, S.; Ham, J., *Tetrahedron* **2011**, *67*, 1062-1070.

96) Wessels, M.; Mahajan, V.; Boßhammer, S.; Raabe, G.; Gais, H.-J., *Eur. J. Org. Chem.* **2011**, *2011*, 2431-2449.

97) Snieckus, V., *Chem. Rev. (Washington, DC, U. S.)* **2002**, *90*, 879-933.

98) Itami, K.; Mitsudo, K.; Yoshida, J.-i., *J. Org. Chem.* **1999**, *64*, 8709-8714.

99) Missaghi, M. N.; Galloway, J. M.; Kung, H. H., *Organometallics* **2010**, *29*, 3769-3779.

100) Wood, P. M.; Woo, L. W. L.; Labrosse, J.-R.; Trusselle, M. N.; Abbate, S.; Longhi, G.; Castiglioni, E.; Lebon, F.; Purohit, A.; Reed, M. J.; Potter, B. V. L., *J. Med. Chem.* **2008**, *51*, 4226-4238.

101) Hepler, L. G., *Can. J. Chem.* **1971**, *49*, 2803-2807.

102) Chung, M.-K.; Orlova, G.; Goddard, J. D.; Schlaf, M.; Harris, R.; Beveridge, T. J.; White, G.; Hallett, F. R., *J. Am. Chem. Soc.* **2002**, *124*, 10508-10518.

103) Biffis, A.; Braga, M.; Basato, M., *Adv. Synth. Catal.* **2004**, *346*, 451-458.

104) Sommer, L. H.; Lyons, J. E., *J. Am. Chem. Soc.* **1967**, *89*, 1521-1522.

105) Yamamoto, K.; Takemae, M., *Bull. Chem. Soc. Jpn.* **1989**, *62*, 2111-2113.

106) Kim, S.; Marie Jacobo, S.; Chang, C.-T.; Bellone, S.; Powell, W. S.; Rokach, J., *Tetrahedron Lett.* **2004**, *45*, 1973-1976.

107) Terunuma, D.; Senda, K.; Sanazawa, M.; Nohira, H., *Bull. Chem. Soc. Jpn.* **1982**, *55*, 924-927.

108) Tran, N. T.; Min, T.; Franz, A. K., *Chem. Eur. J.* **2011**, *17*, 9897-9900.

109) Barnes, G. H.; Daughenbaugh, N. E., *J. Org. Chem.* **1966**, *31*, 885-887.

110) Späth, E.; Gruber, W., *Ber. Dtsch. Chem. Ges.* **1938**, *71*, 106-113.

111) Gammill, R. B.; Hyde, B. R., *J. Org. Chem.* **1983**, *48*, 3863-3865.

112) Ravina, E.; Kubinyi, H., *The Evolution of Drug Discovery: From Traditional Medicines to Modern Drugs*. John Wiley & Sons: 2011.

113) Wulff, H.; Castle, N. A.; Pardo, L. A., *Nat Rev Drug Discov* **2009**, *8*, 982-1001.

114) Baell, J.; Gable, R.; Harvey, A.; Toovey, N.; Herzog, T.; Hansel, W.; Wulff, H., *J. Med. Chem.* **2004**, 2326-2336.

115) Reed, M.; Moore, H., *J. Org. Chem.* **1988**, 4166-4171.

116) Yamashita, A.; Toy, A.; Scahill, T., *J. Org. Chem.* **1989**, 3625-3634.

117) Gammill, R., *Tetrahedron Lett.* **1985**, 1385-1388.

118) Clarke, J. R.; Robertson, A., *J. Chem. Soc. D* **1949**, *0*, 302-307.

119) Gammill, R. B., *J. Org. Chem.* **1984**, *49*, 5035-5041.

120) Yamashita, A., *J. Am. Chem. Soc.* **1985**, *107*, 5823-5824.

121) Geissman, T. A.; Halsall, T. G., *J. Am. Chem. Soc.* **1951**, *73*, 1280-1284.

122) Schönberg, A.; Sina, A., *J. Am. Chem. Soc.* **1950**, *72*, 1611-1616.

123) Gammill, R. B.; Day, C. E.; Schurr, P. E., *J. Med. Chem.* **1983**, *26*, 1672-1674.

124) Gardner, T. S.; Wenis, E.; Lee, J., *J. Org. Chem.* **1950**, *15*, 841-849.

125) Baxter, R. A.; Ramage, G. R.; Timson, J. A., *J. Chem. Soc. D* **1949**, *0*, S30-S33.

126) Brimble, M. A.; Flowers, C. L.; Trzoss, M.; Tsang, K. Y., *Tetrahedron* **2006**, *62*, 5883-5896.

127) Jager, G.; Geiger, R.; Siedel, W., *Chem. Ber.* **1968**, 2762-2770.

128) Griffen, E. J.; Roe, D. G.; Snieckus, V., *J. Org. Chem.* **1995**, *60*, 1484-1485.

129) Singh, K. J.; Collum, D. B., *Journal of the American Chemical Society* **2006**, *128*, 13753-13760.

130) Wentworth, P.; Datta, A.; Smith, S.; Marshall, A.; Partridge, L. J.; Blackburn, G. M., *Journal of the American Chemical Society* **1997**, *119*, 2315-2316.

131) Metallinos, C.; Nerdinger, S.; Snieckus, V., *Org. Lett.* **1999**, *1*, 1183-1186.

132) Kauch, M.; Snieckus, V.; Hoppe, D., *J. Org. Chem.* **2005**, *70*, 7149-7158.

133) van Otterlo, W. A. L.; Morgans, G. L.; Madeley, L. G.; Kuzvidza, S.; Moleele, S. S.; Thornton, N.; de Koning, C. B., *Tetrahedron* **2005**, *61*, 7746-7755.

134) Mathouet, H.; Elomri, A.; Lameiras, P.; Daïch, A.; Vérité, P., *Phytochemistry* **2007**, *68*, 1813-1818.

135) Cruz, A.; Garduño, L.; Salazar, M.; Martínez, E.; Jiménez-Vázquez, H. A.; Díaz, F.; Chamorro, G.; Tamariz, J., *Arzneimittelforschung* **2001**, *51*, 535-544.

136) Fraile, J.; Garcia, J.; Gomez, M.; Vazquez, E., *Eur. J. Org. Chem.* **2001**, 2891 - 2899.

137) Kotsuki, H.; Asao, K.; Ohnishi, H., *Bull. Chem. Soc. Jpn.* **1984**, *57*, 3339-3340.

138) Brion, F., *Tetrahedron Lett.* **1982**, *23*, 5299-5302.

139) Safaei-Ghomi, J.; Tajbakhsh, M.; Kazemi-Kani, Z., *Acta Chim. Slov.* **2004**, 545-550.

140) Shoji, M., *Bull. Chem. Soc. Jpn.* **2007**, *80*, 1672-1690.

141) Nelson, T. D.; Crouch, R. D., *Synthesis* **1996**, *1996*, 1031-1069.

142) Schelhaas, M.; Waldmann, H., *Angew. Chem. Int. Ed.* **1996**, *35*, 2056-2083.

143) Lalonde, M.; Chan, T. H., *Synthesis* **1985**, *1985*, 817-845.

144) Mori, Y.; Yaegashi, K.; Furukawa, H., *J. Org. Chem.* **1998**, *63*, 6200-6209.

145) Romo, D.; Meyer, S. D.; Johnson, D. D.; Schreiber, S. L., *J. Am. Chem. Soc.* **1993**, *115*, 7906-7907.

146) Wiles, C.; Watts, P., *Green Chem.* **2012**, *14*, 38-54.

147) Webb, D.; Jamison, T. F., *Chemical Science* **2010**, *1*, 675-680.

148) Warner, J. C.; Cannon, A. S.; Dye, K. M., *Environmental Impact Assessment Review* **2004**, *24*, 775-799.

149) ThalesNano Commercially available microreactor.

150) Sudhakar, S.; Luh, T.-Y., *J. Org. Chem.* **2002**, *67*, 6860-6862.

151) Goh, S. S.; Baars, H.; Gockel, B.; Anderson, E. A., *Org. Lett.* **2012**, *14*, 6278-6281.

152) Mader, M. M.; Norrby, P.-O., *Chem. Eur. J.* **2002**, *8*, 5043-5048.

153) Nikolin, A. A.; Kramarova, E. P.; Shipov, A. G.; Baukov, Y. I.; Negrebetsky, V. V.; Korlyukov, A. A.; Arkhipov, D. E.; Bowden, A.; Bylikin, S. Y.; Bassindale, A. R.; Taylor, P. G., *Organometallics* **2012**, *31*, 4988-4997.

154) Bassindale, A. R.; Sohail, M.; Taylor, P. G.; Korlyukov, A. A.; Arkhipov, D. E., *Chem. Commun. (Cambridge, U. K.)* **2010**, *46*, 3274-3276.

155) Pauling, L., *The Nature of the Chemical Bond, 3rd Ed.* Cornell University Press: 1960.

156) Galbraith, J. M., *J. Chem. Educ.* **2007**, *84*, 783.

157) Pimentel, G. C., *J. Chem. Phys.* **1951**, *19*, 446-448.

158) Hach, R. J.; Rundle, R. E., *J. Am. Chem. Soc.* **1951**, *73*, 4321-4324.

159) Pierrefixe, S. C. A. H.; Fonseca Guerra, C.; Bickelhaupt, F. M., *Chem. Eur. J.* **2008**, *14*, 819-828.

160) Chuit, C.; Corriu, R. J. P.; Reye, C.; Young, J. C., *Chem. Rev. (Washington, DC, U. S.)* **1993**, *93*, 1371-1448.

161) Corriu, R. J. P.; Dabosi, G.; Martineau, M., *J. Organomet. Chem.* **1978**, *154*, 33-43.

162) Kin-ya-Akiba, *Organo Main Group Chemistry*. Wiley: 2011.

163) Holmes, R. R., *Chem. Rev. (Washington, DC, U. S.)* **1996**, *96*, 927-950.

164) Deiters, J. A.; Holmes, R. R., *J. Am. Chem. Soc.* **1990**, *112*, 7197-7202.

165) Corriu, R. J. P.; Guerin, C.; Henner, B. J. L.; Wong Chi Man, W. W. C., *Organometallics* **1988**, *7*, 237-238.

166) Razuvaev, G. A.; Yablokov, V. A.; Ganyushkin, A. V.; Yablokova, N. V.; Kalinina, G. S., *J. Organomet. Chem.* **1979**, *165*, 281-286.

167) Knölker, H.-J.; Wanzl, G., *Synlett* **1995**, *1995*, 378-382.

168) Mader, M. M.; Norrby, P.-O., *J. Am. Chem. Soc.* **2001**, *123*, 1970-1976.

169) Kunai, A.; Ohshita, J., *J. Organomet. Chem.* **2003**, *686*, 3-15.

170) Jacobsen, N. E., *NMR Spectroscopy Explained: Simplified Theory, Applications and Examples for Organic Chemistry and Structural Biology*. Wiley: 2007.

171) Denmark, S. E.; Ober, M. H., *Adv. Synth. Catal.* **2004**, *346*, 1703-1714.

172) OriginLab *OriginPro 8.5.1 SR2*, Northampton, 1991-2011.

173) Murto, J., Hydroxide-Alkoxide Ion Equilibria. In *The Chemistry of the Hydroxyl Group*, Patai, S., Ed. Interscience Publishers: 1971.

174) Murto, J., *Acta Chem. Scand.* **1964**, *18*, 1029-1042.

175) Burns, R. G.; England, B. D., *J. Chem. Soc. B* **1966**, *0*, 864-867.

176) Burns, R. G.; England, B. D., *Tetrahedron Lett.* **1960**, *1*, 1-6.

177) Reichardt, C. W., T, *Solvents and Solvent Effects in Organic Chemistry*. 4th ed.; Wiley: Weinheim, 2011.

178) Abrash, H. I., *J. Chem. Educ.* **2001**, *78*, 1496.

179) Kickelbick, G., *Hybrid Materials*. Wiley: 2007.

180) West, R.; Baney, R. H., *J. Am. Chem. Soc.* **1959**, *81*, 6145-6148.

181) Koskikallio, J., *Suomen Kemistilehti* **1957**, *30B*, 111.

182) Rochester, C. H., *J. Chem. Soc., Dalton Trans.* **1972**, *0*, 5-8.

183) Macey, R. O., G; Zahnley, T *Berkeley Madonna Modelling and Analysis of Dynamic Systems*, University of California at Berkeley, 1993.

184) Fina, N. J.; Edwards, J. O., *Int. J. Chem. Kinet.* **1973**, *5*, 1-26.

185) Kira, M.; Miyazawa, T.; Sugiyama, H.; Yamaguchi, M.; Sakurai, H., *J. Am. Chem. Soc.* **1993**, *115*, 3116-3124.

186) Ishikawa, M.; Watanabe, K.; Sakamoto, H.; Kunai, A., *J. Organomet. Chem.* **1993**, *455*, 61-68.

187) Pitt, C. G.; Friedman, A. E.; Rector, D.; Wani, M. C., *Tetrahedron* **1975**, *31*, 2369-2377.

188) Lipowitz, J., *J. Am. Chem. Soc.* **1972**, *94*, 1582-1589.

189) Hevesi, L.; Dehon, M.; Crutzen, R.; Lazarescu-Grigore, A., *J. Org. Chem.* **1997**, *62*, 2011-2017.

190) Rich, J. D.; Burnell, T. B., *Synth. Commun.* **1990**, *20*, 1033 - 1037.

191) Schott, G.; Kuhla, S., *Z. Anorg. Allg. Chem.* **1970**, *374*, 86-93.

192) Itami, K.; Mitsudo, K.; Nishino, A.; Yoshida, J.-i., *J. Org. Chem.* **2002**, *67*, 2645-2652.

193) Denmark, S. E.; Kallemeyn, J. M., *Org. Lett.* **2003**, *5*, 3483-3486.

194) Yoshida, H.; Yamaryo, Y.; Ohshita, J.; Kunai, A., *Chem. Commun. (Cambridge, U. K.)* **2003**, 1510-1511.

195) Hirabayashi, K.; Ando, J.-i.; Kawashima, J.; Nishihara, Y.; Mori, A.; Hiyama, T., *Bull. Chem. Soc. Jpn.* **2000**, *73*, 1409-1417.

196) Scheim, U.; Porzel, A.; Rühlmann, K., *J. Organomet. Chem.* **1988**, *354*, 31-37.

197) Yen, *Collect. Czech. Chem. Commun.* **1973**, *38*, 3167,3168,3171,3172

198) Grogger, C.; Loidl, B.; Stueger, H.; Kammel, T.; Pachaly, B., *J. Organomet. Chem.* **2006**, *691*, 105-110.

199) Koehler, P.; Geissler, H.; Jakoubkova, M.; Dube, G.; Licht, K.; Kriegsmann, H., *Z. Anorg. Allg. Chem.* **1978**, *440*, 183-196.

200) Eaborn, C.; Jones, K. L.; Lickiss, P. D., *J. Organomet. Chem.* **1994**, *466*, 35-42.

201) Zhang, G.; Wen, X.; Wang, Y.; Mo, W.; Ding, C., *J. Org. Chem.* **2011**, *76*, 4665-4668.

202) Magano, J.; Chen, M. H.; Clark, J. D.; Nussbaumer, T., *J. Org. Chem.* **2006**, *71*, 7103-7105.

203) Inamoto, K.; Nozawa, K.; Yonemoto, M.; Kondo, Y., *Chem. Commun. (Cambridge, U. K.)* **2011**, *47*, 11775-11777.

204) Chan, C.-C.; Chen, Y.-W.; Su, C.-S.; Lin, H.-P.; Lee, C.-F., *Eur. J. Org. Chem.* **2011**, *2011*, 7288-7293.

205) Gonzalez, R. R. g.; Gambarotti, C.; Liguori, L.; Bjarsvik, H.-R., *J. Org. Chem.* **2006**, *71*, 1703-1706.

206) Del Giudice, M. R.; Settimj, G.; Delfini, M., *Tetrahedron* **1984**, *40*, 4067-4080.

207) Jiang, F.; Bézier, D.; Sortais, J.-B.; Darcel, C., *Adv. Synth. Catal.* **2011**, *353*, 239-244.

208) Rajagopal, G.; Lee, H.; Kim, S. S., *Tetrahedron* **2009**, *65*, 4735-4741.

209) Xu, J.; Luo, D.-F.; Xiao, B.; Liu, Z.-J.; Gong, T.-J.; Fu, Y.; Liu, L., *Chem. Commun. (Cambridge, U. K.)* **2011**, *47*, 4300-4302.

210) Clayden, J., Helliwell, M., McCarthy, C. and Westlund, N., *J. Chem. Soc., Perkin Trans. 1* **2000**, 3232 - 3249.

211) Rahmathullah, S. M.; Hall, J. E.; Bender, B. C.; McCurdy, D. R.; Tidwell, R. R.; Boykin, D. W., *J. Med. Chem.* **1999**, *42*, 3994-4000.

212) Viallon, L.; Reinaud, O.; Capdevielle, P.; Maumy, M., *Synthesis* **1995**, *1995*, 1534-1538.

213) Changtam, C.; de Koning, H. P.; Ibrahim, H.; Sajid, M. S.; Gould, M. K.; Suksamrarn, A., *Eur. J. Med. Chem.* **2010**, *45*, 941-956.

214) Testaferri, L.; Tiecco, M.; Tingoli, M.; Chianelli, D.; Montanucci, M., *Tetrahedron* **1982**, *38*, 3687-3692.

215) Zhang, Q.; Botting, N. P., *Tetrahedron* **2004**, *60*, 12211-12216.

216) Schafer, W.; Geyer, I.; Leute, R., *Chem. Ber. Recl.* **1967**, 930-&.

217) Zhang, Y.; Zhang, Y.; Sun, Y. L.; Du, X.; Shi, J. Y.; Wang, W. D.; Wang, W., *Chem. Eur. J.* **2012**, *18*, 6328-6334.

218) Shaw, A. Y.; Chang, C.-Y.; Liau, H.-H.; Lu, P.-J.; Chen, H.-L.; Yang, C.-N.; Li, H.-Y., *Eur. J. Med. Chem.* **2009**, *44*, 2552-2562.

219) Reddy, B. P.; Krupadanam, G. L. D., *J. Heterocycl. Chem.* **1996**, *33*, 1561-1565.

220) Sharma, A.; Joshi, B. P.; Singh, N. P.; Sinha, A. K., *Tetrahedron* **2006**, *62*, 847-851.

221) Wu, H.-J.; Yen, C.-H.; Chuang, C.-T., *The Journal of Organic Chemistry* **1998**, *63*, 5064-5070.

222) Kelly, T. R.; Bell, S. H.; Ohashi, N.; Armstrong-Chong, R. J., *J. Am. Chem. Soc.* **1988**, *110*, 6471-6480.

223) Morita, N.; Kudo, M.; Yokoyama, R.; Ito, S., *Heterocycles* **2001**, 679-+.

224) Deshpande, A. M.; Natu, A. A.; Argade, N. P., *Synthesis* **2002**, *2002*, 1010-1012.

225) Mahajna, M.; Quistad, G. B.; Casida, J. E., *Chemical Research in Toxicology* **1996**, *9*, 241-246.

226) Maras, A.; Altay, A.; Ballini, R., *Synth. Commun.* **2008**, 212-216.

227) Cordonnier, M.-C. A. Palladium-Catalysed Cascade Cyclisation of Alkynyl Silanes. University of Oxford, DPhil Thesis, 2011.

228) Yamada, H.; Kushibe, K.; Okujima, T.; Uno, H.; Ono, N., *Chem. Commun. (Cambridge, U. K.)* **2006**, 383-385.

229) Harrison, A. N.; Reichau, S.; Parker, E. J., *Bioorg. Med. Chem. Lett.* **2012**, *22*, 907-911.

230) Tour, J. M.; John, J. A.; Stephens, E. B., *J. Organomet. Chem.* **1992**, *429*, 301-310.

231) Min, G. K.; Skrydstrup, T., *J. Org. Chem.* **2012**, *77*, 5894-5906.

232) Yeom, C.-E.; Kim, Y. J.; Lee, S. Y.; Shin, Y. J.; Kim, B. M., *Tetrahedron* **2005**, *61*, 12227-12237.